D&C R. Rapp

250pgs 12 fold out

MSC-PA-R-69-1

NATIONAL AERONAUTICS AND SPACE ADMINISTRATION

APOLLO 8 MISSION REPORT

DISTRIBUTION AND REFERENCING

This paper is not suitable for general distribution or referencing. It may be referenced only in other working correspondence and documents by participating organizations.

MANNED SPACECRAFT CENTER

HOUSTON, TEXAS

FEBRUARY 1969

MSC-PA-R-69-1

APOLLO 8 MISSION REPORT

PREPARED BY

Mission Evaluation Team

APPROVED BY

George M. Low
Manager, Apollo Spacecraft Program

NATIONAL AERONAUTICS AND SPACE ADMINISTRATION
MANNED SPACECRAFT CENTER
HOUSTON, TEXAS
February 1969

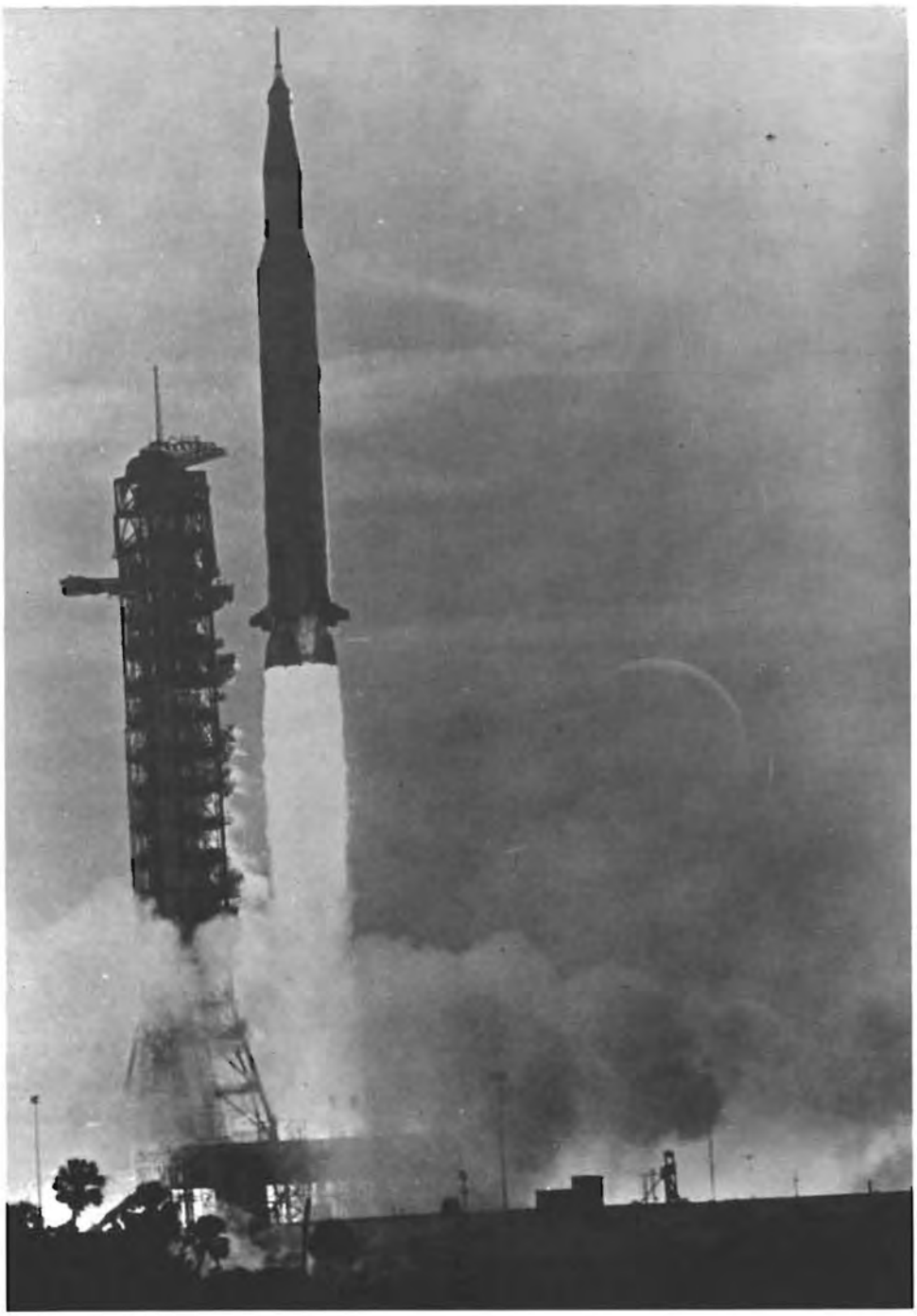

Apollo 8 lift-off.

CONTENTS

1.0 SUMMARY

Apollo 8 was the second manned flight in the program and the first manned lunar orbit mission. The crew were Frank Borman, Commander; James A. Lovell, Command Module Pilot; and William A. Anders, Lunar Module Pilot.

The Apollo 8 space vehicle was launched on time from Kennedy Space Center, Florida, at 7:51:00 a.m. e.s.t. on December 21, 1968. Following a nominal boost phase, the spacecraft and S-IVB combination was inserted into a parking orbit of 98 by 103 nautical miles. After a post-insertion checkout of spacecraft systems, the 319-second translunar injection maneuver was initiated at 2:50:37 by reignition of the S-IVB engine.

The spacecraft separated from the S-IVB at 3:20:59, followed by two separation maneuvers using the service module reaction control system. The first midcourse correction, made with a velocity change of 24.8 feet per second, was conducted at 11:00:00. The translunar coast phase was devoted to navigation sightings, two television transmissions, and various systems checks. The second midcourse correction, conducted at 60:59:55, was a velocity change of 1.4 feet per second.

The 246.9-second lunar orbit insertion maneuver was performed at 69:08:20, and the initial lunar orbit was 168.5 by 60.0 nautical miles. A maneuver to circularize the orbit was conducted at 73:35:07 and resulted in a lunar orbit of 59.7 by 60.7 nautical miles. The coast phase between maneuvers was devoted to orbit navigation and ground track determination. Ten revolutions were completed during the 20 hours 11 minutes spent in lunar orbit.

The lunar orbit coast phase involved numerous landing-site/landmark sightings, lunar photography, and preparation for transearth injection. The transearth injection maneuver, 204 seconds in duration, was conducted at 89:19:17 using the service propulsion system.

When possible during both the translunar and transearth coast phases, passive thermal control maneuvers of about one revolution per hour were effected to maintain temperatures within nominal limits. The transearth coast period involved a number of star/horizon navigation sightings using both the earth and moon horizons. The only transearth midcourse correction was a maneuver of 4.8 feet per second made at 103:59:54.

Command module/service module separation was at 146:28:48, and the command module reached the entry interface (400 000 feet altitude) at 146:46:14. Following normal deployment of all parachutes, the spacecraft landed in the Pacific Ocean at 8 degrees 8 minutes north latitude and

165 degrees 1 minute west longitude, as determined by the primary recovery ship *USS Yorktown*. The total flight duration was 147 hours 42 seconds.

Almost without exception, spacecraft systems operated as intended. All temperatures varied in a predictable manner within acceptable limits, and consumables usage was always maintained at safe levels. Communications quality was exceptionally good, and live television was transmitted on six occasions. The crew superbly performed the planned mission.

2.0 INTRODUCTION

The Apollo 8 mission was the eighth in a series of flights using specification Apollo hardware, the second manned flight of a block II spacecraft, and the first manned flight using a Saturn V launch vehicle. The mission was the first to the vicinity of the moon and was the continuation of a program to develop manned lunar landing capability.

The overall objectives of the mission were to demonstrate command and service module performance in a cislunar and lunar-orbit environment, to evaluate crew performance in a lunar-orbit mission, to demonstrate communications and tracking at lunar distances, and to return high-resolution photography of proposed Apollo landing areas and other locations of scientific interest.

Because of the excellent performance of spacecraft systems in both the Apollo 7 and Apollo 8 missions, this report will present only the Apollo 8 mission results that are either unique to the lunar environment or significantly different from Apollo 7. Consequently, some of the report sections presented in previous Mission Reports have been deleted to permit greater emphasis on lunar observations of scientific or operational interest.

All times in this report are based on range zero, the integral second before lift-off. Range zero for this mission was 12:51:00 G.m.t.

3.0 MISSION DESCRIPTION

The Apollo 8 mission followed the prescribed flight plan in every major respect. The space vehicle was launched at 7:51:00 a.m. e.s.t. on December 21, 1968, and the spacecraft was inserted into a 103- by 98-n. mi. parking orbit. The launch vehicle was a 3-stage Saturn V (no. 503), and the spacecraft was a standard block II command and service module configuration (no. 103). A lunar module test article (LTA-B) was mounted in the spacecraft/launch vehicle adapter for mass loading purposes. The adapter used on this mission was the first to incorporate a panel-jettison mechanism.

After a parking-orbit coast period devoted to inflight systems checks, the third stage (S-IVB) of the launch vehicle was reignited at 2:50:37 for the translunar injection maneuver (see fig. 3-1). This maneuver lasted for 319 seconds. At approximately 3:21:00, the spacecraft was separated from the S-IVB by a small maneuver with the service module reaction control system.

After separation and transposition, the crew observed and photographed the S-IVB, then performed reaction control system maneuvers at 3:40:01 and at 4:45:01 to increase the separation distance. At 4:55:56, a liquid-oxygen dump procedure was initiated in the S-IVB to provide impulse for changing its path to a trailing-edge lunar flyby and for insertion into solar orbit. The first midcourse correction was performed with the service propulsion system at 11:00:00 and produced a velocity change of 24.8 ft/sec. This maneuver reduced the injection pericynthion altitude from 459 to 66.3 n. mi.

The conditions at cutoff of the translunar injection maneuver were so nearly perfect that only one midcourse correction, approximately 8 ft/sec, would have been sufficient to achieve the desired altitude of about 65 n. mi. at lunar orbit insertion. However, the unplanned maneuver of 7.7 ft/sec at 4:45:01 altered the trajectory so that the predicted altitude was 458.1 n. mi., which required a 24.8-ft/sec correction to achieve the desired conditions. An additional midcourse correction of 1.4 ft/sec was performed to further refine the initial conditions.

During translunar coast, the crew completed systems checks, navigation sightings, two television transmissions, and a second midcourse correction (1.4 ft/sec at 60:59:54). The spacecraft high-gain antenna, installed for the first time on this mission, was tested successfully during the translunar coast phase.

Lunar orbit insertion was initiated at 69:08:20 with a 2997-ft/sec service propulsion maneuver, resulting in a 60- by 168.5-n. mi. orbit.

After approximately 4 hours of navigation checks and ground orbit determination, a lunar orbit circularization maneuver of 135 ft/sec resulted in an orbit of 60.7 by 59.7 n. mi.

The next 12 hours of crew activity in lunar orbit involved near- and far-side photography, landing-area sightings, and television transmissions. The final 4 hours in lunar orbit included a second television broadcast, but most of the remaining non-critical flight-plan activities were deleted because of crew fatigue, and this period was devoted to rest periods and preparation for the transearth injection maneuver. This maneuver was initiated at 89:19:17, lasted for 303 seconds, and resulted in a velocity change of 3517 ft/sec.

The transearth coast activities included a number of star/horizon navigation sightings, using both the moon and earth limbs. Passive thermal control, requiring roll rates of approximately one revolution per hour, was used during most of the translunar and transearth coast phases to maintain nearly stable onboard temperatures. This method of thermal control was interrupted only when specific vehicle attitudes were required. The only transearth midcourse correction required provided a velocity change of 4.8 ft/sec, made with the service module reaction control system at 103:59:54.

Command module/service module separation was performed at 146:28:48, and subsequent command module entry (400 000 feet) occurred at 146:46:14. The spacecraft followed a guided entry profile and landed at 147:00:42 in the Pacific Ocean at 8 degrees 8 minutes north latitude and 165 degrees 1 minute west longitude. The crew were retrieved and were aboard the *USS Yorktown* at 17:20 G.m.t., and the spacecraft was taken aboard approximately 1 hour later.

With only minor discrepancies, all spacecraft systems operated as intended, and all mission objectives were successfully accomplished on this first manned lunar mission. The flight plan was followed closely, and crew performance was excellent throughout the 6.1-day mission. A sequence of events for the mission is shown in table 3-I.

TABLE 3-I.- SEQUENCE OF EVENTS

Event	Time, hr:min:sec
Range zero (12:51:00 G.m.t.)	
Lift-off	00:00:00.7
Maximum dynamic pressure	00:01:18.9
S-IC center engine cutoff	00:02:05.9
S-IC outboard engine cutoff	00:02:33.8
S-IC/S-II separation	00:02:34.5
S-II engine ignition	00:02:35.2
Interstage jettison	00:03:04.5
Launch escape tower jettison	00:03:08.6
S-II engine cutoff	00:08:44.0
S-II/S-IVB separation	00:08:44.9
S-IVB engine ignition	00:08:45.0
S-IVB engine cutoff	00:11:25.0
Earth orbit insertion	00:11:35.0
Translunar injection ignition	02:50:37.1
Translunar injection cutoff	02:55:55.5
Spacecraft/S-IVB separation	03:20:59.3
First separation maneuver	03:40:01
Second separation maneuver	04:45:01
First midcourse correction ignition	10:59:59.5
First midcourse correction cutoff	11:00:01.9
Second midcourse correction	60:59:56
Lunar orbit insertion ignition	69:08:20.4
Lunar orbit insertion cutoff	69:12:27.3
Lunar orbit circularization ignition	73:35:07
Lunar orbit circularization cutoff	73:35:16
Transearth injection ignition	89:19:16.6
Transearth injection cutoff	89:22:40.3
Third midcourse correction	103:59:54

TABLE 3-I.- SEQUENCE OF EVENTS - Concluded

Event	Time, hr:min:sec
Command module/service module separation	146:28:48
Entry interface (400 000 feet)	146:46:12.8
Begin blackout	146:46:37
End blackout	146:51:42
Drogue deployment	146:54:47.8
Main parachute deployment	146:55:38.9
Landing	147:00:42

NASA-S-69-605

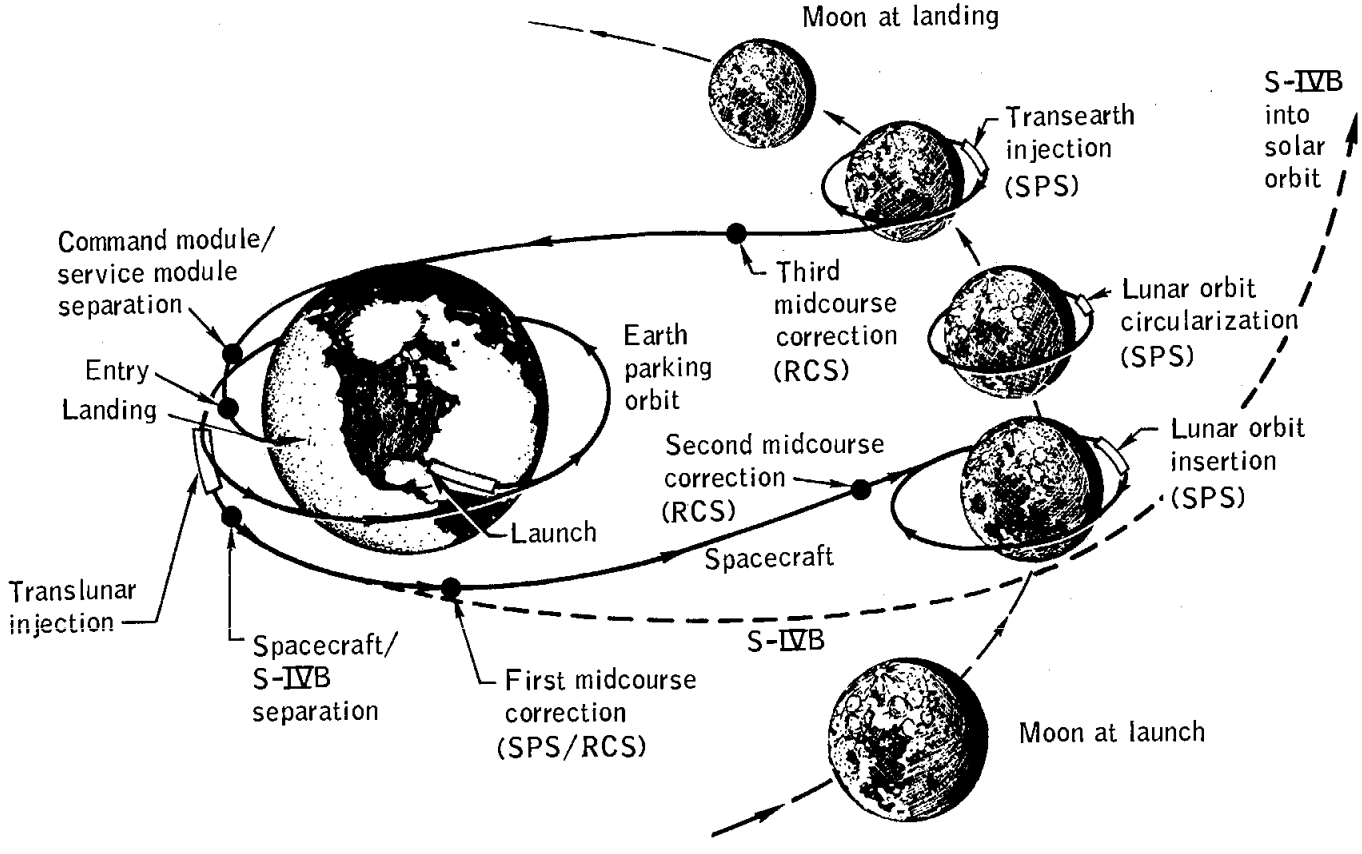

Figure 3-1.- Apollo 8 mission profile.

4.0 THE MOON

The preliminary analysis of the scientific activities planned and accomplished during the Apollo 8 mission is discussed in this section. A formal evaluation of the lunar photography and observations entitled "Apollo 8 Lunar and Space Science Report" will be published in April 1969 as a NASA special publication. Although no formal scientific experiments were planned, recommendations were solicited from scientists regarding tasks and observations that could be accomplished within the equipment and schedule constraints. The principal recommendations were for modifications to initial photographic plans and equipment.

During the mission, seven 70-mm film magazines were exposed and yielded more than 150 photographs of the earth and more than 700 photographs of the moon. Five 16-mm color magazines were also exposed. A summary of these photographs is provided in table 4-I.

Approximately 90 percent of the photographic objectives of the mission were accomplished. Approximately 60 percent of the additional lunar photographs requested as targets of opportunity were also taken despite early curtailment of crew photographic activities. Many smaller lunar features, heretofore undiscovered, were photographed. These features are located principally on the far side of the moon in areas which had been photographed only at much greater distances by automated spacecraft.

4.1 PHOTOGRAPHIC OBJECTIVES

The principal photographic objectives were to obtain vertical and oblique overlapping photographs during at least two revolutions, photographs of specified targets of opportunity, and photographs through the spacecraft sextant of a potential landing site.

The purpose of the overlapping, or stereo-strip, photography was to determine elevation and geographical position of lunar far side features. The positions will be determined with respect to the control points sighted with the onboard telescope and sextant and by the Lunar Orbiter and earth-based telescopic photography. The area to be covered was dependent on the launch day and consisted of one pass with the optical axis in a near-vertical plane and another pass with the axis inclined 20 degrees. The photographs were to be taken at 20-second intervals and at a shutter speed of 1/250 second.

The targets of opportunity were those areas recommended for photography if time and circumstances permitted. All lunar surface areas where photographic coverage was desired were plotted on target-of-opportunity

planning charts as a function of launch day. Lunar-lighting limits, orbital inclination, and spacecraft attitude were used to determine which targets could be photographed for a given launch date. Exposure data were developed to assist the crew and included all supplemental information for accomplishing the recommended photography.

Sextant photography was included to provide image comparisons for landmark evaluation and navigation training purposes. The 16-mm camera used for this study was attached to the sextant by a special adapter mount. A secondary objective was to photograph one of the certified Apollo landing sites (fig. 4-1).

4.2 FILM DESCRIPTION AND PROCESSING

4.2.1 Onboard Film

Special care was taken in the selection, preparation, calibration, and processing of flight film to maximize the information content and retrieval from returned exposures. The types of film used during Apollo 8 are listed in table 4-II and are discussed briefly in the following paragraphs.

Film type SO-368, which has been used extensively during previous manned missions, was stored onboard in two 70-mm and nine 16-mm magazines for photography of the lunar surface, S-IVB, and earth. Film type 3400, a thin-base panchromatic black-and-white negative film, was selected for its high contrast and extended red sensitivity for lunar photometric studies. Film type SO-121, a slow-speed, high definition color reversal film on a thin base, has about twice the resolution of SO-368 and was primarily included for use in earth orbit had the lunar mission been aborted. Film type 2485, a very high-speed panchromatic thin-base film, was selected for photography of various dim-light phenomena, such as gegenschein, zodiacal light, dim stars, solar corona, and the lunar surface in earthshine. Film type SO-168, a high-speed color reversal 16-mm film, was included in two magazines for photographing the spacecraft interior.

4.2.2 Film Sensitometric Calibration

The Apollo 8 photography afforded the first opportunity to analyze the intensity and spectral distribution of lunar surface illumination free from the atmospheric modulation that is present in earth telescopic photography and without the electronic processing losses that are present

in Ranger, Surveyor, and Lunar Orbiter photography. A series of sensitometric strips were exposed on the flight film to allow extraction of densitometric information. The primary purpose of these strips is to reconstruct the density/exposure relationship as a function of processing chemistry, temperature, and time.

4.2.3 Exposure Settings

Prior to the mission, camera aperture settings were determined for all targets to be photographed with the 70-mm film. These settings were applicable to the 80-mm lens and, with some limitations, to the 250-mm lens. A system restriction existed with the 250-mm lens that prohibited use of aperture settings larger than f/5.6. It was recommended that the shutter rate remain fixed at 1/250 second because, at slower speeds, image smear would cause loss of resolution. With the wide latitude inherent in the film types, adequate exposure control could be maintained by aperture regulation only.

Computing the f-stop for each photographic target involved two operations: prediction of the average value and range of the film plane illumination (exposure) as a function of the scene geometry and the albedo of the surface area to be photographed; and evaluation of the sensitivity of the film to the predicted illumination, with subsequent selection of the appropriate camera setting (f-stop) required to achieve the optimum exposure at the film plane.

Three sets of aperture changes were recommended to correspond to each of the general camera-pointing orientations — vertical, obliques to the east and west of the ground track, and obliques to the north and south. These data were printed on the photographic target of opportunity chart with the changes indicated as a function of selenographic longitude.

In addition, procedures had been established and simulated for real-time revisions of the entire set of exposure recommendations should an off-nominal situation have occurred.

4.2.4 Processing

Standards for processing onboard films were developed before flight from the standard process specified by the manufacturer and modified for specific requirements and sensitometric results. The films were refrigerated from the time of emulsion coating until processing, except for the time they were actually in the spacecraft.

After return of the films to the Manned Spacecraft Center, postflight sensitometric data were derived, where appropriate, before actual processing. The SO-368 and SO-168 films were processed in the General Photography Laboratory, and the SO-121, 3400, and 2485 films were processed in the Precision Laboratory.

The SO-368 film was processed under pre-established controls using ME-2A chemistry. The 70-mm film was processed at 3.5 ft/min. and the 16-mm film at 34 ft/min, both at 75° F. No problems were encountered, and the results are excellent.

The SO-168 film was adjusted in speed from its manufactured level of 160 to 1000; therefore, a substantial modification to the processing technique was required. A high-speed processor (42 ft/min) was used with a modified ME-4 chemistry. The color developer was at 110° F, the first developer at 98° F, the pre-hardener at 95° F, and other chemicals at normal room temperature. The operation was satisfactory, and no problems were encountered.

The 1411 M color Versamat was required for the SO-121 film. The manufacturer's chemistry was modified, however, based on trial emulsion batch. Film speed during processing was 3.2 ft/min. The original flight film was spliced with other films as follows:

a. Scratch test, 10 feet

b. Head leader threads machine, 80 feet

c. Leading edge sensitometry, 3 feet

d. Flight film, 38 feet

e. Trailing edge sensitometry, 3 feet

f. Colormetric, resolution, photogrammetric, sensitometric frisket, 20 feet

g. Trailer, 80 feet

The black-and-white Versamat was used to process the type 3400 film. A special developer and fixer comprised the chemistry. However, since roll C was not normally exposed, a low gamma developer was recommended. During the entire eighth revolution, the lunar surface had been photographed from terminator to terminator at f/5.6 and 1/250 second. A low-gamma developer was formulated and tested in the Precision Laboratory. The resultant gamma was lowered from 1.70 to 0.70. The processed negatives show far more detail and information than the two films processed by conventional means.

Processing techniques for the high-speed type-2485 film were established before flight. A Versamat Model M-11C cycle (standard D-19 developer at 3 ft/min or 150 seconds, two tanks, 95° F) would have produced a gamma of 1.95. A 0.5-base fog rise due to radiation fogging was anticipated.

However, the film was not used for the dim light astronomical experiments, as planned, but for general lunar surface photography, and a film speed of 80 was erroneously assumed, rather than the actual 2000. This difference is about a six-stop overexposure and far beyond the latitude of the film. A special chemistry and processing technique was formulated to preserve the recorded data, but it was discovered that the chemistry could not be changed fast enough to prevent the image from chemically destroying itself. A procedure was developed to use special film reels in a large tank. The process was accomplished at 68° F, including a bleach step to remove the effect of the vastly overexposed silver and produce a more normal negative. The technique proved highly successful and satisfactory images were obtained. The wide-latitude processing could significantly reduce workload on future flight crews by permitting more nearly constant exposure settings.

4.3 PHOTOGRAPHIC RESULTS

Approximately 90 percent of the photographic objectives were achieved, despite the curtailment of photographic activity in the later portion of lunar orbit coast. In general, the stereo and target-of-opportunity photographic results will complement and in many cases improve upon the coverage obtained from Lunar Orbiter. At the end of this section are charts which show all areas of the lunar surface photographed during this mission. The sextant photography of a potential landing site was valuable, particularly from a training standpoint for future crews.

4.3.1 Stereo Strip Photography

The objective of the stereo strip photography was to obtain vertical and oblique stereo photographs with the bracket-mounted still camera and 80-mm lens. These photographs would include the lunar surface from the far-side terminator to about 60 degrees from the near-side terminator. By using the intervalometer, an exposure could be taken every 20 seconds. Each photograph would overlap the previous photograph by approximately 60 percent and allow viewing from photographic positions separated by about 16 n. mi. At an orbital altitude of 60 n. mi., this overlap produces a base-to-height ratio of about 0.27, which is acceptable for stereo viewing. By combining the vertical strip with a second convergent strip, the geometry of the stereo view could be made stronger; hence, the ability to measure height differences would be better by a factor of 2.

The vertical strip photography was accomplished on the fourth and eighth revolutions and extends from the far-side terminator (longitude 150 degrees west) to about 60 degrees from the near-side terminator. The photography is of good quality and appears to have good forward overlap in all areas. An extra exposure was triggered every 5 minutes, but the time was not recorded. By using the fixed interval and fitting to the navigational control points, the scale of the photography can be established and related to the known orbit.

With the two stereo strip exposures, far-side features can be located with respect to control points. Because of the early launch date and termination of both passes at about 90 degrees east, information concerning relative positions between the eastern limb and the Apollo zone will depend on the photography of this region obtained after transearth injection. Both passes included many frames taken with a zero phase angle in the field of view. It is significant that the photometric washout was less than generally expected, and surface detail remains readily apparent. Photographs taken near zero phase indicate that albedo changes of the surface are quite clear at this high sun angle. In most cases, albedo changes correlate with particular structure, and there are indications that the younger features have brighter albedos. Sufficient surface detail is available to permit photogrammetric reconstruction of the surface.

Four magazines of 16-mm color film were taken through the rendezvous window. The coverage generally extends 25 n. mi. to either side of the ground track from terminator to terminator. A review of this film indicates that good surface detail was obtained and that exposures were good.

4.3.2 Photographic Targets of Opportunity

Photographic targets of opportunity were all outside the area of planned lunar stereo-strip photography.

Lists of proposed targets of opportunity were submitted by the following organizations:

a. U.S. Geological Survey; Flagstaff and Menlo Park, Arizona

b. Lunar and Planetary Laboratory, University of Arizona

c. Science and Applications Directorate, Manned Spacecraft Center

The targets were selected to provide either detailed coverage of specific features or broad coverage of areas not adequately covered by Lunar Orbiter IV photographs. Most of the recommended sites were proposed to improve knowledge of areas on the earth-facing hemisphere. Table 4-I briefly describes and locates the targets of opportunities that were taken

during the mission. The majority of these 51 targets were programmed to be taken during the fourth and ninth lunar orbits, in order to have as much of this photography as possible taken during the two planned photographic orbits. The fourth orbit was the planned vertical stereo photography, and the ninth orbit was the planned convergent stereo photography. The loss of photography on the ninth orbit because of flight-plan constraints resulted in some loss of target-of-opportunity photography.

About 60 percent of the targets of opportunity applicable for the Apollo 8 launch date were photographed, as well as many crew-selected targets. Most of the targets photographed are to the south of the ground track because of attitude constraints and camera location.

The crew reported that the preplanned exposure data were satisfactory and that targets, when time was available, could be photographed at a higher rate than had been planned. Most of the targets of opportunity were photographed in the first few revolutions of the moon. Among the more outstanding photographs are the near-full-moon views of the eastern hemisphere. These are centered near Mare Symthii and show that this mare is a circular rather than an irregular feature and includes several resolvable mare units. Other maria in these photographs also display a number of units of varying albedo. The photographs confirm that the Soviet Mountains are non-existent and are most probably rays from the bright-rayed crater Giordano Bruno. The bright-rayed crater that has long been believed to exist near the north pole on the lunar far side was confirmed (fig. 4-2).

4.3.3 Sextant Photography

For this flight, a special adapter allowed the 16-mm sequence camera to be attached to the command module sextant. In this configuration, the camera could record on color film the target centered in the scanning telescope.

Sextant photography was performed over the proposed landing site during the fourth revolution and over the three control points during the fifth revolution navigation exercise. Several sequences of control-point sightings with the sextant were recorded at a frame rate of 6 frames/sec. The effects of brighter surface features seen through the fixed landmark line of sight are clearly displayed. Sequence photography near the proposed landing site compare favorably in resolution and image quality with the still photographs taken through the window.

In summary, sextant photography indicates that landmark identification and tracking will be readily performed on lunar landing missions. Although the sextant photographs near landing site 1 in Mare Tranquillitatis are

underexposed, they provide a qualitative example of how brightness decreases with the change of the phase angle.

During transearth coast, sextant photographs were taken of the moon at about 123 hours and of the earth at 124 hours. Although the range is too great for an accurate horizon analysis, the appearance of the earth through the red tinting of the landmark line of sight should be an effective familiarization aid for future crews.

4.3.4 Comparison With Lunar Orbiter

The Apollo 8 photography complements the extensive coverage of Lunar Orbiter. Lunar Orbiter provided excellent high-resolution photography of the near side of the moon, and Apollo 8 provided excellent coverage of selected areas on the far side. The Apollo 8 photography was taken through the entire range of sun angles, yielding excellent high-sun-angle photographs. The photographs have revealed albedo variations not previously detected and have also revealed many bright-rayed craters ringed with high albedo material. These craters are interspersed among both old and younger craters which have no high albedo rings.

The broad coverage obtained in Apollo 8 photography after transearth injection is free from mosiac effects and local rectification errors inherent in an array of photography such as Lunar Orbiter mosiacs. This is the same effect obtained by using a space photograph of the earth and comparing it with a mosiac of photographs obtained at lower altitudes. These large-area photographs aid significantly in the identification and delineation of regional features.

4.4 CREW OBSERVATIONS

During the lunar orbit phase, the crew described the color of the lunar surface as "black-and-white, absolutely no color" or "whitish gray, like dirty beach sand." The color photographs show a gray surface modified by weak-to-strong overtones of green, brown, or blue. The human eye readily detects intense hues but commonly does not recognize faint hues present in a dark gray surface unless color standards are available for direct comparison. Based on the crew observations, intense color overtones within the area observed are precluded, but there remains a possibility that faint hues modify the dark gray that is typical of the lunar surface. The crew report of the absence of sharp color boundaries is significant, whether the surface color is gray or near gray. The lack of visible contrast from an altitude of 60 n. mi. reduces the probability that a flight crew will be able to use color to distinguish geologic units while operating near or on the lunar surface.

The observation of surface features was somewhat difficult because of window degradation, unfavorable spacecraft attitudes, and conflicting activities when spacecraft attitude was favorable. Near the terminator, topographic details were enhanced by the conspicuous shadows. Within the shadow areas, scattered light permitted the observation of features that cannot be seen on the photographs. The human eye could also detect features on bright slopes that appear washed out in the photographs. It is quite possible that the additional detail can be enhanced by special processing of the photographs.

The crew reported that the terminator was sharp and distinct and that more light than expected was reflected from the smooth surfaces near the terminator (fig. 4-3).

High sun angles enhanced albedo differences, yet reduced the visual ability to detect topographic relief near the subsolar point, as expected. Conspicuous, bright-haloed craters occur in sizes that range downward to the resolution limit. Similar craters probably are distributed somewhat uniformly across the moon, but they are detectable only at the high sun angles. Although topographic relief is difficult to detect at high sun incidence, numerous craters were conspicuous because of their bright walls.

Fault scarps, rilles, and other linear features were described by the crew. Few sinuous rilles were visible, and none were near the ground track. Boulders were observed only at the central peak in crater Tsiolkovsky, where light-colored boulders contrasted sharply with the dark-colored crater fill.

Probable flows were observed on the west wall of a crater located at 163.5 degrees west, 6 degrees south. Photographs confirm the description of features that suggest material flowed from high on the crater rim to a pond on the crater wall (fig. 4-4).

Ray patterns were observed in the highlands only near the subsolar point. On the dark mare surface, rays were detected at much lower sun angles. The crew examined the rays from Messier A in the Sea of Fertility and stated that no depth to the ray material could be observed.

The Command Module Pilot observed what is believed to be zodiacal light and solar corona through the telescope just prior to sunrise on one of the early lunar orbit revolutions. The Lunar Module Pilot visually observed what he described as a cloud or bright area in the sky during lunar darkness on two successive revolutions and sketched the area in his log. By correlating spacecraft attitude and the Lunar Module Pilot's position in the spacecraft, it appears that he was looking near the south celestial pole. A rough correlation of his star sketch was achieved with a star chart. The identification, if correct, indicates that the Lunar Module Pilot visually observed one of the Magellanic clouds.

Although earthshine observations were limited, the crew reported that the peaks and terraced walls of crater Copernicus were clearly visible.

Figures 4-5 through 4-16 are typical examples of the excellent lunar photography obtained during Apollo 8. These figures are not specifically discussed within this section; however, the subtitle on each figure specifies the area photographed and discusses pertinent details.

4.5 LUNAR LIGHTING OBSERVATIONS

In addition to the lighting comments presented in the Crew Observations section, certain conclusions regarding lunar surface lighting as it affects the lunar landing maneuver are pertinent. These conclusions concern two types of lighting constraint: the washout limits, and the operational limits.

The crew observed the magnitude of the washout effect (i.e., surface viewing near the sun line or zero phase angle) to be much less than expected. Although the cone of washout was considered small, required viewing along the sun line should still be avoided.

The operational limits for lunar lighting are influenced on the lower end by the extensive area of shadow coverage and on the higher end by the lack of feature definition because the flight path is below the sun line. Prior to Apollo 8, the lower limit was believed to be practically bound at approximately 6 degrees. The Apollo 8 crew observed surface detail at sun angles in the vicinity of 2 or 3 degrees and stated that these low angles should present no problem for a lunar landing. Landing sites in long shadow areas, however, are to be avoided. At the higher limit, an upper bound of 16 degrees would still provide very good definition of surface features for most of the critical landing phase near touchdown. Between 16 degrees and 20 degrees, lighting was judged acceptable for viewing during final descent. As expected, a sun angle above 20 degrees was considered unsatisfactory for a manual landing maneuver.

4.6 INFORMAL OBSERVATIONS FROM EARTH

4.6.1 Lunar Surveillance

More than 30 professional and 70 private observatories were organized into an international network of lunar observers by the Lunar and Planetary Laboratory at the University of Arizona. A system was instituted for communication of events to network observers and to the Science Support

Room at the Manned Spacecraft Center to support the period of intense lunar surveillance during the Apollo 8 mission. This organization witnessed some significant transient events but because of other conflicts and the secondary nature of the observations, they were not reported to the crew.

4.6.2 Translunar Injection Photography

The Maui, Hawaii, station of the Smithsonian Astrophysical Observatory obtained Baker-Nunn photographs of the J-2 rocket plume at translunar injection. The plume became visible only when the spacecraft came into sunlight during the engine firing. The illumination photographed seems to come from a thin conical surface with its apex at the vehicle. Many lineations are apparent in the plume. The plume covered about 10 degrees in the sky. The photographs spanned about a 2-minute period.

The Baker-Nunn camera at the Spain station of the Smithsonian Astrophysical Observatory obtained about a 2-hour sequence of photographs of the spacecraft, the S-IVB, and the ice cloud resulting from an S-IVB venting. The photographic coverage began about 14 minutes after this venting. The cloud appears to have an expansion velocity in the range of 0.1 to 0.2 km/sec. It grows to an apparent diameter of several hundred kilometers.

TABLE 4-I.- TARGETS-OF-OPPORTUNITY FRAME NUMBERS

Target no.	Name	Location, deg		Frame nos.				
				Magazine A	Magazine B	Magazine C	Magazine D	Magazine E
10	Various targets	020.9 S	161.0 W					2319
11	Basin with pitted plains fill ofloor	002.9 S	162.9 W			2827		
12	Fresh crater with trails of birdsfoot secondaries	009.1 S	164.0 W		2412 - 2415			2244 - 2247 2318
14	12-km central peak in 40-km crater	021.0 S	172.4 W					2320
15	25-km central peak in 85-km crater	004.7 S	173.7 W					
16	18-km central peak in 60-km crater	020.6 S	177.5 W					
19	Patches of 2-km bulbous hills with mare	017.4 S	174.3 E					2322 - 2324
20	15-km young craters on rim of Mendellev	014.1 S	173.5 E					2321
21	Patches of bulbous hills in small crater in mare	027.1 S	173.3 E					
23	Fractured tumescent floor	017.1 S	167.8 E					2325
26	Bulbous hills and ridges in bottom	026.1 S	158.2 E					
28	Mare on floor of 100-km crater and bright crater	019.2 S	147.5 E				2197	2327
29	Fractured tumescent crater floors (2 craters)	004.2 S	146.1 E				2197	
30	Large crater floored by old pitted plains	003.7 N	139.8 E					
31	Tsiolkovsky secondaries	017.3 S	139.2 E				2197	2328
32	Medium age crater	004.1 S	138.4 E				2197, 2198	
33	Medium age crater	002.0 S	138.1 E				2197, 2198	
34	Various crater materials	006.0 N	136.8 E					
35	Medium age crater	010.2 S	135.9 E			2730	2197, 2198	
36	Fractured tumescent crater floor	015.0 S	129.3 E				2197, 2198	2249 - 2251
37	Crater chains	000.3 S	129.5 E				2197, 2198	
38	Dark, probable flows of old crater near Tsiolkovsky	026.9 S	128.5 E				2214	
40	Fractured mare dome and other Tsiolkovsky	020.1 S	128.0 E		2447 - 2451			2248 2252 - 2255
41	Crater chains	005.7 S	128.0 E				2197, 2198	
44	Young crater	017.4 S	122.7 E				2197 - 2199	
45	Soviet Mountains	005.7 S	121.9 E				2198 - 2200	
49	20-km, fairly young crater	020.0 S	116.4 E		2446		2214	2256
51	Bright spot in Luna photographs	000.2 S	107.5 E					

TABLE 4-I.- TARGETS-OF-OPPORTUNITY FRAME NUMBERS - Concluded

Target no.	Name	Location, deg		Frame nos.				
				Magazine A	Magazine B	Magazine C	Magazine D	Magazine E
52	Mare patches and light-dark center	027.2 S	104.0 E		2455 - 2462		2212 - 2214	
54	Probable young crater; probable Sklowdowska Curie	022.3 S	100.3 E				2195, 2213	
55	Very bright small crater	004.8 N	099.8 E					
57	Very bright small crater	008.0 N	096.1 E					
58	Fresh large crater with secondaries	017.9 S	093.7 E				2201, 2189, 2190, 2193	2262 - 2265
59	Mare Smythii ring-craters	002.9 S	083.8 E				2202 - 2205 2207	2331, 2332
63	Crater Behaim, especially central peak	017.0 S	078.4 E				2189, 2193	2268, 2269
64	Very bright crater northwest of La Perouse	010.1 S	074.2 E					
65	Crater Kapteyn	010.5 S	070.6 E				2181, 2182 2203	2270
66	E Crisium rim fill-in for poor Lunar Orbiter IV	015.0 N	068.9 E				2206	
67	S Crisium rim fill-in for poor Lunar Orbiter IV	004.6 N	057.7 E				2204 - 2206	2334 - 2338 2344 - 2350
68	Langrenus; to compare with Copernicus	008.8 S	060.7 E	2613 - 2616			2184, 2203	
71	Petarius B missing rim material	019.1 S	057.4 E					
72	McClure crater cluster	013.4 S	051.4 E					2215 - 2227
80	West of Lubbock Sharp irregular depression and hills	002.2 S	040.0 E			2805 - 2826		2340 - 2343 2257 - 2261
87	Cauchy dome	007.4 N	038.3 E					2244
90	Crater Capella	007.6 S	035.0 E					2228 - 2242

TABLE 4-II.- FILM USED

Type		Camera	ASA speed	Resolution, lines/mm	
				High contrast	Low contrast
368	Color	16-mm 70-mm	64	80	35
3400	Black & white	70-mm	[a]40	170	65
121	Color	70-mm	50	160	70
2485	Black & white	70-mm	[b]2000	55	20
SO-168	Color	16-mm	[c]160	80	36

[a]Manufacturer quotes ASA of 80.

[b]Special process can boost speed up to 8000.

[c]Special process can boost speed up to 1000.

NASA-S-69-606

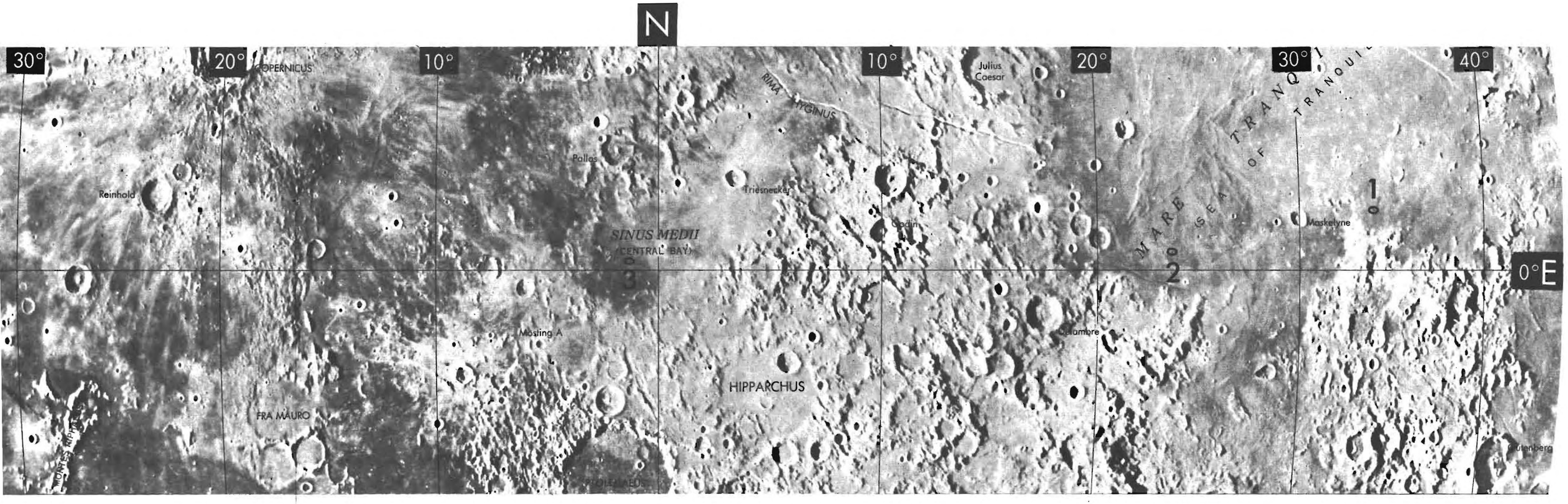

Figure 4-1.- Apollo landing sites.

NASA-S-69-606

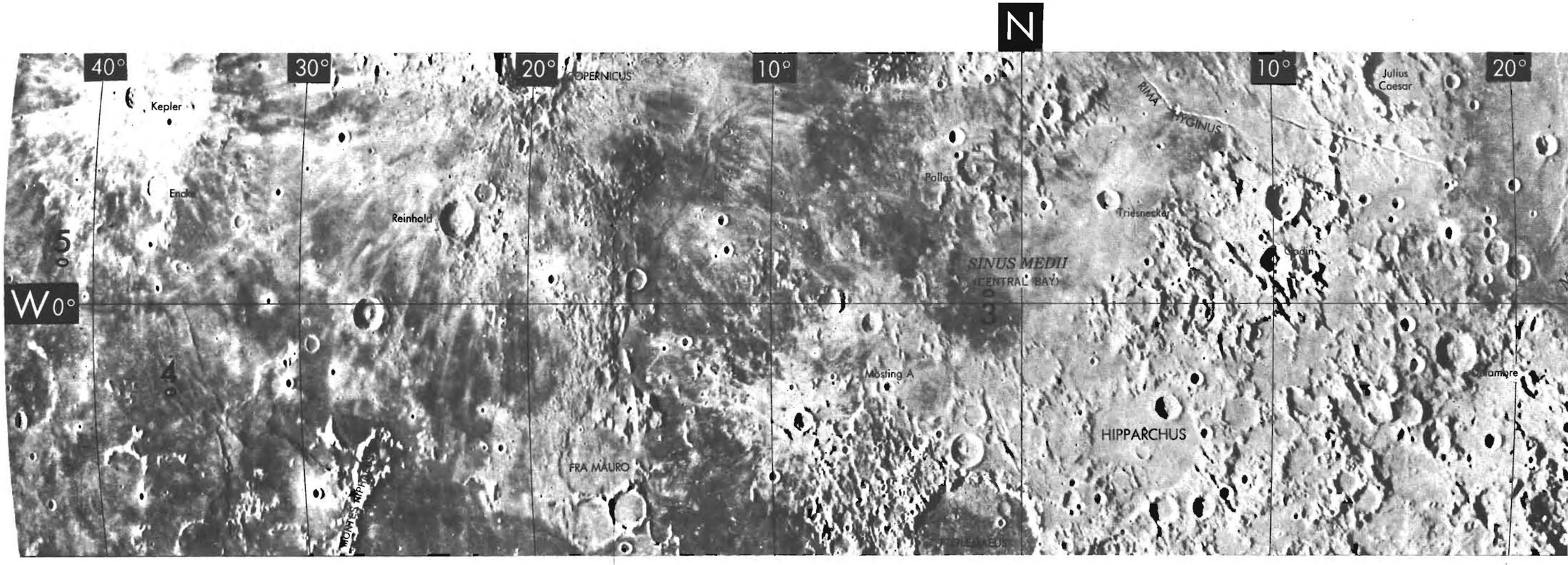
N
40°
30°
20°
10°
10°
20°
W0°
Kepler
Encke
Reinhold
OPERNICUS
Pallas
RIMA
BYGINUS
Julius
Caesar
Triesnecker
Godin
SINUS MEDII
(CENTRAL BAY)
Mösting A
Delambre
HIPPARCHUS
FRA MAURO
WOLF'S RIFT
5
4
3

NASA-S-69-607

The crater Joliot Curie, about 110 statute miles in diameter and centered near 94 degrees east, 27 degrees north, is near the center of the left side. The bright-rayed crater near the horizon probably is located near 105 degrees east, 45 degrees north. Long, narrow rays that have been reported in the polar region of the earth-facing hemisphere may radiate from this crater. The dark-bottomed crater is Lomonosou, which is approximately 50 statute miles in diameter.

Figure 4-2.- High-altitude oblique view looking northeasterly.

NASA-S-69-608

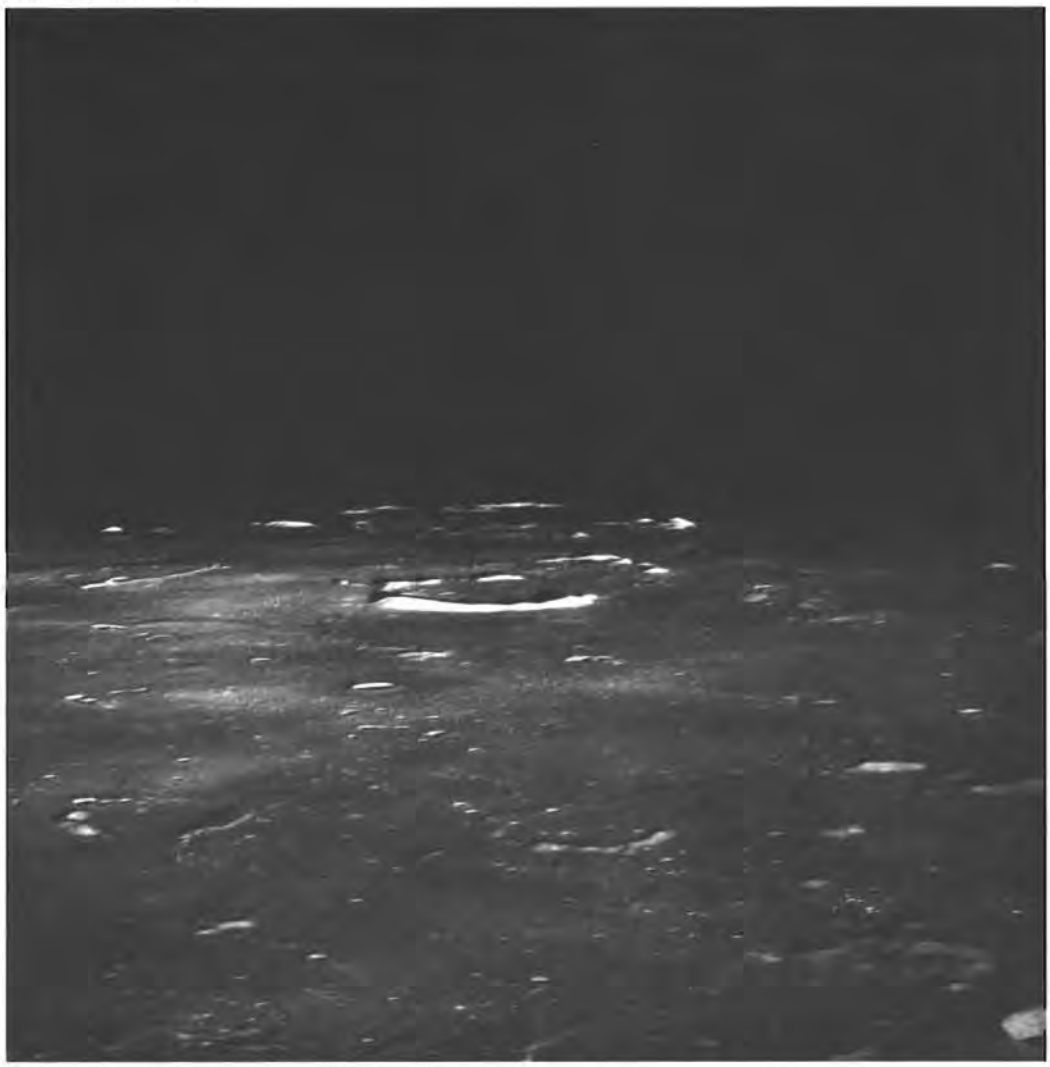

The feature at the center in Maskelyne F, and the crater in the lower right corner is Tauruntius F. The distance between these features in about 90 statute miles. The terminator is near the horizon, as evidenced by light reflected from only high ridges, making them appear to be suspended.

Figure 4-3.- Oblique view looking west across the Sea of Tranquility.

NASA-S-69-609

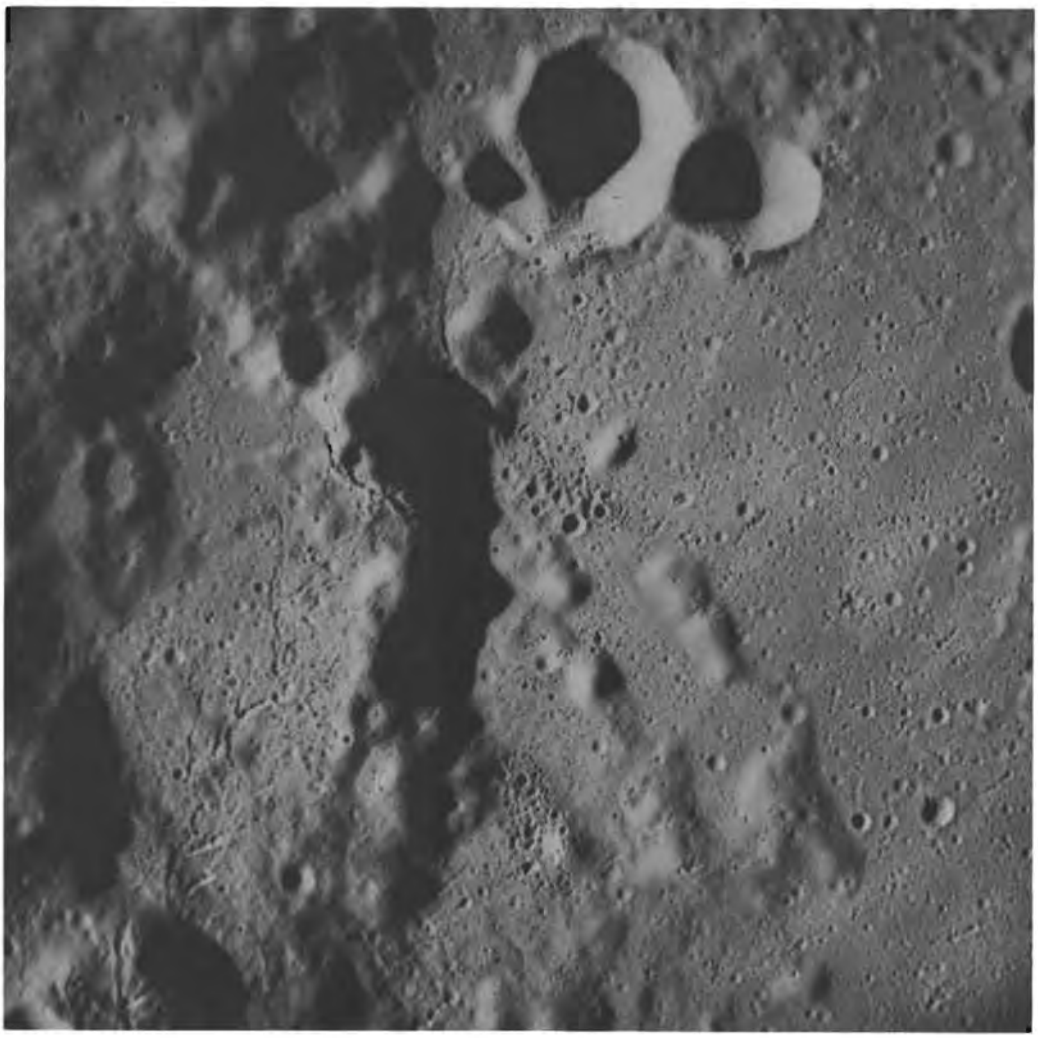

The floor of crater with possible flows was described by the Lunar Module Pilot. The feature is located 163.5 degrees west longitude and 6 degrees south latitude.

Figure 4-4.- Near-vertical view of large crater.

NASA-S-69-610

This unnamed crater, located at 11 degrees south latitude, 164.5 degrees west longitude, has a diameter of about 28 statute miles, has an irregular shape, and appears creased on the crater walls.

Figure 4-5.- Oblique view of a crater on the far side of the moon.

NASA-S-69-611

The photographed area is approximately 20 by 20 statute miles. It is located on the far side of the moon and within a crater about 100 statute miles in diameter. The crater is at 10 degrees south latitude and 160 degrees east longitude.

Figure 4-6.- Near-vertical view taken with a telephoto lens.

NASA-S-69-612

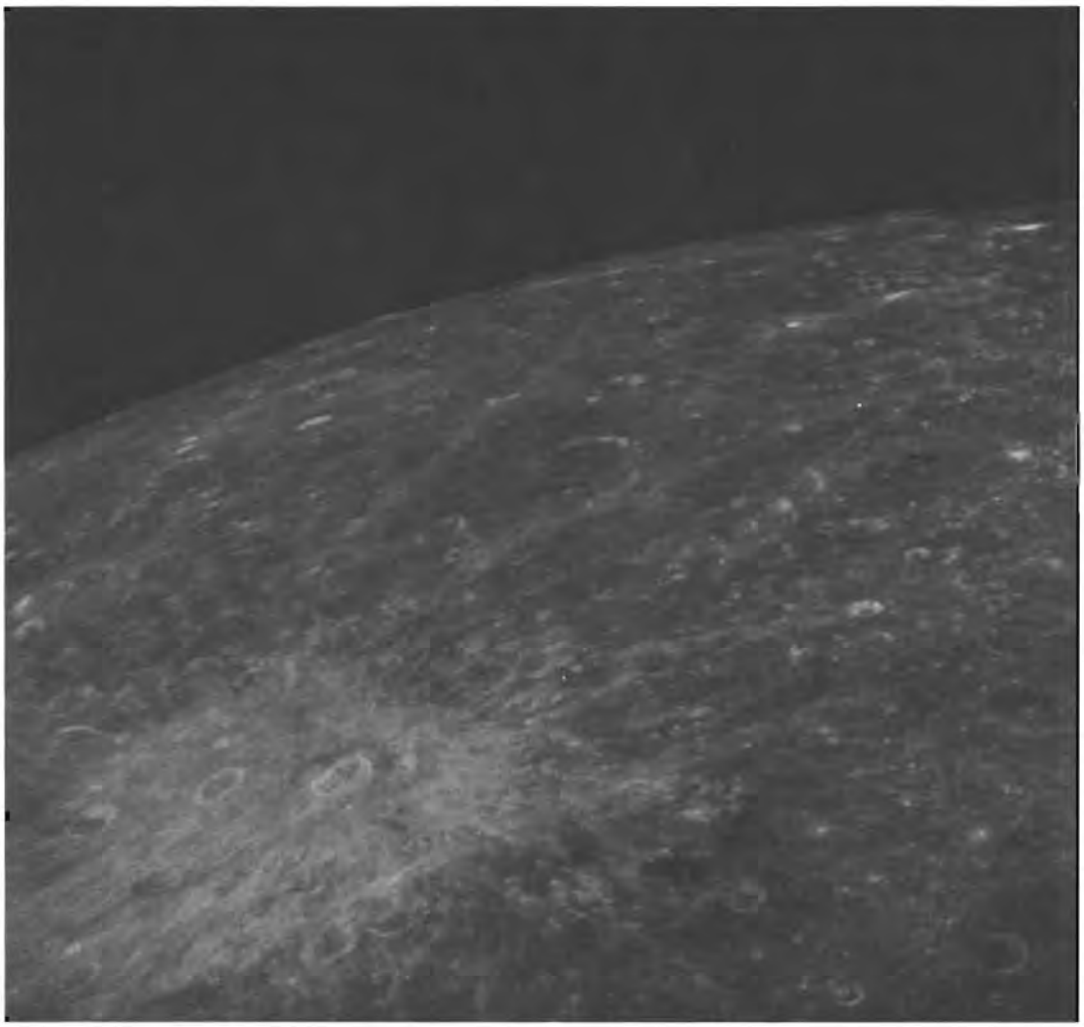

None of the features are named, but the crater Tsiolkovsky is just out of view to the right. The bright crater to the lower left is approximately 55 statute miles in diameter.

Figure 4-7.- An eastward view of the far side.

NASA-S-69-613

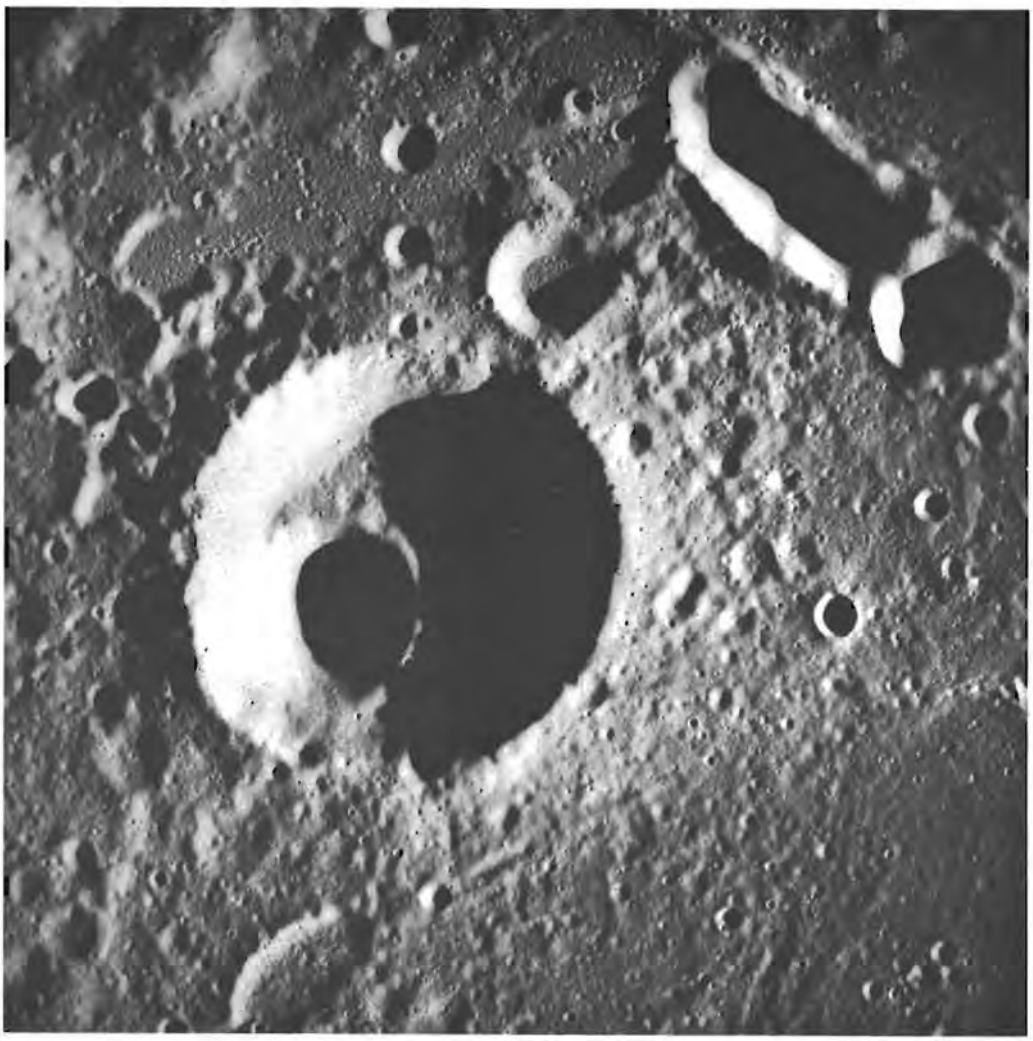

None of the features in this frame have been named; however, the key-hole shaped crater was used for crew tracking training. The large crater is approximately 20 statute miles in diameter. Note the range in sizes of craters visible at the low (7 degrees) sun angle.

Figure 4-8.- A near-vertical view of the far side.

NASA-S-69-614

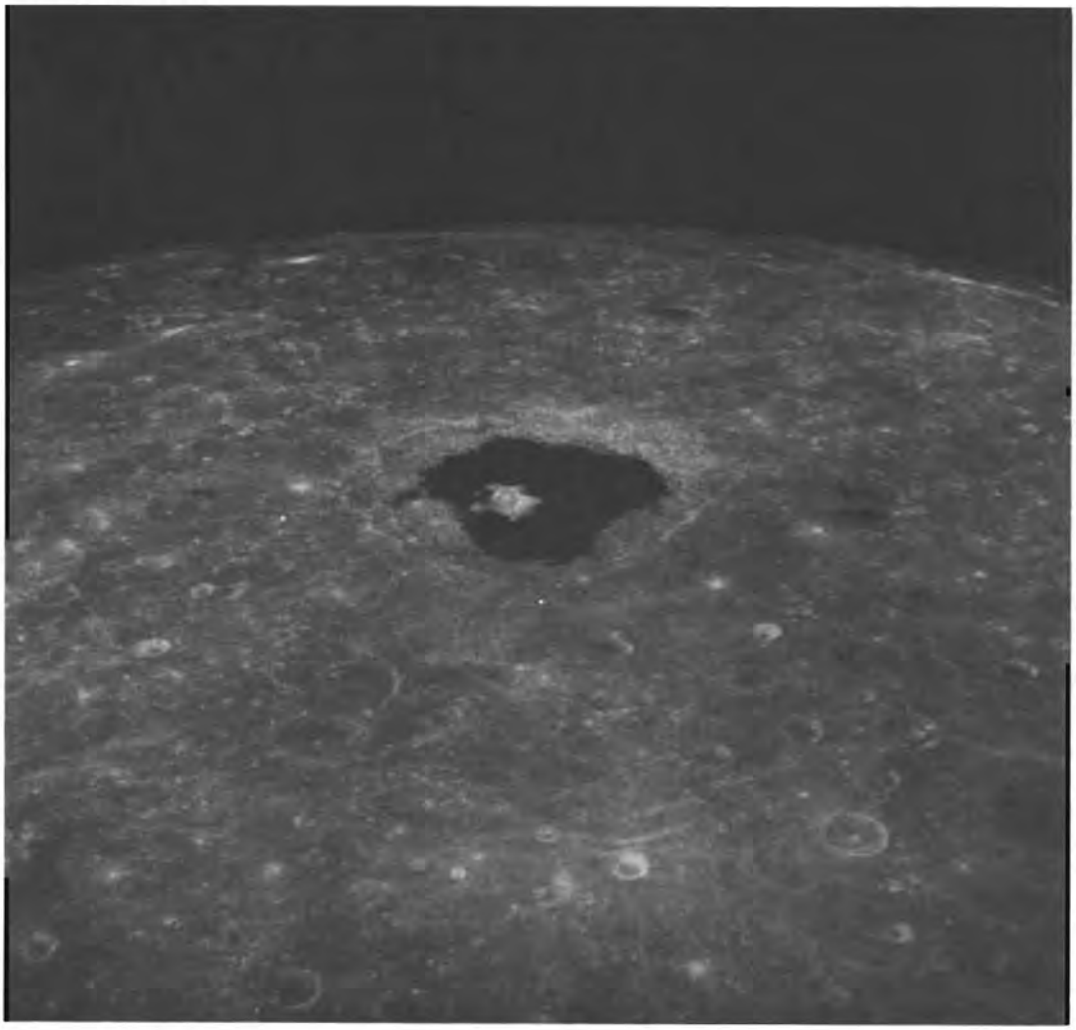

The crater Tsiolkovsky near the center is 94 statute miles in diameter and is located at 129 degrees east, 21 degrees south.

Figure 4-9.- Oblique view eastward across the lunar surface from about 115 degrees east to the horizon near 180 degrees longitude.

NASA-S-69-615

The Mare Symthii is the dark area at the right center. Crater Humboldt is 150 statute miles in diameter and is located at the bottom center. Crater Langrenus is located at the center near the horizon. Numerous rays and light material are visible throughout photograph.

Figure 4-10.- Eastward view of moon.

NASA-S-69-616

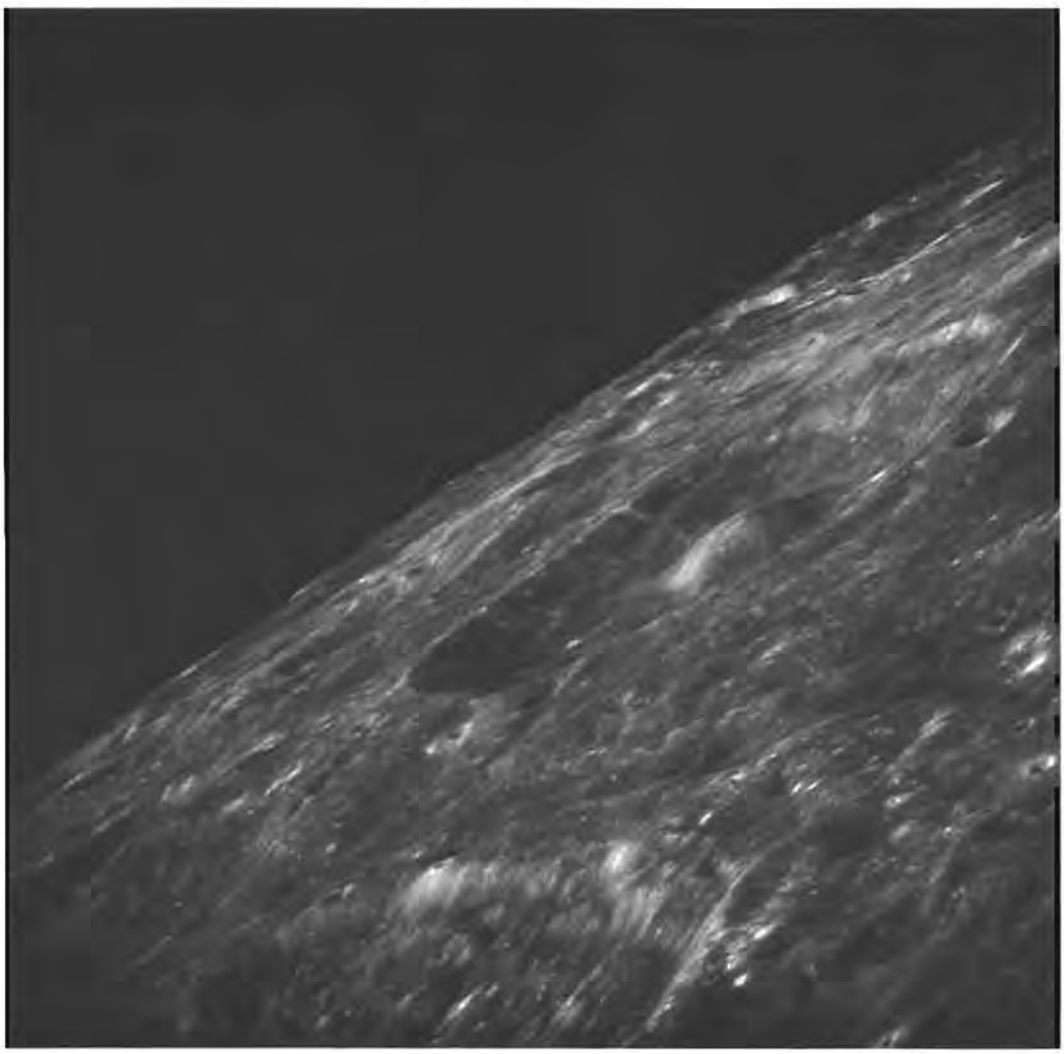

Behaim is located at 79 degrees east, 18 degrees south. Partially visible in the foreground is the rim of the crater La Perouse, and the edge of crater Angarius is on the left. Behaim has a smooth dome at the center and is approximately 35 statute miles in diameter. Crater Gibbs is located beyond Behaim on the horizon to the left.

Figure 4-11.- Oblique view of crater Behaim.

NASA-S-69-617

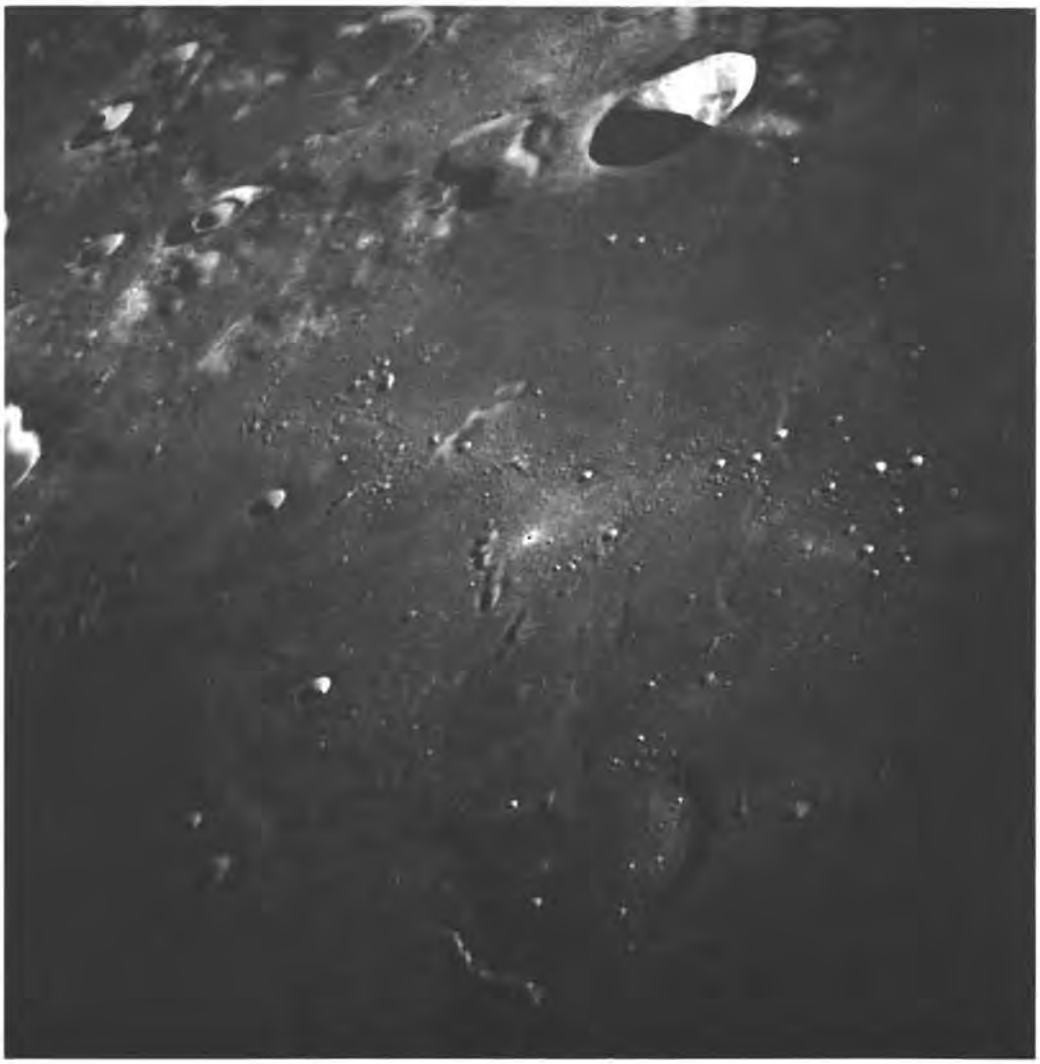

The larger crater at the top is Bellot, about 13 statute miles in diameter. The interesting double crater to the upper left is Bellot B. A small bright ray crater in the Sea of Fertility near the center is less than 1 statute mile in diameter and is located near a small crater chain.

Figure 4-12.- Oblique view looking south near the crater Colombo at the Sea of Fertility.

NASA-S-69-618

Figure 4-13.- Oblique view looking southwest toward the crater Gibbs with earthrise over the lunar horizon.

NASA-S-69-619

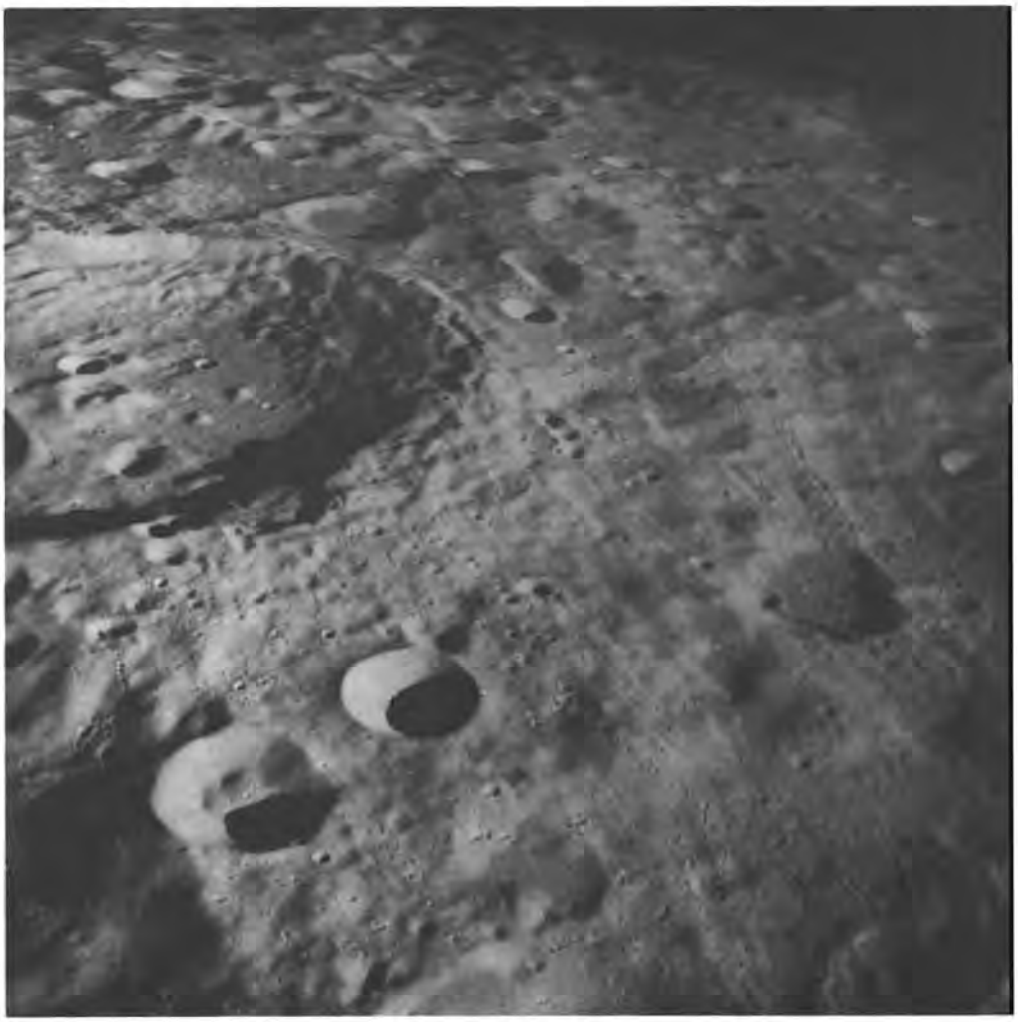

This southward view at 162 degrees west longitude shows rugged terrain characteristic of the lunar far-side hemisphere. The large crater at the left side is about 70 statute miles in diameter and is centered about 125 statute miles south of the spacecraft. The sharp circular crater in the foreground is about 9 statute miles wide. Conspicuous surface lineations that extend from the lower right corner of the photograph toward the upper left resemble a radial texture observed near Mare Orientale on Lunar Orbiter IV photographs. The lineations in the area probably are related to another major crater because the observed trend is not radial to Mare Orientale.

Figure 4-14.- Southward view across a large far-side crater.

NASA-S-69-620

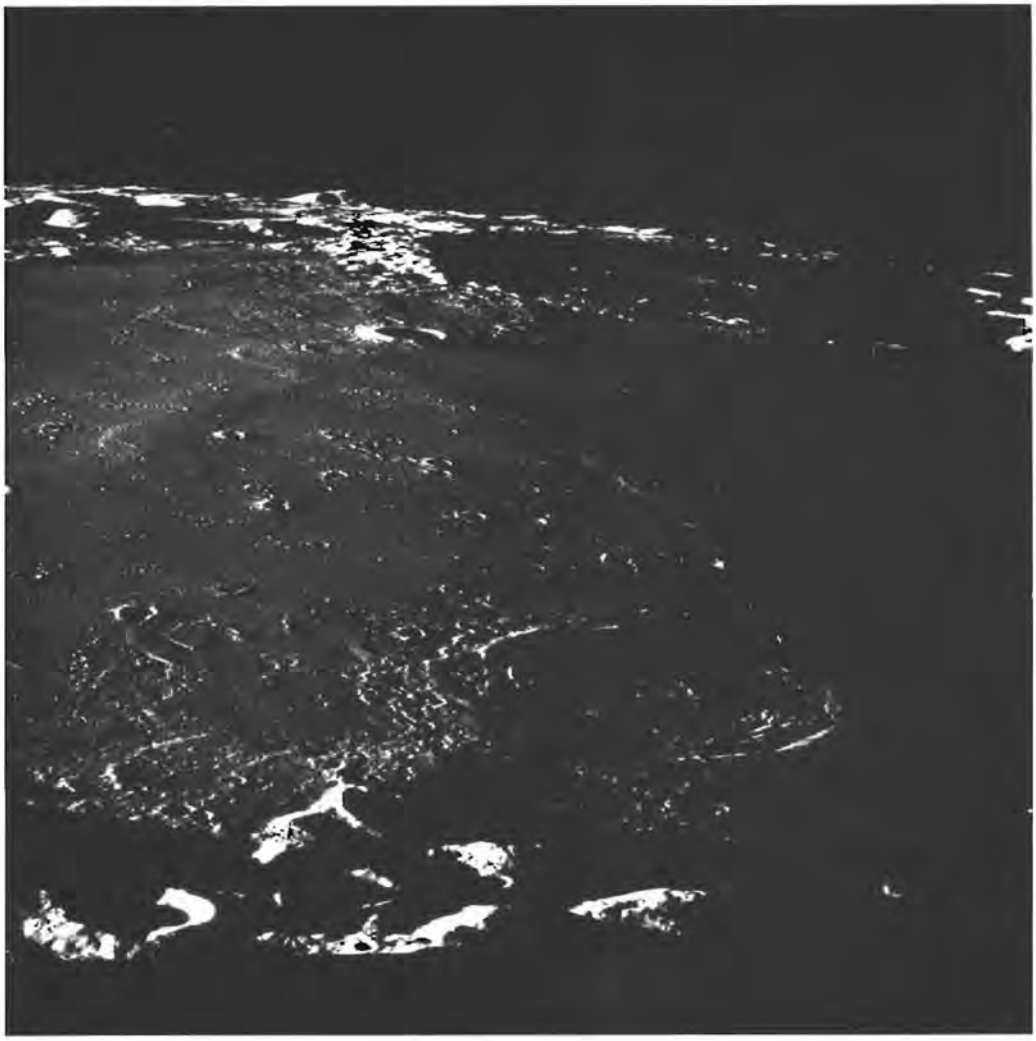

The crater Fracastorius is the large crater on the horizon. The shallow crater in the foreground surrounded by the Sea of Nectar is Daguerre which is about 27 statute miles in diameter. The peak visible on the horizon is about 270 statute miles from crater Daguerre.

Figure 4-15.- Oblique view looking south across the Sea of Nectar at the crater Fracastorius.

NASA-S-69-621

The Pyrennes Mountains can be seen in the center background at the top edge. The large crater Goclenius in the foreground lies on the southern edge of the Sea of Fertility and measures approximately 45 statute miles in diameter. The numerous rilles scarring the floor of Goclenius can be seen, one of which extends across the entire width of the crater floor, over the central peak, and across the rim into the smooth Mare.

Figure 4-16.- Oblique view looking south near crater Colombo.

NASA-S-69-622

Figure 4-17.- View of earth from approximately 200 000 statute miles, as seen through telephoto lens following the transearth injection maneuver.

PREPARED UNDER THE DIRECTION OF THE DEPARTMENT OF DEFENSE BY THE AERONAUTICAL CHART AND INFORMATION CENTER, UNITED STATES AIR FORCE FOR THE NATIONAL AERONAUTICS AND SPACE ADMINISTRATION.

EDITION 2, 4 FEBRUARY 1969
Lithographed by ACIC 2-69

180
165W
150W
135W
120W
105W
90W
30S
15S
15N
30N

2685
2076
2688
2062
2675
2082
2669
2664
2052
2659
2046

EASTERN SEA

ROOK MOUNTAINS

SCHLÜTER

D'ALEMBERT MOUNTAINS

HARTWIG

BOHR

EINSTEIN

MOSELEY

DALTON

VASCO DA GAMA

BALBOA

CORDED

EASTERN SEA

90W

ROOK MOUNTAINS

SCHLÜTER

D'ALEMBERT MOUNTAINS

EINSTEIN

MOSELEY

90W

BOHR

DALTON

VASCO DA GAMA

BALBOA

30S

CORDED MOUNTAINS

15S

HARTWIG

15N

30N

EICHSTÄDT

STRUVE

OLBERS

RUSSELL

75W

RICCIOLI

ROCCA

KRAFFT

EDDINGTON

75W

LAGRANGE

CARDANUS

DARWIN

BYRGIUS

BYRGIUS RILLE

Crüger

HEVELIUS

CAVALERIUS

Seleucus

GRIMALDI

Sirsalis

60W

SIRSALIS RILLE

60W

Schiaparelli

VIETA

Reiner

Cavendish

Hansteen

Billy

Marius

OCEAN OF STORMS

Herodotus

SCHRÖTER'S VALLEY

MERSENIUS

Aristarchus

45W

Flamsteed

45W

Prinz

DOPPELMAYER

LETRONNE

SEA OF MOISTURE

Lee

GASSENDI

Vitello

Kepler

Encke

30S

15S

15N

30N

Delisle

Hippalus

30W

30W

Euler

CAMPANUS

MERCATOR

RIPHAEN MOUNTAINS

KNOWN SEA

Lansberg

CARPATHIAN MOUNTAINS

BULLIALDUS

Reinhold

Pytheas

SEA OF RAINS

Lambert

COPERNICUS

FRA MAURO

15W

SEA OF CLOUDS

15W

PITATUS

Guericke

Stadius

Eratosthenes

Timocharis

STRAIGHT WALL

SEETHING BAY

Mosting

Mosting A

ALPHONSUS

APENNINE MOUNTAINS

CHIMEDES

REGIOMONTANUS

PURBACH

ARZACHEL

PTOLEMAEUS

Pallas

MARSH OF DECAY

0

0

Autolycus

ALBATEGNIUS

HIPPARCHUS

Triesnecker

SEA OF VAPORS

LIACENSIS

APIANUS

HYGINUS RILLE

MERCATOR PROJECTION
APPROXIMATE SCALE 1:7,500,000 AT THE EQUATOR

FRA MAURO
15W
SEA OF CLOUDS
PITATUS
Guericke
Stadius
Eratosthenes
Timocharis
STRAIGHT WALL
Mösting
Mösting A
SEETHING BAY
APENNINE MOUNTAINS
APPROXIMATE SCALE 1:7,500,000 AT THE EQUATOR
MERCATOR PROJECTION
CHIMEDES
MARSH OF DECAY
Autolycus
REGIOMONTANUS
PURBACH
ARZACHEL
ALPHONSUS
PTOLEMAEUS
Pallas
0
Triesnecker
SEA OF VAPORS
ALBATEGNIUS
HIPPARCHUS
HYGINUS RILLE
APIANUS
Manilius
HAEMUS MOUNTAINS
ABULFEDA
ARIADAEUS RILLE
JULIUS CAESAR
15E
SEA OF SERENITY
DELAMBRE
WILKINS
30 S
15S
15N
30N
CATHARINA
CYRILLUS
Plinius
THEOPHILUS
POSIDONIUS
30E
PICCOLOMINI
FRACASTORIUS
SEA OF NECTAR
Vitruvius
SEA OF TRANQUILITY
Le Monnier
Chacornac
Maraldi
TAURUS MOUNTAINS
PYRENEES
MOUNTAINS
GUTENBERG
SANTBECH
Newcomb
45E
MARSH OF SLEEP
COLOMBO
SEA OF FERTILITY
TARUNTIUS
MACROBIUS
Picard
SNELLIUS
CLEOMEDES
60E
PETAVIUS
VENDELINUS
LANGRENUS
SEA OF CRISES
Apollonius
Firmicus
LAMÉ
FOAMING SEA
30S
15S
30N
ADAMS
2796
SEA OF WAVES
CONDORCET
LEGENDRE
BALMER
Kapteyn
HAHN
75E
2780
La Pérouse
GILBERT
KÄSTNER
Behaim
2728
HECATAEUS
ANSGARIUS
2805
PLUTARCH
HUMBOLDT
Gibbs
NEPER
BORDER SEA
BARNARD
2772
SMYTH'S SEA
GODDARD
HUBBLE
Jansky

APOLLO MISSION 8
LUNAR PHOTOGRAPHY INDEX

SHEET 1 OF 4

STEREOGRAPHIC STRIP (70mm)

Magazine C

Magazine D

HAHN

PLUTARCH

HUBBLE

Liapunov

RAYLEIGH

JOLIOT-CURIE

Lomonosov

SEA OF MOSCOW

BORDER SEA

NEPER

GODDARD

Jonsky

GILBERT

KÄSTNER

ANSGARIUS

SMYTH'S SEA

Lo Pacuvius

Baboim

HECATAEUS

Gibbs

HUMBOLDT

BARNARD

TSIOLKOVSKY

75E 90E 105E 120E 135E 150E 165E 180

30N 15N 30S 15S

2789 2778 2785 2172 2165 2158 2146 2140 2135 2122 2117 2111 2088 2085

PREPARED UNDER THE DIRECTION OF THE DEPARTMENT OF DEFENSE BY THE
AERONAUTICAL CHART AND INFORMATION CENTER, UNITED STATES
AIR FORCE FOR THE NATIONAL AERONAUTICS AND SPACE ADMINISTRATION.

EDITION 2, 4 FEBRUARY 1969
Lithographed by ACIC 2-69

180
165W
150W
135W
120W
105W
90W
30S
15S
15N
30N

EASTERN SEA

ROOK MOUNTAINS

SCHLÜTER

HARTWIG

D'ALEMBERT MOUNTAINS

BOHR

EINSTEIN

MOSELEY

DALTON

VASCO DA GAMA

BALBOA

CORDED

EASTERN SEA

90W

ROOK MOUNTAINS

SCHLÜTER

D'ALEMBERT MOUNTAINS

EINSTEIN

MOSELEY

BOHR

DALTON

VASCO DA GAMA

BALBOA

90W

30S

CORDED MOUNTAINS

15S

HARTWIG

15N

30N

EICHSTÄDT

OLBERS

STRUVE

RUSSELL

75W

RICCIOLI

ROCCA

KRAFFT

EDDINGTON

CARDANUS

LAGRANGE

DARWIN

BYRGIUS

BYRGIUS RILLE

Crüger

GRIMALDI

HEVELIUS

CAVALERIUS

Seleucus

60W

Sirsalis

SIRSALIS RILLE

Schiaparelli

VIETA

Reiner

Cavendish

Hansteen

Billy

Marius

Herodotus

SCHRÖTER'S VALLEY

OCEAN OF STORMS

MERSENIUS

Aristarchus

45W

Flamsteed

Prinz

DOPPELMAYER

LETRONNE

Lee

SEA OF MOISTURE

GASSENDI

Vitello

30S

15S

Kepler

Encke

15N

30N

Delisle

Hippalus

30W

RIPHAEN MOUNTAINS

Euler

CAMPANUS

MERCATOR

KNOWN SEA

Lansberg

CARPATHIAN MOUNTAINS

BULLIALDUS

Reinhold

Pytheas

SEA OF RAINS

Lambert

COPERNICUS

FRA MAURO

15W

SEA OF CLOUDS

Guericke

Stadius

Timocharis

PITATUS

Eratosthenes

STRAIGHT WALL

SEETHING BAY

Mösting

Mösting A

ALPHONSUS

CHIMEDES

REGIOMONTANUS

PURBACH

ARZACHEL

PTOLEMAEUS

Pallas

APENNINE MOUNTAINS

MARSH OF DECAY

0

0

Autolycus

ALBATEGNIUS

HIPPARCHUS

Triesnecker

SEA OF VAPORS

ALIACENSIS

APIANUS

HYGINUS RILLE

Manilius

MERCATOR PROJECTION
APPROXIMATE SCALE 1:7,500,000 AT THE EQUATOR

FRA MAURO
15W
SEA OF CLOUDS
PITATUS
Guericke
Stadius
Eratosthenes
Timocharis
STRAIGHT WALL
Mösting
Mösting A
SEETHING BAY
APENNINE MOUNTAINS
APPROXIMATE SCALE 1:7,500,000 AT THE EQUATOR
MERCATOR PROJECTION
CHIMEDES
ALPHONSUS
REGIOMONTANUS
PURBACH
ARZACHEL
PTOLEMAEUS
Pallas
MARSH OF DECAY
0
Autolycus
Triesnecker
SEA OF VAPORS
ALBATEGNIUS
HIPPARCHUS
HYGINUS RILLE
ALIACENSIS
APIANUS
Manilius
HAEMUS MOUNTAINS
ABULFEDA
ARIADAEUS RILLE
JULIUS CAESAR
15E
DELAMBRE
SEA OF SERENITY
WILKINS
30 S
15S
15N
30N
CATHARINA
CYRILLUS
Plinius
LINDENAU
THEOPHILUS
POSIDONIUS
30E
Vitruvius
Le Monnier
PICCOLOMINI
FRACASTORIUS
SEA OF NECTAR
SEA OF TRANQUILITY
Chacornac
Maraldi
TAURUS MOUNTAINS
PYRENEES
MOUNTAINS
GUTENBERG
SANTBECH
MARSH OF SLEEP
Newcomb
45E
COLOMBO
SEA OF FERTILITY
TARUNTIUS
MACROBIUS
Picard
SNELLIUS
CLEOMEDES
SEA OF CRISES
60E
PETAVIUS
VENDELINUS
LANGRENUS
Apollonius
LAME
Firmicus
FOAMING SEA
30S
15S
30N
ADAMS
SEA OF WAVES
CONDORCET
LEGENDRE
BALMER
Kapteyn
HAHN
75E
La Pérouse
GILBERT
KÄSTNER
Behaim
HECATAEUS
ANSGARIUS
PLUTARCH
HUMBOLDT
Gibbs
NEPER
BORDER SEA
BARNARD
SMYTH'S SEA
GODDARD
Jansky
HUBBLE

APOLLO MISSION 8
LUNAR PHOTOGRAPHY INDEX

SHEET 2 OF 4
SEQUENCE PHOTOGRAPHY (16mm)

Magazine H
Magazine I
Magazine J
Magazine K
Magazine Q

HAHN
PLUTARCH
HUBBLE
Liapunov
RAYLEIGH
JOLIOT-CURIE
Lomonosov
SEA OF MOSCOW
BORDER SEA
NEPER
GODDARD
Jonsky
GILBERT
KASTNER
ANSGARIUS
SMYTH'S SEA
HECATAEUS
Babbage
HUMBOLDT
Gibbs
BARNARD
TSIOLKOVSKY
75E
90E
105E
120E
135E
150E
165E
180
30N
15N
15S
30S

PREPARED UNDER THE DIRECTION OF THE DEPARTMENT OF DEFENSE BY THE
AERONAUTICAL CHART AND INFORMATION CENTER, UNITED STATES
AIR FORCE FOR THE NATIONAL AERONAUTICS AND SPACE ADMINISTRATION.

EDITION 2, 4 FEBRUARY 1969
Lithographed by ACIC 2-69

180
165W
150W
135W
120W
105W
90W
30S
15S
15N
30N

2423
2422
2421
2420
2419
2417
2416
2418
2415
2412
2414
2413
2411
2410
2409
2408
2407
2406
2405
2404
2403
2402
2401
2400
2399
2398
2397
2836
2835
2834
2831
2830
2829
2828
2833
2832

EASTERN SEA
ROOK MOUNTAINS
SCHLÜTER
D'ALEMBERT MOUNTAINS
HARTWIG
CORDED
EINSTEIN
MOSELEY
BOHR
DALTON
VASCO DA GAMA
BALBOA

EASTERN SEA

90W

ROOK MOUNTAINS

SCHLÜTER

D'ALEMBERT MOUNTAINS

EINSTEIN

MOSELEY

90W

BOHR

DALTON

VASCO DA GAMA

BALBOA

30S

CORDED MOUNTAINS

15S

HARTWIG

15N

30N

EICHSTÄDT

OLBERS

STRUVE

RUSSELL

75W

RICCIOLI

75W

ROCCA

KRAFFT

EDDINGTON

LAGRANGE

CARDANUS

DARWIN

BYRGIUS

BYRGIUS RILLE

Crüger

HEVELIUS

CAVALERIUS

Seleucus

GRIMALDI

Sirsalis

60W

SIRSALIS RILLE

60W

Schiaparelli

VIETA

Reiner

Cavendish

Hansteen

Billy

Marius

Herodotus

SCHRÖTER'S VALLEY

OCEAN OF STORMS

MERSENIUS

Aristarchus

45W

Flamsteed

45W

Prinz

DOPPELMAYER

LETRONNE

Lee

SEA OF MOISTURE

GASSENDI

Vitello

Kepler

30S

15S

Encke

15N

30N

Delisle

Hippalus

30W

30W

Euler

CAMPANUS

MERCATOR

RIPHAEN MOUNTAINS

KNOWN SEA

Lansberg

CARPATHIAN MOUNTAINS

BULLIALDUS

Reinhold

SEA OF RAINS

Pytheas

Lambert

COPERNICUS

FRA MAURO

15W

SEA OF CLOUDS

15W

Guericke

Stadius

Timocharis

PITATUS

Eratosthenes

STRAIGHT WALL

SEETHING BAY

Mösting

Mösting A

ALPHONSUS

APENNINE MOUNTAINS

CHIMEDES

REGIOMONTANUS

PURBACH

ARZACHEL

PTOLEMAEUS

Pallas

MARSH OF DECAY

0

0

Autolycus

Triesnecker

SEA OF VAPORS

ALBATEGNIUS

HIPPARCHUS

HYGINUS RILLE

ALIACENSIS

APIANUS

Manilius

MERCATOR PROJECTION
APPROXIMATE SCALE 1:7,500,000 AT THE EQUATOR

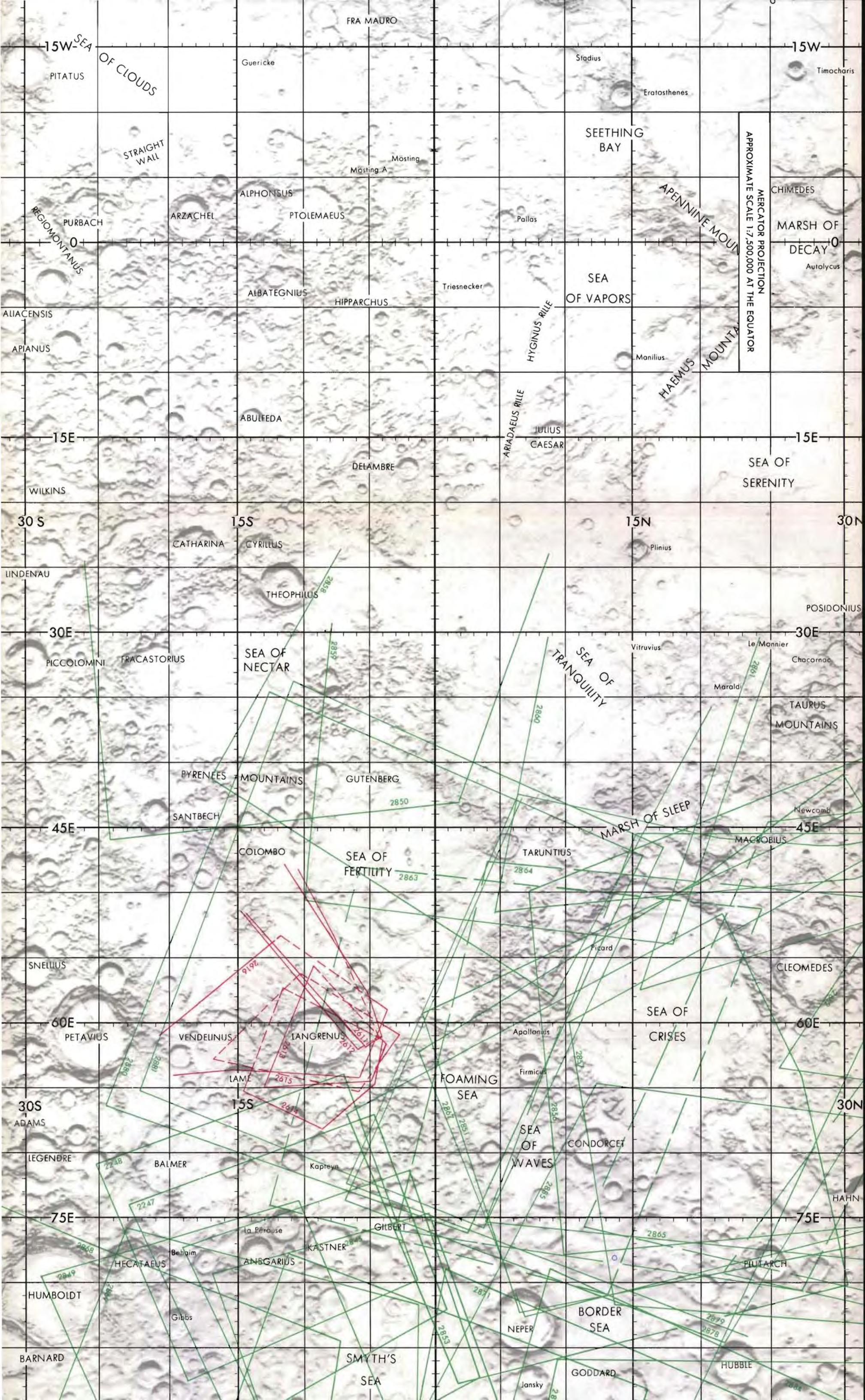
FRA MAURO
15W
SEA OF CLOUDS
PITATUS
Guericke
Stadius
Eratosthenes
Timocharis
STRAIGHT WALL
Mösting
Mösting A
SEETHING BAY
APENNINE MOUNTAINS
MERCATOR PROJECTION
APPROXIMATE SCALE 1:7,500,000 AT THE EQUATOR
CHIMEDES
MARSH OF DECAY
Autolycus
ALPHONSUS
PTOLEMAEUS
ARZACHEL
PURBACH
REGIOMONTANUS
Pallas
0
Triesnecker
SEA OF VAPORS
ALBATEGNIUS
HIPPARCHUS
ALIACENSIS
APIANUS
HYGINUS RILLE
Manilius
HAEMUS MOUNTAINS
ABULFEDA
ARIADAEUS RILLE
IULIUS CAESAR
15E
DELAMBRE
SEA OF SERENITY
WILKINS
30 S
15S
15N
30N
CATHARINA
CYRILLUS
Plinius
LINDENAU
THEOPHILUS
2858
POSIDONIUS
30E
PICCOLOMINI
FRACASTORIUS
SEA OF NECTAR
2859
Vitruvius
SEA OF TRANQUILITY
Le Monnier
Chacornac
Maraldi
2861
2860
TAURUS MOUNTAINS
PYRENEES MOUNTAINS
GUTENBERG
2850
SANTBECH
MARSH OF SLEEP
Newcomb
45E
MACROBIUS
COLOMBO
SEA OF FERTILITY
2863
TARUNTIUS
2864
Picard
SNELLIUS
CLEOMEDES
2616
60E
PETAVIUS
VENDELINUS
LANGRENUS
SEA OF CRISES
Apollonius
2880
2881
LAME
2615
2614
Firmicus
2852
FOAMING SEA
30S
15S
30N
ADAMS
2867
2851
2856
SEA OF WAVES
CONDORCET
LEGENDRE
BALMER
Kapteyn
2248
2247
2885
HAHN
75E
La Pérouse
GILBERT
2865
2868
Behaim
KÄSTNER
2849
HECATAEUS
ANSGARIUS
PLUTARCH
2849
HUMBOLDT
2871
Gibbs
BORDER SEA
2879
2878
NEPER
2853
BARNARD
SMYTH'S SEA
GODDARD
HUBBLE
Jansky

APOLLO MISSION 8
LUNAR PHOTOGRAPHY INDEX

SHEET 3 OF 4

TARGETS OF OPPORTUNITY (70mm)

Magazine A

Magazine B

Magazine G

PREPARED UNDER THE DIRECTION OF THE DEPARTMENT OF DEFENSE BY THE AERONAUTICAL CHART AND INFORMATION CENTER, UNITED STATES AIR FORCE FOR THE NATIONAL AERONAUTICS AND SPACE ADMINISTRATION.

EDITION 2, 4 FEBRUARY 1969
Lithographed by ACIC 2-69

180
165W
150W
135W
120W
105W
90W
30S
15S
15N
30N

2320
2247
2246
2245
2318
2244
2317
2319
2827
2316
2310
2311
2312
2313
2314
2315
2044

EASTERN SEA

ROOK MOUNTAINS
SCHLÜTER
HARTWIG
D'ALEMBERT MOUNTAINS
BOHR
EINSTEIN
MOSELEY
DALTON
VASCO DA GAMA
BALBOA
CORDED

EASTERN SEA

90W

ROOK MOUNTAINS

SCHLÜTER

D'ALEMBERT MOUNTAINS

EINSTEIN

MOSELEY

90W

BOHR

DALTON

VASCO DA GAMA

BALBOA

30S

CORDED MOUNTAINS

15S

HARTWIG

15N

30N

EICHSTÄDT

STRUVE

OLBERS

RUSSELL

75W

RICCIOLI

ROCCA

KRAFFT

EDDINGTON

75W

LAGRANGE

DARWIN

CARDANUS

BYRGIUS

BYRGIUS RILLE

Crüger

GRIMALDI

HEVELIUS

CAVALERIUS

Seleucus

Sirsalis

60W

SIRSALIS RILLE

60W

Schiaparelli

VIETA

Reiner

Cavendish

Hansteen

Billy

Marius

Herodotus

SCHRÖTER'S VALLEY

MERSENIUS

OCEAN OF STORMS

Aristarchus

45W

Flamsteed

Prinz

45W

DOPPELMAYER

LETRONNE

Lee

SEA OF MOISTURE

GASSENDI

Vitello

Kepler

30S

15S

Encke

15N

30N

Delisle

Hippalus

30W

RIPHAEN MOUNTAINS

Euler

30W

CAMPANUS

MERCATOR

KNOWN SEA

Lansberg

BULLIALDUS

Reinhold

CARPATHIAN MOUNTAINS

SEA OF RAINS

Pytheas

Lambert

COPERNICUS

FRA MAURO

15W

SEA OF CLOUDS

15W

Guericke

Stadius

Timocharis

PITATUS

Eratosthenes

STRAIGHT WALL

SEETHING BAY

Mösting

Mösting A

ALPHONSUS

APENNINE MOUNTAINS

CHIMEDES

REGIOMONTANUS

PURBACH

ARZACHEL

PTOLEMAEUS

Pallas

MARSH OF DECAY

0

0

Autolycus

Triesnecker

SEA OF VAPORS

ALBATEGNIUS

HIPPARCHUS

ALIACENSIS

HYGINUS RILLE

APIANUS

Manilius

MERCATOR PROJECTION
APPROXIMATE SCALE 1:7,500,000 AT THE EQUATOR

FRA MAURO
COPERNICUS
15W
SEA OF CLOUDS
PITATUS
Guericke
Stadius
Eratosthenes
Timocharis
STRAIGHT WALL
Mösting
Mösting A
SEETHING BAY
APENNINE MOUNTAINS
APPROXIMATE SCALE 1:7,500,000 AT THE EQUATOR
MERCATOR PROJECTION
CHIMEDES
REGIOMONTANUS
PURBACH
ARZACHEL
ALPHONSUS
PTOLEMAEUS
Pallas
MARSH OF DECAY
Autolycus
0
ALBATEGNIUS
HIPPARCHUS
Triesnecker
SEA OF VAPORS
HYGINUS RILLE
APIANUS
Manilius
HAEMUS MOUNTAINS
ABULFEDA
ARIADAEUS RILLE
JULIUS CAESAR
15E
DELAMBRE
SEA OF SERENITY
WILKINS
30 S
15S
CATHARINA
CYRILLUS
15N
Plinius
30N
LINDENAU
THEOPHILUS
POSIDONIUS
30E
PICCOLOMINI
FRACASTORIUS
SEA OF NECTAR
TRANQUILLITY
Vitruvius
Le Monnier
Chacornac
Maraldi
TAURUS MOUNTAINS
PYRENEES
MOUNTAINS
GUTENBERG
SANTBECH
MARSH OF SLEEP
Newcomb
45E
COLOMBO
SEA OF FERTILITY
TARUNTIUS
MACROBIUS
Picard
SNELLIUS
CLEOMEDES
60E
PETAVIUS
VENDELINUS
LANGRENUS
Apollonius
SEA OF CRISES
LAME
FOAMING SEA
Firmicus
30S
15S
30N
ADAMS
SEA OF WAVES
CONDORCET
LEGENDRE
BALMER
Kapteyn
HAHN
75E
La Pérouse
GILBERT
KÄSTNER
Behaim
HECATAEUS
ANSGARIUS
PLUTARCH
HUMBOLDT
Gibbs
BORDER SEA
NEPER
BARNARD
SMYTH'S SEA
GODDARD
HUBBLE
Jansky

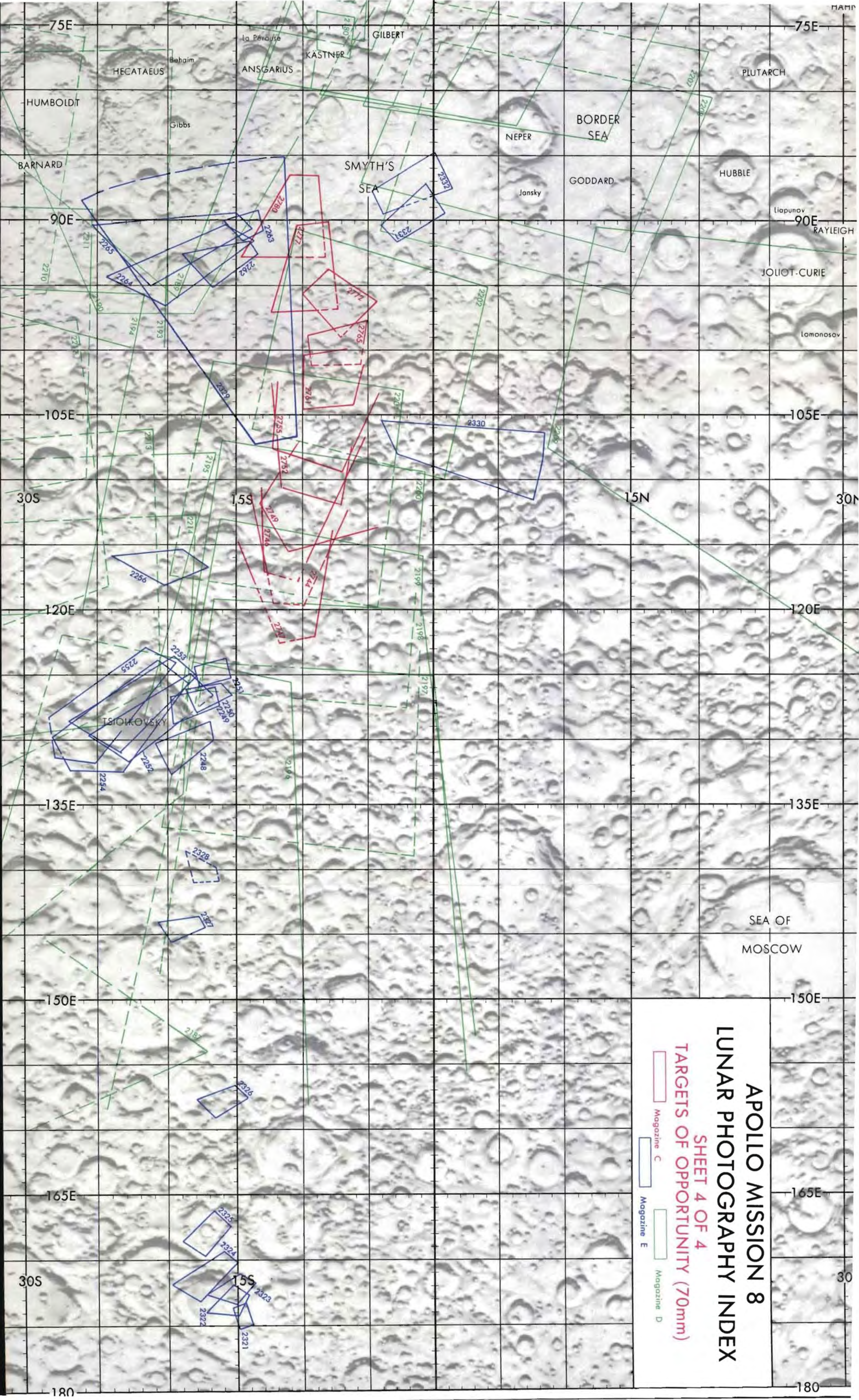
APOLLO MISSION 8
LUNAR PHOTOGRAPHY INDEX
SHEET 4 OF 4
TARGETS OF OPPORTUNITY (70mm)
Magazine C
Magazine E
Magazine D
75E
90E
105E
120E
135E
150E
165E
180
30S
15S
15N
30N
HUMBOLDT
HECATAEUS
Behaim
Gibbs
BARNARD
La Pérouse
ANSGARIUS
KÄSTNER
GILBERT
PLUTARCH
NEPER
BORDER SEA
SMYTH'S SEA
GODDARD
Jansky
HUBBLE
Liapunov
RAYLEIGH
JOLIOT-CURIE
Lomonosov
TSIOLKOVSKY
SEA OF MOSCOW

5.0 TRAJECTORY

The Marshall Space Flight Center (MSFC) provided the trajectory data for the phase from lift-off to spacecraft/S-IVB separation, and a detailed analysis of these data is presented in reference 1. The actual spacecraft trajectories are based on Manned Space Flight Network (MSFN) data reduced and analyzed after the mission. For the analysis, the earth model was a Fischer ellipsoid and contained gravitational constants for the spherical harmonics, and the moon model was a sphere and contained gravitational constants for the triaxial potential. The trajectory and orbital parameters are defined in table 5-I.

5.1 LAUNCH PHASE

The S-IC stage trajectory was essentially nominal (fig. 5-1). Mach 1 occurred at 0:01:01 at an altitude of 24 128 feet, within 1 second and 91 feet of the planned conditions. A maximum dynamic pressure of 777 lb/sq ft occurred at 0:01:18.9 and was 3.1 seconds later than predicted. The times for S-IC center and outboard engine cutoff were within 2.5 seconds of the planned times. At outboard engine cutoff, velocity was high by 41 ft/sec, and flight-path angle and altitude were low by 1.12 degrees and 3246 feet, respectively.

The S-II stage trajectory was nominal (fig. 5-1). The launch escape tower was jettisoned at 0:03:08.6, within 1.5 seconds of the predicted time. S-II stage engine cutoff was 2.8 seconds later than the predicted time. At S-II cutoff, velocity and flight-path angle were high by 35 ft/sec and 0.24 degree, respectively, and altitude was low by 4606 feet.

The small trajectory deviations resulting from the powered flight of the S-IC and S-II stages converged during the S-IVB stage flight, and the trajectory followed the predicted profile. S-IVB engine cutoff was within 1 second of the planned time. At cutoff, velocity was high by 1 ft/sec, flight-path angle was nominal, and altitude was low by only 97 feet.

5.2 EARTH PARKING ORBIT

The spacecraft/S-IVB was inserted into an earth parking orbit at 0:11:35; the conditions are shown in table 5-II, and a ground track in figure 5-2. Before preparations were begun for S-IVB restart, the parking orbit was perturbed by liquid oxygen venting through the J-2

engine. This expected perturbation increased apogee by 6.4 n. mi. between insertion and S-IVB reignition. The increase, however, was only 0.7 n. mi. greater than predicted. The S-IVB restart preparation phase began at 2:40:59.5, which was 0.7 second later than that predicted, and table 5-II shows the conditions for this event.

5.3 TRANSLUNAR INJECTION

The S-IVB engine was ignited at 2:50:37 and resulted in a nominal translunar injection maneuver (fig. 5-3). The time of ignition was within 0.5 second of the predicted time. Engine cutoff was at 2:55:56, with translunar injection arbitrarily assumed to be 10 seconds later to account for tail-off and other transient effects. Table 5-II presents the conditions for this phase. The pericynthion solution resulting from the maneuver is presented in table 5-III.

The command and service module was separated from the S-IVB at 3:20:59, and the crew practiced station-keeping with the S-IVB. At 3:40:01, a 1.1-ft/sec separation maneuver was performed prior to injecting the S-IVB into a solar orbit. The S-IVB/spacecraft separation distance did not appear to be increasing as rapidly as the crew expected; consequently, an additional separation maneuver (7.7 ft/sec) was performed at 4:45:01 to increase the separation rate before the S-IVB maneuver. The pericynthion solutions resulting from the two separation maneuvers are shown in table 5-III.

5.4 TRANSLUNAR MIDCOURSE CORRECTIONS

The translunar trajectory is shown in figure 5-4. Because of acceptable guidance errors, only two of the planned four translunar midcourse corrections were required. The first was made at 11:00:00 and was calculated to be a 2.4-second, 24.8-ft/sec service propulsion maneuver to satisfy the pericynthion target conditions; however, a velocity change of only 20.4 ft/sec was achieved because the thrust was less than expected. (Cutoff for service propulsion maneuvers from 1 to 6 seconds is based on firing time rather than velocity. Further discussion is contained in section 6.9.) The second midcourse correction was made at 60:59:55 and was a 1.4-ft/sec, 11.8-second reaction control maneuver. The ignition and cutoff conditions for the two midcourse corrections are presented in table 5-II, and the resulting pericynthion conditions are shown in table 5-III.

5.5 LUNAR ORBIT INSERTION

A 2997-ft/sec, 246.9-second service propulsion maneuver, performed at 69:08:20, 75.6 n. mi. above the lunar surface, placed the spacecraft in a lunar orbit of 168.5 by 60.0 n. mi. to achieve the desired velocity change. The engine firing time was about 4 seconds longer than expected because of somewhat low thrust characteristics (see section 6.11). About two revolutions later, at 73:35:07, the elliptical lunar orbit was circularized to 60.7 by 59.7 n. mi. The firing time and the resultant velocity change for the lunar orbit circularization maneuver were 9.6 seconds and 134.8 ft/sec, respectively. The moon-referenced conditions for these two service propulsion maneuvers are presented in table 5-II. A lunar ground track for revolutions 1 and 10 is shown in figure 5-5.

5.6 TRANSEARTH INJECTION

Perturbation in the lunar gravitational field continuously changed the spacecraft orbit, and the final lunar orbit was 63.6 by 58.6 n. mi. The transearth injection maneuver was performed with the service propulsion system at the planned time of 89:19:17 at the end of 10 orbital revolutions. The required velocity change of 3519 ft/sec was achieved in 203.7 seconds; however, the reaction control plus X translation added an additional 3.5 ft/sec. The propagated entry interface conditions resulting from this maneuver are presented in table 5-IV.

5.7 TRANSEARTH MIDCOURSE CORRECTION

The trajectory that resulted from the transearth injection maneuver was nearly perfect, and only one of three planned midcourse corrections was required. The slight correction was performed with the reaction control system at 103:59:54 to decrease the inertial velocity by 4.8 ft/sec. The entry interface solution for this maneuver is shown in table 5-IV. The trajectory conditions for transearth injection and the third midcourse correction are shown in table 5-II.

5.8 ENTRY

The planned and actual entry trajectories are shown in figure 5-6. The actual was generated by correcting the guidance and navigation accelerometer data for known errors in the inertial measurement unit. The actual conditions at entry interface are presented in table 5-V.

The entry interface velocity and flight-path angle were only 1 ft/sec faster and 0.02 degree steeper, respectively, than planned. The peak load factor was 6.84g.

The guidance and navigation system indicated a 2.1-n. mi. overshoot at drogue deployment; the postflight reconstructed trajectory indicates a 0.9-n. mi. overshoot at drogue deployment.

Although no radar tracking data for the service module were available during entry, photographic coverage information correlates well with the predicted trajectory in altitude, latitude, longitude, and time.

5.9 TRAJECTORY ANALYSIS

Tracker performance was excellent, with only a few minor problems that had been anticipated before the mission. Two significant perturbations encountered in real time and after the flight affected orbit determination. First, water dumps and boiloff from the environmental control system evaporator disrupted the orbit determination during the translunar and transearth coasts. After each venting period, about 8 hours of tracking data were necessary to provide the Real Time Computer Complex with sufficient velocity information for accurate orbit determination.

Second, during lunar orbit, the lack of knowledge of the lunar potential function was evident in the Doppler tracking data. The data obtained during the 10 lunar revolutions will be used to minimize this problem for future near-moon orbits.

5.10 LUNAR ORBIT DETERMINATION

The real-time orbit determination technique developed for the lunar orbit phase was based on an analysis of Lunar Orbiter III low-altitude data. This technique, using a triaxial moon model, involved processing of tracking data during each separate orbital pass. The resultant solutions for each pass during the mission indicated that pericynthion altitude was decreasing and apocynthion altitude was increasing, both at a rate of approximately 0.3 n. mi. per revolution.

An estimate of propagation errors is determined by comparing position information obtained during the period of interest with the predicted position based on processing of previous tracking data. This comparison in spacecraft position as a function of time is a good measure of the propagation errors using an inexact representation of lunar gravity. For example, an orbit solution for revolution 3 was integrated forward using

the triaxial moon model and compared with the solution based on the processing of revolution 4 data. Figure 5-7 shows the radial and downrange errors in predicting revolution 3 data forward to both revolutions 4 and 5. Similar behavior was noted in comparisons of data during later orbit determination solutions.

The errors observed are approximately twice those indicated from the analysis of Lunar Orbiter results. While these errors did not significantly affect Apollo 8 targeting, uncertainties of this magnitude could influence targeting for a lunar landing. Therefore, an intensive analysis is being performed using other representations of the lunar gravity field and modified processing techniques to reduce these errors to an acceptable level for the lunar landing mission. The results of this analysis will be published as a supplemental report.

TABLE 5-I.- DEFINITION OF TRAJECTORY AND ORBITAL PARAMETERS

Trajectory parameter	Definition
Geodetic latitude	Spacecraft position measured north or south from the earth equator to the local vertical vector, deg
Selenographic latitude	Spacecraft position measured north or south from the true lunar equatorial plane to the local vertical vector, deg
Altitude	Perpendicular distance from the reference body to the point of orbit intersect, ft
Space-fixed velocity	Magnitude of the inertial velocity vector referenced to the body-centered, inertial reference coordinate system, ft/sec
Space-fixed flight-path angle	Flight-path angle measured positive upward from the body-centered, local horizontal plane to the inertial velocity vector, deg
Space-fixed heading angle	Angle of the projection of the inertial velocity vector onto the local body-centered, horizontal plane, measured positive eastward from north, deg
Apogee	Maximum altitude above the oblate earth model, n. mi.
Perigee	Minumum altitude above the oblate earth model, n. mi.
Pericynthion	Minimum altitude above the moon model, n. mi.
Period	Time required for spacecraft to complete 360 degrees of orbit rotation, min

TABLE 5-II.- TRAJECTORY PARAMETERS

Event	Ref. body	Time, hr:min:sec	Latitude, deg	Longitude, deg	Altitude, n. mi.	Space-fixed velocity, ft/sec	Space-fixed flight-path angle, deg	Space-fixed heading angle, deg E of N
Launch Phase								
S-IC center engine cutoff	Earth	0:02:05.9	28.72N	80.19W	22.4	6 214	24.53	76.57
S-IC outboard engine cutoff	Earth	0:02:33.8	28.85N	79.73W	35.5	8 900	20.70	75.39
S-II engine cutoff	Earth	0:08:44.0	31.72N	65.39W	103.4	22 379	0.65	81.78
S-IVB engine cutoff	Earth	0:11:25.0	32.63N	54.06W	103.3	25 562	0.00	88.10
Parking Orbit								
Parking orbit insertion	Earth	0:11:35.0	32.65N	53.20W	103.3	25 567	0.00	88.53
S-IVB restart preparation	Earth	2:40:59.5	11.67S	162.41E	105.3	25 562	0.04	59.38
Translunar Injection								
S-IVB ignition	Earth	2:50:37.1	9.25N	166.55W	106.4	25 558	0.02	58.64
S-IVB cutoff	Earth	2:55:55.5	21.12N	144.79W	179.3	35 532	7.44	67.16
Translunar injection	Earth	2:56:05.5	21.48N	143.02W	187.1	35 505	7.90	67.49
Spacecraft/S-IVB separation	Earth	3:20:59	25.86N	66.23W	3 797.8	24 975	45.11	107.12
Translunar Midcourse Corrections								
First midcourse correction								
Ignition	Earth	10:59:59.5	1.70S	123.74W	52 768.4	8 187	73.82	120.65
Cutoff	Earth	11:00:01.9	1.71S	123.75W	52 771.7	8 172	73.75	120.54
Second midcourse correction								
Ignition	Moon	60:59:55	14.09N	44.96W	21 064.5	4 101	-84.41	-86.90
Cutoff	Moon	61:00:07.8	14.09N	44.97W	21 059.2	4 103	-84.41	-87.01
Lunar Orbit								
Lunar orbit insertion								
Ignition	Moon	69:08:20.4	7.46S	163.98W	76.6	8 391	-6.43	-123.79
Cutoff	Moon	69:12:27.3	9.89S	179.56E	62.0	5 458	-0.79	-117.13
Lunar orbit circularization								
Ignition	Moon	73:35:07	11.61S	160.29E	59.3	5 479	-0.03	-110.18
Cutoff	Moon	73:35:16	11.66S	159.79E	60.7	5 345	-0.02	-110.18

TABLE 5-II.- TRAJECTORY PARAMETERS - Concluded

Event	Ref. body	Time, hr:min:sec	Latitude, deg	Longitude, deg	Altitude, n. mi.	Space-fixed velocity, ft/sec	Space-fixed flight-path angle, deg	Space-fixed heading angle, deg E of N
Transearth								
Transearth injection								
Ignition	Moon	89:19:16.6	9.27S	174.78E	60.2	5 342	-0.16	-118.59
Cutoff	Moon	89:22:40.3	11.17S	160.19E	66.1	8 842	5.10	-115.00
Third midcourse correction								
Ignition	Earth	103:59:54	5.67S	57.27W	165 561.5	4 299	-80.59	52.65
Cutoff	Earth	104:00:08	5.67S	57.33W	167 552.0	4 298	-80.60	52.65

TABLE 5-III.- PERICYNTHION ARRIVAL CONDITIONS

[Based on best estimate trajectory vectors]

Maneuver	Time of nearest approach, hr:min:sec	Pericynthion altitude, n. mi.
Translunar injection	69:13:58	-130.2
First separation maneuver	69:01:03	0.8
Second separation maneuver	68:57:40	458.1
First midcourse correction	69:10:40	66.3
Second midcourse correction	69:10:39	65.8

TABLE 5-IV.- ENTRY INTERFACE CONDITIONS

[Based on best estimate trajectory vectors]

Maneuver	Velocity, ft/sec	Flight-path angle, deg
Transearth injection	36 221.1	-6.117
Third midcourse correction	36 221.2	-6.395

TABLE 5-V.- ENTRY TRAJECTORY PARAMETERS

Entry interface (400 000 feet)	
Time, hr:min:sec	146:46:12.8
Geodetic latitude, deg north	20.83
Longitude, deg west	179.89
Altitude, n. mi.	65.90
Space-fixed velocity, ft/sec	36 221
Space-fixed flight-path angle, deg	-6.50
Space-fixed heading angle, deg east of north	121.57
Maximum conditions	
Velocity, ft/sec	36 303
Acceleration, g	6.84
Drogue deployment	
Time, hr:min:sec	146:54:48
Geodetic latitude, deg north	
Recovery ship report	8.125
Best estimate trajectory	8.100
Onboard guidance	8.100
Target	8.133
Longitude, deg west	
Recovery ship report	165.020
Best estimate trajectory	165.013
Onboard guidance	165.012
Target	165.033

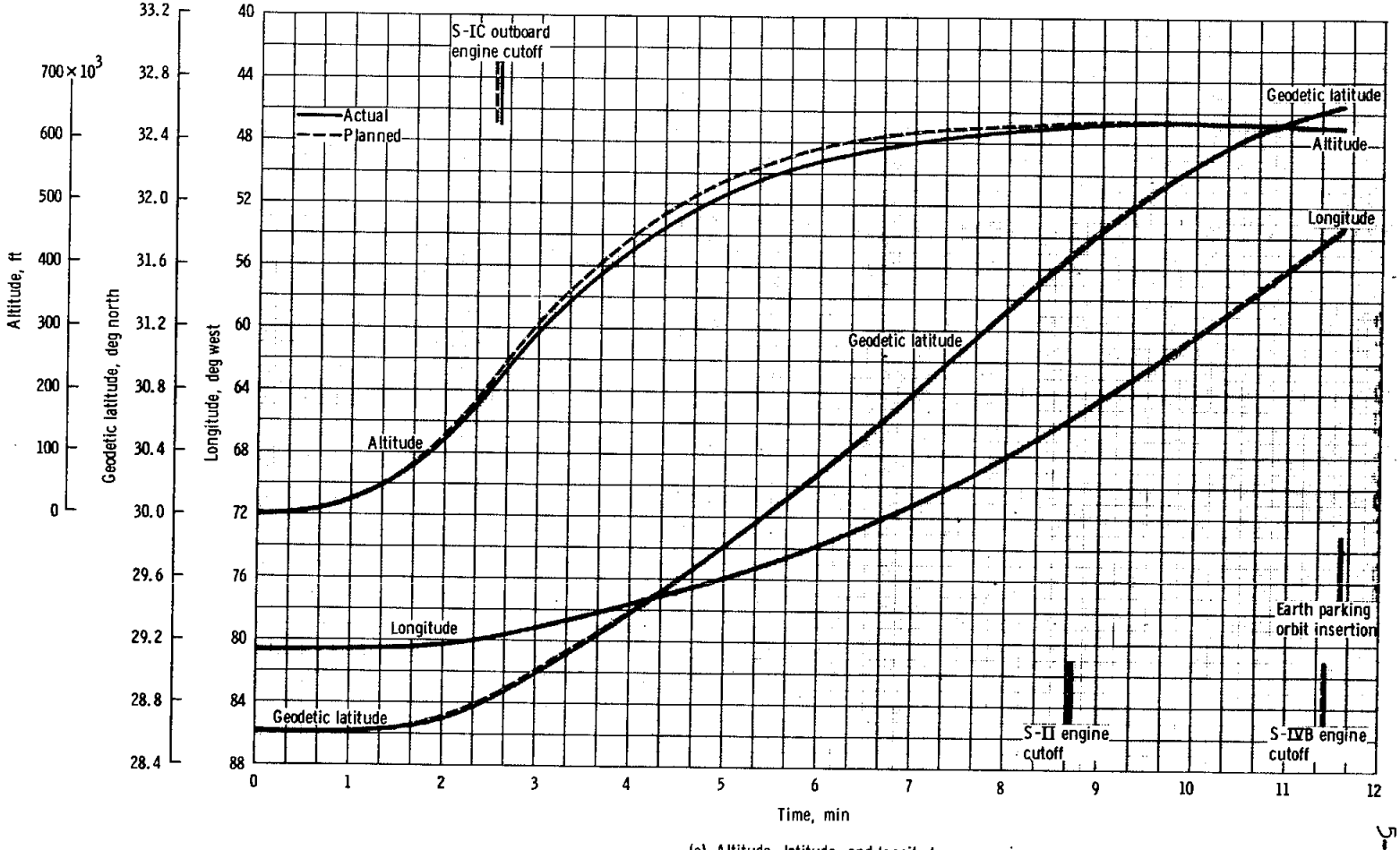

(a) Altitude, latitude, and longitude.

Figure 5-1. - Trajectory parameters during launch phase.

NASA-S-69-624

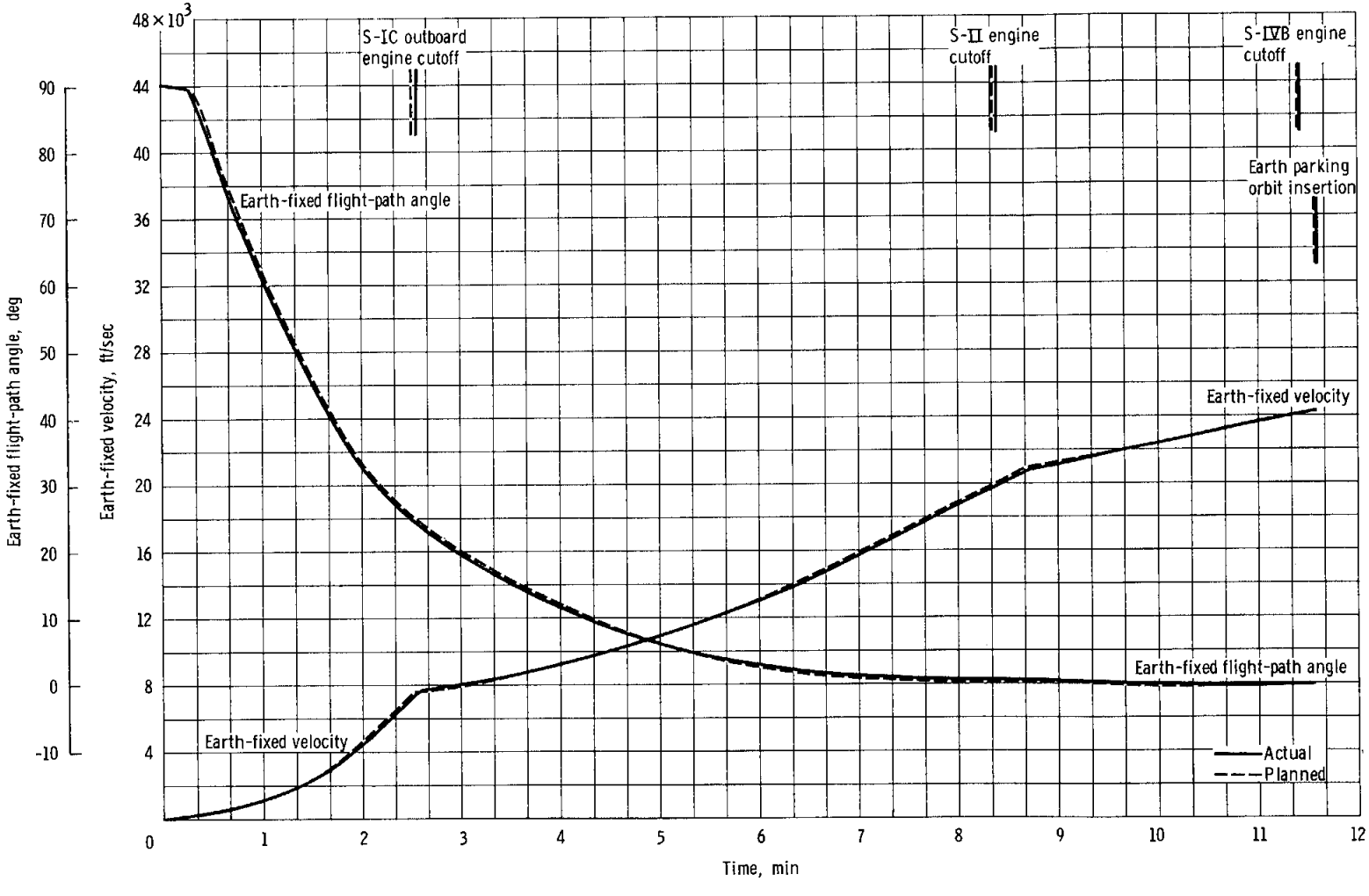

(b) Earth-fixed flight-path angle and velocity.

Figure 5-1. - Continued.

NASA-S-69-625

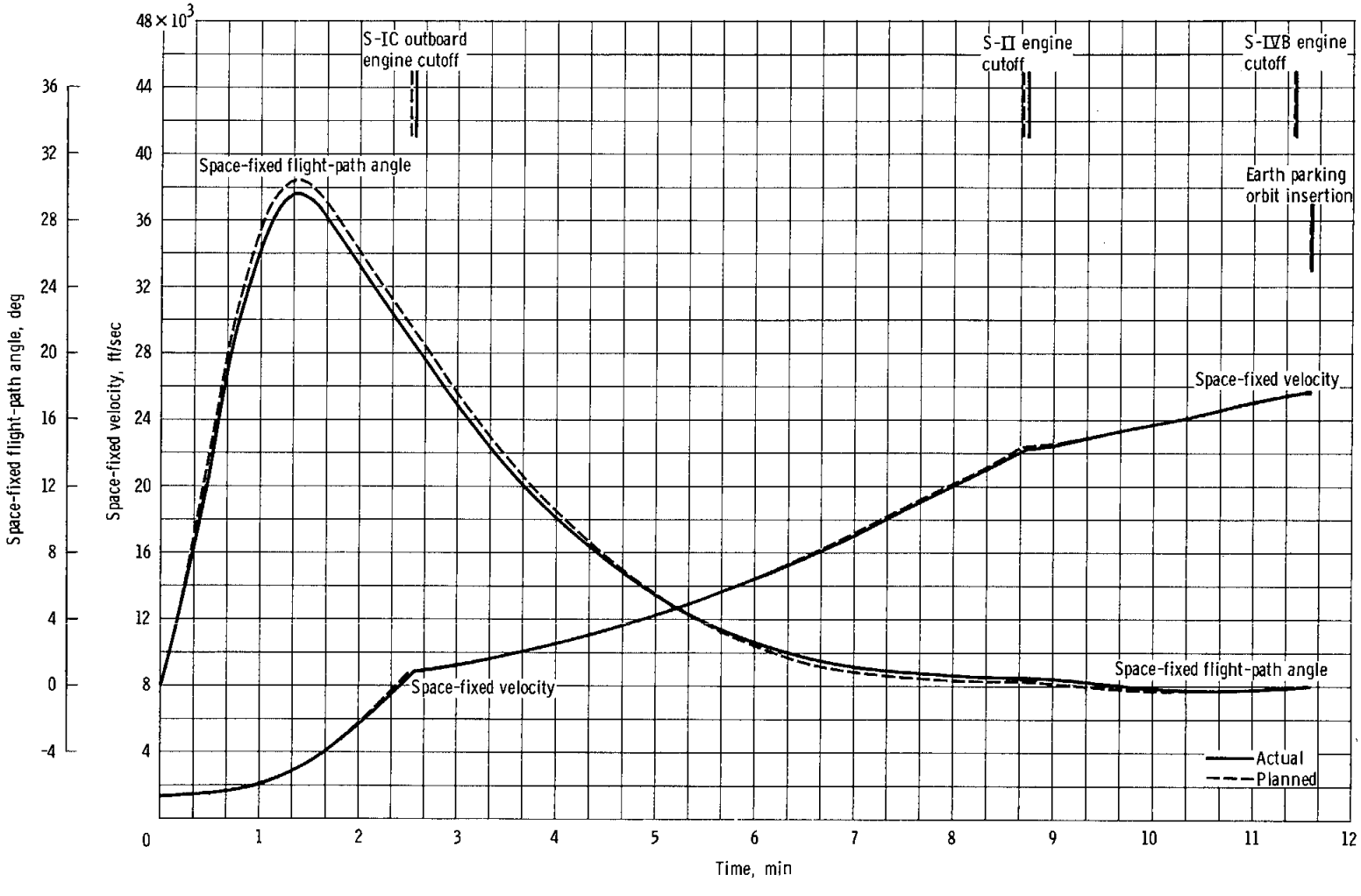

(c) Space-fixed flight-path angle and velocity.

Figure 5-1. - Continued.

NASA-S-69-626

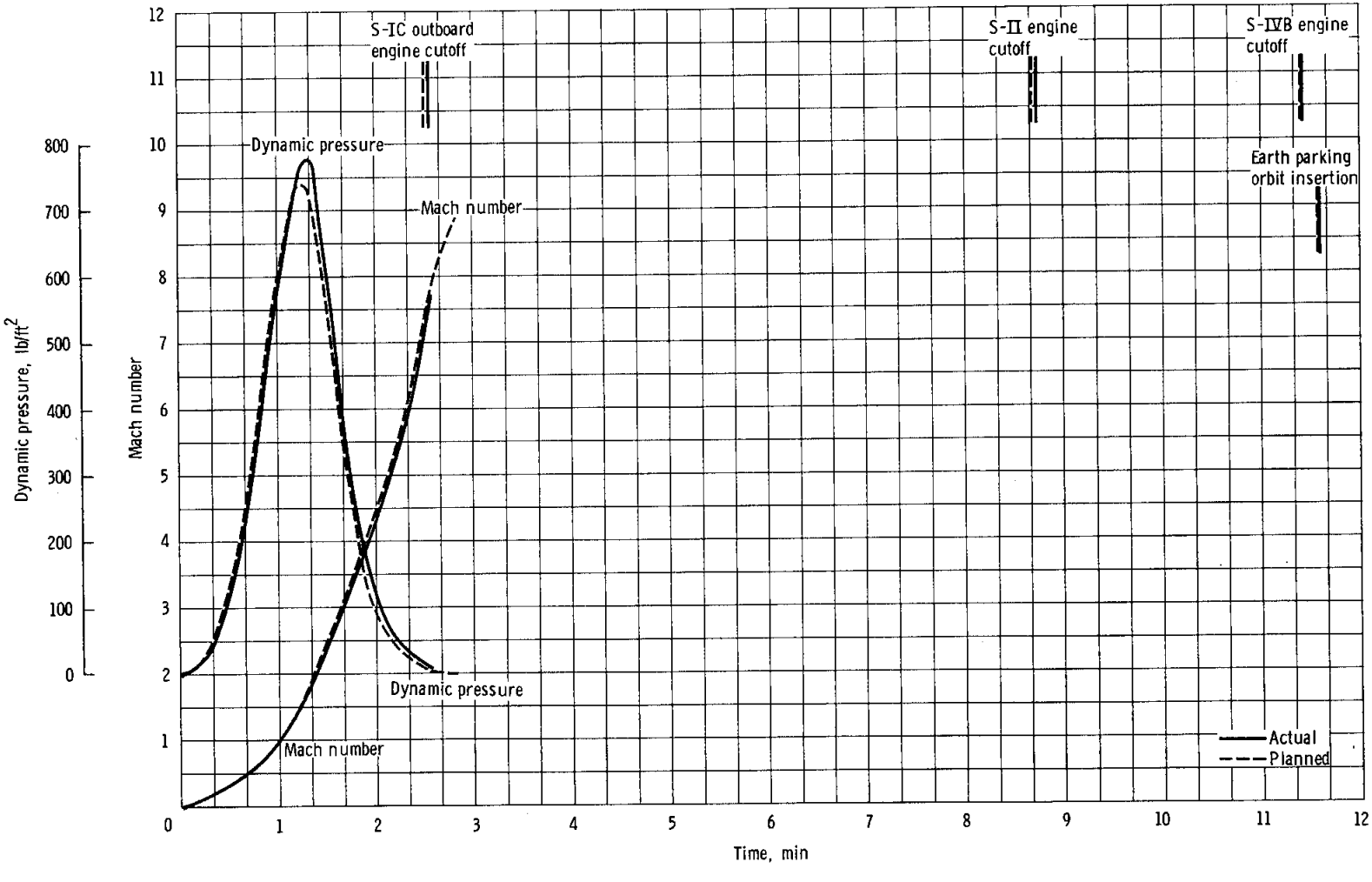

(d) Dynamic pressure and Mach number.

Figure 5-1.- Concluded.

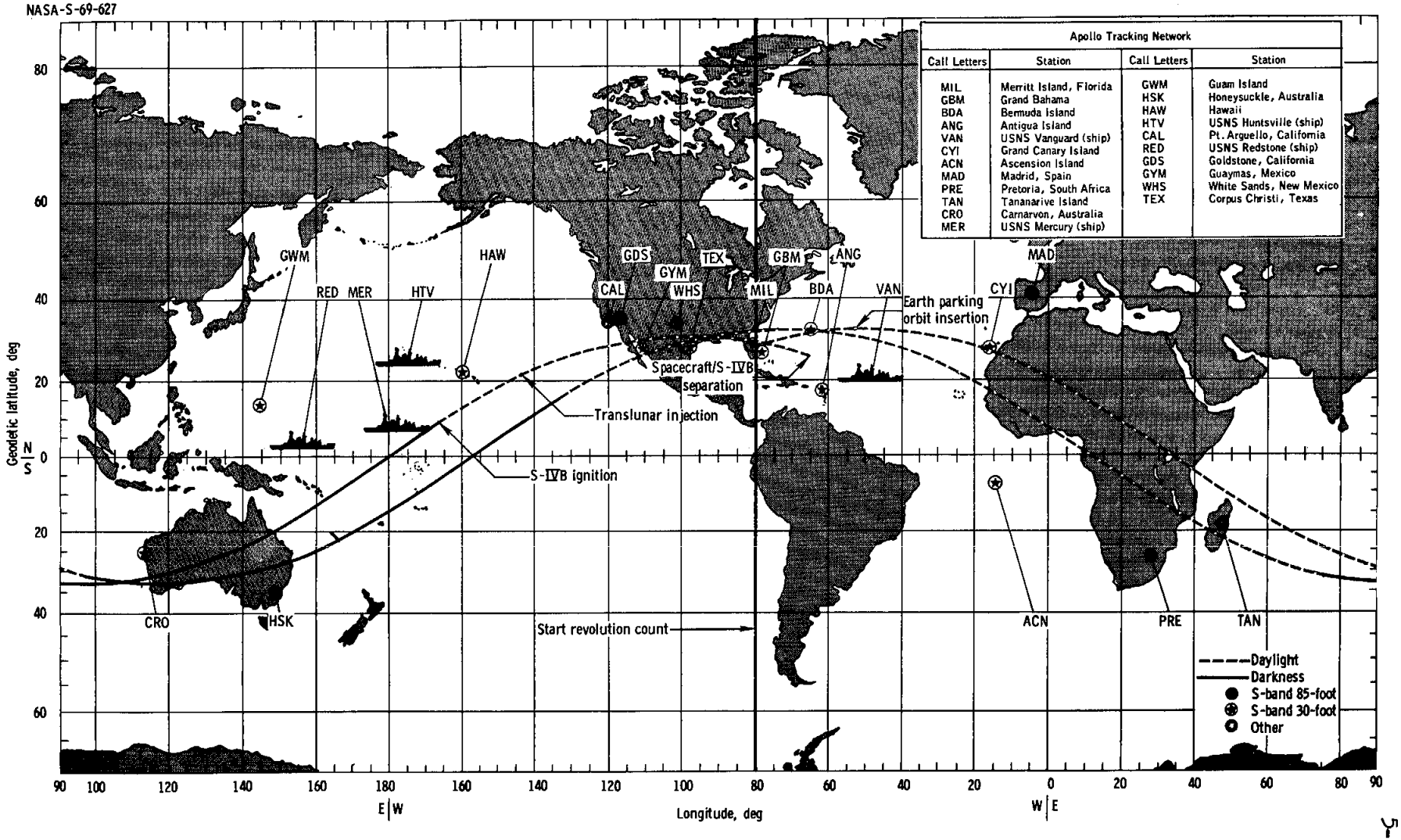

Figure 5-2. - Ground track for earth parking orbits.

NASA-S-69-628

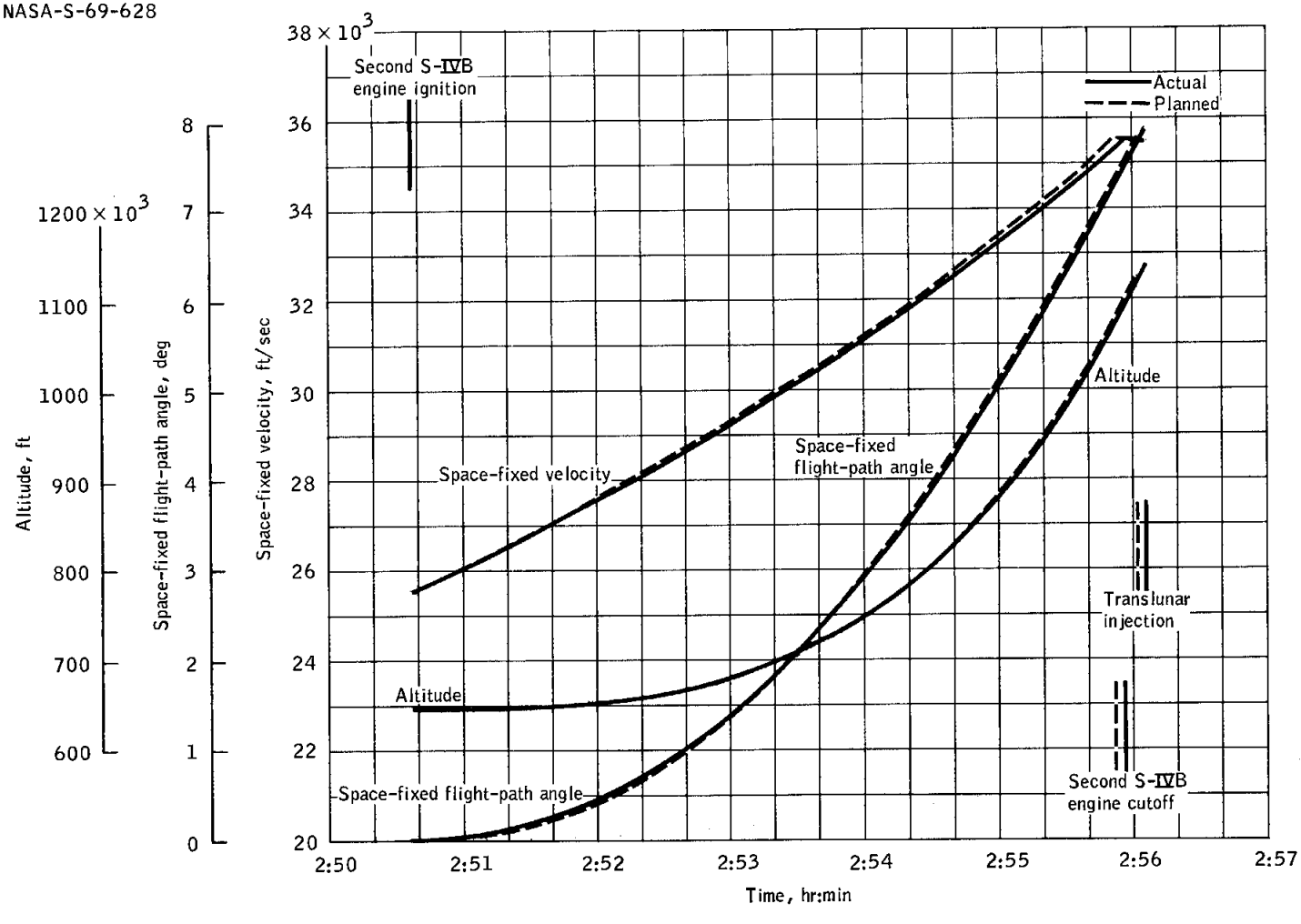

Figure 5-3.- Trajectory parameters during translunar injection.

NASA-S-69-629

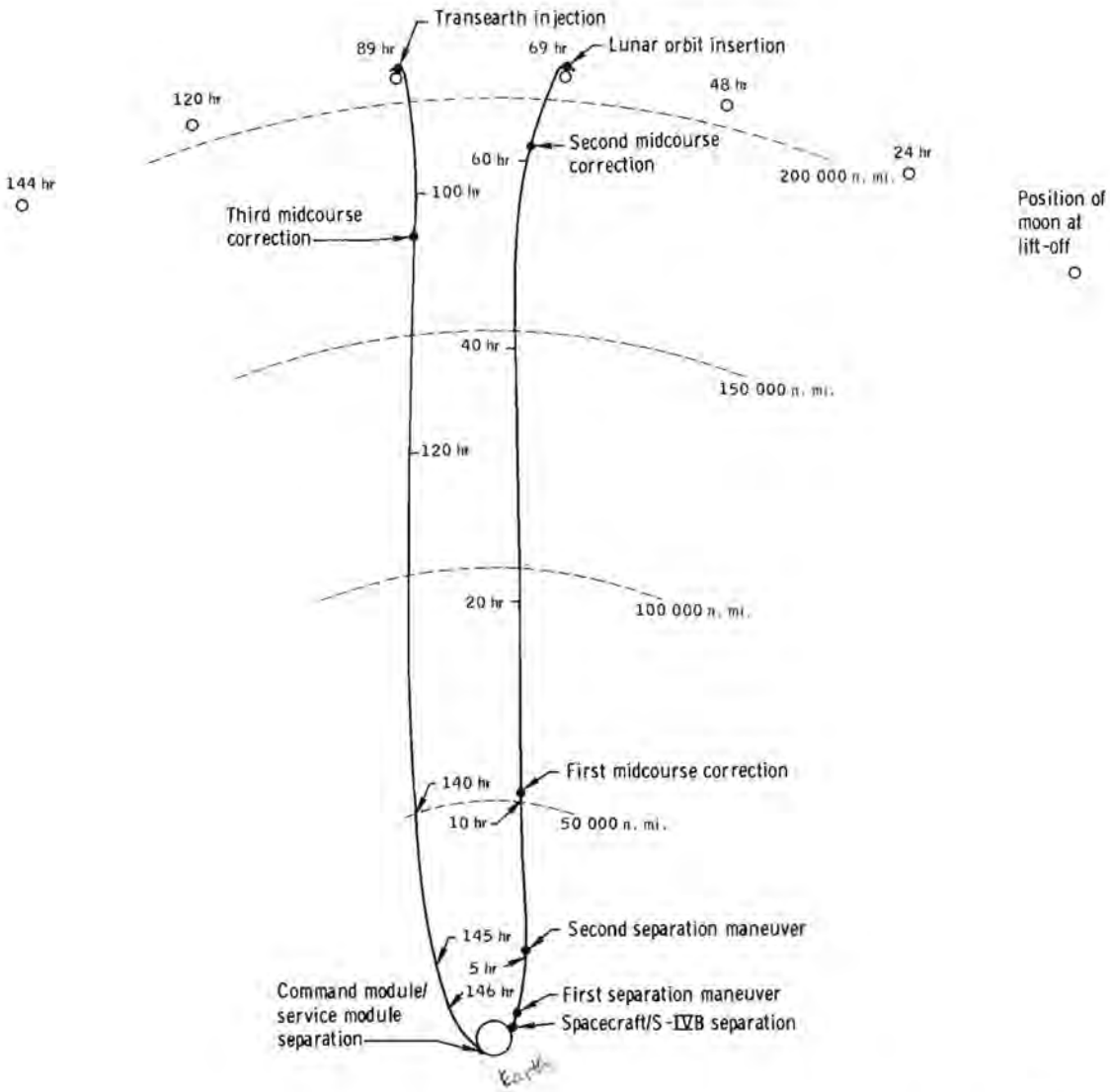

Figure 5-4.- Translunar and transearth trajectories.

Apollo 8

NASA-S-69-631

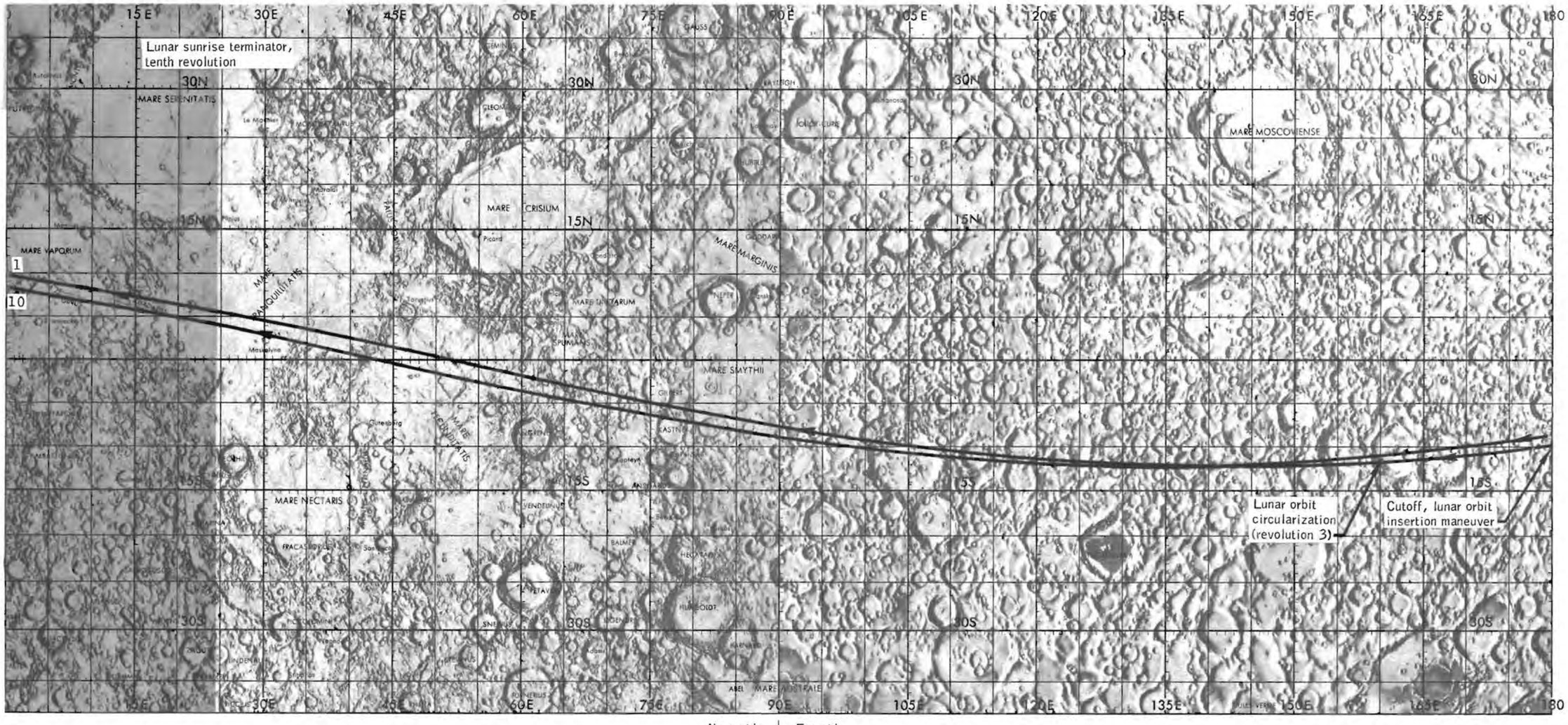

MERCATOR PROJECTION
SCALE 1:11,024,406 AT THE EQUATOR

Figure 5-5.- Ground track for lunar orbits 1 and 10.

NASA-S-69-630

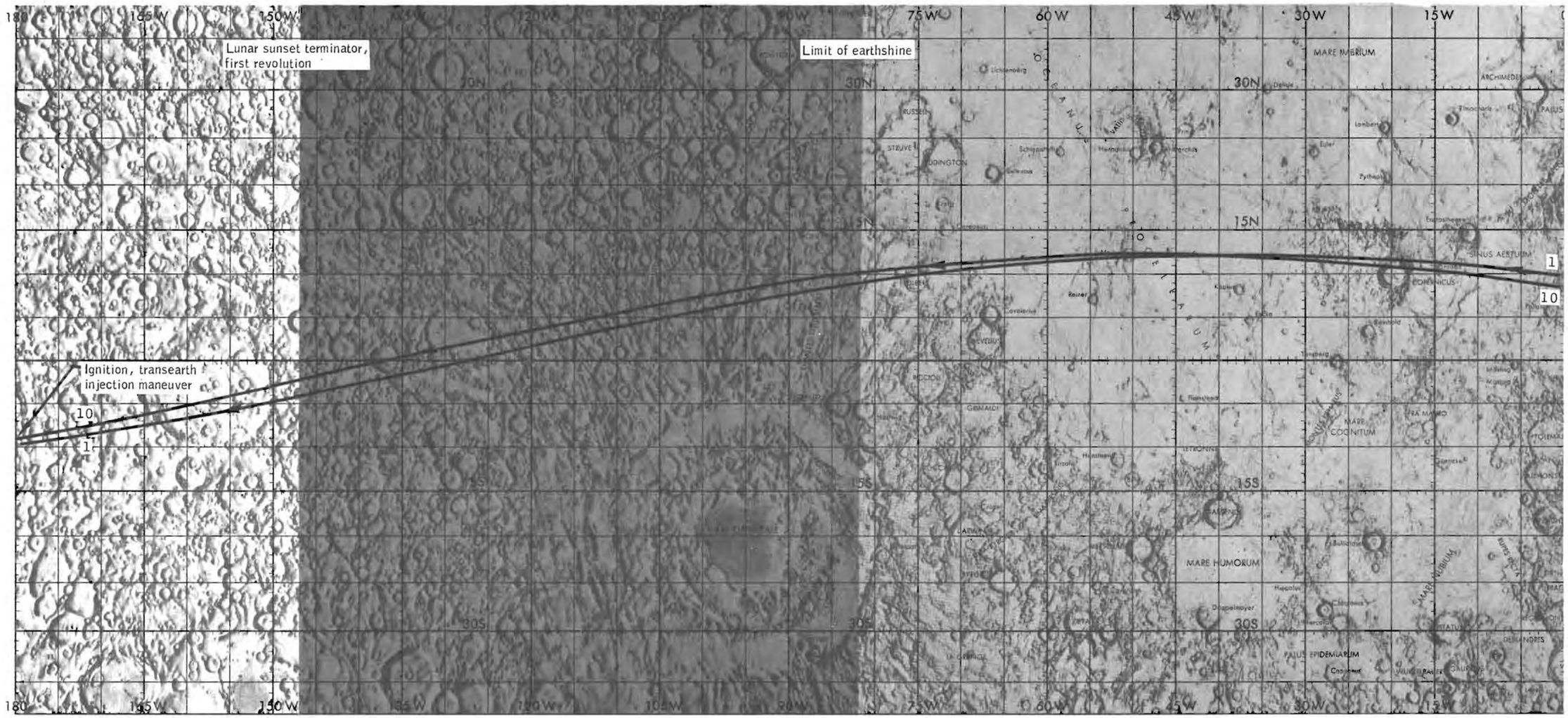

PREPARED UNDER THE DIRECTION OF THE DEPARTMENT OF DEFENSE BY THE AERONAUTICAL CHART AND INFORMATION CENTER, UNITED STATES AIR FORCE FOR THE NATIONAL AERONAUTICS AND SPACE ADMINISTRATION

Figure 5-5.- Ground track for lunar orbits 1 and 10.

NASA-S-69-632

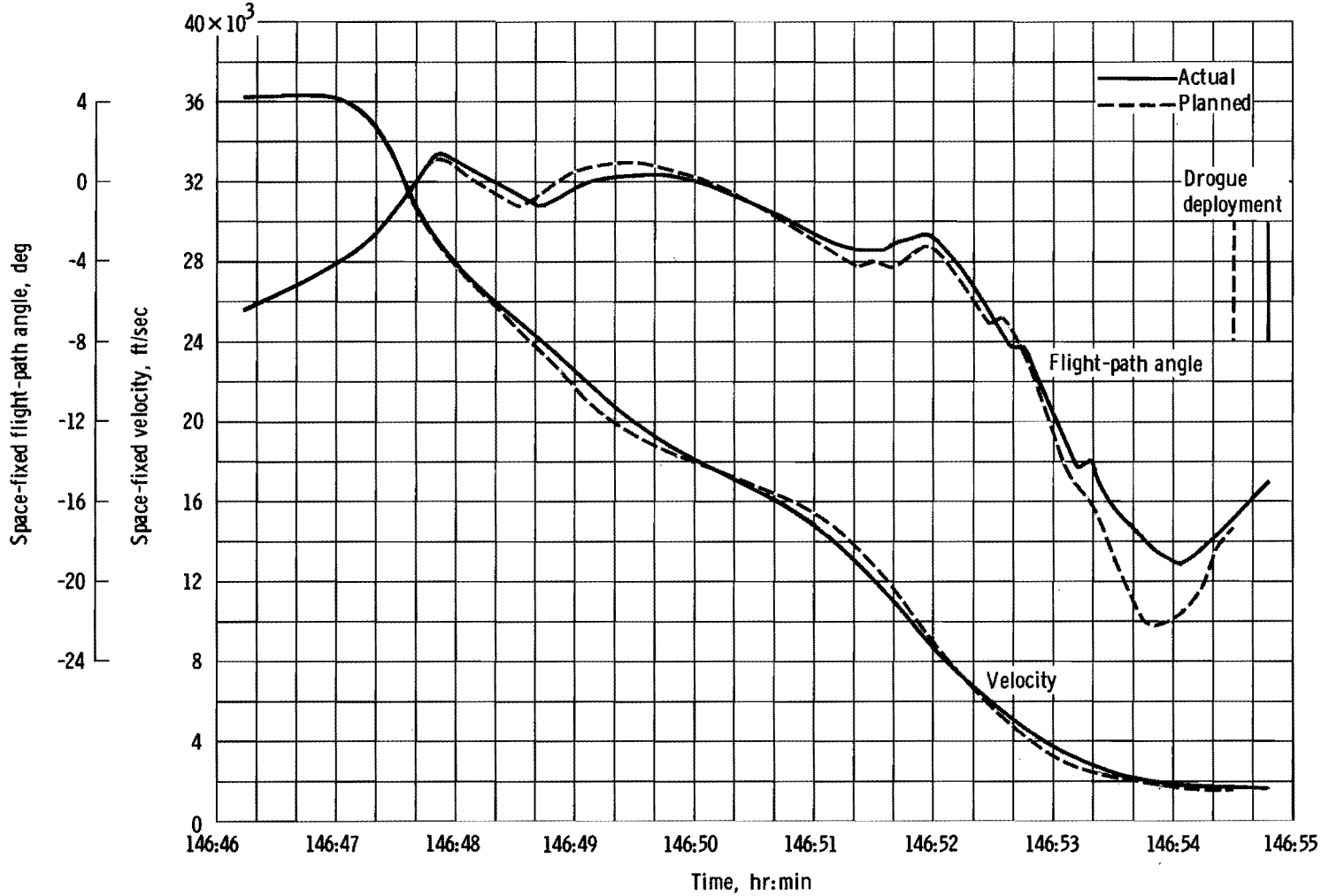

(a) Space fixed flight-path angle and velocity.

Figure 5-6. - Trajectory parameters during entry.

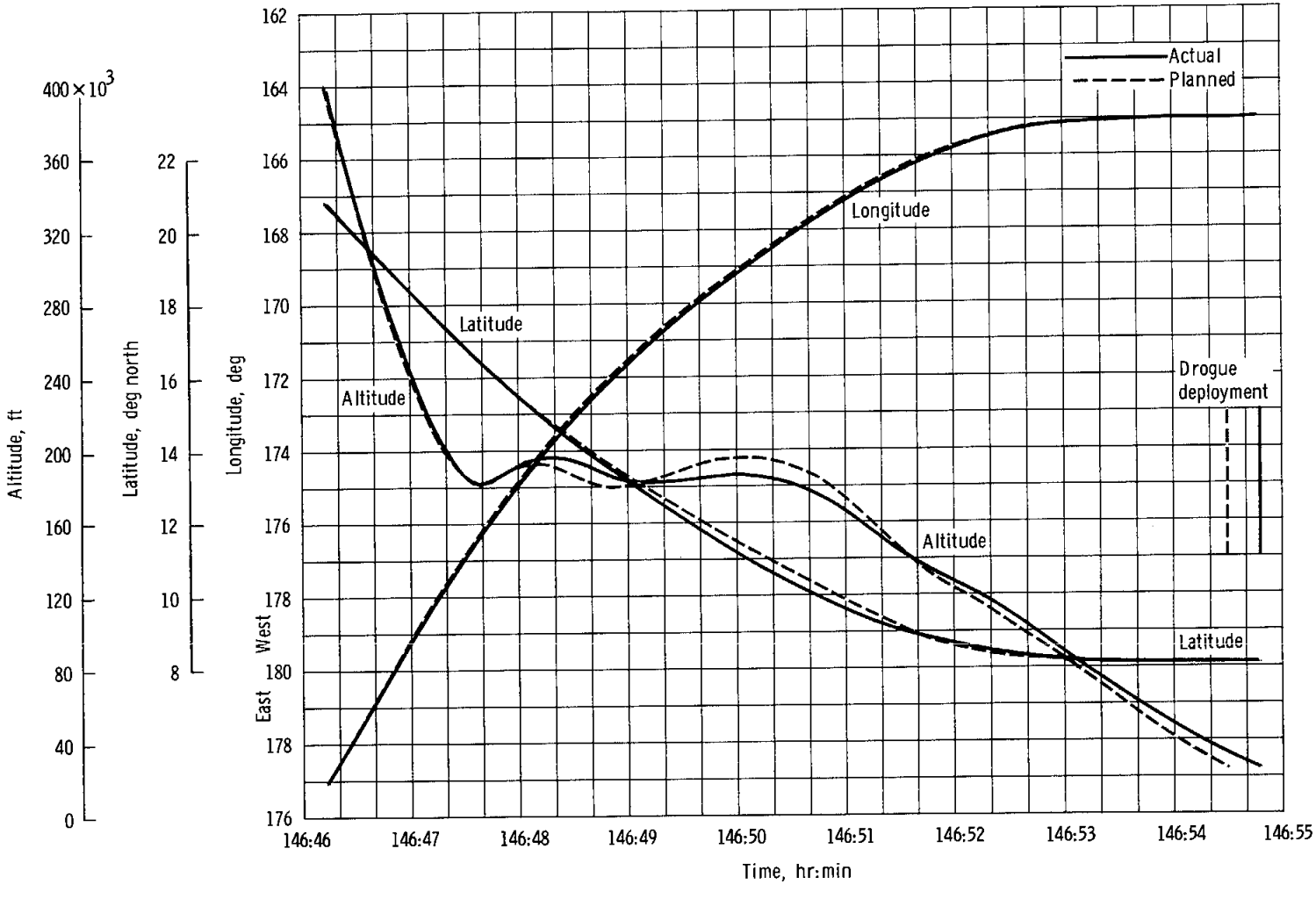

(b) Altitude, latitude, and longitude.

Figure 5-6. - Continued.

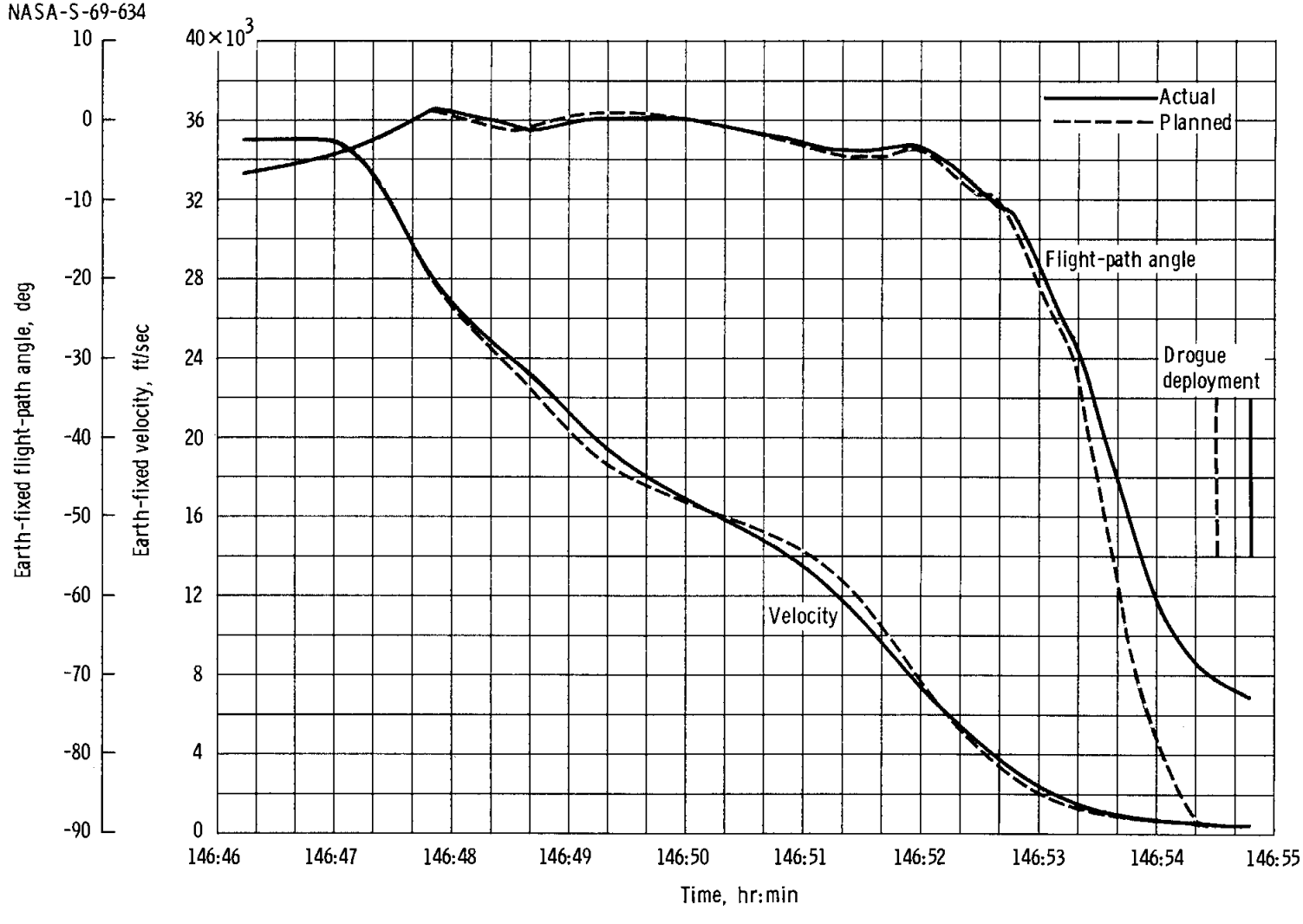

(c) Earth-fixed flight-path angle and velocity.

Figure 5-6.- Concluded.

NASA-S-69-635

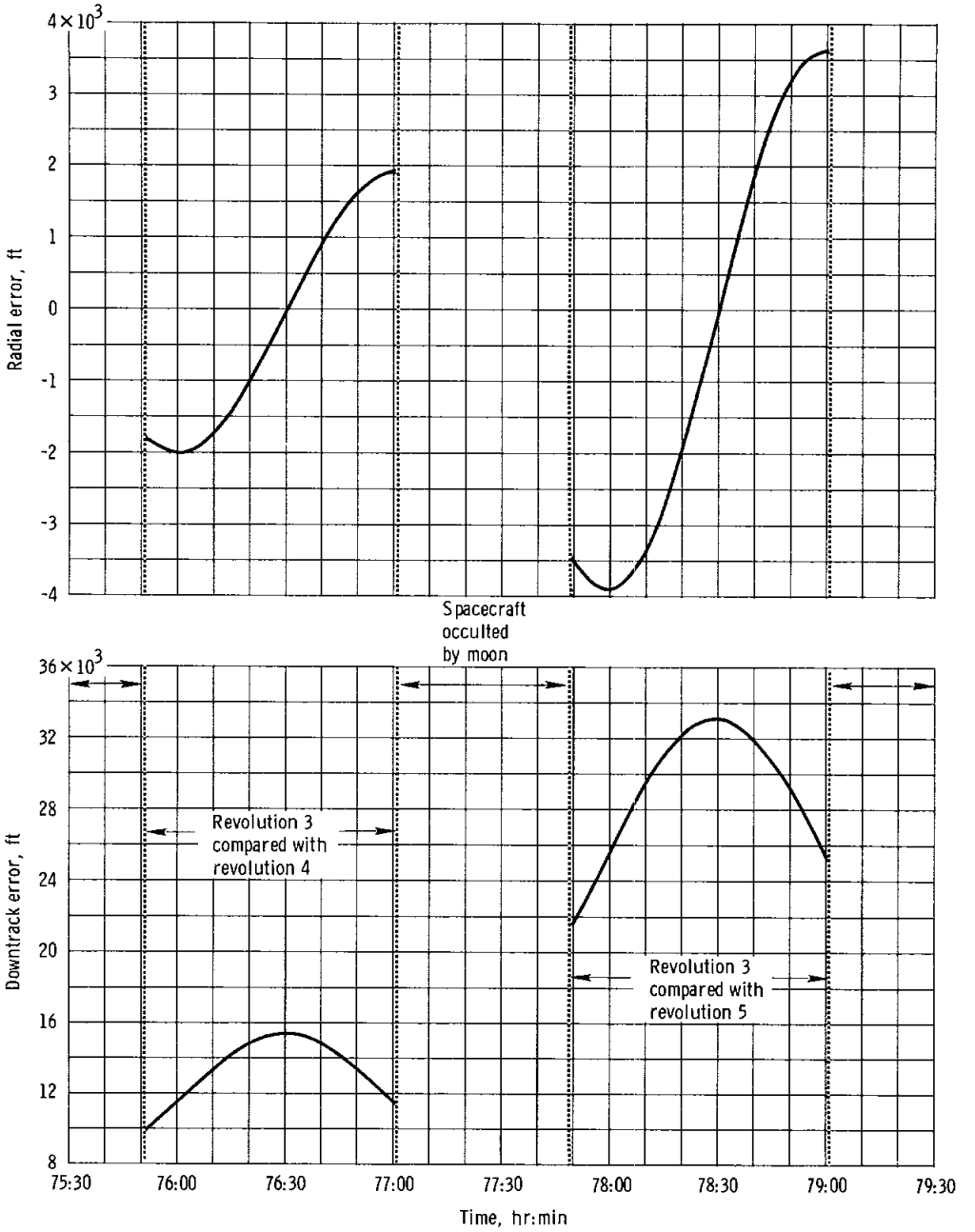

Figure 5-7. - Prediction errors for triaxial moon model.

6.0 COMMAND AND SERVICE MODULE PERFORMANCE

This section presents the specific performance of major system groups in the command and service modules. All spacecraft systems performed satisfactorily during the Apollo 8 mission; only those systems for which performance was unusual or for which results are considered significant to future flights will be discussed. The earth landing, sequential, pyrotechnic, launch escape, and emergency detection systems operated exactly as intended and are not documented. Specific discrepancies and anomalies in other systems are mentioned in this section but are discussed at greater length in section 12, Anomaly Summary. A compilation of liquid consumable quantities is presented at the end of this section.

6.1 STRUCTURAL AND MECHANICAL SYSTEMS

6.1.1 Structural Loads

The analysis of spacecraft structural loads was based on recorded onboard measurements and indicates that the loads were less than design values for all phases of flight.

Ground winds at launch were light. The bending moment monitored at station 790 of the Saturn V launch vehicle was 6.4 million in-lb, as compared to the launch-release limit of 81 million in-lb. Unsymmetrical thrust buildup effects were lower than design values, and the effects of vortex shedding were not detected. Calculated loads of the various interfaces for lift-off are compared with the predicted loads for Apollo 8 design conditions in table 6.1-I.

Also shown in table 6.1-I are spacecraft loads near the period of maximum dynamic pressure (maximum $q\alpha$); these loads were caused primarily by the angle of attack induced by wind shear. The measured winds at this point were from the west with a peak velocity of 100 ft/sec.

A 5.9-Hz longitudinal command module oscillation began at 0:02:14 and lasted until first-stage outboard engine cutoff. This oscillation, which peaked at 0.15g at 0:02:28, was the maximum steady-state oscillation measured at any time during the mission. This oscillation was lower than the 0.22g measured during Apollo 4 and the 0.6g value for Apollo 6 and is an acceptable level for structural components.

Maximum axial acceleration of the spacecraft occurred immediately prior to first-stage outboard engine cutoff. Spacecraft loads for this condition are compared to predicted Apollo 8 loads for Saturn V, block II design conditions in table 6.1-I.

The crew reported longitudinal oscillations near the end of the S-II powered-flight phase. The maximum longitudinal oscillation measured at the command module forward bulkhead was 0.1g peak at 8.9 Hz. Using comparable levels measured at the forward bulkhead during a ground environmental vibration test, a 0.15g peak longitudinal oscillation is calculated for the crew couch in this period. The command module forward bulkhead oscillation was within the acceptable structural level.

Loads were low during service propulsion firings. The maximum steady-state axial acceleration measured during any firing was 0.68g at transearth injection.

The peak acceleration during entry was 6.84g, which is well below the 20g structural design limit.

6.1.2 Structural Strains

For this mission, seventeen strain gage measurements were added to the spacecraft/launch-vehicle adapter and were monitored during the launch phase of the flight to provide additional information on the dynamic response of the adapter. One strain gage was located on the lunar module attachment ring in the adapter; the remaining 16 strain gages were located on the shell in groups of four, approximately 45 degrees between the Y and Z axes and 51 inches aft of the lunar module attachment ring. Each group of strain gages was arranged to measure inner and outer shell axial and circumferential strains.

For the periods of longitudinal oscillation during the S-IC and S-II boost phases, the instrumentation measured neglibible low-frequency structural responses. The strains were greatest during first stage flight and were well below previously demonstrated structural static test levels. The flight strains compared reasonably well with strains attained from static ground tests at loads consistent with those calculated from flight data. The measured axial compressive strains were below 1000 microinches per inch and were less than 65 percent of the ultimate static test levels.

6.1.3 Vibration

The Apollo 8 spacecraft was instrumented with four X-axis accelerometers of ±25g range and 2500 Hz response on the command module forward bulkhead and X-axis and tangential accelerometers of ±75g range and 2000-Hz response at the outer end of the high-gain antenna boom. The X-axis measurement is mounted perpendicular to the antenna boom, oriented in the radial direction when the antenna is stowed during launch and oriented in the longitudinal axis after antenna deployment. The four

measurements on the forward bulkhead were equally spaced about the junction circle with the docking tunnel. One measurement on the forward bulkhead was inoperative prior to launch.

Power spectral density analyses of the operative bulkhead measurements were made for lift-off, the transonic and maximum dynamic pressure regions, and center engine cutoff (approximately 0:02:06); these showed high energy concentrations in narrow frequency bands at approximately 60 and 180 Hz. The amplitude at these frequencies was approximately the same for each analysis time. However, an analysis of data taken just prior to engine ignition shows the vibration data at these frequencies to be invalid. With these peaks excluded, the vibration levels measured on the forward bulkhead are well below the qualification criteria.

The two vibration measurements located on the high-gain antenna boom significantly exceeded the qualification vibration criteria for the antenna during lift-off and in the transonic and maximum dynamic pressure regions. The power spectral density analysis of the X-axis measurement is compared with the qualification criteria in figure 6.1-1, for the time period from 3.5 to 5.0 seconds after lift-off. A tabulation of all cases where the criteria were exceeded is presented as table 6.1-II. The levels measured during Apollo 8 will be incorporated into the existing delta qualification vibro-acoustic test to be conducted on the high-gain antenna assembly prior to the Apollo 10 mission.

For service propulsion firings, the signal-to-noise ratios were insufficient to produce valid data.

The service module/adapter separation shock, as measured on the high-gain antenna boom (fig. 6.1-2), had a peak value of 70g in the X-axis and 58g in the tangential direction. The shock measured during antenna deployment was 13g in the X-axis and 5g in the tangential direction. At present, no shock criteria for the high-gain antenna have been determined. However, the operation of the antenna was satisfactory (see section 6.7).

6.1.4 Mechanical Systems

All components of the mechanical systems performed properly during the flight. However, the crew stated that the pressurizing mechanism for the side-hatch counterbalance was difficult to operate. The correct procedure for pressurizing the counterbalance is to turn a knob that punctures a rupture disc in a nitrogen pressure bottle. However, the checklist directed the crew to set the flow valve in the wrong position, which prevented the pressurized gas in the punctured bottle from entering the counterbalance cylinder. The crew was therefore misled to believe that the turned knob had not punctured the bottle, and they kept turning until the knob bottomed, making the turning forces excessive. Postflight inspection revealed that the bottle was punctured and that the knob was

bottomed. Future checklists will be corrected. However, for crew convenience, a ratchet mechanism is being designed to replace the knob.

Windows 1, 3, and 5 (two side and one center hatch window) became contaminated and fogged over, similar to the problem during Apollo 7. An analysis of the Apollo 8 window contaminants confirmed the Apollo 7 conclusion, that is, outgassing products from the sealant compound (RTV) appear to be the major cause of the window contamination. This contamination was found on the interior surfaces of the outer heat shield panes. Further discussion is presented in section 12.

TABLE 6.1-I.- MAXIMUM SPACECRAFT LOADS DURING LAUNCH PHASE

Interface	Load	Lift-off		Maximum qα		End of first stage boost	
		Calculated[a]	Predicted[b]	Calculated[a]	Predicted[b]	Calculated[a]	Predicted[b]
Launch escape system/command module	Bending moment, in-lb . . .	740 000	2 630 000	342 000	1 165 000	63 200	95 000
	Axial force, lb	-12 400	-12 425	-19 372	-24 850	-35 000	-35 900
Command module/ service module	Bending moment, in-lb . . .	922 000	3 470 000	523 000	1 967 000	270 000	412 000
	Axial force, lb	-29 800	-29 800	-83 509	-89 900	-84 600	-85 900
Service module/ adapter	Bending moment, in-lb . . .			2 036 000	7 028 000	2 140 000	2 498 000
	Axial force, lb			-134 767	-193 000	-289 600	-293 000
Adapter/instrument unit	Bending moment, in-lb . . .			5 136 000	19 636 000	2 017 000	3 900 000
	Axial force, lb			-188 000	-264 290	-385 600	-390 200

Note: Negative axial force indicates compression.

The flight conditions at maximum qα were:

Condition	Calculated[a]	Predicted[b]
Flight time, sec	77.4	68.1
Mach no.	1.74	1.34
Dynamic pressure, psf . .	772	732.3
Angle of attack, deg . . .	1.33	6.7
Maximum qα, psf-deg . . .	1033	4910

The accelerations at the end of first stage boost were:

Acceleration	Calculated[a]	Predicted[b]
Longitudinal, g	3.97	4.04
Lateral, g	0.03	0.05

[a]Calculated from flight data.

[b]Predicted Apollo 8 loads for Saturn V, block II design conditions.

TABLE 6.1-II.- HIGH-GAIN ANTENNA VIBRATION

Sensitive axis	Frequency, Hz	Above criteria, dB		
		Lift-off	Transonic (Mach 1)	Maximum q
X-axis	70	3.2	--	--
	120	6.2	--	--
	1500	--	8.5	8.8
	1860	--	--	4.0
Tangential	1200	--	--	4.0

NASA-S-69-636

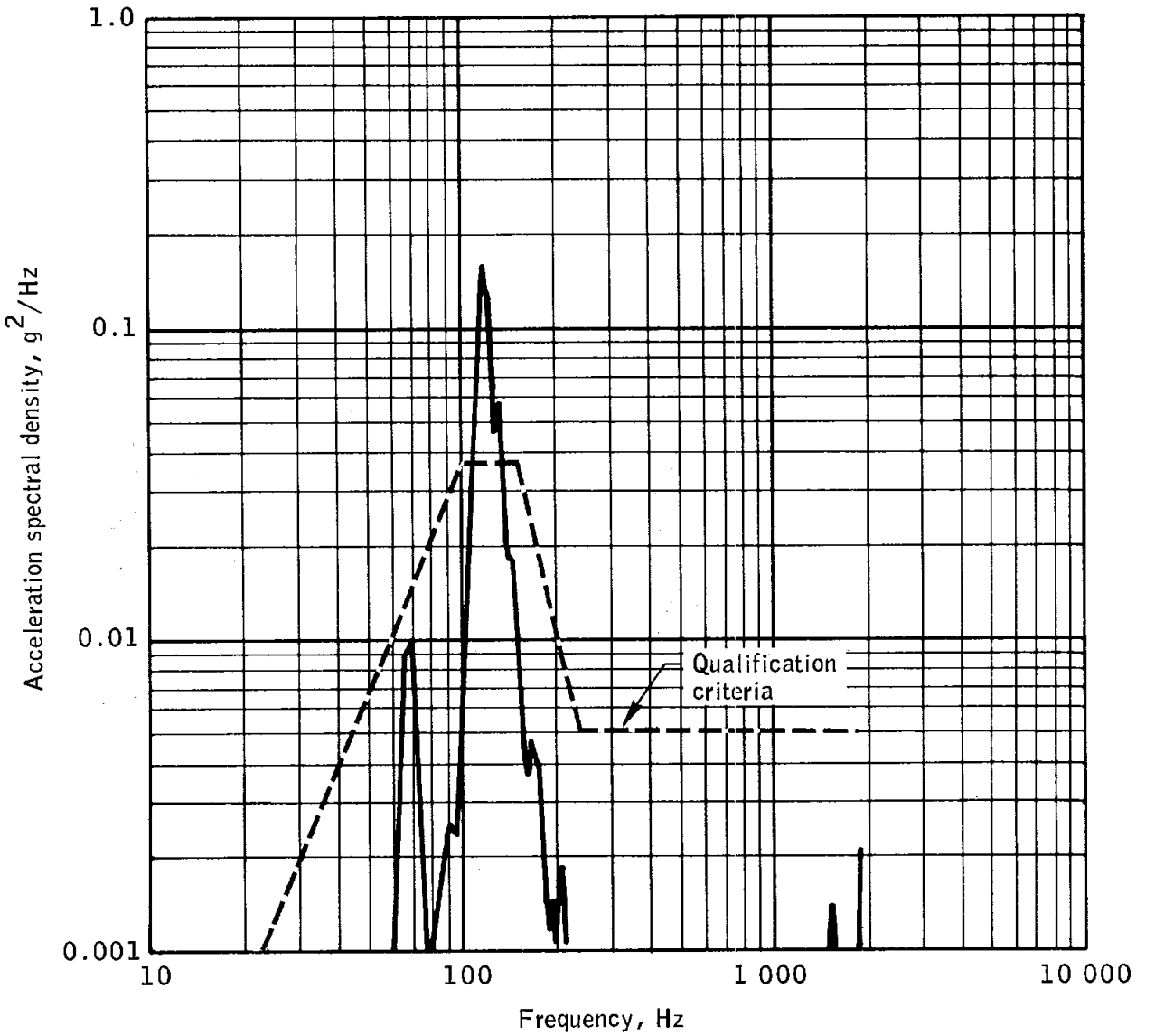

Figure 6.1-1.- Comparison of high-gain antenna vibration at lift-off with criteria.

NASA-S-69-637

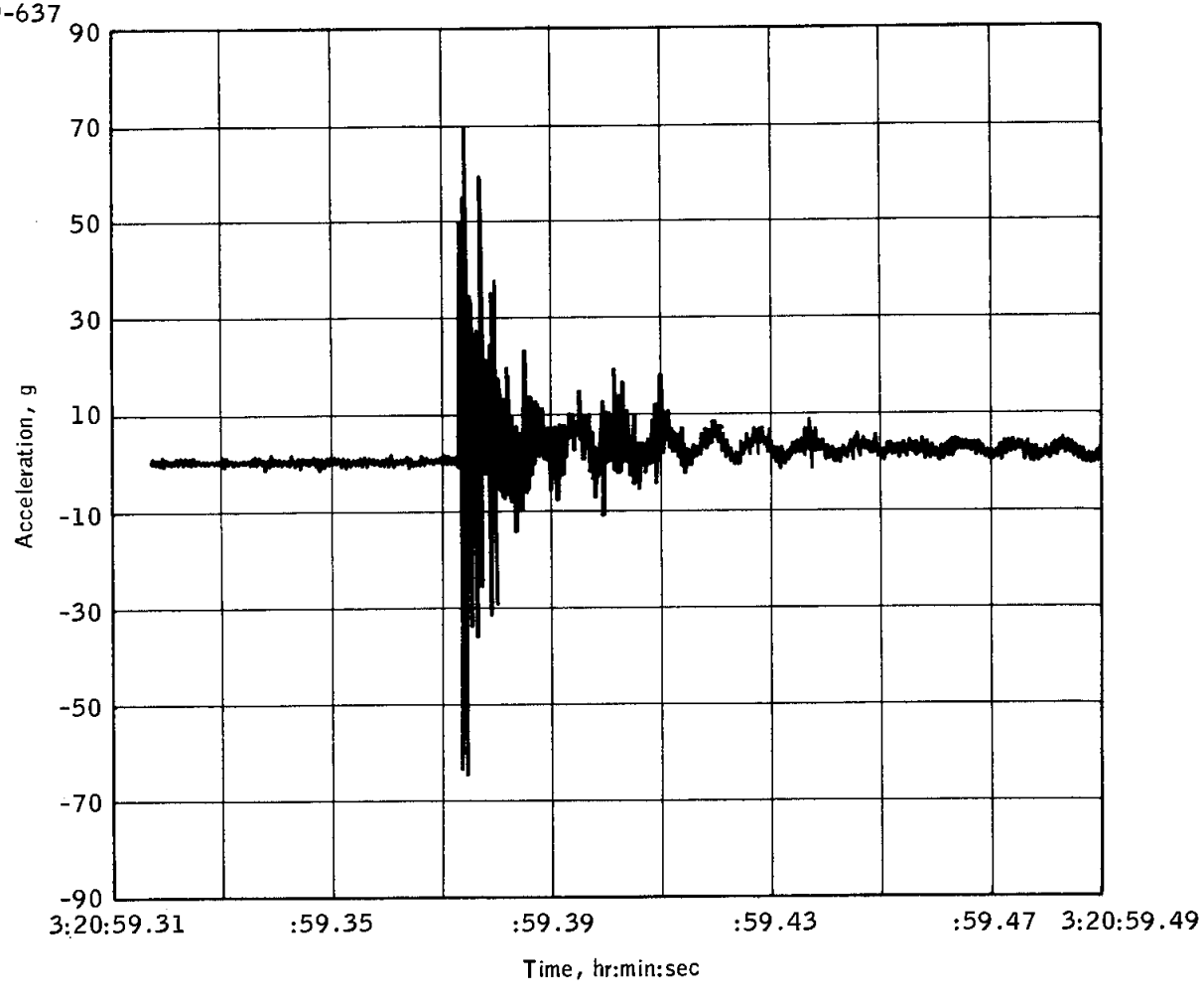

Figure 6.1-2.- X-axis accelerations on high-gain antenna during spacecraft/S-IVB separation.

6.2 AERODYNAMICS

As noted in all previous flights, the trend for the hypersonic trim lift-to-drag ratio to increase with decreasing Mach number was observed. The flight-derived lift-to-drag ratio was within the predicted uncertainty band of ±0.3 from the beginning of entry to a Mach number of 4.0.

The predicted and flight-derived lift-to-drag ratios and the predicted and estimated trim angle of attack are shown in figure 6.2-1.

Accelerometer data and the onboard guidance system entry position and velocity information were used to obtain the flight lift-to-drag ratios. The accelerometer data were corrected for known preflight bias and scale factor errors. The estimated trim angle of attack was obtained from the flight-derived lift-to-drag ratio and the wind tunnel variation of lift-to-drag ratio with angle of attack.

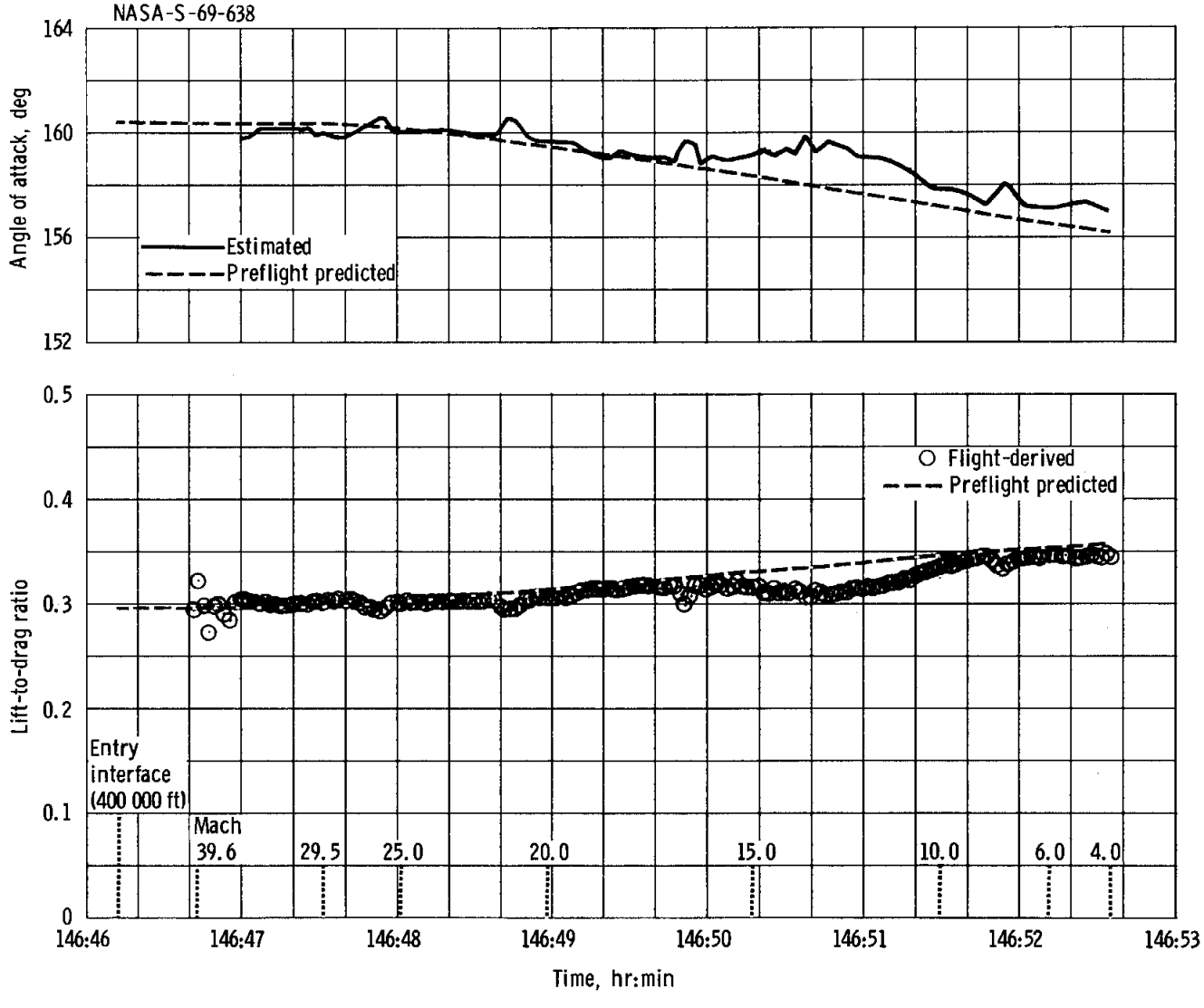

Figure 6.2-1. - Command module hypersonic entry aerodynamics.

6.3 THERMAL CONTROL

This section discusses the thermal response for the spacecraft elements that lack active temperature control. A passive thermal control technique, which required the spacecraft to be rolled about the major axis, generally positioned perpendicular to the sun vector, was used during most of the translunar and transearth phases and resulted in nominal temperatures.

The temperature response for the service module reaction control system helium tanks and service propulsion propellant tanks for each bay are shown in figure 6.3-1. As the service propulsion storage tanks became empty, the temperature measurement showed a greater fluctuation and generally followed the trend of the helium tank temperature. The service propulsion propellant sump tanks never emptied; consequently, they consistently maintained a temperature of 70° (±2°) F, assisting the passive thermal control technique in maintaining nominal temperatures.

The service propulsion feedline temperatures remained well within operating limits (25° to 110° F) throughout the mission. The temperatures ranged from 65° to 86° F at the engine fuel and oxidizer interface, from 62° to 84° F on the oxidizer and fuel transfer feedlines, and from 59° to 83° F on the propellant utilization valve.

The command module ablator temperatures were normal and remained between minus 30° F and plus 100° F throughout the flight, except for a 4-hour period when the temperature on the thick side of the ablator reached 138° F. This would be expected for the 4-hour period in which a cold soak of service module reaction control system quad A and a television transmission took place. The temperatures in the command module reaction control system helium tanks also remained within a normal range of 57° to 74° F.

Passive thermal control was very effective in maintaining measured temperatures midway between the hot and cold extremes of the allowable, and little deviation was noted from this condition while in lunar orbit.

NASA-S-69-639

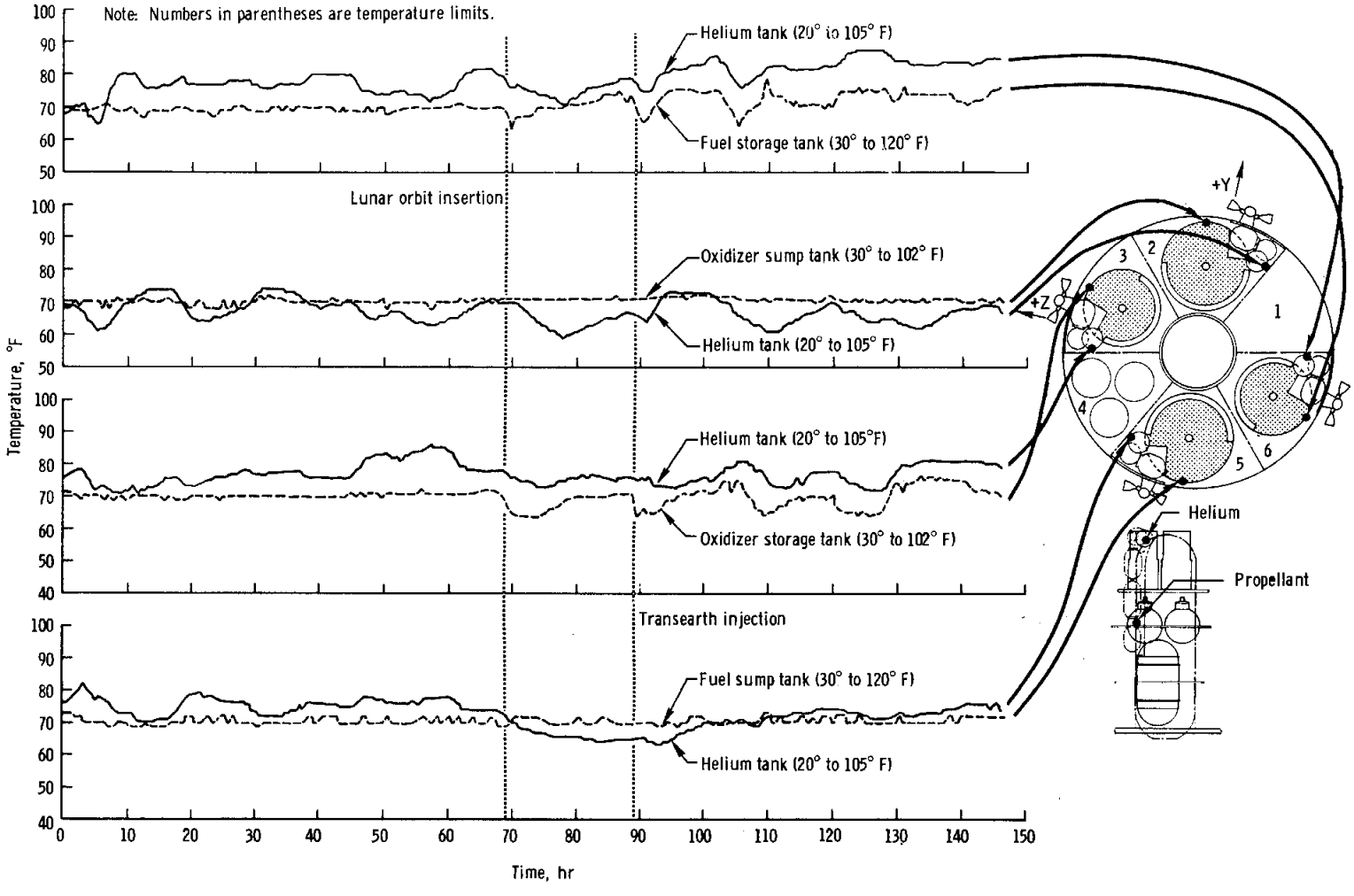

Figure 6.3-1.- Temperatures on service module reaction control system helium tanks and service propulsion propellant tanks.

6.4 HEAT PROTECTION SYSTEM

Visual inspection of the command module heat shield indicates satisfactory thermal performance, in that the degree and distribution of ablator charring are consistent with preflight calculations. The heat shield system was not adversely affected by exposure to cislunar space or to the lunar environment.

The Apollo 8 heat shield charred less than that flown on Apollo 4 because of the less severe entry environment. Char depths on the aft (blunt) heat shield ranged from 0.6 inch at the stagnation zone to 0.4 inch in the downstream (-Z) area. The windward conic heat shield was charred only lightly, and the leeward conic ablator was virtually undegraded.

Pieces of charred ablator were broken from a large area in the general stagnation region (fig. 6.4-1). Examination of the damaged area and char thickness measurements at adjacent locations definitely indicate that the char was intact during entry. Similar damage was noted on Apollo 4 and 6 heat shields but over a much smaller area. The damage most likely resulted from landing shock, and, therefore, does not relate to ablator performance.

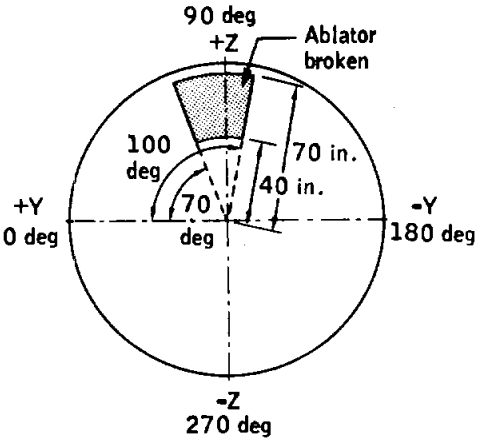

Figure 6.4-1.- Location of damaged ablator.

From a thermal standpoint, external heat-shield components endured the lunar return entry environment satisfactorily.

The condition of crew-compartment heat=shield components is very good. Umbilical bundles were cleanly severed, and discoloration on the window, plus blistered splotches on identification decals, are the only indications of entry heating on the unified hatch. All other crew-compartment and forward-heat-shield components show entry effects similar to or less severe than those observed on Apollo 4 and 6.

The condition of the truncated apex, first exposed to supercircular entry environment on spacecraft 103, appeared as expected based on analysis and extrapolation of spacecraft 101 flight test data.

6.5 ELECTRICAL POWER

This section is a discussion of fuel-cell and battery performance. The power distribution system exhibited nominal performance during the mission, and no separate discussion is provided.

6.5.1 Fuel Cells

The fuel cells and radiators performed satisfactorily during all prelaunch and flight phases. All three fuel cells were activated 48 hours prior to launch and thereafter shared spacecraft electrical loads with ground support equipment until 2 hours prior to launch, when they assumed the full spacecraft power load.

During the mission, the fuel cells provided approximately 290 kilowatt-hours of energy at an average current of 22.7 amperes per fuel cell and an average command module bus voltage of 28.6 V dc. The bus voltage was maintained between 28.2 and 30.0 V dc during all mission phases when fuel cell power was being used. The maximum deviation from equal load sharing between individual fuel cells was an acceptable 3.5 amperes.

Prior to flight, an unexpected drop in fuel-cell current prompted an oxygen purge, and subsequent performance indicated a substandard oxygen purity. (See section 12.) Reservicing of cryogenic oxygen corrected the observed degradation. Figure 6.5-1 shows that the actual performance agreed very closely with predicted performance, and no significant degradation was noted during the mission.

Thermal performance of the three fuel cells as a function of load current is summarized in figure 6.5-2. All thermal parameters, including condenser exit temperature, remained within normal ranges of operation.

Periodic fuel cell oxygen and hydrogen purges did not noticeably increase performance, indicating that high-purity reactants were being supplied to the fuel cells from the cryogenic tanks. Reactant consumption rates calculated from fuel cell currents agreed very well with indicated reactant quantities, as discussed in section 6.6.

6.5.2 Batteries

The three entry and postlanding batteries and two pyrotechnic batteries performed all required functions. Battery charging during this mission was more successful than on Apollo 7, primarily because the charger had a higher output potential. Entry battery A was charged twice,

with a total of 17.14 A-h restored, and battery B was charged three times, with a total of 23.16 A-h restored. The first charge on battery B was interrupted temporarily for the first midcourse correction.

The battery capacity status throughout the mission is shown in figure 6.5-3. Battery C was isolated shortly after launch and was not used again until initiation of the earth entry phase. The total capacity remaining just prior to command module/service module separation was 113.9 A-h (37.5, 38.0, and 38.4 A-h on batteries A, B, and C, respectively). Just after separation, when the entry batteries assumed all of the spacecraft electrical load, the minimum main-bus voltage recorded was 26.8 V dc. The voltage was lower than desired, but it gradually increased to 27.8 V dc 3 seconds after separation. A repetition of the Apollo 7 low-voltage alarm was prevented by maintaining a high state of charge on the entry batteries, preloading the batteries prior to separation to increase internal temperature, and reducing loads after separation.

The total capacity remaining at landing was estimated to have been 86.34 A-h (28.6, 30.4, and 27.8 A-h for batteries A, B, and C, respectively).

NASA-S-69-640

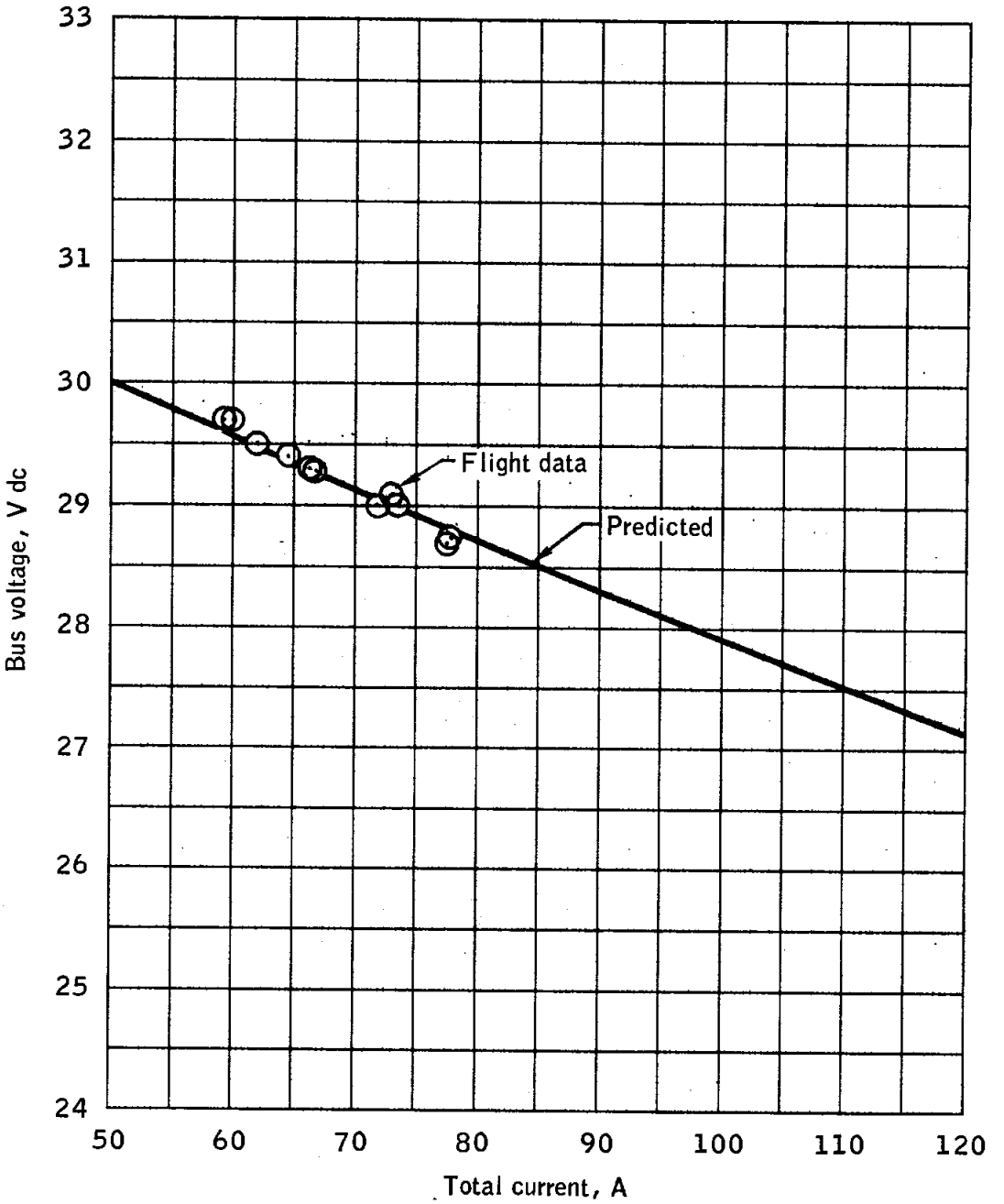

Figure 6.5-1.- Performance of three-fuel-cell system.

NASA-S-69-641

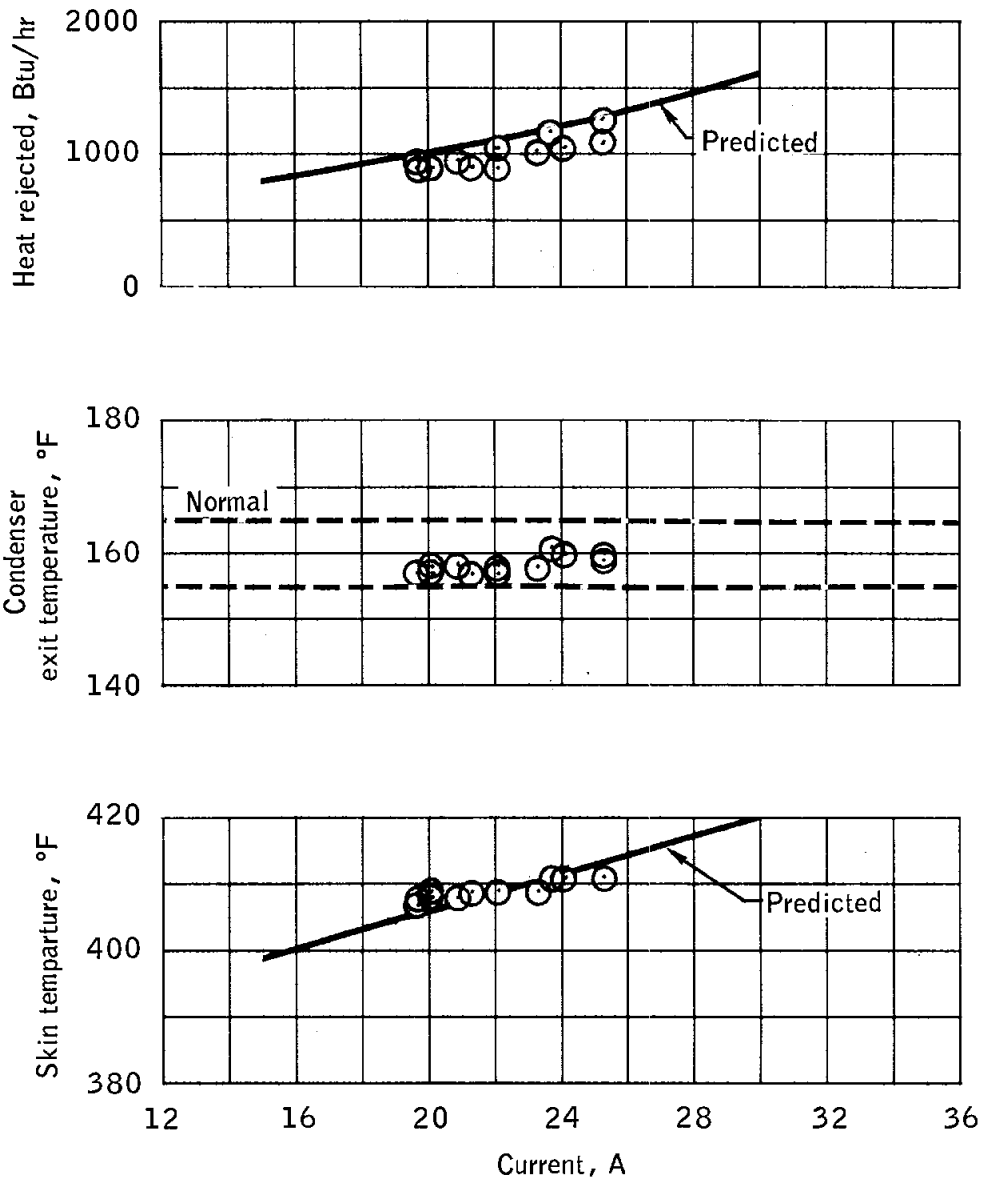

(a) Fuel cell 1.

Figure 6.5-2.- Thermal performance of fuel cells.

NASA-S-69-642

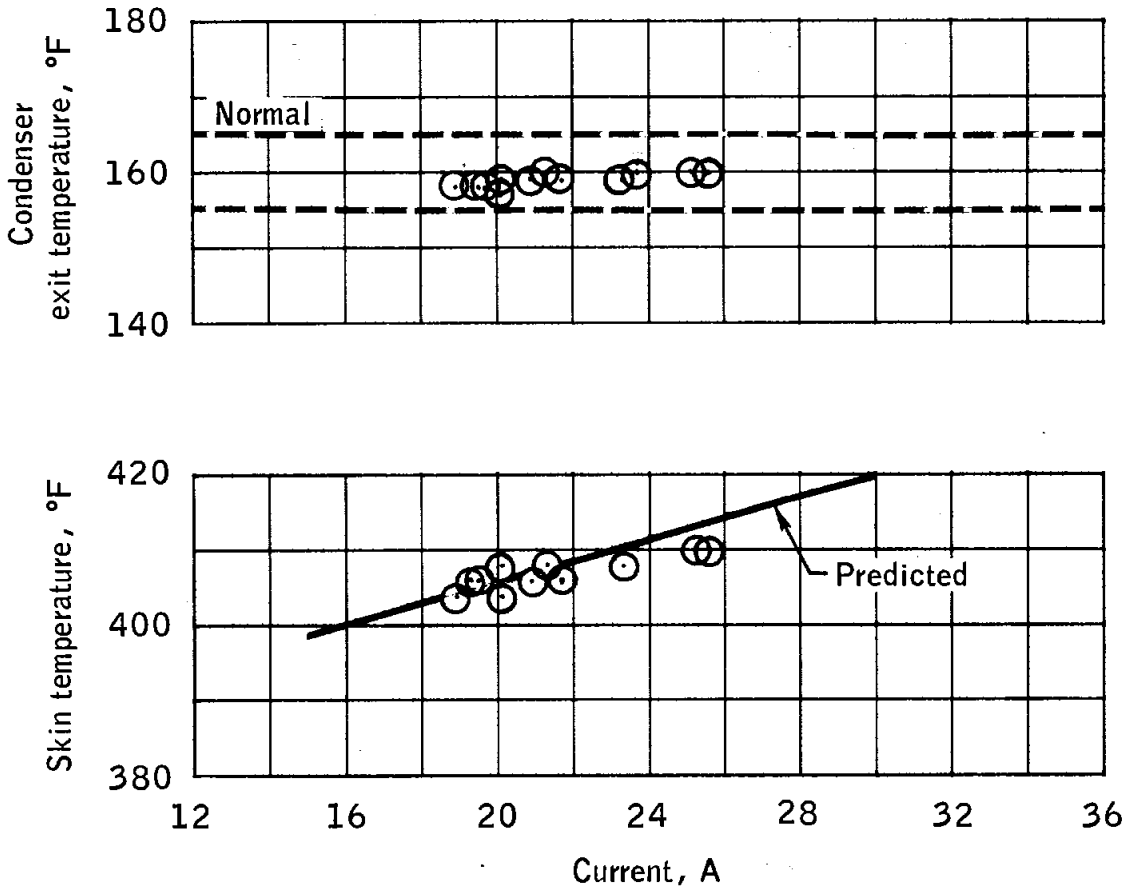

(b) Fuel cell 2.

Figure 6.5-2.- Continued.

NASA-S-69-643

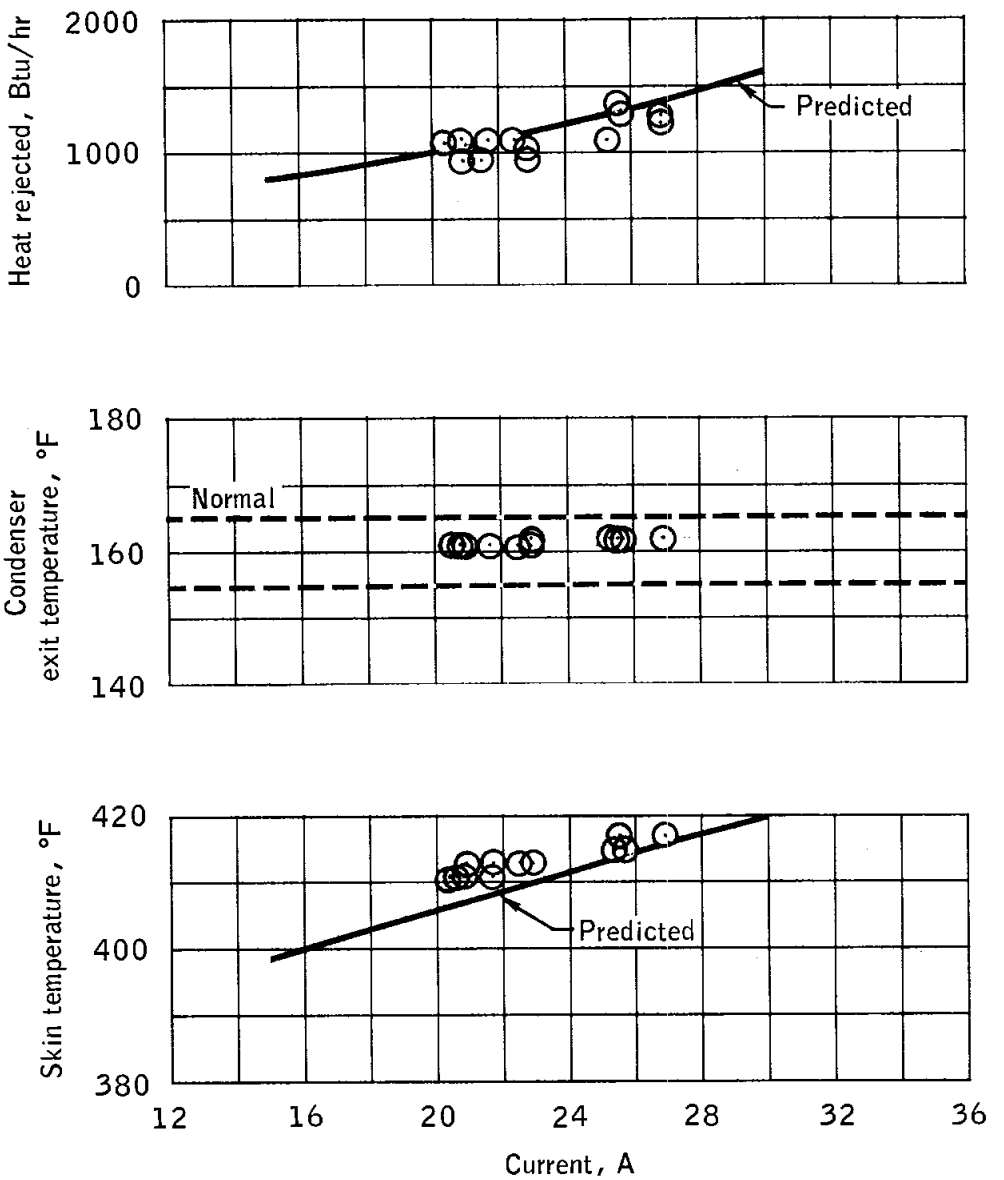

(c) Fuel cell 3.

Figure 6.5-2.- Concluded.

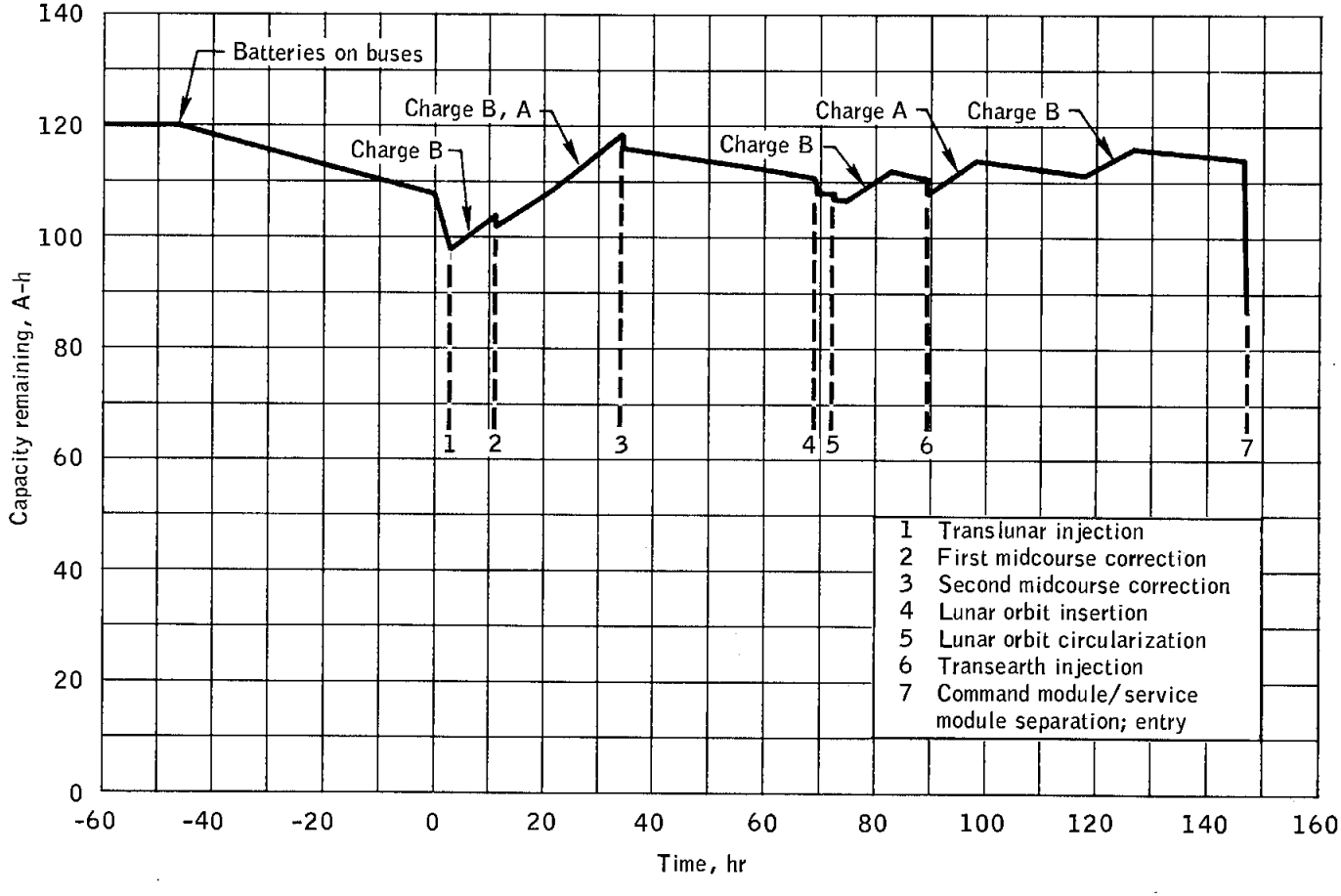

Figure 6.5-3.- Battery capacity history.

6.6 CRYOGENIC STORAGE

The cryogenic storage system satisfactorily supplied reactants to the fuel cells and metabolic oxygen to the environmental control system. At launch, the total oxygen quantity was 639.4 pounds (154.4 pounds above the minimum requirements) and the total hydrogen quantity was 49.1 pounds (2.3 pounds above minimum requirements). The overall consumption from the system was less than expected, a direct result of a lower-than-predicted average power level.

The oxygen and hydrogen quantities at various mission phases are shown in figure 6.6-1. During the mission, 254 pounds of oxygen and 26.6 pounds of hydrogen were consumed. This overall consumption corresponds to an average fuel cell current of 70.6 amperes with an environmental control system flow rate of 0.3 lb/hr of oxygen.

The heat leak for the oxygen tanks is shown in figure 6.6-2. Testing prior to the flight indicated that the calculated heat leak for these systems is very sensitive to system volumetric changes during pressure decays and to errors in the pressure measurement. Also, the effect of launch vibration and acceleration on the heat leak is brief and low in magnitude (approximately 10 percent). As a result of the Apollo 8 data, the heat leaks for Apollo 7 were reevaluated and are shown in the figure for comparison. The data scatter is a result of the confined range in the pressure instrumentation.

The allowable heat leak for cryogenic oxygen before the tanks require venting depends on the quantity remaining. In the worst case, a heat leak of 28 Btu/hr is allowable for a quantity remaining of 109 pounds per tank. The allowable heat leak becomes greater (less restrictive) at all other remaining quantity levels. The observed heat leak for Apollo 8 was always well within the allowable heat-leak criteria, and venting was not required. Since the actual heat leak after approximately 40 hours elapsed time was less than 28 Btu/hr, venting would not have occurred thereafter at any quantity level, including the design point of 109 pounds.

NASA-S-69-645

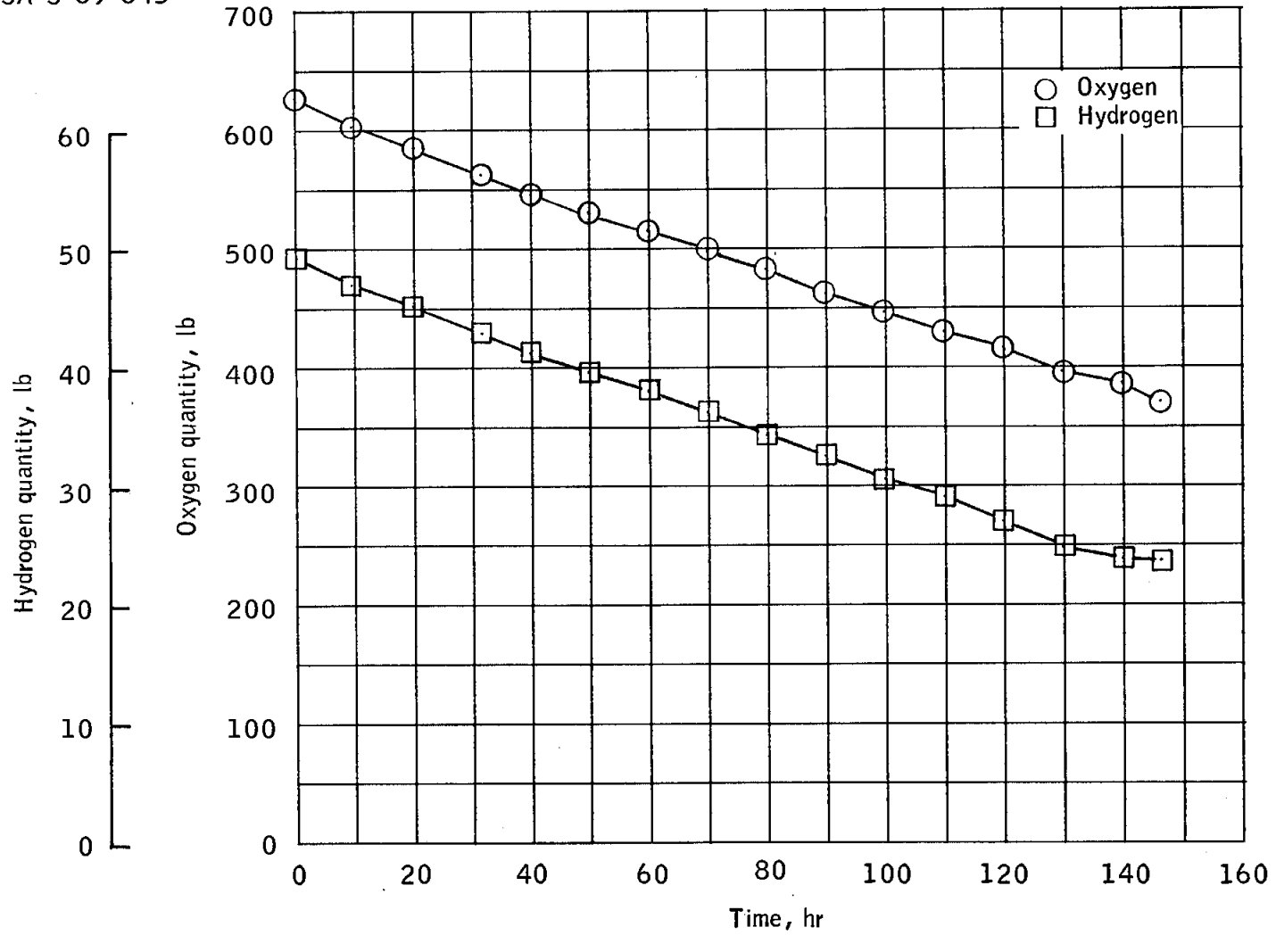

Figure 6.6-1.- Cryogenic quantity profiles.

NASA-S-69-646

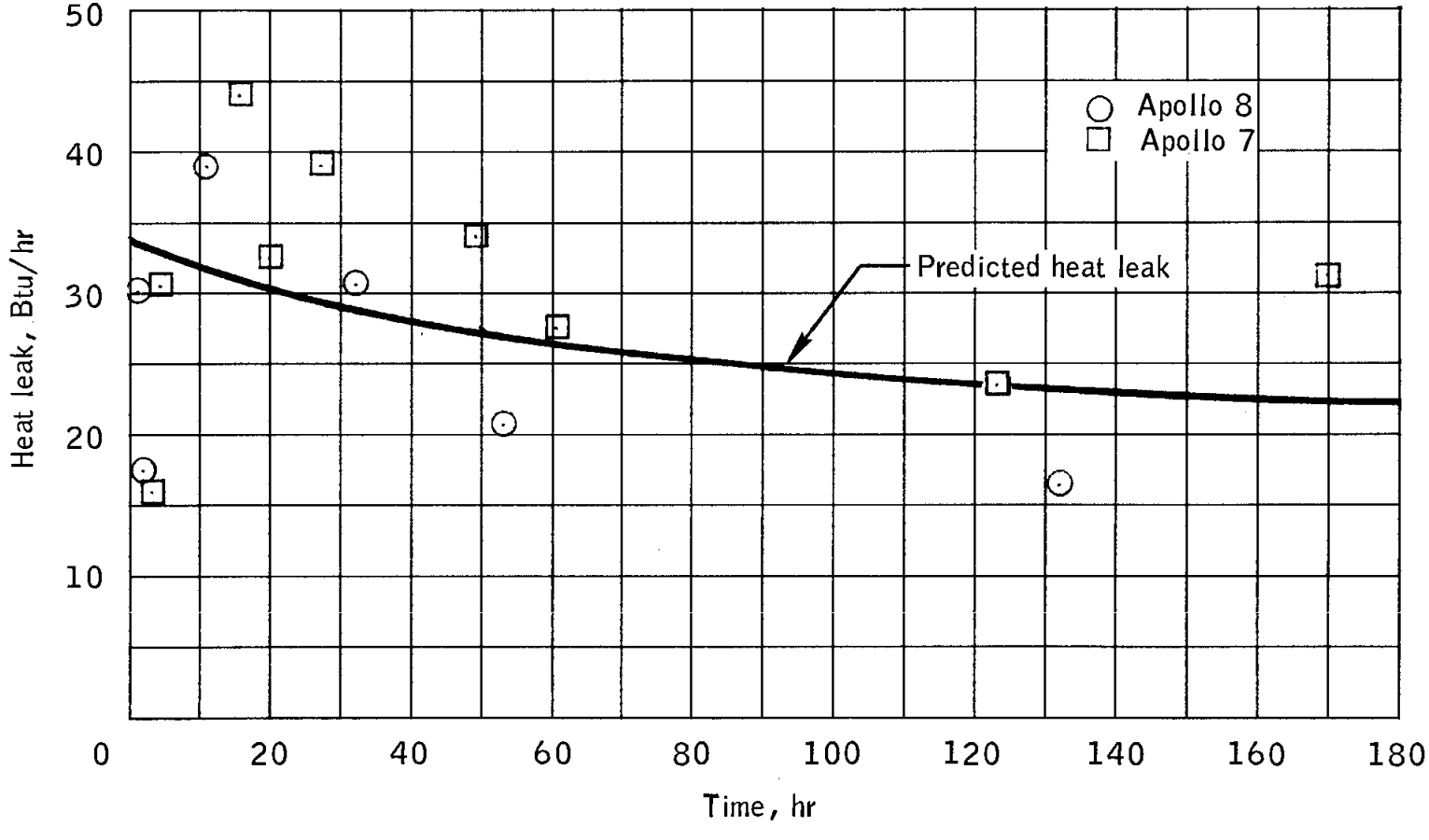

Figure 6.6-2 - Thermal performance for the cryogenic oxygen system on Apollo 8 and Apollo 7.

6.7 COMMUNICATIONS

The communication system satisfactorily supported the mission, and the applicable mission objectives were acheived. The S-band communications system provided good quality voice throughout the mission, and the VHF link provided good voice within its normal range capabilities. The quality of recorded voice played back through the data storage equipment varied from very good to unusable. The performance of the real-time and playback telemetry channels was excellent and consistent with received power levels. The quality of television pictures ranged from good to excellent. The received downlink S-band signal levels for both the phase modulation (PM) and the frequency modulation (FM) links corresponded to preflight predictions. Communication system management, including antenna switching, was very good.

6.7.1 Spacecraft Equipment Performance

The onboard communications equipment provided the necessary mission support throughout the flight, and the only discrepancy was after landing, when a recovery swimmer was unable to communicate with the crew through the swimmer interphone. Testing of the actual hardware, however, did not reveal a problem, and no conclusive explanation can be given for this discrepancy (see section 12). During the mission, all S-band communication modes were verified (with the exception of the emergency key mode), and performance was nominal in all cases. Table 6.7-I is a summary of significant communications events.

The VHF system was used during launch and earth orbit. Reception of a VHF signal at distances up to 34 000 n. mi. during transearth coast greatly exceeded expectations, although intelligible voice was not received.

The S-band equipment was used as the primary air-to-ground link throughout the mission. After the operation of both the primary and secondary transponders was verified, the secondary transponder was utilized continously until landing. This transponder transmitted through the secondary power amplifier, which was operated continuously in the high-power mode until just prior to entry.

The S-band FM transmitter was used to transmit television, recorded voice, and recorded telemetry data through the primary power amplifier. The updata link, including a digital decoder and logic relays, was used successfully for computer updates and real-time commands, such as rewinding and playing back recorded data, switching data, rates, switching from normal to backup voice, and switching spacecraft antennas. The VHF recovery beacon was turned on shortly after main parachute deployment and operated normally.

The crew was dissatisfied with the lightweight headsets because of mechanical difficulties in wearing them. Rapid head movements and the spring action of the connecting cabling would sometimes move the whole assembly off the head, as had been observed before flight. The electrical performance of the headsets was satisfactory. A new headset configuration to be used on subsequent flights should resolve the problem.

The Apollo 8 mission was the initial flight for the high-gain antenna. This antenna, which deployed in 8.4 seconds after adapter panel jettison, was used in all three beam widths for communications.

Because of an installation discrepancy, the antenna control about the yaw axis was reverse connected, and a decal was placed on the panel before flight to correct the erroneous indication. Gains observed for the high-gain antenna were similar to those measured during ground checkout, as shown in the following table.

Mode	Gain change, db	
	Ground checkout	Inflight
Transmit:		
Narrow to wide beam	17.1	16.5
Narrow to medium beam	5.3	5.5
Receive:		
Narrow to wide beam	16.4	10.0

An area of concern had involved antenna performance when the line of sight to earth passed through a service module reflection area. However, acquisition beyond and automatic tracking within this region were successfully performed during the second television transmission.

A special test of the automatic acquisition mode of the high-gain antenna began at approximately 110:14:00, and results indicate that the antenna performed as predicted. During this test, the pitch and yaw plane look angles to earth were monitored by telemetry. These angles, which correspond to the antenna pointing direction when tracking the earth, are plotted in figure 6.7-1 for two spacecraft revolutions about the roll axis. Figure 6.7-2 shows the downlink signal strength for the first revolution of this test. The strong signal at the time of the test provided an earth presence signal; consequently, the antenna remained against the gimbal limits for approximately 10 minutes during each revolution. However, this position is dependent on spacecraft orientation and for such a brief period is not detrimental to antenna operation.

Test results indicate that automatic reacquisition will operate satisfactorily without crew participation.

Six television transmissions were made during the flight and included pictures of the spacecraft interior, the lunar surface, and the earth. The quality of all transmissions was satisfactory, except for the initial attempt at viewing the earth with the 100-mm telephoto lens. These initial views were of poor quality because of the higher-than-expected contrast between the earth and its background. The automatic light control of the camera adjusts to a value determined by averaging the light over the entire viewfield, thereby considerably overexposing bright objects. A procedure was developed for use of filters from the 70-mm camera, and subsequent telecasts of the earth using the telephoto lens with a red filter were satisfactory. During the lunar orbit period, a wide-angle 9-mm lens and suitable filters were used to obtain excellent views of the lunar surface. The six telecasts are summarized in the following table.

Transmission	Acquisition time, hr:min:sec	Duration, min:sec	Remarks
1	31:10:36	23:37	Good interior
2	55:02:45	25:38	Good earth scenes
3	71:40:52	12:00	Some good lunar
4	85:43:03	26:43	Excellent lunar and some earth scenes
5	104:24:04	9:31	Interior
6	127:45:33	19:54	Earth scenes

6.7.2 Spacecraft/Network Performance

Two-way phase lock with the spacecraft S-band equipment was established by the Manned Space Flight Network prior to launch. The Merritt Island, Grand Bahama Island, Bermuda Island, and *USNS Vanguard* sites successfully maintained the phase lock through orbital insertion, except during station-to-station handovers. Communication system performance was nominal throughout this time period. Proper operation of the normal and backup communication systems was verified during parking-orbit checkout.

The *USNS Mercury* and Hawaii sites provided coverage of the translunar injection maneuver. This coverage was continuous except from 2:52:00 to 2:53:00, when the line-of-sight to the spacecraft was interrupted by a mechanical limit in the Hawaii S-band antenna pattern.

A time history of the S-band system management during translunar coast is presented in figure 6.7-3. Included in this figure is the nominal received carrier power levels at the three primary Manned Space Flight Network sites; the site transmitting the uplink S-band signal; and the utilization of omnidirectional and high-gain antennas, high- and low-bit-rate telemetry, and normal and backup downvoice.

Communications during passive thermal control were maintained by switching sequentially through the four omnidirectional antennas or by switching between the high-gain antenna and one or more omnidirectional antennas. During translunar coast, the passive thermal control attitude was such that optimum sequential switching between the four omnidirectional antennas would have provided gains greater than zero dB during the entire revolution. Although no means was available for optimum antenna switching, antenna management produced good signal strengths throughout the mission.

The spacecraft omnidirectional antenna system was used for communications during most of the translunar coast. The maximum received carrier power level during operation on these antennas agreed with predictions, based primarily on measured spacecraft/ground parameters and slant range.

As shown in figure 6.7-3, checkout of the spacecraft high-gain antenna was initiated in the wide-beam mode at 6:33:04. The received downlink carrier power level during this check agreed with predictions. Basic compatibility between the high-gain antenna tracking system and the various S-band uplink signal combinations was verified during the two periods of high-gain antenna operation between 12:00:00 and 13:00:00.

The high-gain antenna was used periodically during the remainder of translunar coast with excellent results.

A time history of S-band system management during the lunar orbit phase is presented in figure 6.7-4. The high-gain antenna was used at least once during each lunar orbit. The received downlink power level of the PM system carrier averaged minus 103 dBm during coverage by the Goldstone site, when the downlink signal combination consisted of normal voice, high-bit-rate telemetry, and turnaround ranging. This power level agreed favorably with the predicted value of minus 102 dBm. The received FM signal power level during the same time periods averaged minus 97 dBm. The received uplink carrier power level with narrow-beam operation of the high-gain antenna was from 4 to 9 dB below the predicted value, but this did not affect communications.

Telemetry and voice data recorded while the spacecraft was behind the moon were played back through the high-gain antenna during each revolution. Solid frame synchronization by the telemetry decommutation

system was reported during each of these playbacks. The quality of the recorded voice was dependent on the playback-to-record data storage equipment tape-speed ratios and the receiving Manned Space Flight Network site. Good quality voice was obtained during playbacks accomplished at the record speed. However, the quality of the voice received at Madrid during the playbacks at 32 times the record speed was, in general, unusable because of a high level of background noise. The quality of the voice received at the Goldstone and Honeysuckle sites during playbacks at 32 times the record speed was good. Therefore, it appears that the unusable voice may have been caused by equipment or procedural problems at the Madrid site.

The only significant communications difficulty occurred as the spacecraft emerged from lunar occlusion following transearth injection. Two-way phase lock was established at 89:28:47 (approximate predicted time); however, two-way voice contact and telemetry decommutation system synchronization were not achieved until approximately 5-1/2 and 14-1/2 minutes later, respectively. These delays were caused by a combination of events and procedural errors. As shown in figure 6.7-5, an unsuccessful high-gain antenna acquisition was attempted at 89:30:45. If this acquisition had been successful, normal communications capability would have been established prior to the first attempt to contact the crew. The data indicate that the high-gain antenna acquisition may have been attempted while the line-of-sight to the earth was within the service module reflection region and that the reflections may have caused the antenna to track on a side lobe.

The spacecraft was configured for high-bit-rate transmission (transearth-injection recording requirement). Therefore, the command (89:29:29), which configured the spacecraft for normal voice and subsequent playback of the data storage equipment, selected an S-band signal combination which was not compatible with the received carrier power. Two-way voice communications were not achieved until backup down-voice was reselected by command at 89:33:28. Telemetry decommutation frame synchronization was not achieved until the high-gain antenna was reacquired in the wide beamwidth at approximately 89:43:00. A history of S-band system management during the transearth coast is presented in figure 6.7-6.

During passive thermal control, communications were maintained by ground command switching between two diametrically opposite omnidirectional antennas (B and D), thus verifying the feasibility of such a procedure. Low-bit-rate telemetry data and backup down-voice were received during most of each spacecraft revolution of passive thermal control. High-bit-rate telemetry data were received during the periods when the line-of-sight to earth passed through the highest portion of the active omnidirectional antenna lobe.

The management of the communication system during translunar and transearth coast provided an excellent opportunity to compare high-bit-rate telemetry capability with predictions. Generally, the mean time between losses of telemetry frame synchronization decreased rapidly when the received carrier power was below minus 120 dBm. Predictions show that within a received power range of minus 119 to 122 dBm, the bit error rate for an 85-foot antenna would be approximately 0.001, and for a received carrier power range of minus 122 to 125 dBm, the bit error rate would be approximately 0.01. Figure 6.7-7 shows the relationship between received carrier power levels and telemetry performance during transearth coast. The measured threshold for 0.001-bit-error-rate telemetry occurred between minus 121 and 123 dBm and for 0.01-bit-error-rate telemetry, between minus 124 and 126 dBm.

During portions of both the translunar and transearth coast phases, the 210-foot antenna at Goldstone was used for reception of high-bit-rate telemetry, while the spacecraft was transmitting through the omnidirectional antennas. This coverage provided more continuous high-bit-rate data than would have been possible using the 85-foot antenna.

Communications performance was nominal during transearth coast and entry, and voice contact with the spacecraft was established after communications blackout and before landing.

TABLE 6.7-I.- COMMUNICATIONS EVENTS

Time, hr:min:sec	Event	Remarks
00:00:00	Lift-off	VHF and S-band voice and data excellent
00:02:00	S-band handover, MILA to GBM	First S-band handover
01:31:31	Backup voice check	Weak but clear
01:32:18	Normal S-band voice check	Loud and clear
03:20:55	Spacecraft/S-IVB separation, high gain antenna deployment	Nominal. Antenna deployed successfully and latched in position 8 seconds after separation
04:39:54	Last reported VHF up-link reception	Range of 20 000 n. mi. slightly greater than expected
04:48	Last reported VHF down-link reception	Good reception after ground squelch adjusted
06:33:04	First high gain antenna usage	Nominal.
12:03:01	Begin S-band mode testing	All modes functioned as expected.
31:10:36	First television transmission	Inside spacecraft picture good but earth picture very poor due to unexpected high light intensity of earth and no filter for television camera
110:16:55	Test of high gain antenna automatic acquisition	Operation time of 52 minutes 9 seconds; successfully reacquired twice and performed normally
142:16:00	First reception of ground VHF during transearth coast	Range approximately 34 000 n. mi.
145:52:00	Good 2-way VHF voice	Signal strength improved by switching VHF antenna
146:49	Enter S-band blackout	
146:55:38	Recovery antennas deployed	Main parachutes deployed
146:56:01	VHF and recovery beacon turned on	Excellent two-way VHF voice
146:57:05	First reported recovery beacon contact	Reported by helicopter 2
147:00:09	End of onboard voice recording when recording equipment turned off	Approximate spacecraft altitude of 600 to 1000 feet
147:00:50	Recovery voice interrupted	Spacecraft turned to stable II after landing

NASA-S-69-647

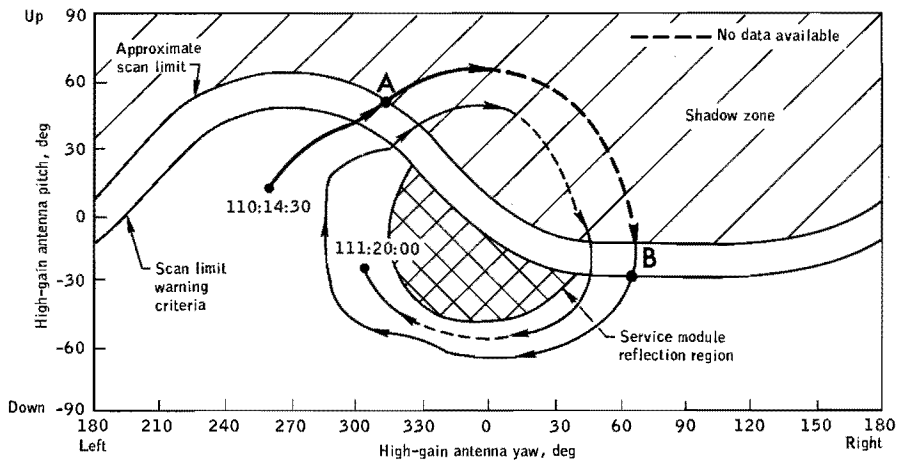

Figure 6.7-1.- High-gain antenna line of sight to earth during automatic reaquisition test.

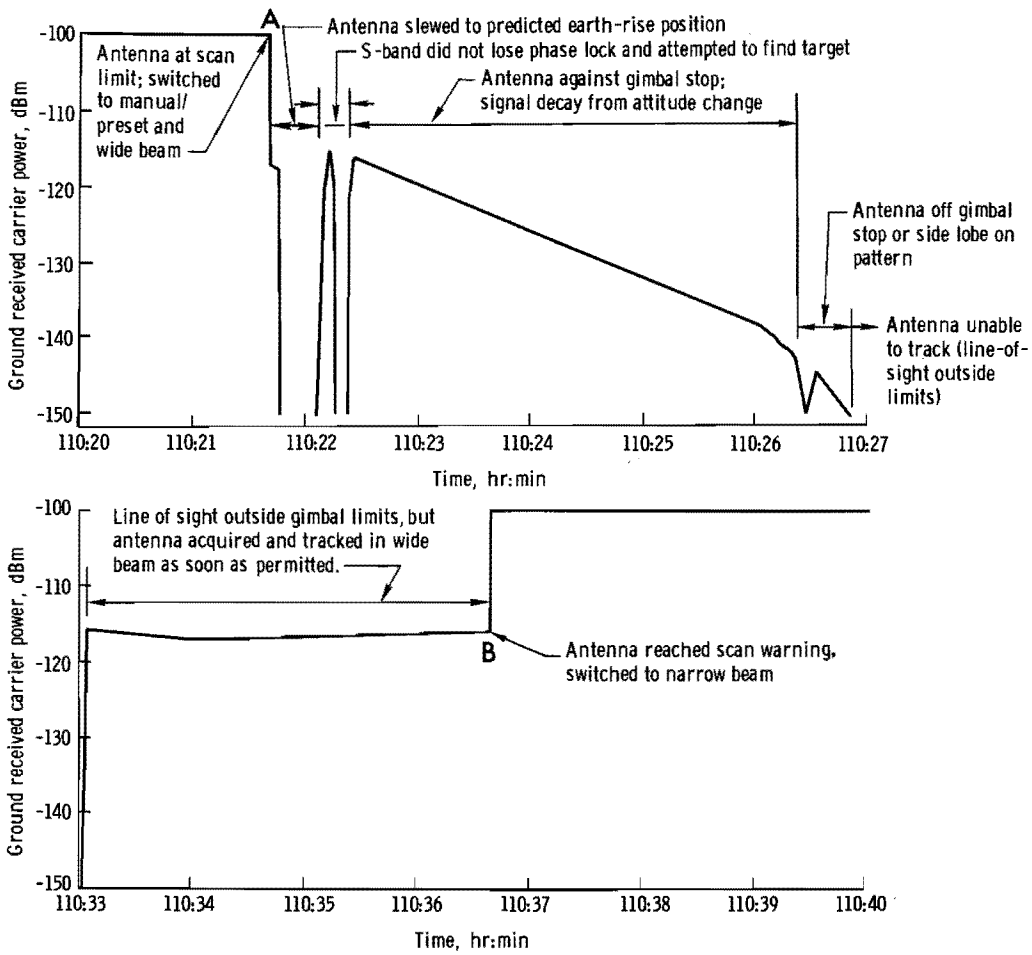

Figure 6.7-2. - Carrier power levels during antenna test.

NASA-S-69-648

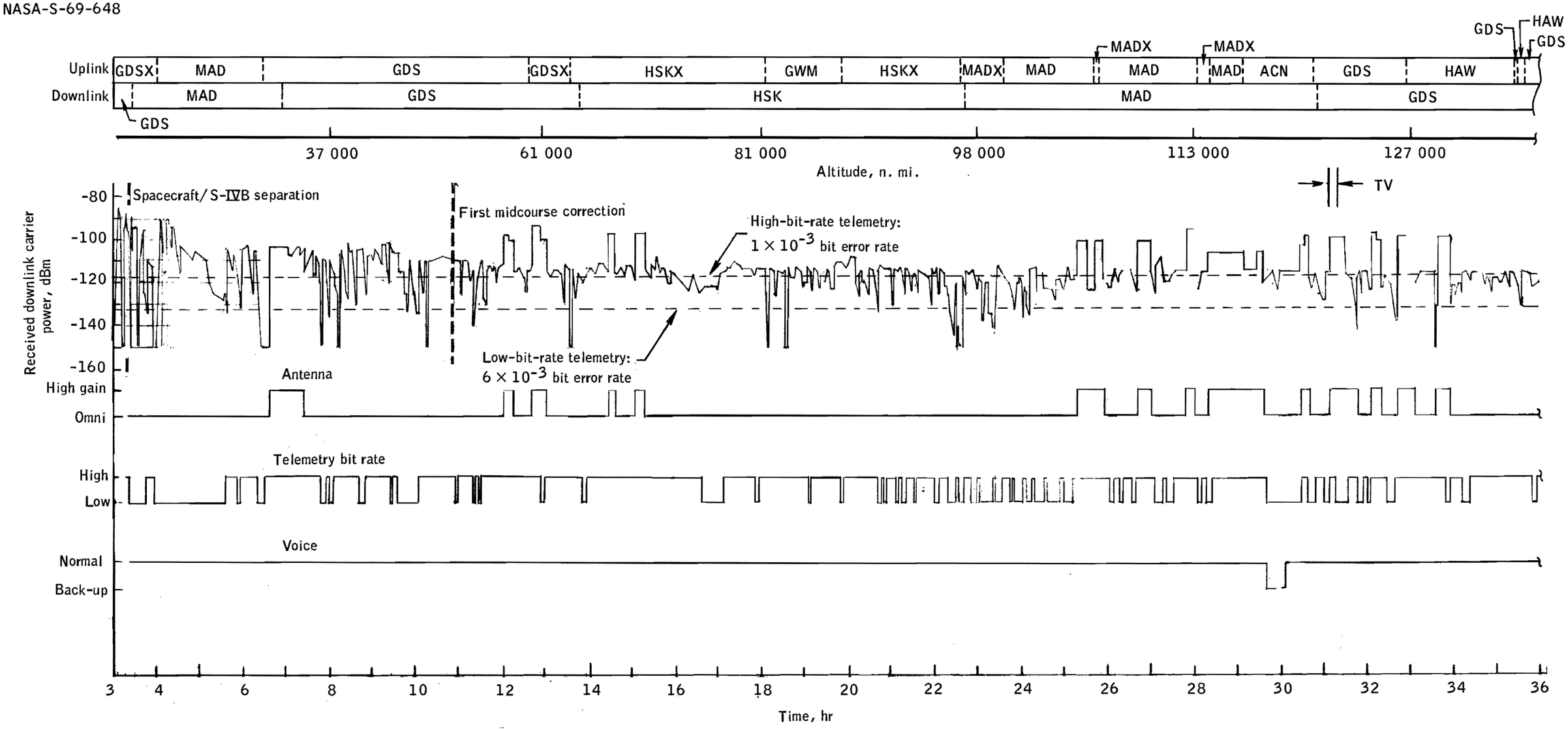

(a) 3 to 36 hours.

Figure 6.7-3.- Communications timeline, translunar.

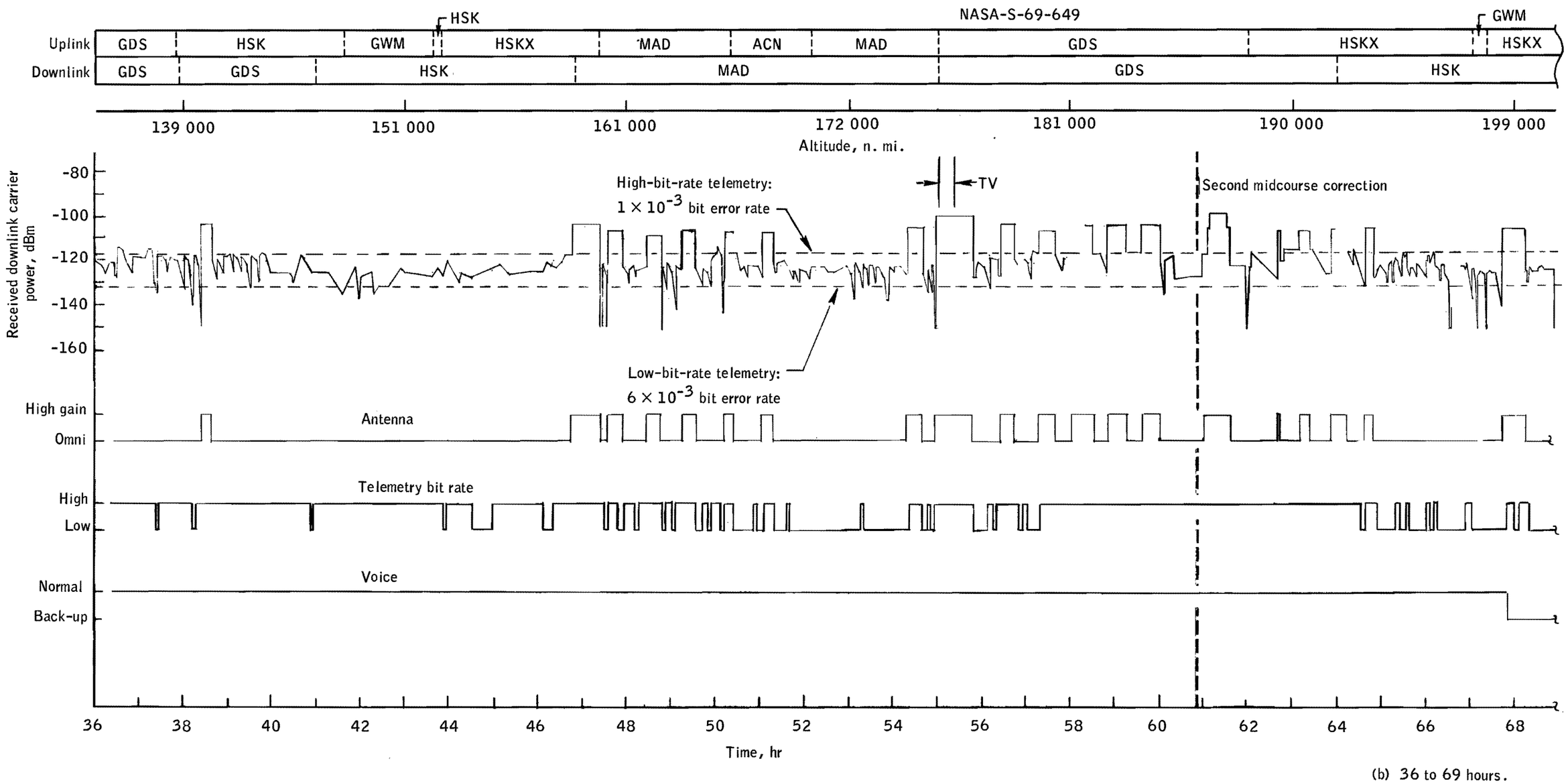

(b) 36 to 69 hours.

Figure 6.7-3.- Concluded.

NASA-S-69-650

Uplink		HSKX		MAD		MAD		MADX → MAD		MAD		GDS		GDS		GDS		HSKX		HSKX
Downlink		HSK		MAD		MAD		MAD		MAD		GDS		GDS		GDS		GDS		GDS HSK

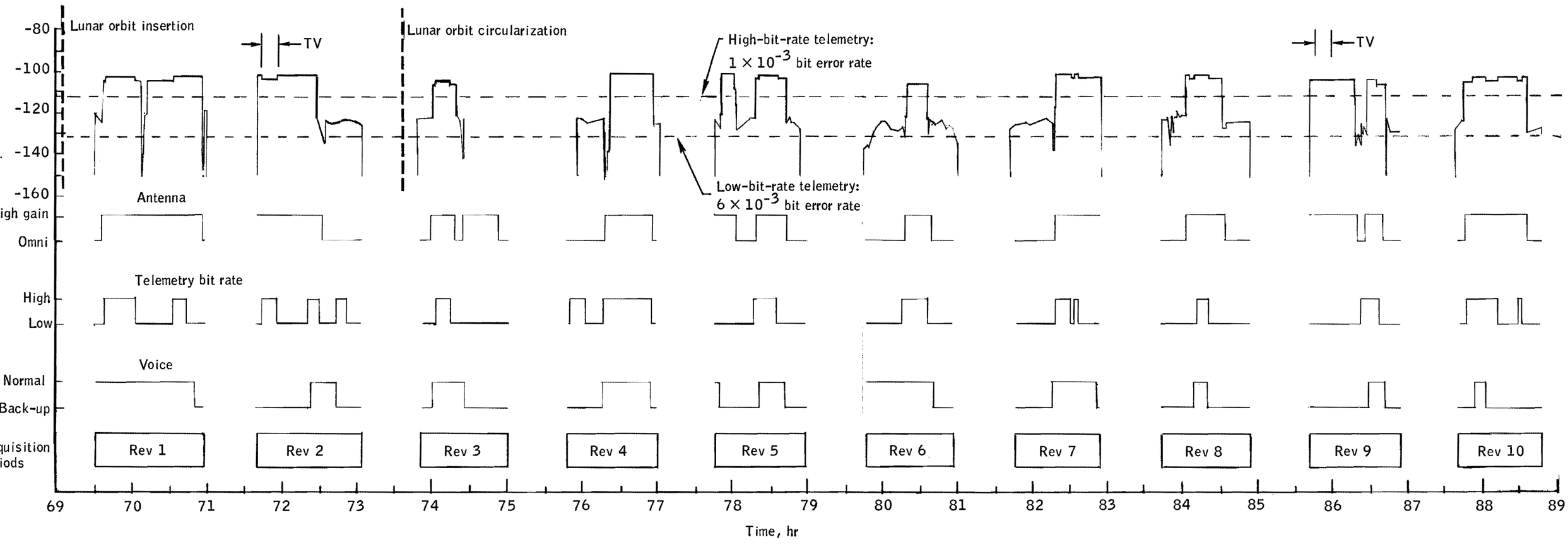

Figure 6.7-4.- Communications timeline, lunar orbit.

NASA-S-69-650

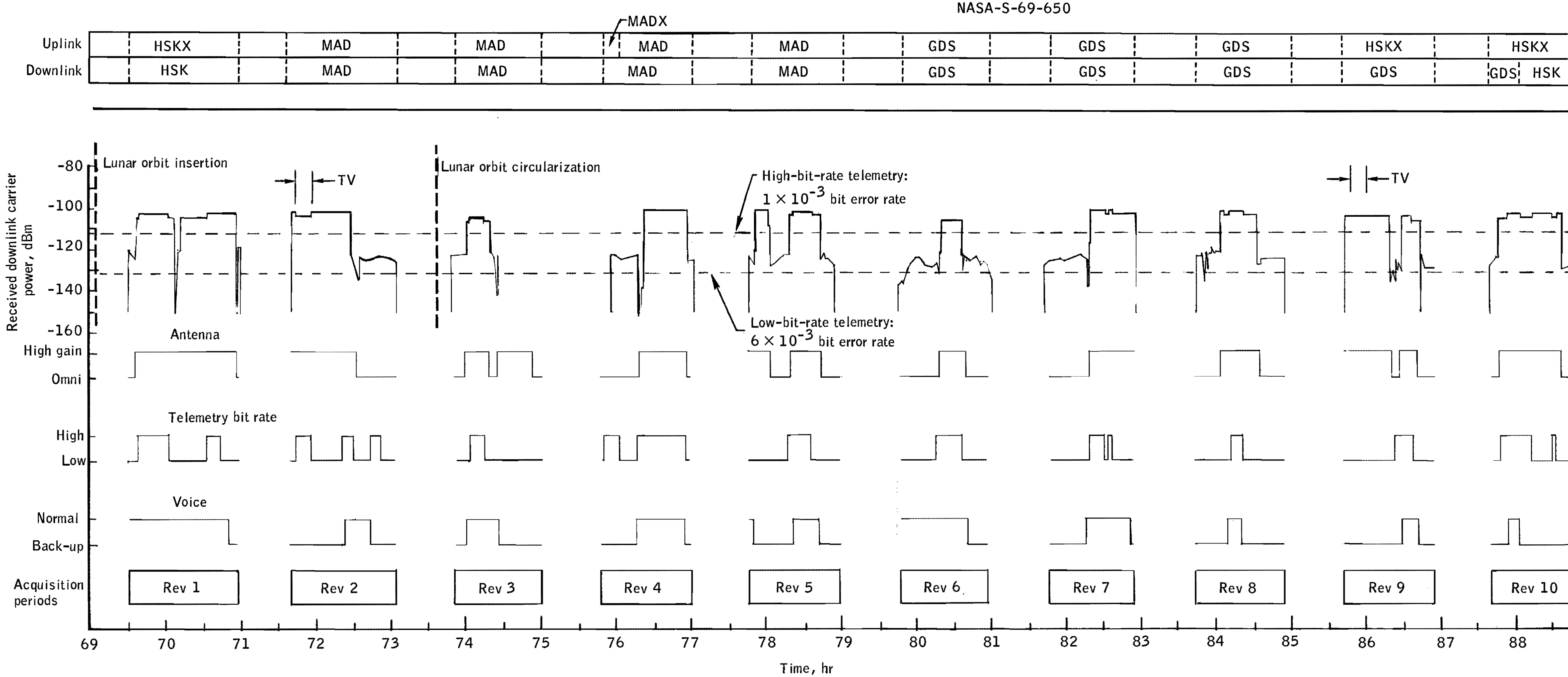

Figure 6.7-4.- Communications timeline, lunar orbit.

NASA-S-69-651

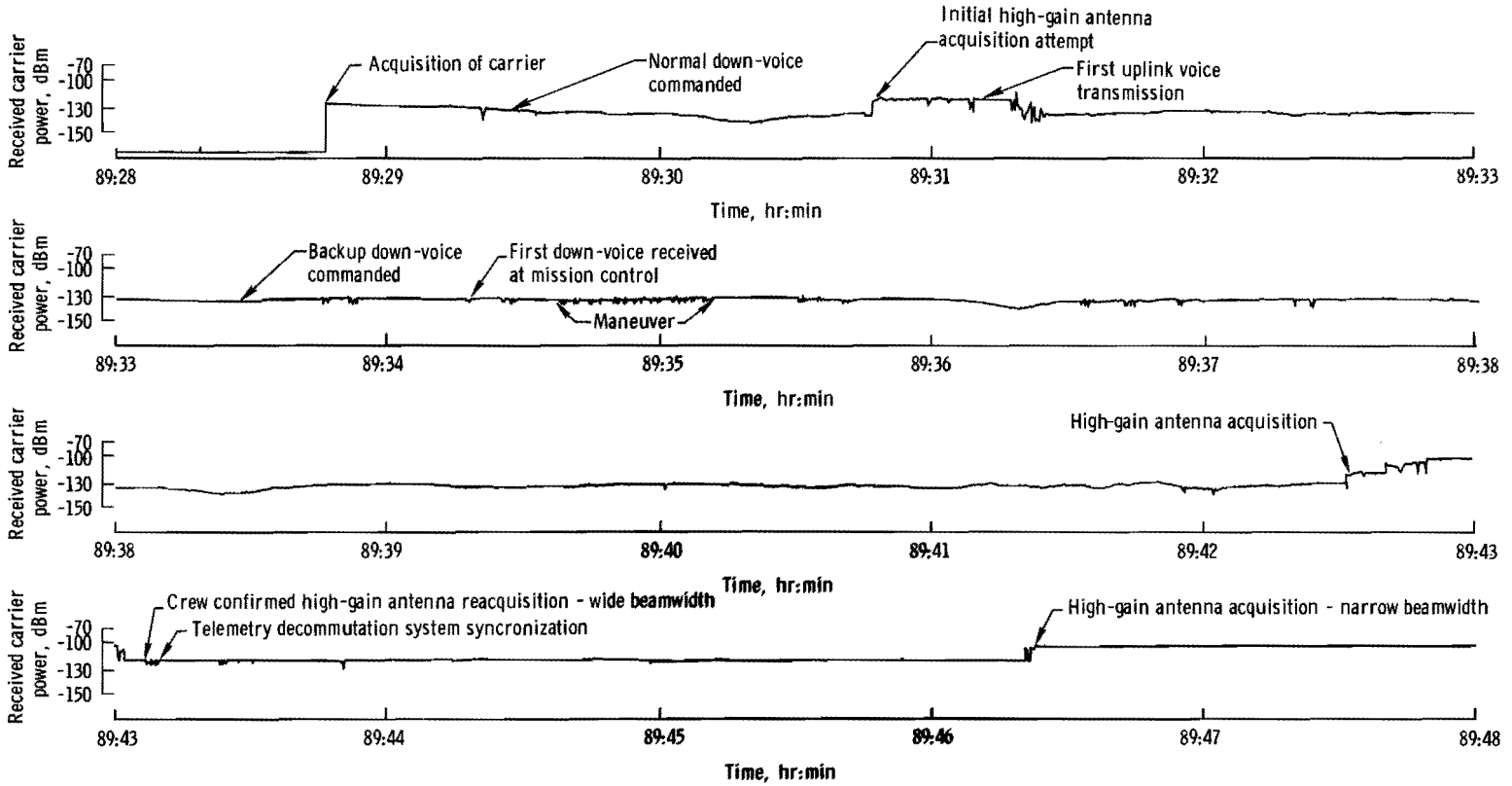

Figure 6.7-5.- Received carrier power at Honeysuckle primary site following transearth injection maneuver.

NASA-S-69-652

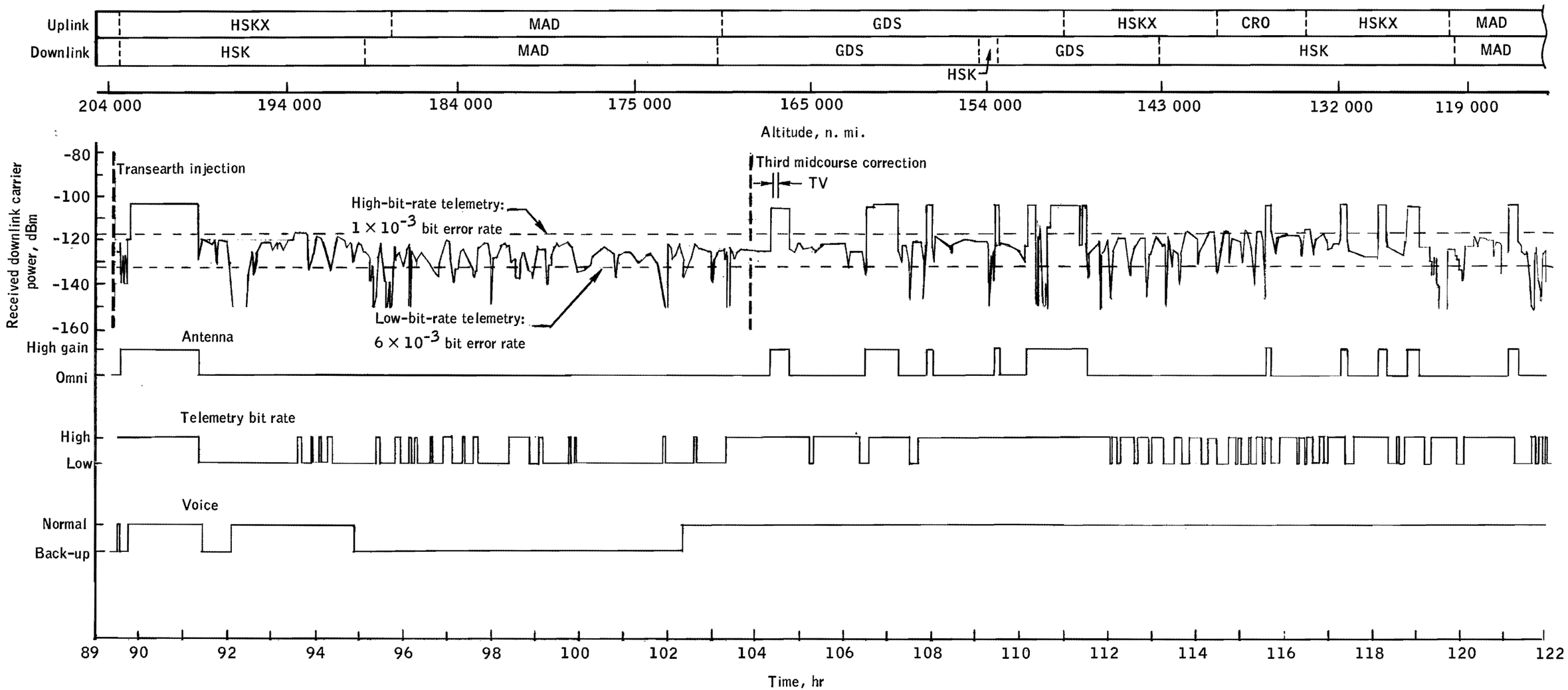

(a) 89 to 122 hours.

Figure 6.7-6.- Communications time line, transearth.

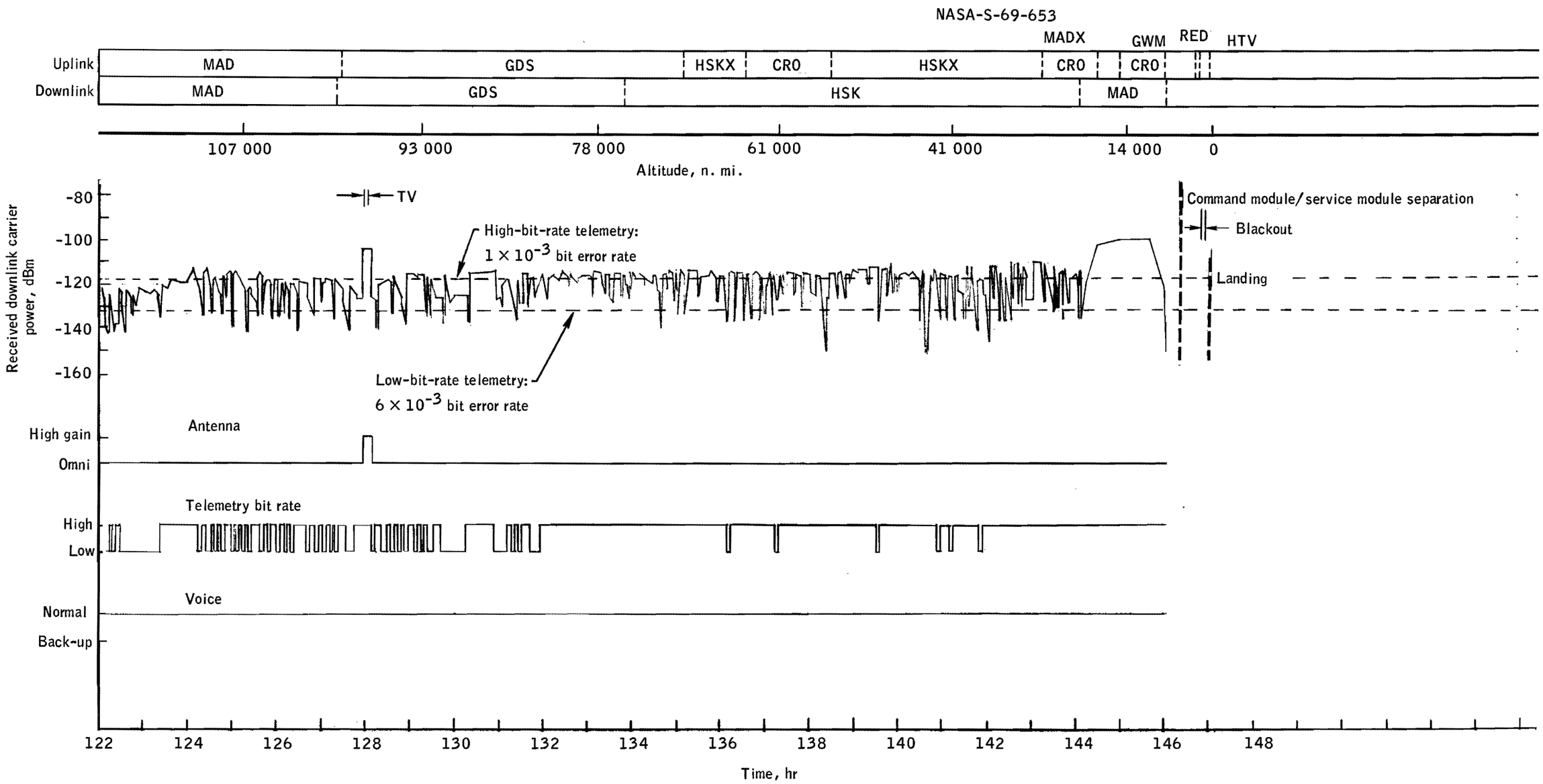

(b) 122 to 147 hours.

Figure 6.7-6.- Concluded.

NASA-S-69-654

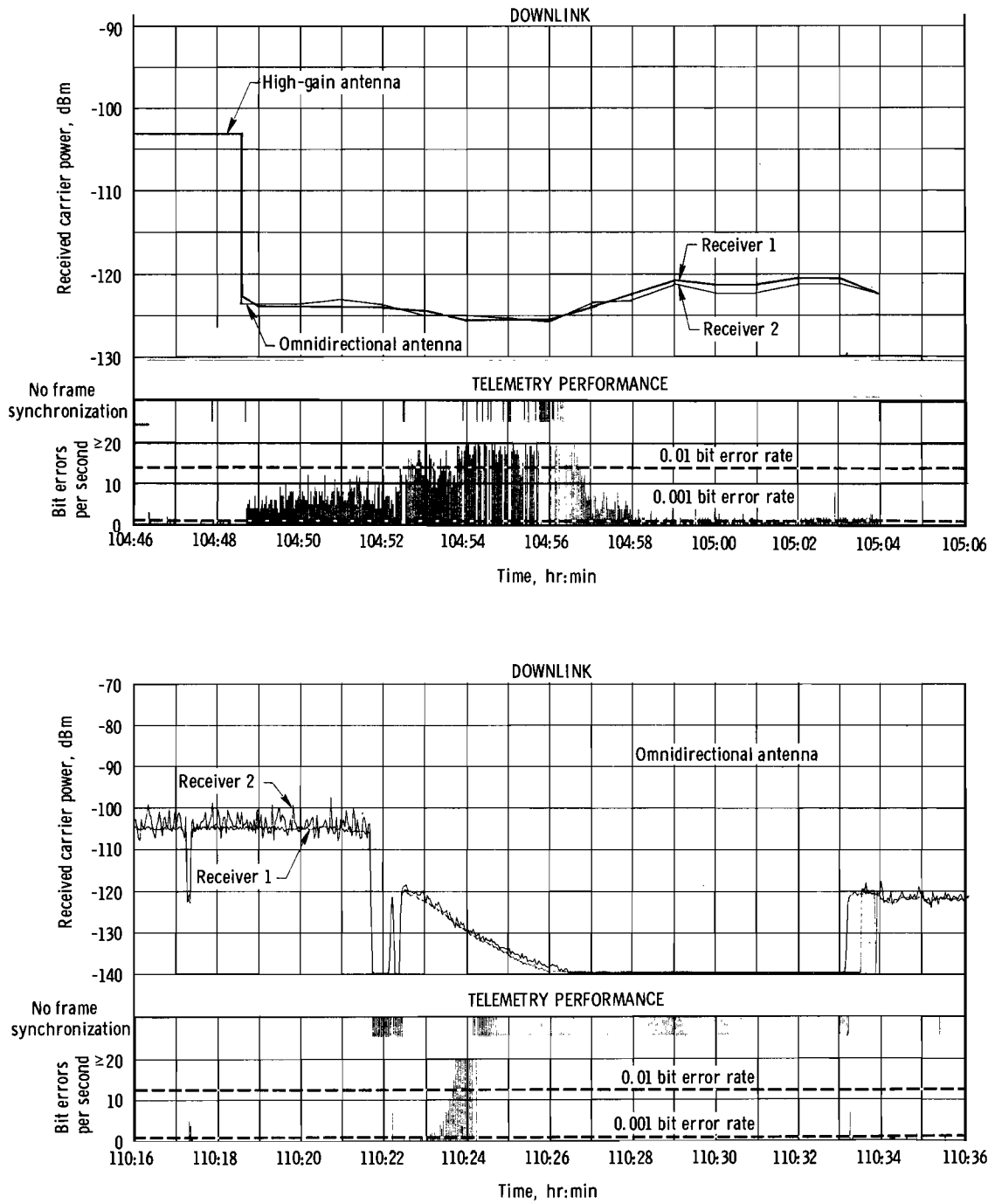

Figure 6.7-7. - Comparison of bit error rate and carrier power level.

6.8 INSTRUMENTATION

The instrumentation system provided for monitoring of 316 operational and 36 flight qualification parameters in the command and service modules and 6 flight qualification parameters in the lunar module test article. Of these, seven were inoperative.

6.8.1 Operational Instrumentation

The performance of the operational measurements and associated equipment was good. Prior to flight, two measurements required waivers, and one measurement exhibited a calibration shift. The propellant utilization and gaging system was believed to have shorted in the fuel sump tank and was disabled prior to launch. After lift-off, all operational instrumentation performed satisfactorily with the exception of three measurements. Additionally, the biomedical instrumentation experienced intermittent electrocardiogram output, suspected to be a loose sensor on the Lunar Module Pilot. Readings from two of the three personnel radiation dosimeters did not agree with the more sensitive telemetry instrumentation. During postflight testing, the dosimeters operated satisfactorily at acceptance-test input levels (higher than experienced inflight). An aluminized particle, which could have been suspended under zero-g conditions, was found inside the ionization chamber of the unit that indicated high values during flight.

The temperature measurements of the nuclear particle detector and the analyzer were noisy, and the requirements for these measurements were waived prior to launch. Both measurements returned to normal quality after translunar injection. The outlet pressure of the secondary glycol pump in the environmental control system exhibited a positive calibration shift of approximately 4.4 pounds during spacecraft checkout. The constant bias was considered in real-time system monitoring. This calibration is believed to have resulted from over-pressurization during preflight servicing, a discrepancy that has been observed in previous tests.

The primary radiator outlet temperature failed at 120:04:00. The rubber insert in the connector between the sensor and signal conditioner was cracked and moisture was found in the connector.

At 143:53:00, data from the potable water quantity measurements exhibited a rapid decrease in quantity from 100 percent to 57 percent and became erratic thereafter, decreasing gradually to 20 percent just prior to entry. The potable water tank was observed to be full after the flight, and postflight tests isolated the failure to the tank sensor. (See section 12 for further discussion.)

The fuel-cell 2 radiator outlet temperature, located in the service module, exhibited erroneous data during the mission. This temperature was inconsistent with similiar temperature measurements in fuel cells 1 and 3, and since other performance data indicated proper fuel cell operation, the measurement was considered invalid.

6.8.2 Flight Qualification Instrumentation

The flight qualification instrumentation system performed satisfactorily. During the powered flight phases, vibration levels were recorded on six occasions. Three measurement discrepancies were noted and four measurements were practically unusable.

One of the four X-axis vibration measurements located on the forward bulkhead near the tunnel was noisy prior to launch and was not usable during the mission. The radial acceleration measurement mounted in the adapter failed at 2:51:00, but this time was after the period of critical adapter load analysis.

6.9 GUIDANCE, NAVIGATION, AND CONTROL SYSTEMS

Performance of the guidance, navigation, and control systems was excellent throughout the mission. Ascent, earth orbit, and translunar injection monitoring functions provided adequate go/no-go information onboard as well as on the ground. Attitude and translation maneuver control was very good. Preliminary midcourse (star/horizon) navigation analyses indicate very close agreement with the Manned Space Flight Network trajectory. The inertial platform was aligned in earth orbit, cislunar, and in lunar orbit, under widely varying visibility conditions, all with satisfactory results. Data were obtained for assessment of landmark tracking navigation accuracy in lunar orbit. Zero-g accelerometer bias and gyro drift stability was good. Onboard return-to-earth targeting appears to have been sufficiently accurate for a safe return had communications been lost. Entry was performed under automatic control with excellent results.

6.9.1 Mission Related Performance

Ascent, parking orbit, and translunar injection.- The inertial measurement unit was inertially fixed at 0.91 second, upon recognition of the lift-off discrete transmitted by the launch vehicle instrument unit. Figure 6.9-1 contains a time history of the attitude errors displayed to the crew on the flight director attitude indicator. These errors represent the difference between the attitude history programmed in the onboard computer and that actually flown by the launch vehicle. The divergences noted immediately after lift-off are characteristic of normal

timing errors, while those near 0:01:10 are attributed to effects of maximum dynamic pressure.

S-IVB and spacecraft gimbal angles were compared during first stage operation. The differences noted were less than on any previous flight (less than 0.1 degree after lift-off transients had subsided).

The initial onboard computer calculation of the reference matrix at lift-off was slightly in error. The reference matrix relates the inertial platform coordinate frame to the earth-centered inertial frame in which both onboard and ground navigation is performed. The error resulted from an inadvertent omission of the centrifugal acceleration correction from the launch pad gravitational direction calculation and caused an approximate 280-arc-second misalignment of the reference matrix. The error had no effect other than to cause errors in the spacecraft/S-IVB go/no-go velocity comparison during ascent.

The translunar injection maneuver and spacecraft/S-IVB separation were performed nominally.

Attitude reference alignments.- The inertial platform was aligned optically 30 times during the mission. Table 6.9-I contains pertinent data for each alignment. The long relief eyepieces, provided for use with the helmet in place and flown for the first time, were used for the initial alignments after translunar injection and no problems were reported. The star angle difference checks shown in the table provide a measure of the alignment accuracy through a comparison of the actual and computed angle between the stars used. In several instances, the crew performed an alignment check using a third star, and they reported excellent checks in all cases.

The orientation determination program (P51) was used once, at 106:42:00, because reference was inadvertently lost as a result of an incorrect program selection. Consequently, the use of the scanning telescope for constellation recognition and coarse alignment in cislunar space was demonstrated. The Command Module Pilot performed the reorientation of the platform with relative ease using the manual procedure required.

The backup attitude reference (stabilization and control system gyro display coupler) was repeatedly aligned to the inertial platform with very good results.

Midcourse navigation.- Midcourse navigation, using both star/earth and star/moon horizon measurements, were performed during the translunar and transearth phases with excellent results; 80 sightings were made translunar and 138 transearth. The initial sets of earth sightings made

between 40 and 50 thousand n. mi. from the earth were used to establish and verify the altitude of the visible horizon threshold. As a result, the onboard computer correction factor for horizon altitude was changed from 32.8 to 18.2 kilometers.

The translunar sightings were evaluated by propagating the resulting state vector forward to pericynthion and comparing the resulting altitude with that computed by the ground tracking network. Preliminary indications are that the pericynthion difference was about 0.1 n. mi. when the data were processed on the ground using a least-squares technique and approximately 0.4 n. mi. when the onboard computation technique was used.

A similar evaluation of the transearth sightings was made by comparing flight-path angles at entry interface. The postflight least-squares fit in this case compared to within 0.01 degree with respect to the ground computed trajectory.

The return-to-earth targeting program (P37) was exercised several times to calculate midcourse corrections. Preliminary comparison of the velocity change calculated onboard with that calculated on the ground indicates that a safe return could have been made if communications had been lost.

Translation maneuvers.- Pertinent data for all translation maneuvers performed are listed in table 6.9-II. All the maneuvers were performed using the digital autopilot, and all control responses were as predicted in preflight simulations. Figures 6.9-2 through 6.9-5 contain time histories of velocity-to-be-gained for each service propulsion maneuver. System performance was nominal in each case. The only significant velocity residual for any maneuver resulted from service propulsion system performance during the first midcourse correction. This maneuver, the first use of the service propulsion system, was targeted for 24.8 ft/sec, with a firing time of 2.4 seconds; however, the actual velocity change was only 20.4 ft/sec. The firing time for 1- to 6-second maneuvers is calculated by the onboard computer before ignition, based on preflight estimates of service propulsion engine performance. The computed firing time of 2.4 seconds was correct for the constants loaded into the computer but was approximately 0.4 second too short for the actual engine performance (see section 6.11).

The other service propulsion engine firings were longer than 6 seconds, and a different method of calculating firing time was utilized. For these, the time-to-go was recalculated every 2 seconds during the firing, based on the actual acceleration, the velocity to be gained, and a prestored estimate of thrust decay after cutoff. Therefore, the low engine thrust discussed in section 6.11 did not affect the desired change in velocity. As shown in table 6.9-II, the residuals were much smaller and within expectations.

Attitude control.- The performance of the digital autopilot and the stabilization and control functions was excellent. The digital autopilot was used extensively for the first time and provided all the capability required. Figure 6.9-6 shows a three-axis automatic attitude maneuver which is typical of the performance throughout the mission.

Passive thermal control, in which the vehicle is slowly rotated about one control axis, was used extensively during the cislunar phases. The rotation was about the roll axis with automatic pitch and yaw axis control enabled in all but two attempts. All cases with active pitch and yaw control were successful, although the duration of the reaction control system pulses was longer than nominal (70 to 85 milliseconds rather than the nominal 14-millisecond minimum impulse). The relatively long firings occurred because the limit cycle switch enabling the stabilization and control system pseudo-rate capability was not actuated. Figure 6.9-7 shows the gimbal angle time histories during a representative period.

The two attempts at passive thermal control without automatic pitch and yaw control were made during the transearth phase, one at 0.1 deg/sec and one at 0.3 deg/sec roll rate. Rapid divergences from the initial orientation were experienced in both cases and were caused by excessive initial rates or by disturbance torques from venting.

Orbital navigation.- The preliminary analysis of onboard lunar orbit navigation using landmark tracking indicates that as on Apollo 7, the results improved with experience. The lunar landing site and control points were tracked with both the scanning telescope and the sextant. The resulting data will add to establishing the accuracy of the onboard initialization point for lunar descent. Although no comparisons with the ground-calculated trajectory are available, the landing site coordinates calculated onboard on successive revolutions appear to be consistent.

Entry.- Figure 6.9-8 contains a time history of dynamic parameters during the entry phase. The pitch and yaw oscillations noted were comparable to those experienced during the Apollo 4 and 6 missions, with long periods of operation within the rate deadbands. Automatic digital autopilot control was enabled approximately 1 minute before 0.05g. As on Apollo 7, most of the pitch and yaw axis control activity occurred in the transonic region during the final 2 minutes before drogue deploy. The propellant usage distribution among the control axes is shown in the following table.

Control axis	Propellant, lb	
	0.05g to drogue deploy	2-minute period just prior to drogue deploy
Plus roll	10.19	
Minus roll	11.71	
Total	21.90	
Plus pitch	0.76	0.73
Minus pitch	1.97	1.97
Total	2.73	2.70
Plus yaw	3.20	2.85
Minus yaw	1.32	1.11
Total	4.52	3.96

The entry interface velocity and flight-path angle calculated onboard were 36 217 ft/sec and minus 6.50 degrees, respectively. These entry parameters compare favorably with the 36 221-ft/sec velocity and minus 6.50-degree flight-path angle obtained from ground tracking data.

The system operated properly throughout the entry phase. Events during entry, reconstructed from telemetry, are shown in figure 6.9-9.

The spacecraft reached the entry interface (400 000 feet altitude) with guidance program 63 (entry initialization) in command. The system indicated a desired inertial range of 1373.9 n. mi. and a predicted cross-range error of minus 22.3 n. mi. Approximately 30 seconds later, the command module had passed through the 0.05g level and the computer transferred control to program 64 (entry, post-0.05g).

The trajectory-planning guidance phase of program 64 was entered at a velocity of 32 598.8 ft/sec and at an inertial range of 910.1 n. mi. This phase searches for a reference trajectory for the computer to guide to during the subsequent guidance phase. The spacecraft had an excessive amount of energy when it entered the trajectory-planning phase; consequently, a constant drag trajectory was flown to dissipate this excess energy. The computer followed the constant drag logic until an exit velocity of less than 18 000 ft/sec was predicted. At that time, the computer properly sequenced directly to program 67 (entry, final phase). Program 67 was entered at a velocity of 24 900.8 ft/sec and at an inertial range of 623.6 n. mi. This phase guides the vehicle with respect to a reference trajectory obtained from a prestored table.

The system indicated the first peak deceleration (6.84g) at a velocity of 31 840.8 ft/sec. The minimum altitude calculated onboard during the first entry was 183 000 feet. The peak deceleration during second entry (3.92g) was sensed at a velocity of 10 714 ft/sec. The computer terminated guidance at a relative velocity of less than 1000 ft/sec. At drogue deployment, the system indicated an overshoot of 2.094 n. mi.

The commanded actual bank angles are presented as a function of time in figure 6.9-10; a comparison of the two parameters indicates proper response of the spacecraft to the bank angle commands. Table 6.9-III is a comparison of the telemetered navigation data with a reconstructed set developed by performing the navigation postflight with telemetered accelerometer data. This comparison indicates that the computer interpreted the accelerometer data correctly.

Figure 6.9-11 shows a summary of the landing point data for this mission. The onboard computer position at drogue deployment was 165 degrees 1.6 minutes west longitude and 8 degrees 6 minutes north latitude, 2.1 n. mi. from the target point. The recovery forces estimated the landing point to be 165 degrees 1.2 minutes west longitude and 8 degrees 7.5 minutes north latitude, 0.5 n. mi. from the desired target point.

Absolute navigation accuracy could not be obtained because of lack of tracking data during entry. The best-estimate trajectory shows a landing point of 165 degrees 0.7 minutes west longitude and 8 degrees 6.0 minutes north latitude, 2.2 n. mi. from the target point. A comparison of the computer navigation data with the best-estimate trajectory is contained in table 6.9-IV. This comparison shows that at entry interface, the computer navigation error was 0.6 n. mi. in position and 4 ft/sec in velocity. This error propagated throughout entry to a navigation error of about 1.3 n. mi. at drogue deployment. This error is well within a one-sigma touchdown accuracy.

The only abnormality during the entry phase involved the entry monitor system. Figure 6.9-12 shows the entry velocity/load-factor scroll from the entry monitor system. Plotted on the scroll is the actual velocity/g trace and one reconstructed from guidance system data. As this figure shows, the g trace contained several jumps during entry. (See section 12 for further discussion.) The apparent violation of the exit guidance is not a true violation, since during the period of tangency, the guidance system was commanding the proper roll attitude (180 degrees, lift down).

Guidance system values of range-to-go were found to be consistent with the manner in which the trace crossed the range potential lines. Further evidence of consistency and proper operation was obtained when the crew compared the range potential, range-to-go counter, and computer

range-to-go displays and found all to be in agreement at 50 miles to go. The system performed its monitoring function properly and could have been used for entry ranging, if needed.

6.9.2 Guidance and Navigation System Performance

Inertial subsystem.- The preflight test history of the inertial components is contained in table 6.9-V, along with the compensation values loaded into the computer. Although the inertial component error coefficients derived from ascent comparisons with the launch-vehicle platform are not yet available, the overall performance indicates that the errors were small.

Figure 6.9-13 contains a summary of inflight accelerometer bias measurements made throughout the mission. Also shown are the one-sigma allowable deviations, which indicate extremely stable performance. The slight variations noted in the period from 50 to 70 hours appear to be correlated with venting activity.

Figure 6.9-14 contains a similar record of gyro bias drift estimates calculated from the torquing angles recorded during each alignment. Again the instruments showed excellent stability and operation within one-sigma tolerances.

Optical subsystem.- The sextant and scanning telescope operated properly throughout the mission. The crew reported that the shaft and trunnion drive systems worked smoothly in all modes and that control capability was adequate. A trunnion readout circuit malfunction was suspected several times during the mission when the trunnion angle counter in the computer rapidly drove from zero to 45 degrees with some intermediate oscillations. Following each case, attempts to use the automatic optics positioning capability were unsuccessful until the system was re-zeroed. It was verified postflight that the apparent malfunction was a procedural oversight and that the behavior of the counter was correlated with the optics power-up sequence. If the optics is powered down while in the ZERO OPTICS mode, the trunnion mechanism drifts off zero in response to torque produced by an anti-backlash spring. With no power applied, the coupling data unit and computer counters do not follow this drift but remain at zero. When power is reapplied, with the mode still in ZERO OPTICS, the trunnion rapidly drives back toward zero; however, the two counters, which are now active, follow the motion and the computer counter drives off zero by an amount dependent on the trunnion drift. As a result, the computer's knowledge of trunnion position is in error, and subsequent optics drive commands will also be in error. The proper procedure is to re-actuate the zero optics switch following each power-up sequence and remove the effect of any power-down motion. The switch must be re-actuated each time because the counters are zeroed only once for each sequence through the mode.

The data received on star visibility through both instruments indicate that the light gathering qualities are adequate for all lunar mission operations involving the command and service module only. Figure 6.9-15 illustrates a series of observations made by the crew during one passive thermal control revolution and shows the effect of incident sun, earth, and moon light. The wide band in the figure portrays the scanning telescope field of view in relation to the sun, moon, and earth as the vehicle rolled 180 degrees. The comments are those of the crew. The data indicate that if the optics surfaces are properly shielded by the spacecraft, sufficient stars for constellation recognition can be seen.

Computer.- Computer operation was nominal throughout the mission. A computer clock drift of 0.953 msec/hr was measured prior to and during the flight. A drift of this magnitude is well within the specification limit of 7.2 msec/hr and was accounted for by periodic clock updates from the ground. One restart occurred during the mission when the crew attempted an illegal exit from the landmark tracking program (program 22). The insertion of a verb 34, which requests termination of a function when the program is requesting an optics mark, causes random transfers which, in this case, resulted in a parity fail when an unused memory location was read. Table 6.9-VI is a list of the computer programs used during the flight.

The onboard computer program, Colossus 237, was used for the first time on this mission and was capable of all lunar-orbit mission functions. The capabilities tested for the first time included precision integration in both the lunar and earth spheres of influence, cislunar navigation, and return-to-earth targetting for use in case of a communications loss.

The Apollo 7 program, Sundisk, had been developed for earth-orbit flight and was capable of only certain navigation functions with regard to the lunar mission. Colossus, however, was designed to monitor translunar injection, compute all lunar velocity-change maneuvers, and evaluate certain lunar-mission abort requirements.

A number of software discrepancies were isolated in preflight testing; however, each discrepancy was either insignificant or circumvented procedurally. The fast-return trajectory and the resulting high-speed entry validated the return-to-earth targetting capability of the program as originally coded. An alternate procedure was devised which involved manually changing two memory locations after the program was entered. Other performance aspects of the computer program were also as expected.

6.9.3 Stabilization and Control Systems Performance

The stabilization and control system was used for attitude control and for backup monitoring of propulsion maneuvers and entry. Performance was nominal. From crew reports, the stabilization and control system attitude reference drifted as much as 9 deg/hr, which is a greater rate than that reported on Apollo 7 but is still within specification. The orbital rate drive assembly was utilized extensively in lunar orbit with reportedly excellent results.

6.9.4 Entry Monitor System

The entry monitor system properly performed all assigned mission functions and provided an adequate backup to the primary system. Four malfunctions occurred:

a. During spacecraft/S-IVB separation, the delta V counter jumped 100 ft/sec.

b. After the third midcourse correction switched off, the delta V counter continued to count.

c. Sometimes when the mode switch was moved rapidly from "standby" to "automatic," the delta V counter jumped.

d. During entry, two short g-transients occurred and were scribed on the scroll.

See section 12 for further details.

TABLE 6.9-I.- PLATFORM ALIGNMENT SUMMARY

Time, hr:min	Program option[a]	Star used		Gyro torquing angle, deg			Star angle difference, deg	Gyro drift, mERU		
		No.	Name	X	Y	Z		X	Y	Z
4:24	3	3 36	Navi Vega	-0.034	-0.027	+0.100	000.01	-0.69	-0.54	+2.00
10:12	3	17 30	Regor Menkent	-0.147	+0.041	-0.157	000.01	-1.69	+0.47	+1.81
16:49	3	3 5	Navi Polaris	-0.122	-0.044	+0.172	000.00	-1.23	-0.45	+1.74
27:30	3	7 12	Menkar Rigel	-0.242	+0.049	+0.295	000.01	-1.50	+0.30	+1.85
34:09	3	15 6	Sirius Acamar	-0.136	-0.013	+0.192	000.01	-1.36	-0.13	+1.92
36:10	3	26 27	Spica Aikaid	-0.157	-0.018	+0.216	000.01	-1.23	-0.14	+1.69
44:31	3	6 45	Acamar Fomalhaut	-0.201	-0.003	+0.255	000.00	-1.61	-0.02	+2.05
51:38	3	7 12	Menkar Rigel	-0.143	+0.003	+0.164	000.00	-1.35	+0.03	+1.54
60:36	1	10 12	Mirfak Rigel	-0.624	-0.701	+0.993	000.01	Maneuver		
66:23	1	30 32	Menken Alphecca	-0.089	-0.007	+0.128	000.02	-1.22	-0.10	+1.78
68:15	3	23 30	Denebola Menkent	-0.048	-0.013	+0.064	000.01	-1.73	-0.47	+2.30
70:14	3	13 22	Capella Regulus	-0.077	+0.017	+0.045	000.00	-1.32	+0.29	+0.78
72:30	2	20 21	Dnoces Alphard	-0.053	-0.007	+0.047	000.01	-1.69	-0.23	+1.50
74:34	3	16 23	Procyon Denebola	-0.052	-0.007	+0.053	000.01	-1.55	-0.21	+1.58
76:24	3	22 30	Regulus Menkent	-0.022	-0.006	+0.074	000.01	-0.79	-0.21	+2.64
78:28	3	16 23	Procyon Denebola	-0.060	-0.013	+0.040	000.00	-1.97	-0.43	+1.31
80:28	3	20 21	Dnoces Alphard	-0.052	+0.002	+0.071	000.01	-1.73	+0.07	-2.36
82:30	3	31 22	Arcturua Regulus	-0.022	-0.004	+0.032	000.01	-0.72	-0.13	+1.05
86:30	3	23 32	Denebola Alphecca	-0.078	-0.006	+0.102	000.01	-1.30	-0.10	+1.70
88:20	3	27 31	Alkaid Arcturus	-0.004	-0.002	+0.048	000.00	-0.15	-0.21	+1.74

[a]Using program 52.

Note: All alignments performed by Command Module Pilot, except that at 66:23, made by the Commander, and that at 74:34, made by the Lunar Module Pilot.

TABLE 6.9-I.- PLATFORM ALIGNMENT SUMMARY - Concluded

Time, hr:min	Program option[a]	Star used		Gyro torquing angle, deg			Star angle difference, deg	Gyro drift, mERU		
		No.	Name	X	Y	Z		X	Y	Z
90:10	1	14 16	Canopus Procyon	-0.539	+0.235	-0.141	000.01	After transearth injection		
99:45	3	22 31	Regulus Arcturus	-0.208	-0.010	+0.292	000.00	-1.39	-0.07	+1.61
102:40	3	22 31	Regulus Arcturus	-0.057	-0.000	+0.073	000.01	-1.30	-0.00	+1.64
106:42		12 15	Rigel Sirius	Inertial measurement unit orientation			000.00			
106:55	1	11 16	Aldebaran Procyon	+0.160	-0.560	+0.028	000.01	Inertial measurement unit realignment		
119:36	3	6 11	Acamar Aldebaran	-0.262	-0.021	+0.302	000.00	-1.03	-0.08	+1.18
124:30	3	32 43	Alphecca Deneb	-0.196	-0.061	+0.254	000.00	-1.32	-0.41	+1.70
139:23	3	17 4	Regor Achernar	-0.180	-0.11	+0.235	000.00	-1.21	-0.07	+1.58
143:02	3	10 20	Mirfak Dnoces	-0.096	-0.020	+0.083	000.01	-1.75	-0.36	+1.51
144:49	3	16 23	Procyon Denebola	-0.034	+0.001	+0.043	000.01	-1.23	0.00	+1.60

[a]Using program 52, except at 106:42 program 51 was used.

Note: All alignments performed by Command Module Pilot, except at 139:23, when the Commander made the alignment.

TABLE 6.9-II.- GUIDANCE AND CONTROL MANEUVER SUMMARY

Condition	Maneuver and control mode[a]					
	First midcourse correction	Second midcourse correction	Lunar orbit insertion	Lunar orbit circularization	Transearth injection	Third midcourse correction
	DAP-TVC	DAP-RCS	DAP-TVC	DAP-TVC	DAP-TVC	DAP-RCS
Time						
Ignition, hr:min:sec	10:59:59.2	60:59:55.9	69:08:20.4	73:35:06.6	89:19:16.6	104:00:00
Cutoff, hr:min:sec	11:00:01.6	61:00:07.8	69:12:27.3	73:35:16.2	89:22:40.3	104:00:15
Duration, sec	2.4	11.8	246.9	9.6	203.7	15
Velocity, ft/sec (desired/actual)						
X	8.35/6.85	1.14/1.19	-1303.1/-1303.5	-102.4/-102.0	1913.2/1913.4	1.05/1.14
Y	-23.27/-19.17	0.61/0.43	-2089.2/-2090.0	-77.2/-76.3	2473.4/2474.2	4.00/3.74
Z	2.24/1.99	1.74/1.77	-1705.5/-1706.3	-41.6/-42.0	1621.2/1621.2	2.91/2.87
Velocity residuals, ft/sec						
X	+1.50	-0.05	+0.38	-0.40	-0.20	0.09
Y	-4.10	+0.18	+0.79	-0.87	-0.66	0.25
Z	+0.25	-0.03	+0.83	+0.39	+0.10	0.04
Engine gimbal position, deg		Not applicable				Not applicable
Initial						
Pitch			-1.66	-0.62	-0.49	
Yaw			+1.24	+1.36	+1.49	
Maximum excursion						
Pitch			+0.56	+0.22	-0.17	
Yaw			+0.33	-0.34	-0.25	
Steady-state						
Pitch			-1.49	-0.62	-0.51	
Yaw			+1.32	+1.45	+1.61	
Cutoff						
Pitch			-0.49	-0.45	-0.84	
Yaw			+1.40	+1.53	+0.60	
Rate excursion, deg/sec						
Pitch		-0.31	+0.55	+0.39	+0.12	-0.40
Yaw		+0.09	+0.24	+0.08	-0.12	+0.10
Roll		+0.02	-0.40	0.00	+0.04	-0.28
Attitude error, deg						
Pitch		-0.50	+0.25	+0.21	+0.61	-0.75
Yaw		+0.20	+0.48	+0.35	-0.48	+0.30
Roll		+0.30	+20.90	0.00	-4.78	-0.50

[a]DAP-TVC: digital autopilot-thrust vector control; DAP-RCS: digital autopilot-reaction control system.

TABLE 6.9-III.- ENTRY NAVIGATION AND GUIDANCE RECONSTRUCTION

Parameter	Entry interface		Peak g		Start FINAL PHASE		Drogue deployment minus 50 seconds	
	146:46:12.8		146:47:38.4		146:48:34.4		146:53:56.4	
	Computer	Simulated	Computer	Simulated	Computer	Simulated	Computer	Simulated
X position, ft	-16 793 759	-16 793 652	-18 281 748	-18 281 651	-19 011 720	-19 011 626	-20 269 121	-20 269 216
Y position, ft	10 752 311	10 752 286	8 708 525	8 708 466	7 636 166	7 636 098	4 533 645	4 533 527
Z position, ft	7 542 160	7 542 056	5 945 648	5 945 575	5 116 449	5 116 378	2 947 066	2 946 993
X velocity, ft/sec . . .	-18 912.5	-18 912.5	-15 577.7	-15 577.8	-10 502.4	-10 502.7	152.7	147.5
Y velocity, ft/sec . . .	-24 296.4	-24 296.4	-21 560.2	-21 560.3	-17 874.5	-17 874.7	-1795.5	-1815.2
Z velocity, ft/sec . . .	-19 070.7	-19 070.6	-16 578.5	-16 578.4	-13 793.2	-13 793.2	-385.2	-385.2

TABLE 6.9-IV.- ONBOARD COMPUTER ENTRY NAVIGATION ACCURACY

Parameter	Entry interface		Peak g		Start FINAL PHASE		Drogue deployment minus 50 seconds	
	146:46:12.8		146:47:38.4		146:48:34.4		146:53:56.4	
	Computer	BET*	Computer	BET*	Computer	BET*	Computer	BET*
X position, ft	-16 793 759	-16 793 369	-18 281 748	-18 286 485	-19 011 720	-19 014 936	-20 269 121	-20 268 458
Y position, ft	10 752 311	10 749 608	8 708 525	8 698 350	7 636 166	7 626 768	4 533 645	4 527 719
Z position, ft	7 542 160	7 539 719	5 945 648	5 937 497	5 116 449	5 108 904	2 947 066	2 942 639
X velocity, ft/sec . . .	-18 912.5	-18 912.9	-15 577.7	-15 555.1	-10 502.4	-10 476.9	152.7	157.0
Y velocity, ft/sec . . .	-24 296.4	-24 299.8	-21 560.2	-21 522.5	-17 874.5	-17 867.7	-1795.5	-1795.5
Z velocity, ft/sec . . .	-19 070.7	-19 072.9	-16 578.5	-16 546.0	-13 793.2	-13 786.6	-385.2	-384.2
Total velocity, ft/sec	36 217.2	36 221.1	31 342.5	31 288.2	24 900.8	24 881.5	1842.7	1842.8

*Best-estimate trajectory.

TABLE 6.9-V.- INERTIAL COMPONENT PREFLIGHT HISTORY

Error	Sample mean	Standard deviation	No. samples	Countdown value	Flight load
Accelerometers					
X - Scale factor error, ppm	-76.57	51.25	7	-65	-144
Bias, cm/sec^2	-0.0013	0.089	7	0.0	0.0
Y - Scale factor error, ppm	-329.14	14.89	7	-401	-329
Bias, cm/sec^2	0.803	0.028	7	0.84	+0.80
Z - Scale factor error, ppm	-200.71	42.62	7	-152	-201
Bias, cm/sec^2	0.631	0.02	7	+0.615	+0.60
Gyroscopes					
X - Null bias drift, mERU	2.18	0.75	4	+0.06	-0.8
Acceleration drift, spin reference axis, mERU/g	-2.24	4.75	2	-2.76	+1.6
Acceleration drift, input axis, mERU/g	17.88	16.24	4	-24.90	-4.1
Acceleration drift, output axis, mERU/g	2.52	0.25	8	+2.68	--
Y - Null bias drift, mERU	2.62	0.95	4	-1.62	+0.6
Acceleration drift, spin reference axis, mERU/g	1.66	0.27	4	+4.00	+3.4
Acceleration drift, input axis, mERU/g	-3.22	8.48	2	-32.43	-14.2
Acceleration drift, output axis, mERU/g	2.28	0.80	4	+3.15	--
Z - Null bias drift, mERU	-3.22	0.51	6	-1.4	-2.7
Acceleration drift, spin reference axis, mERU/g	27.59	6.83	3	+24.41	+28.9
Acceleration drift, input axis, mERU/g	28.23	1.38	2	+19.83	+21.3
Acceleration drift, output axis, mERU/g	0.36	0.60	6	-0.8	--

TABLE 6.9-VI.- COMPUTER PROGRAMS USED

No.	Description
00	Command module computer idling
01	Prelaunch initialization
02	Prelaunch gyrocompassing
03	Prelaunch optical verification of gyrocompassing
06	Command module computer power up
11	Earth orbit insertion monitor
21	Ground track determination
22	Orbital navigation
23	Cislunar midcourse navigation
27	Computer update
30	External delta V
37	Return to Earth
40	Service propulsion thrusting
41	Reaction control system thrusting
47	Thrust monitor
51	Inertial measurement unit orientation determination
52	Inertial measurement unit realignment
61	Entry preparation
62	Entry - Command module/service module separation and pre-entry maneuver
63	Entry initialization
64	Entry - Post 0.05g
67	Entry - Final phase

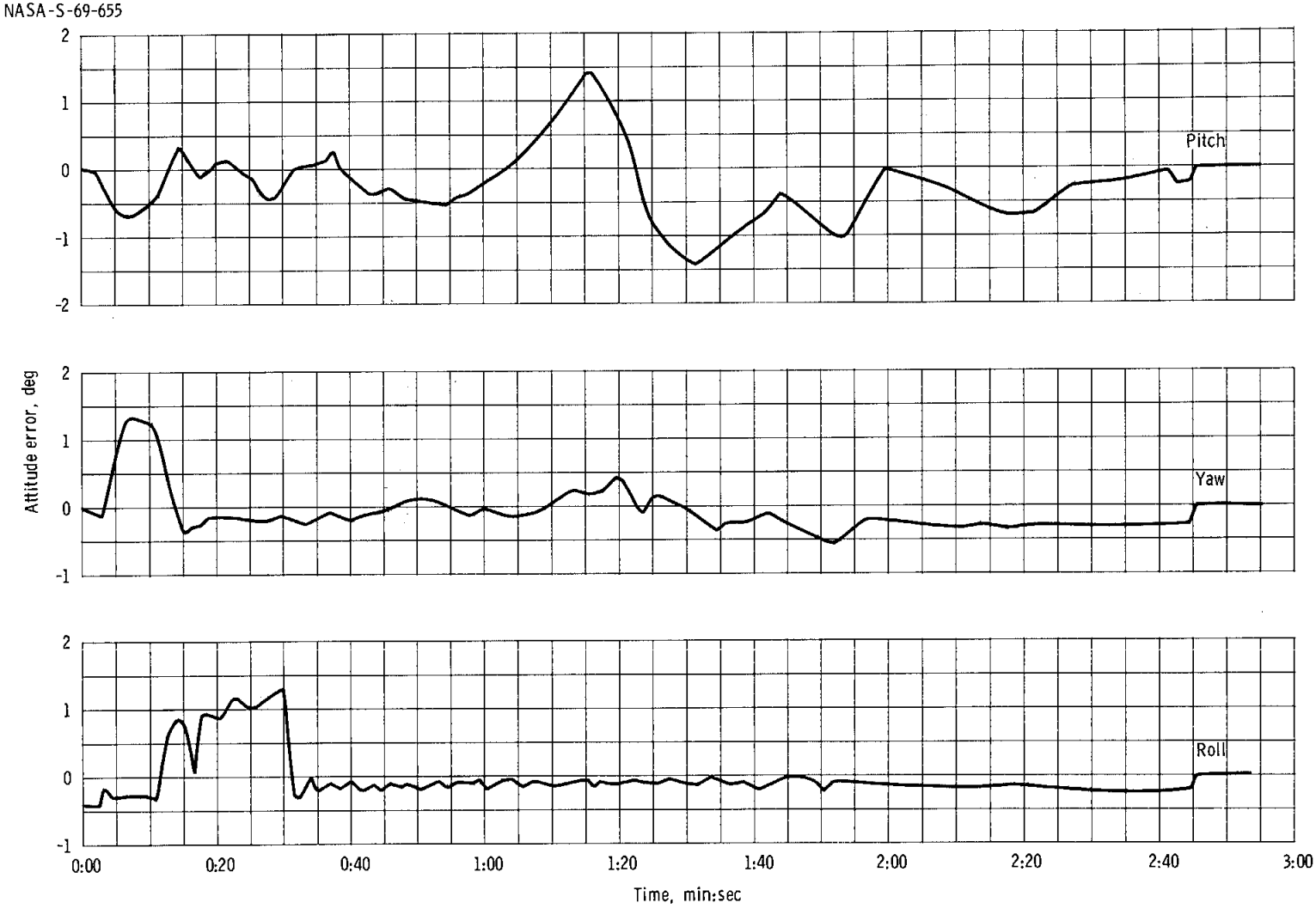

Figure 6.9-1. - Launch phase attitude errors displayed to the crew.

NASA-S-69-656

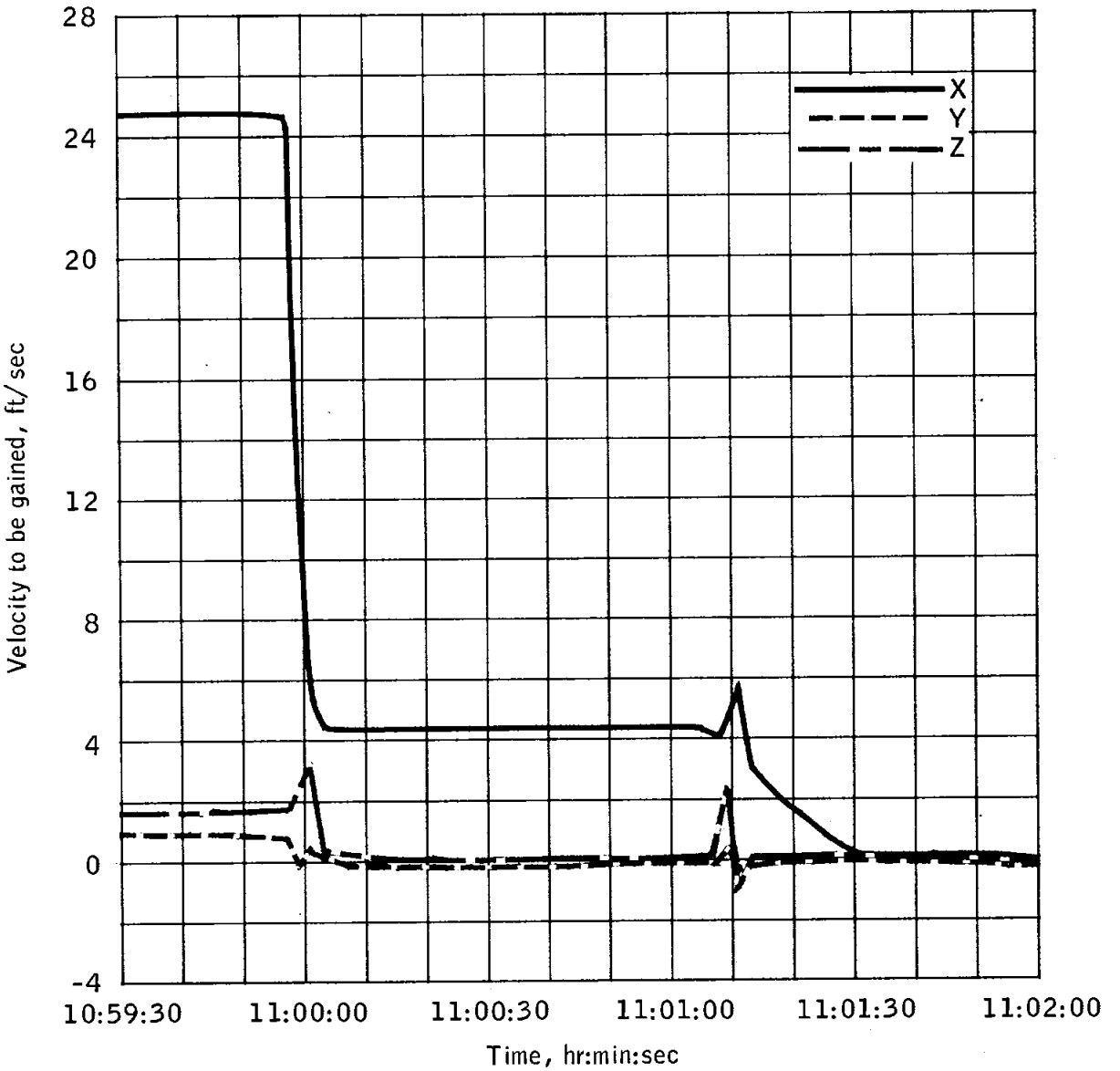

Figure 6.9-2.- Velocity-to-be-gained during first service propulsion maneuver (first midcourse correction).

NASA-S-69-657

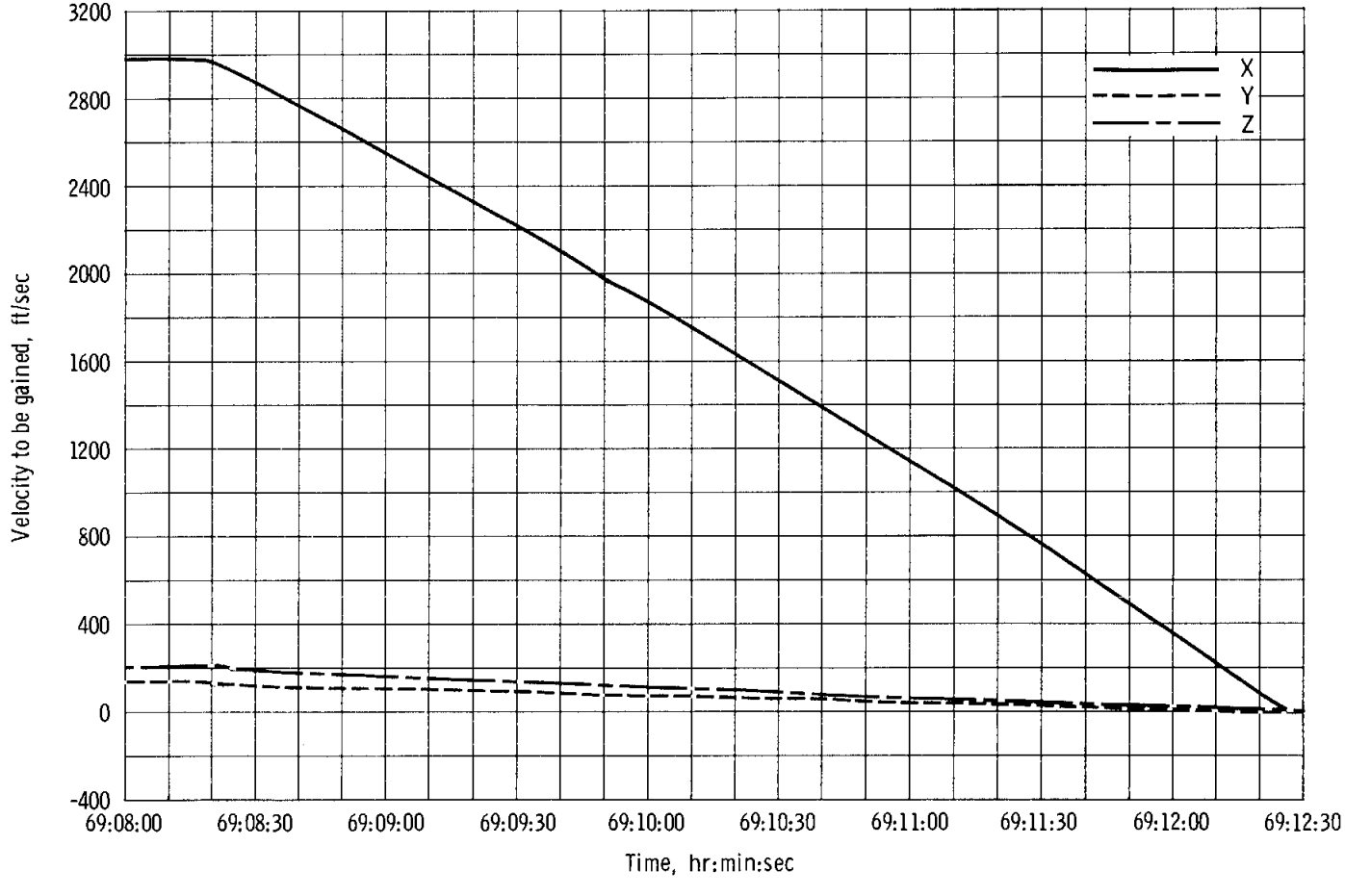

Figure 6.9-3. - Velocity-to-be gained during second service propulsion maneuver (lunar orbit insertion).

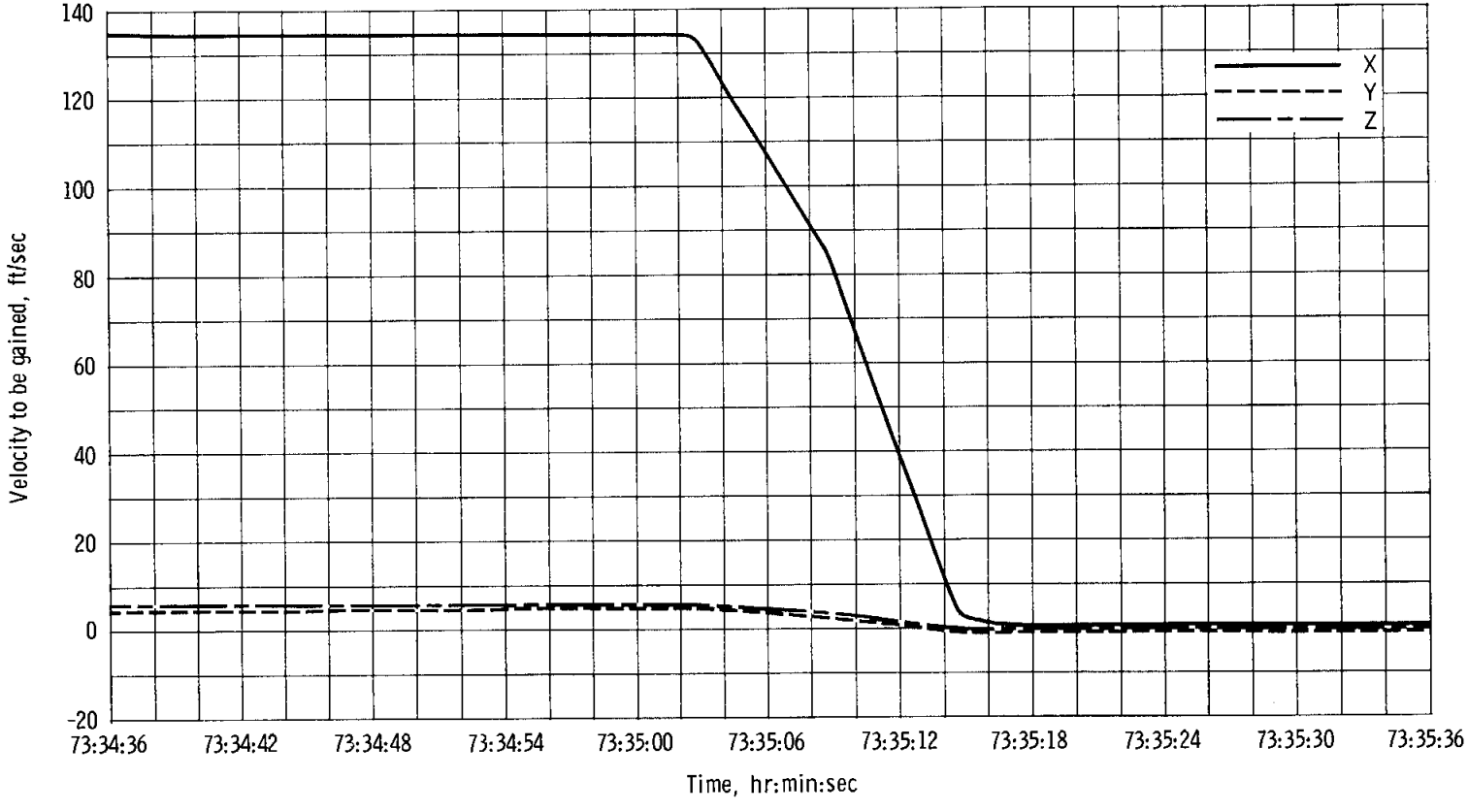

Figure 6.9-4. - Velocity-to-be-gained during third service propulsion maneuver (circularization).

NASA-S-69-659

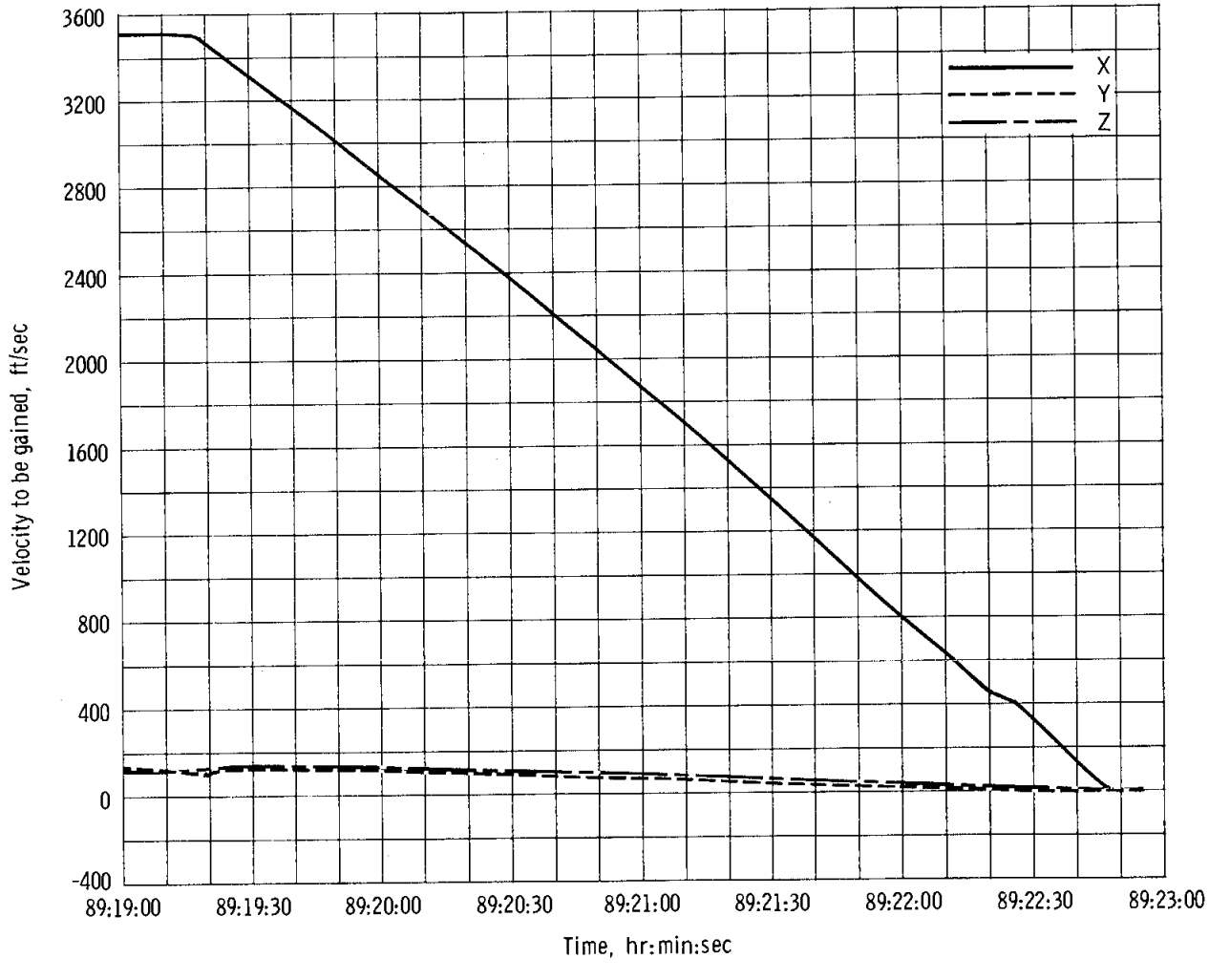

Figure 6.9-5. - Velocity-to-be-gained during fourth service propulsion maneuver (transearth injection).

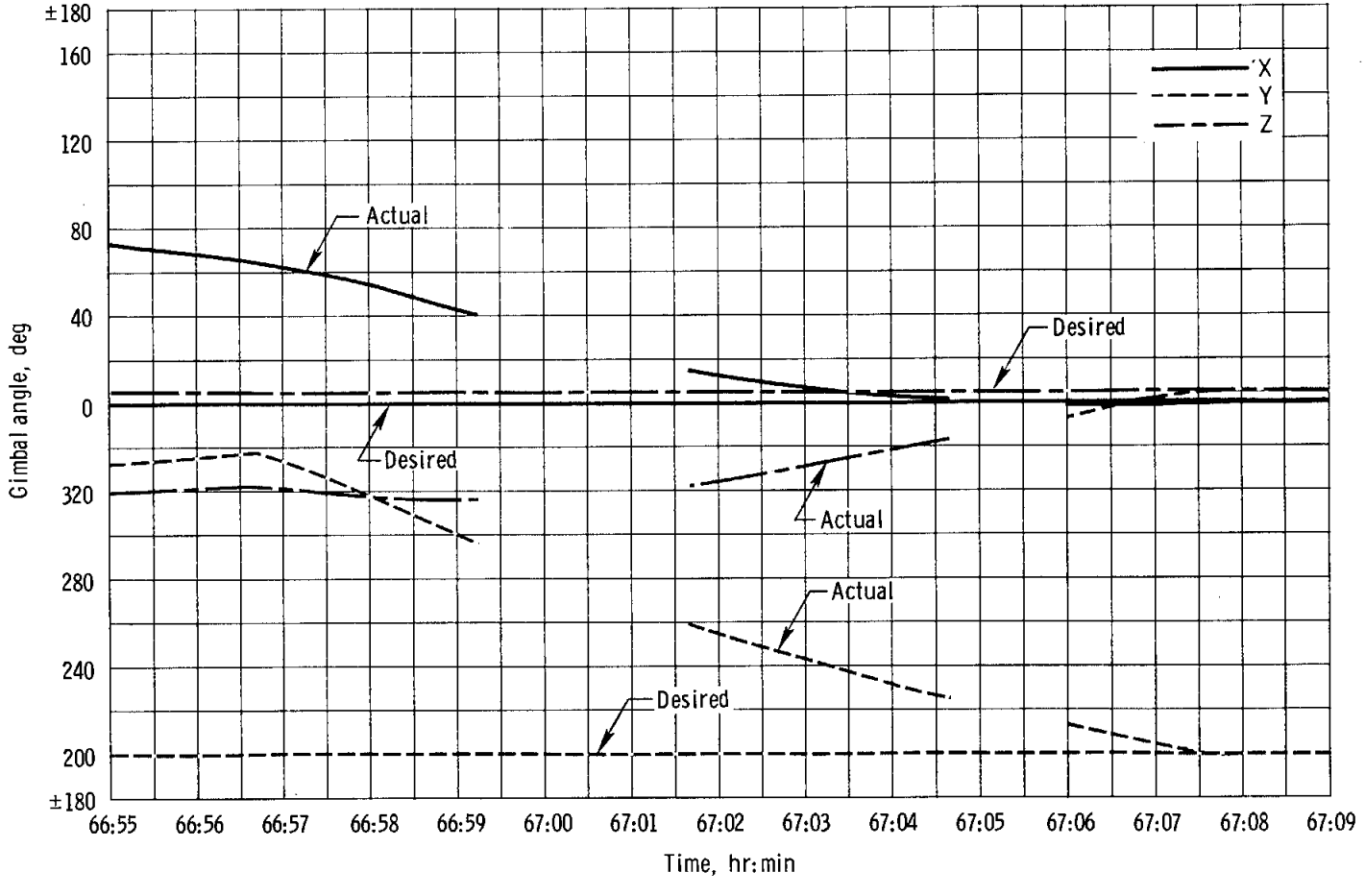

Figure 6.9-6. - Gimbal angles during typical three-axis maneuver.

NASA-S-69-661

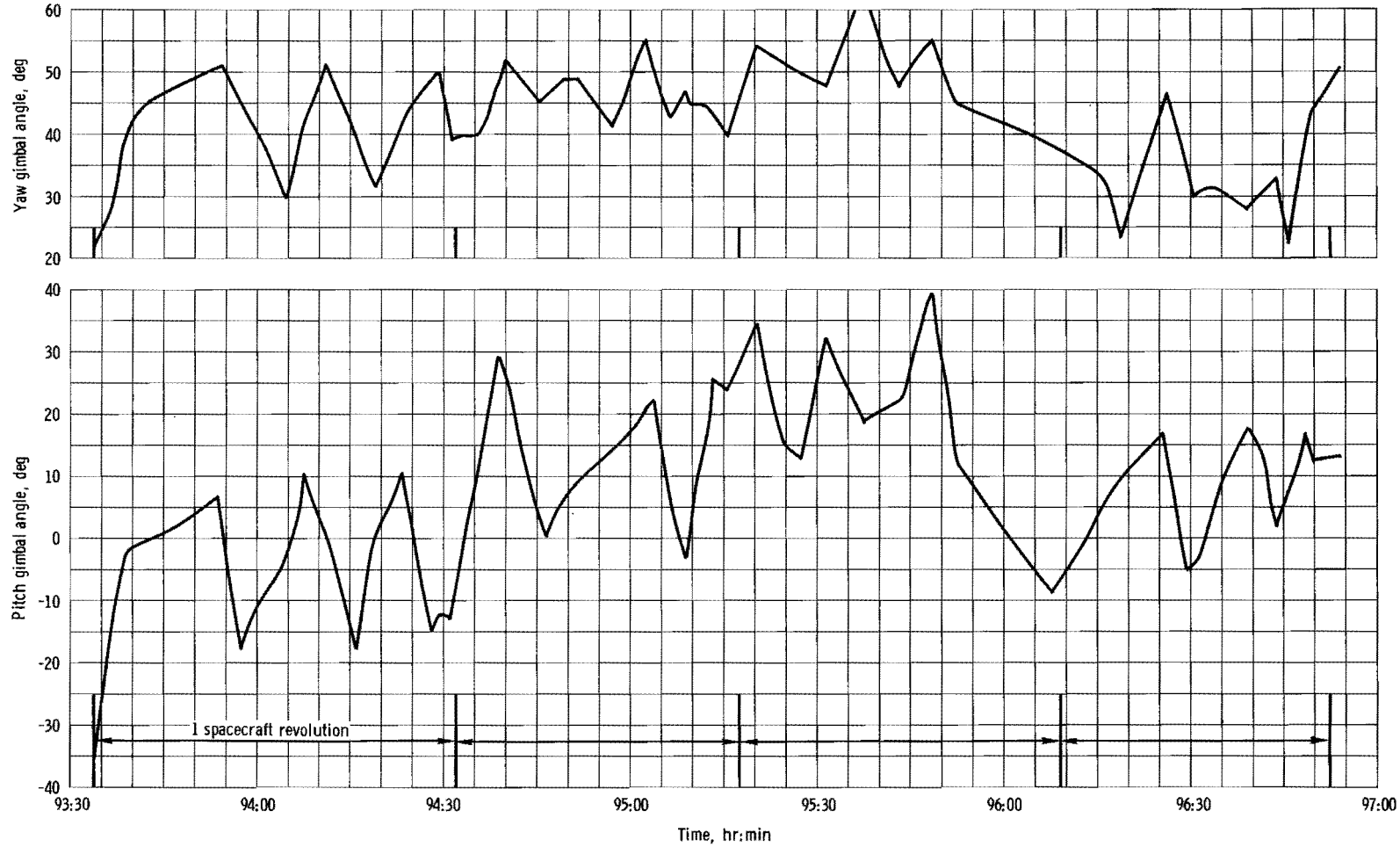

Figure 6.9-7. - Pitch and yaw gimbal angles during passive thermal control.

NASA-S-69-662

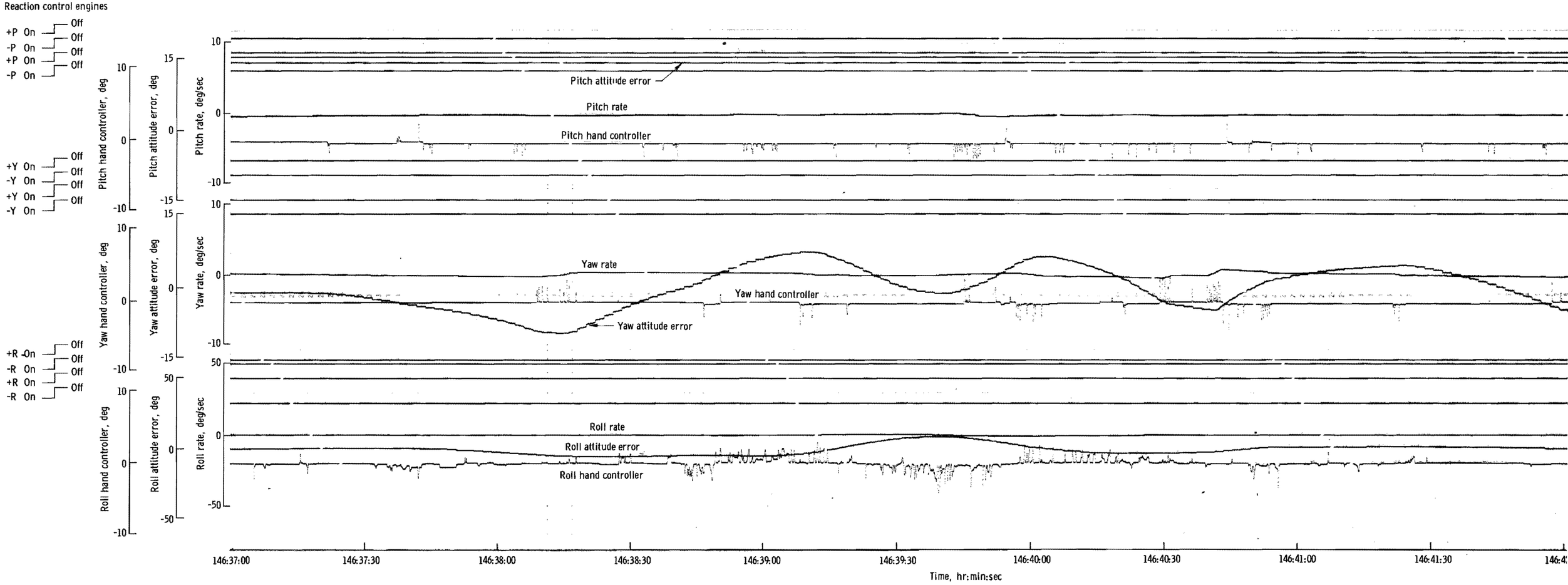

(a) 146:37:00 to 146:42:30.

Figure 6.9-8. - Spacecraft dynamics during entry.

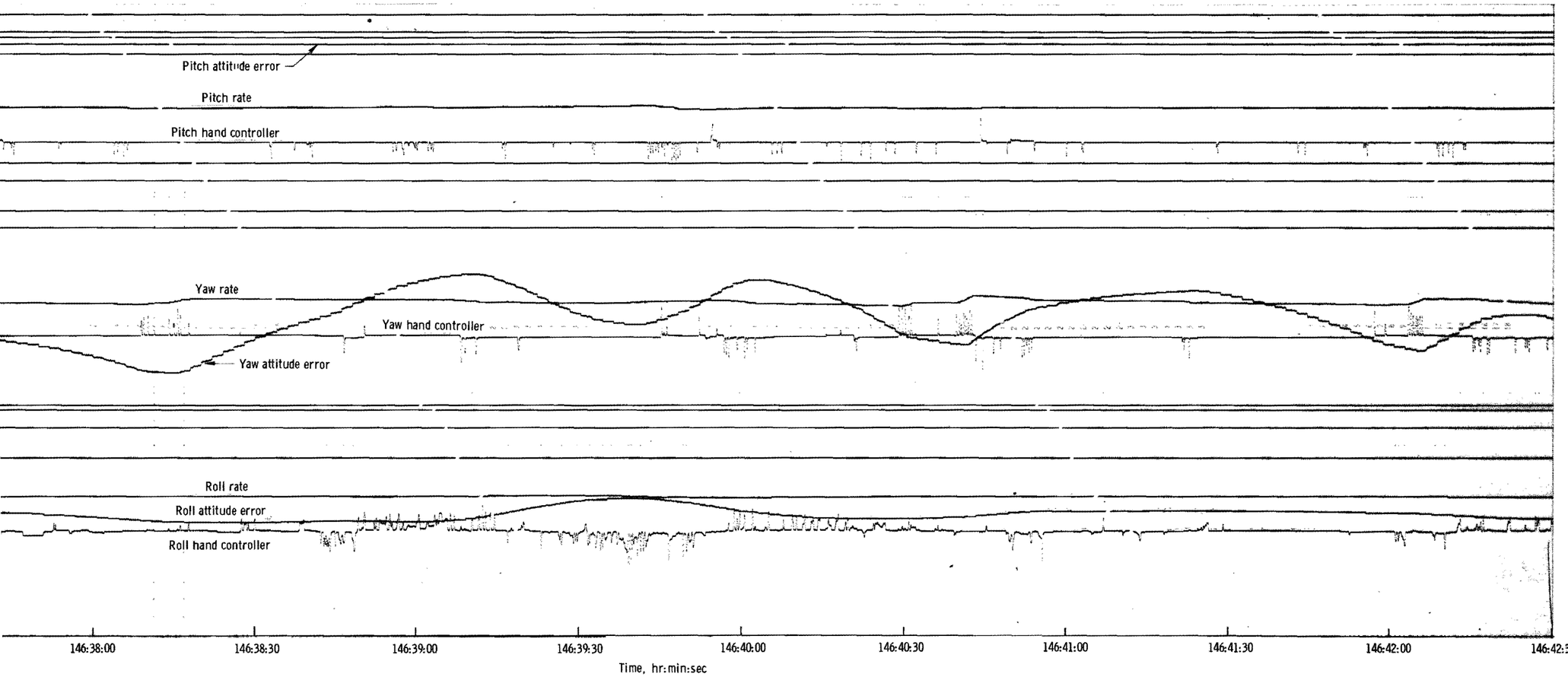
Pitch attitude error
Pitch rate
Pitch hand controller
Yaw rate
Yaw hand controller
Yaw attitude error
Roll rate
Roll attitude error
Roll hand controller
146:38:00
146:38:30
146:39:00
146:39:30
146:40:00
146:40:30
146:41:00
146:41:30
146:42:00
146:42:30
Time, hr:min:sec

NASA-S-69-663

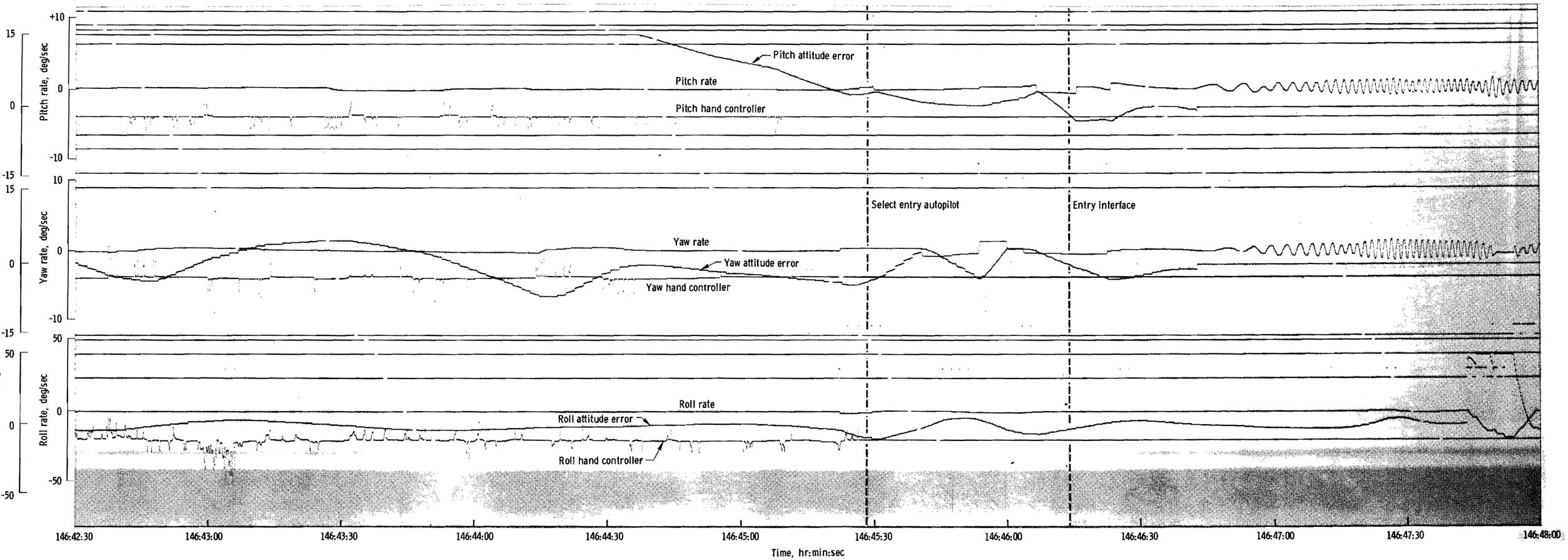

(b) 146:42:30 to 146:48:00.

Figure 6.9-8. - Continued.

NASA-S-69-663

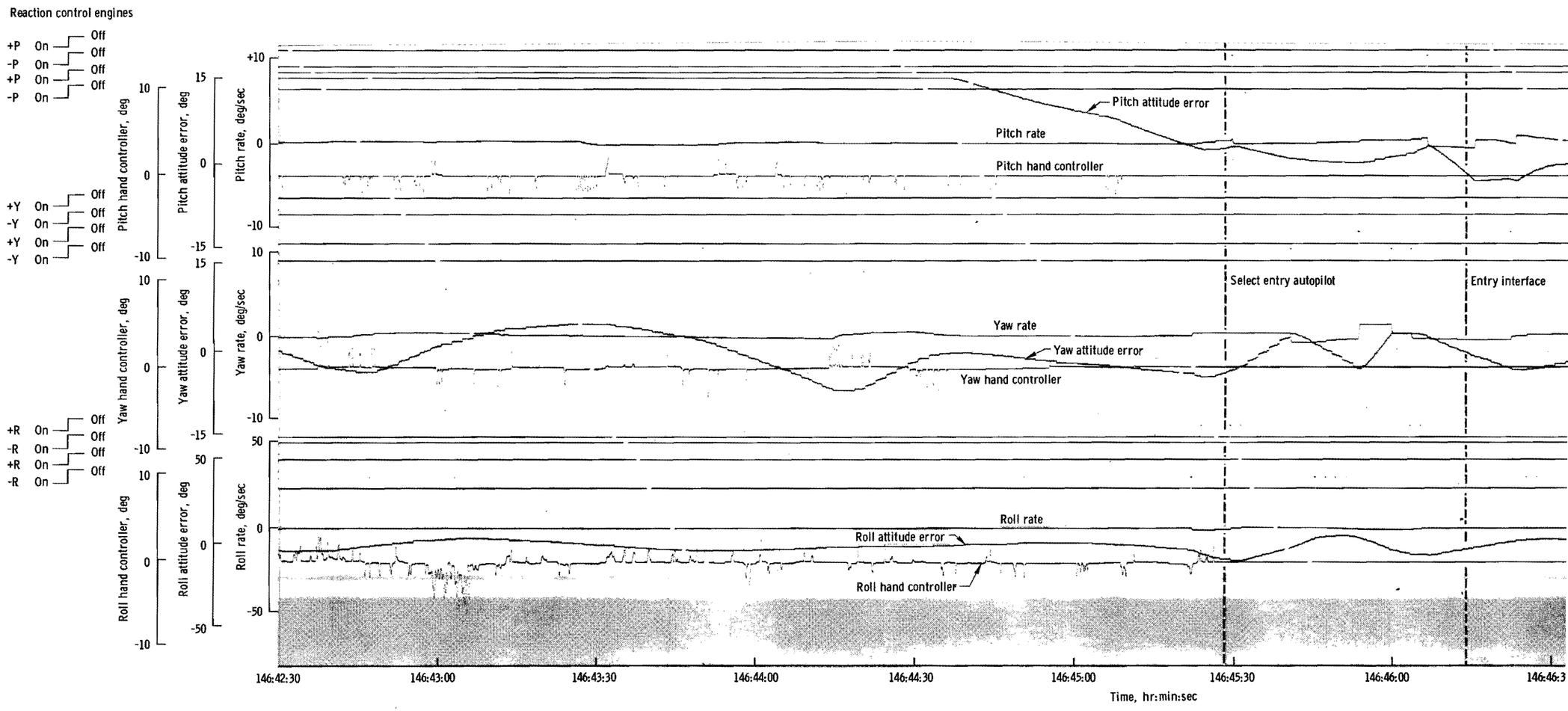
Reaction control engines
+P On
Off
-P On
Off
+P On
Off
-P On
Off
+Y On
Off
-Y On
Off
+Y On
Off
-Y On
Off
+R On
Off
-R On
Off
+R On
Off
-R On
Off
Pitch hand controller, deg
10
0
-10
Pitch attitude error, deg
15
0
-15
Pitch rate, deg/sec
+10
0
-10
Pitch attitude error
Pitch rate
Pitch hand controller
Yaw hand controller, deg
10
0
-10
Yaw attitude error, deg
15
0
-15
Yaw rate, deg/sec
10
0
-10
Yaw rate
Yaw attitude error
Yaw hand controller
Select entry autopilot
Entry interface
Roll hand controller, deg
10
0
-10
Roll attitude error, deg
50
0
-50
Roll rate, deg/sec
50
0
-50
Roll rate
Roll attitude error
Roll hand controller
146:42:30
146:43:00
146:43:30
146:44:00
146:44:30
146:45:00
146:45:30
146:46:00
146:46:3
Time, hr:min:sec

NASA-S-69-664

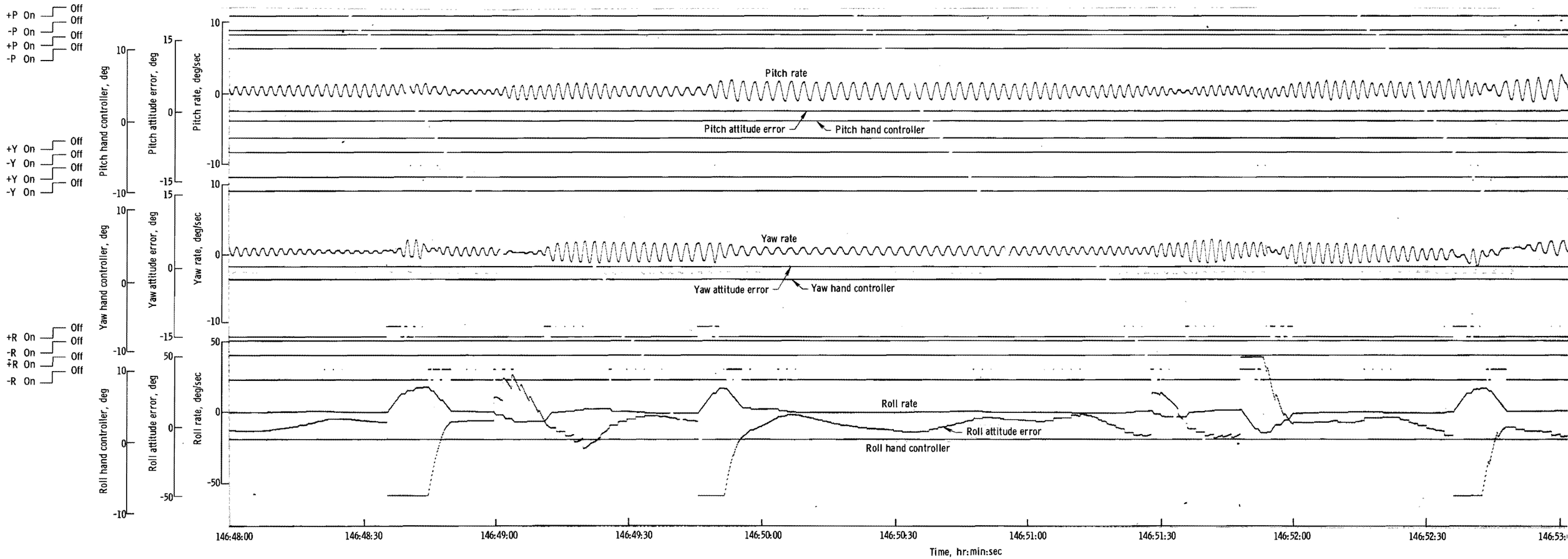

(c) 146:48:00 to 146:53:30.

Figure 6.9-8. - Continued.

NASA-S-69-664

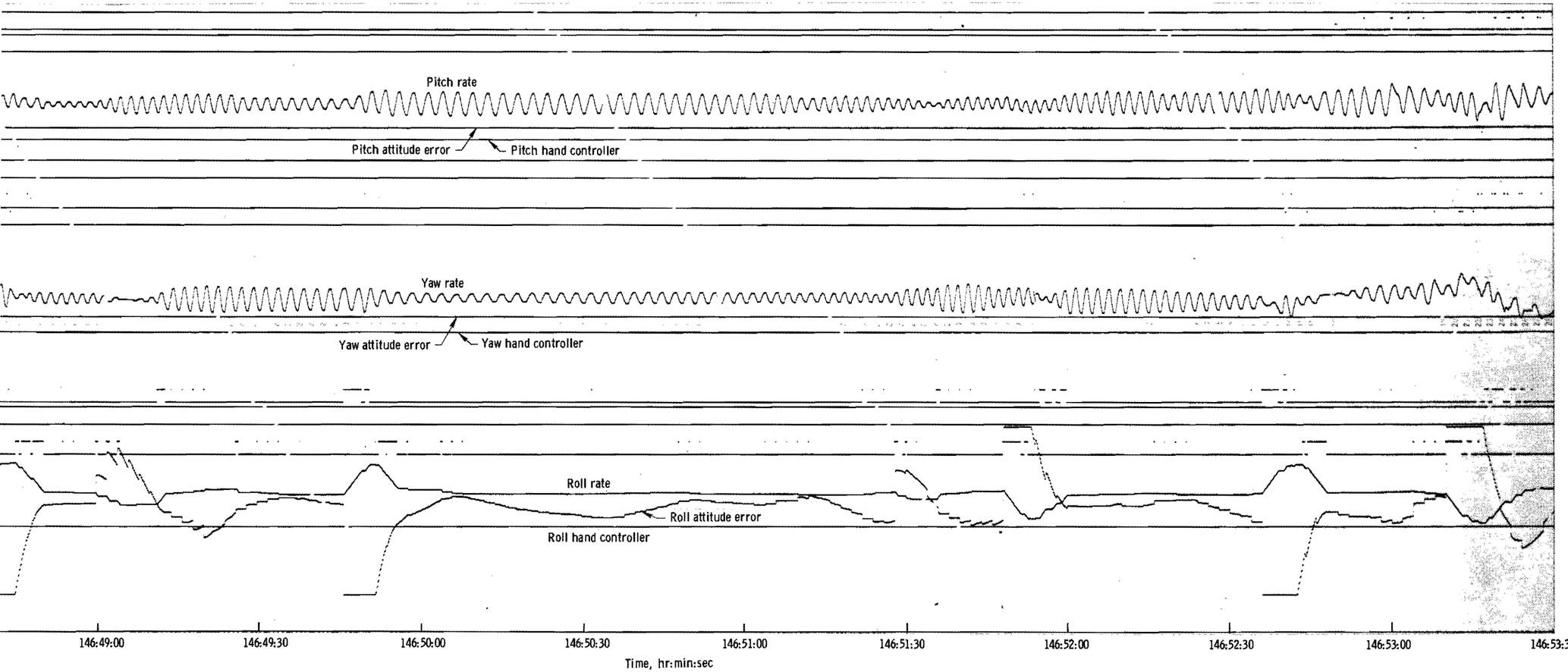

(c) 146:48:00 to 146:53:30.

Figure 6.9-8. - Continued.

NASA-S-69-665

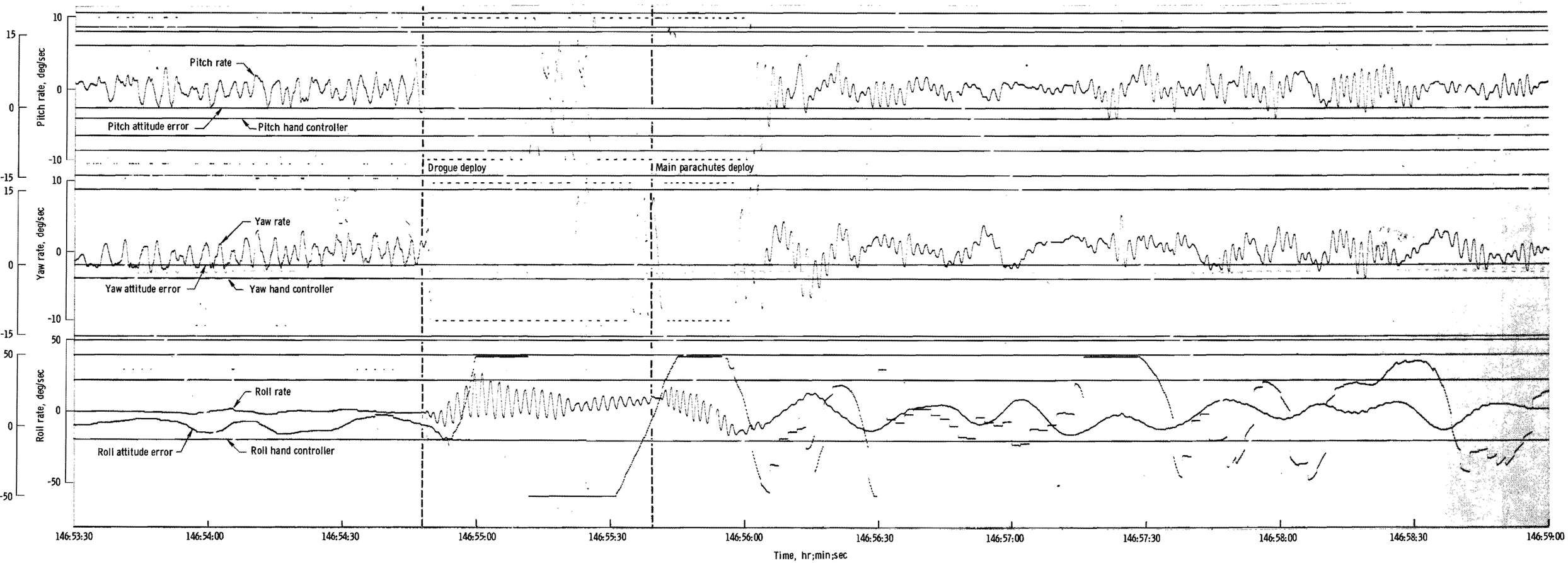

(d) 146:53:30 to 146:59:00.

Figure 6.9-8. - Concluded.

NASA-S-69-665

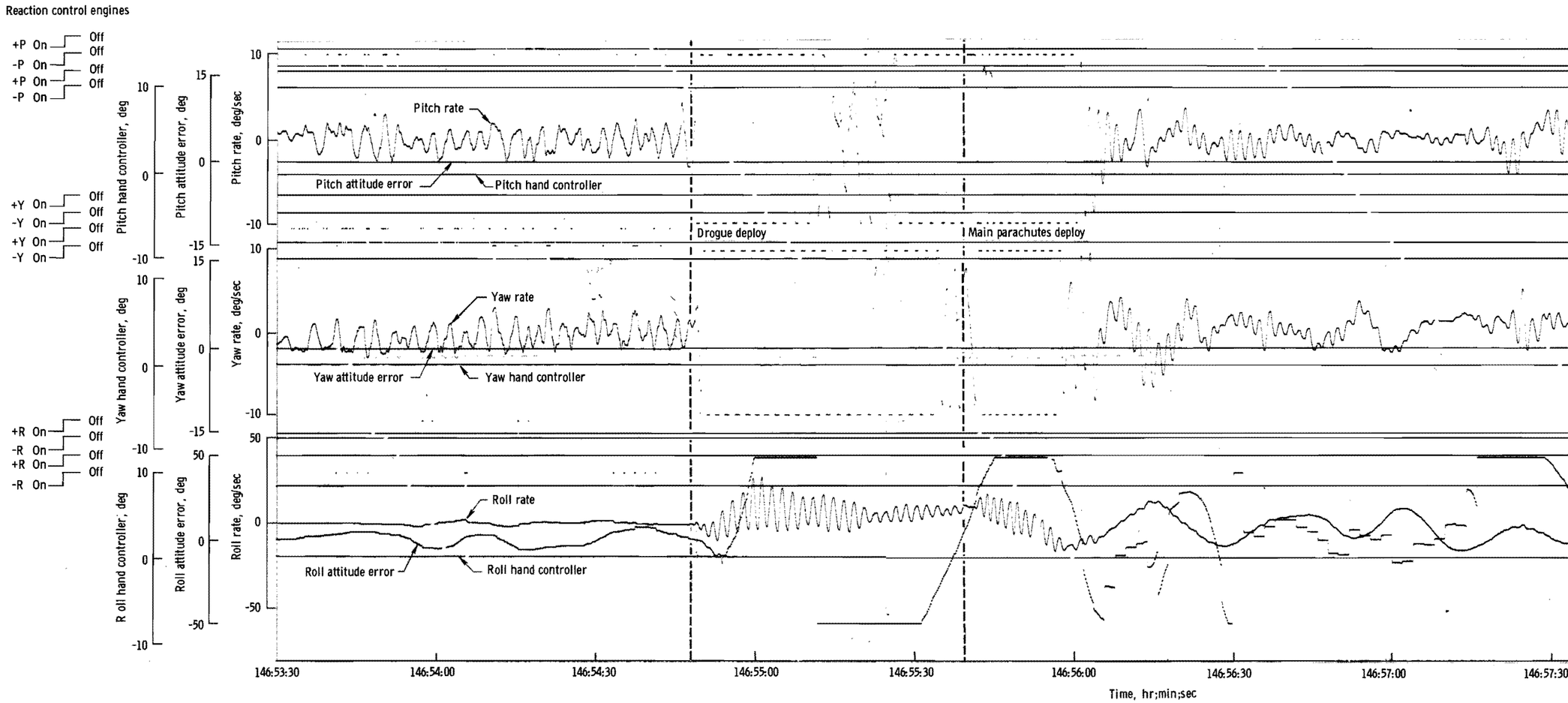
Reaction control engines
+P On
-P On
+P On
-P On
Off
Off
Off
Off
+Y On
-Y On
+Y On
-Y On
Off
Off
Off
Off
+R On
-R On
+R On
-R On
Off
Off
Off
Off
Pitch hand controller, deg
Pitch attitude error, deg
Pitch rate, deg/sec
Yaw hand controller, deg
Yaw attitude error, deg
Yaw rate, deg/sec
Roll hand controller, deg
Roll attitude error, deg
Roll rate, deg/sec
Pitch rate
Pitch attitude error
Pitch hand controller
Drogue deploy
Main parachutes deploy
Yaw rate
Yaw attitude error
Yaw hand controller
Roll rate
Roll attitude error
Roll hand controller
146:53:30
146:54:00
146:54:30
146:55:00
146:55:30
146:56:00
146:56:30
146:57:00
146:57:30
Time, hr;min;sec

NASA-S-69-666

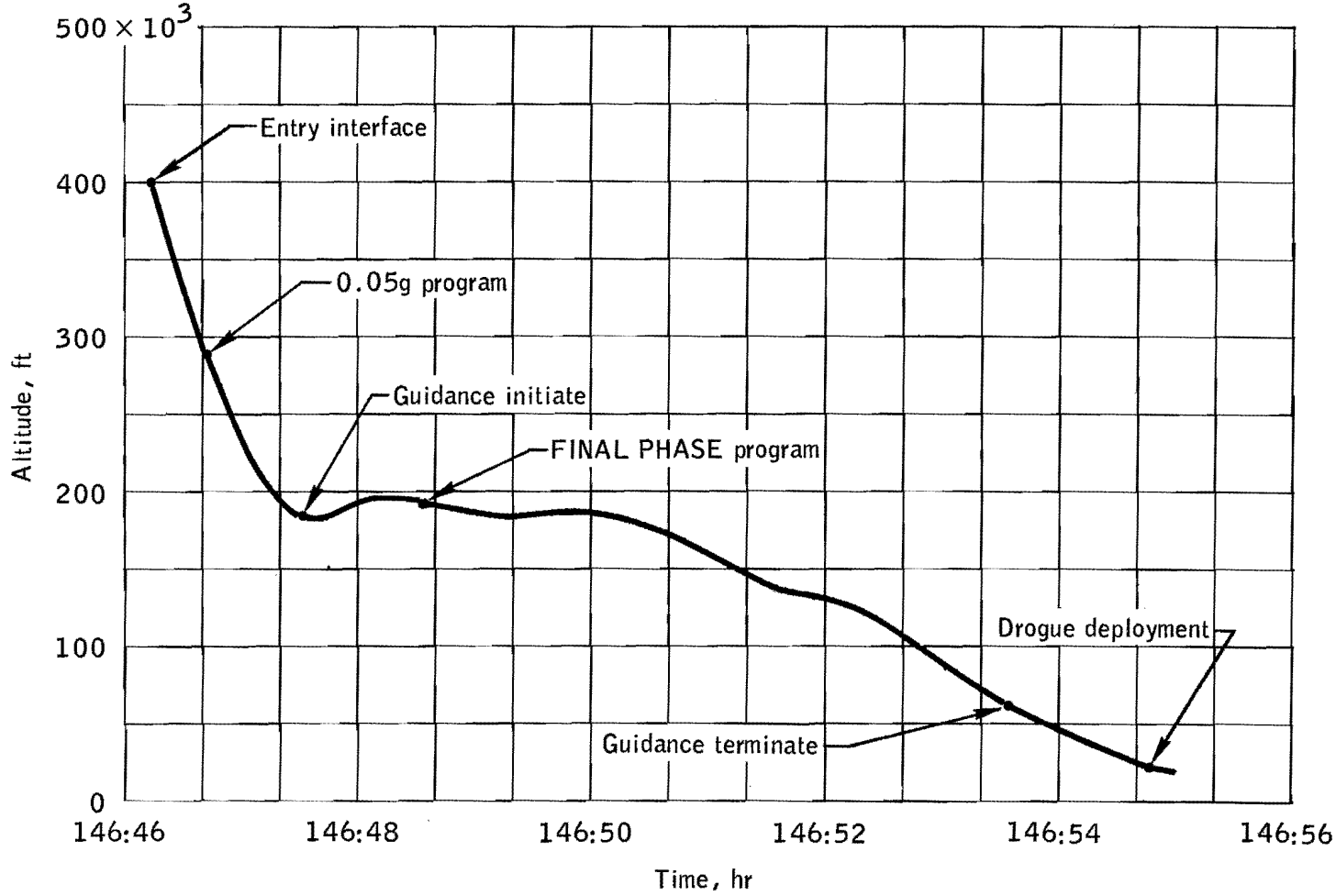

Figure 6.9-9.- Entry sequence of events.

NASA-S-69-667

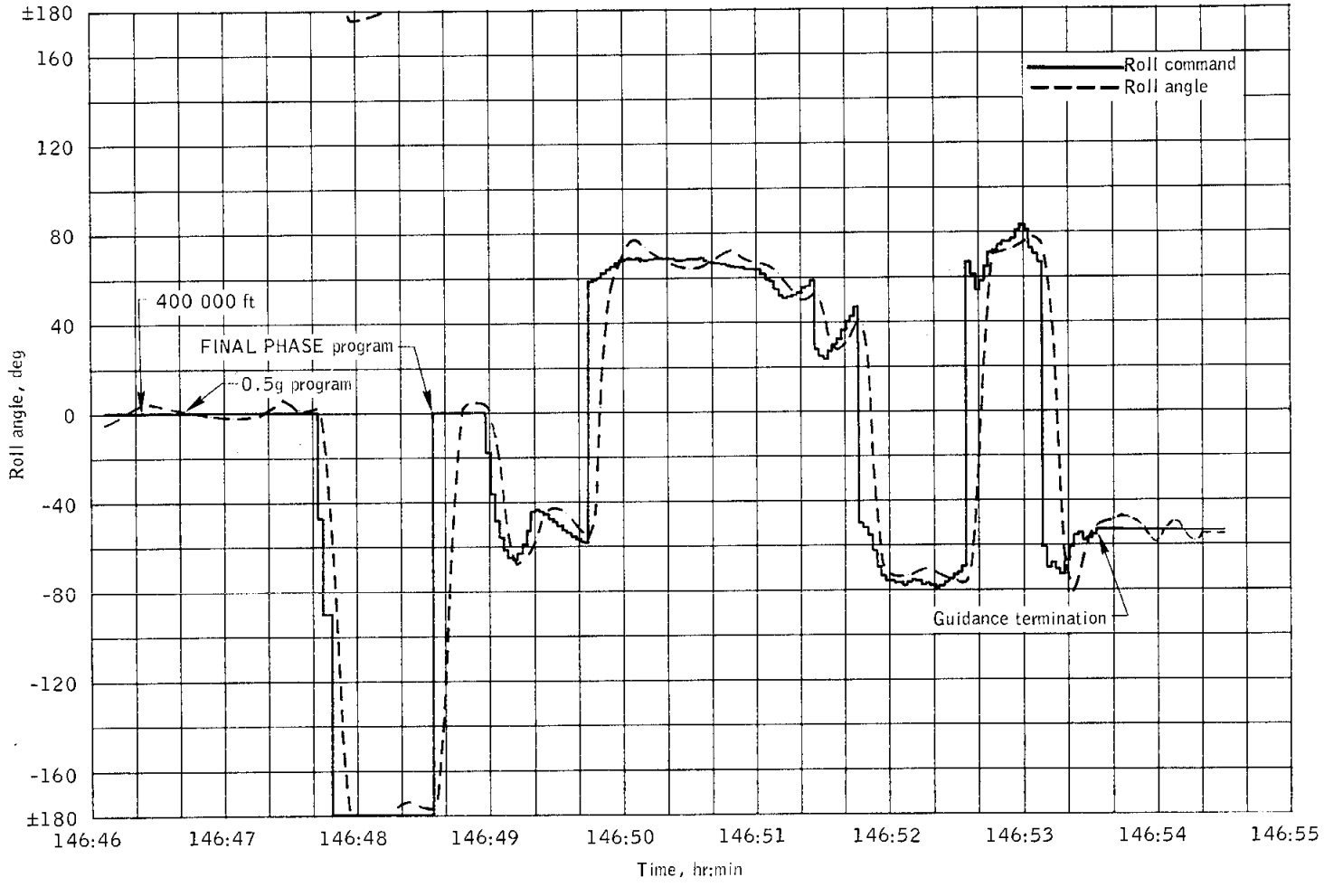

Figure 6.9-10. - Roll command plotted against actual roll.

NASA-S-69-668

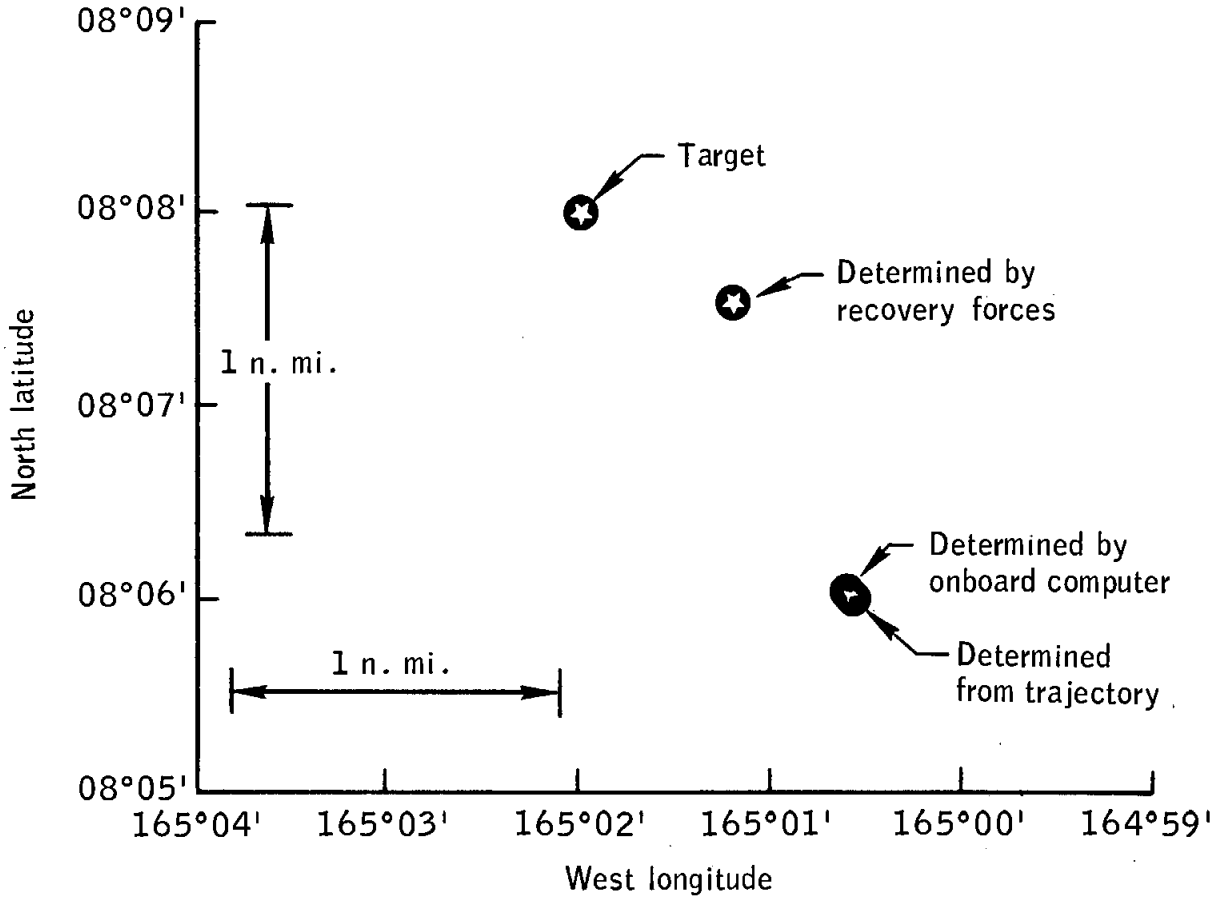

Figure 6.9-11.- Summary of landing point data.

NASA-S-69-669

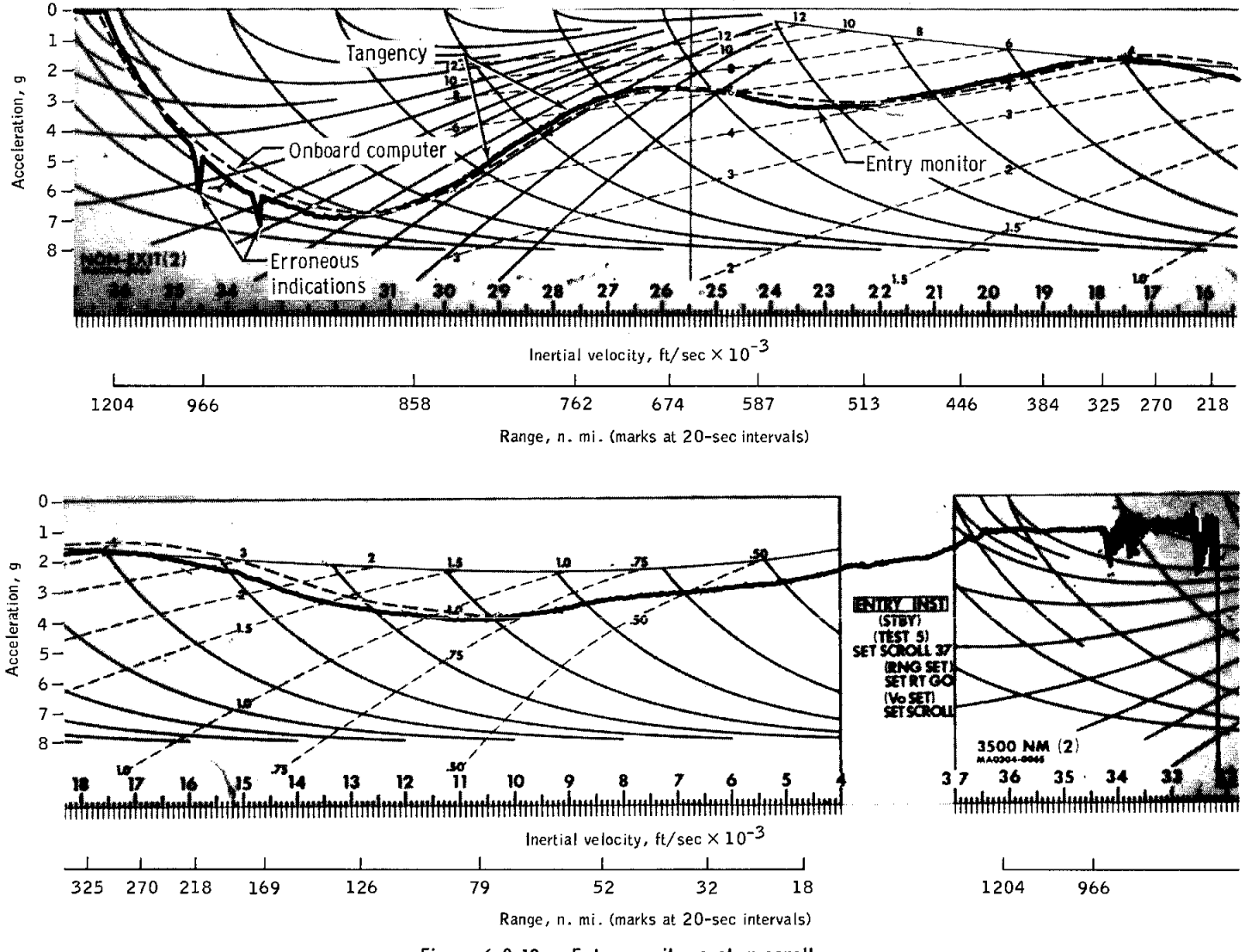

Figure 6.9-12.- Entry monitor system scroll.

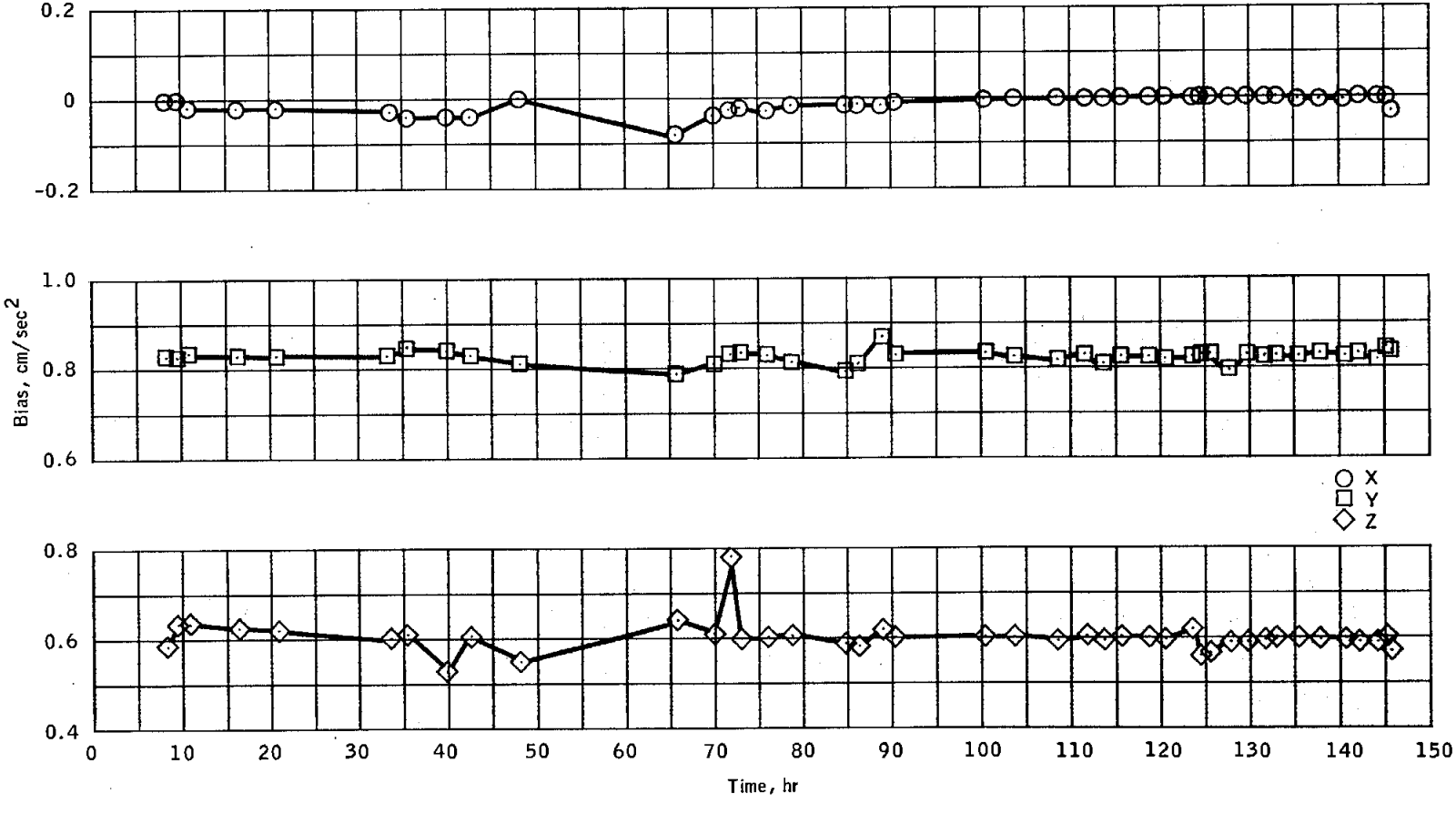

Figure 6.9-13. - Accelerometer bias measured during flight.

NASA-S-69-671

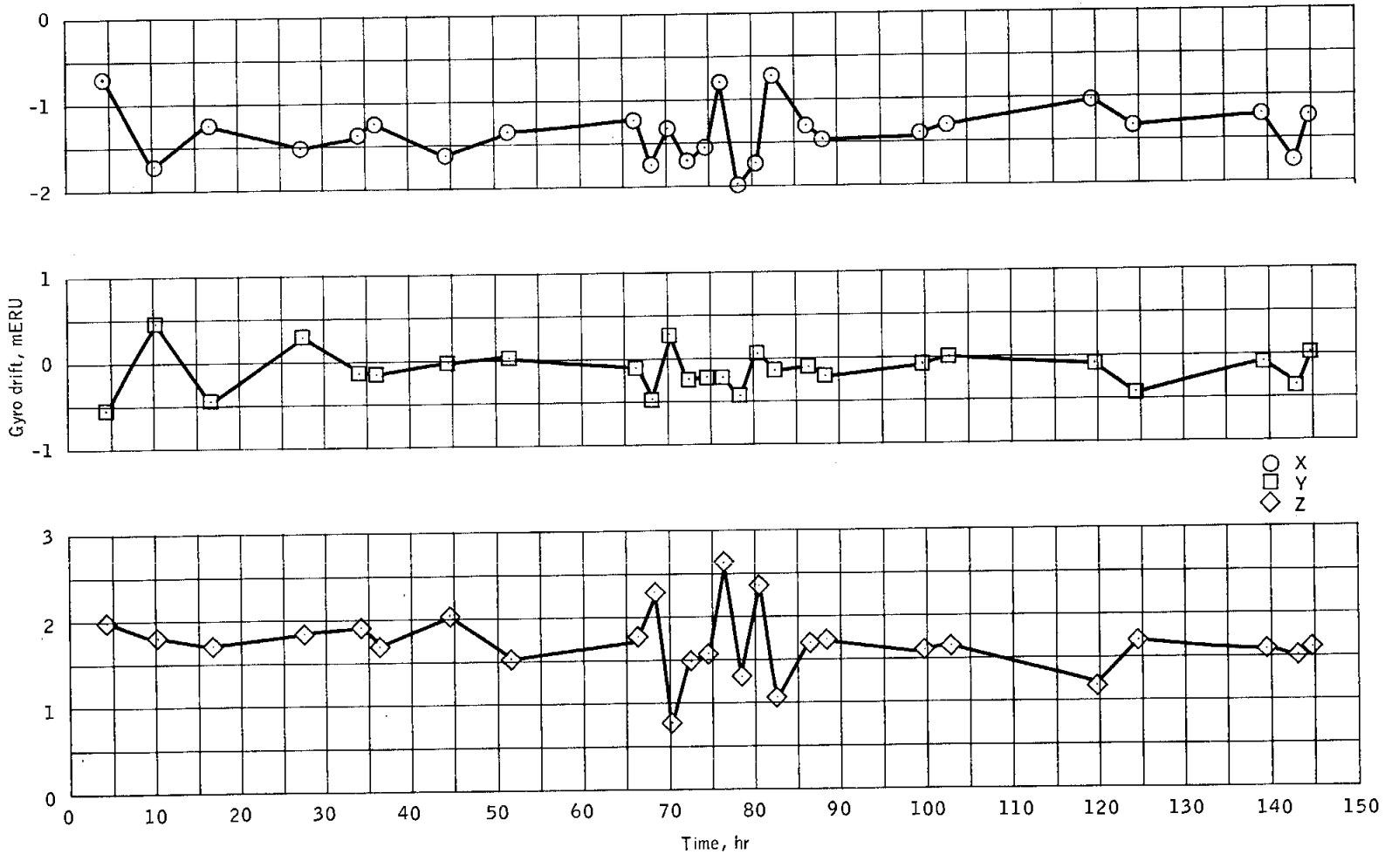

Figure 6.9-14. - Calculated gyro bias drift during flight.

NASA-S-69-672

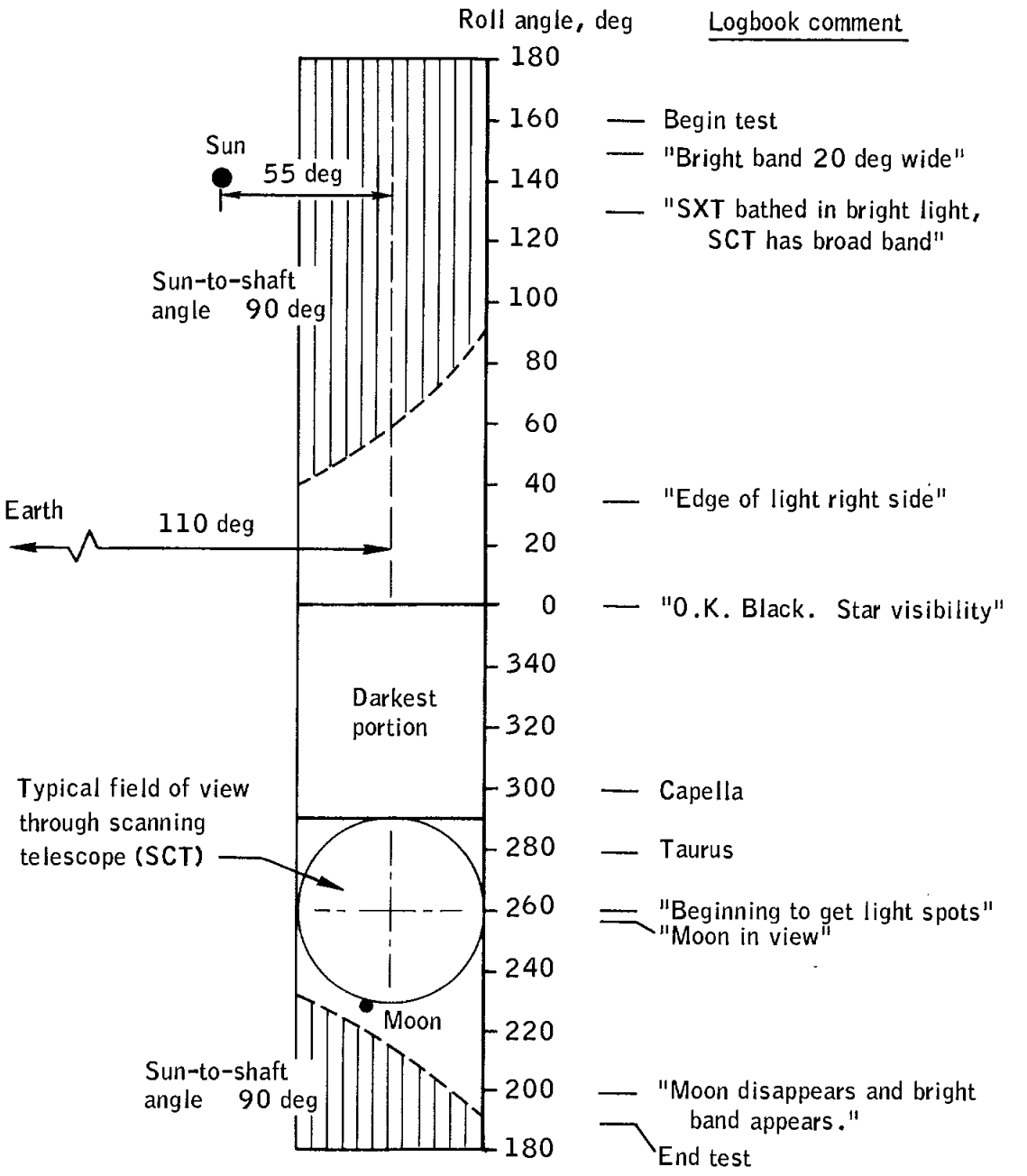

Figure 6.9-15.- Field coverage through scanning telescope at 123 hours.

6.10 REACTION CONTROL SYSTEMS

The performance of the service module and command module reaction control systems was nominal in all respects.

6.10.1 Service Module Reaction Control System

Thermal control of the service module reaction control system was satisfactory, and the quad package temperatures were maintained between 118° and 140° F except during periods of frequent engine activity. All regulated pressures, helium tank temperatures, and propellant usages were normal. A total of 634 pounds of propellant was used; the actual usage is compared with the preflight predicted values in figure 6.10-1. The deviation from the predicted values was primarily caused by the additional separation maneuver after translunar injection. A comparison of ground calculations and corrected onboard readings, converted from percent to expended weight, for each quad is shown in figure 6.10-2.

6.10.2 Command Module Reaction Control System

A brief checkout firing of both command module reaction control systems was performed successfully prior to command module/service module separation. Entry was accomplished using system A for attitude control and a total of approximately 36 pounds of propellant. The amount of propellant used during a particular interval can be determined from figure 6.10-3. The remainder of the propellant and helium was expended during the depletion burn and purge operation. Only a small residual helium pressure remained at landing.

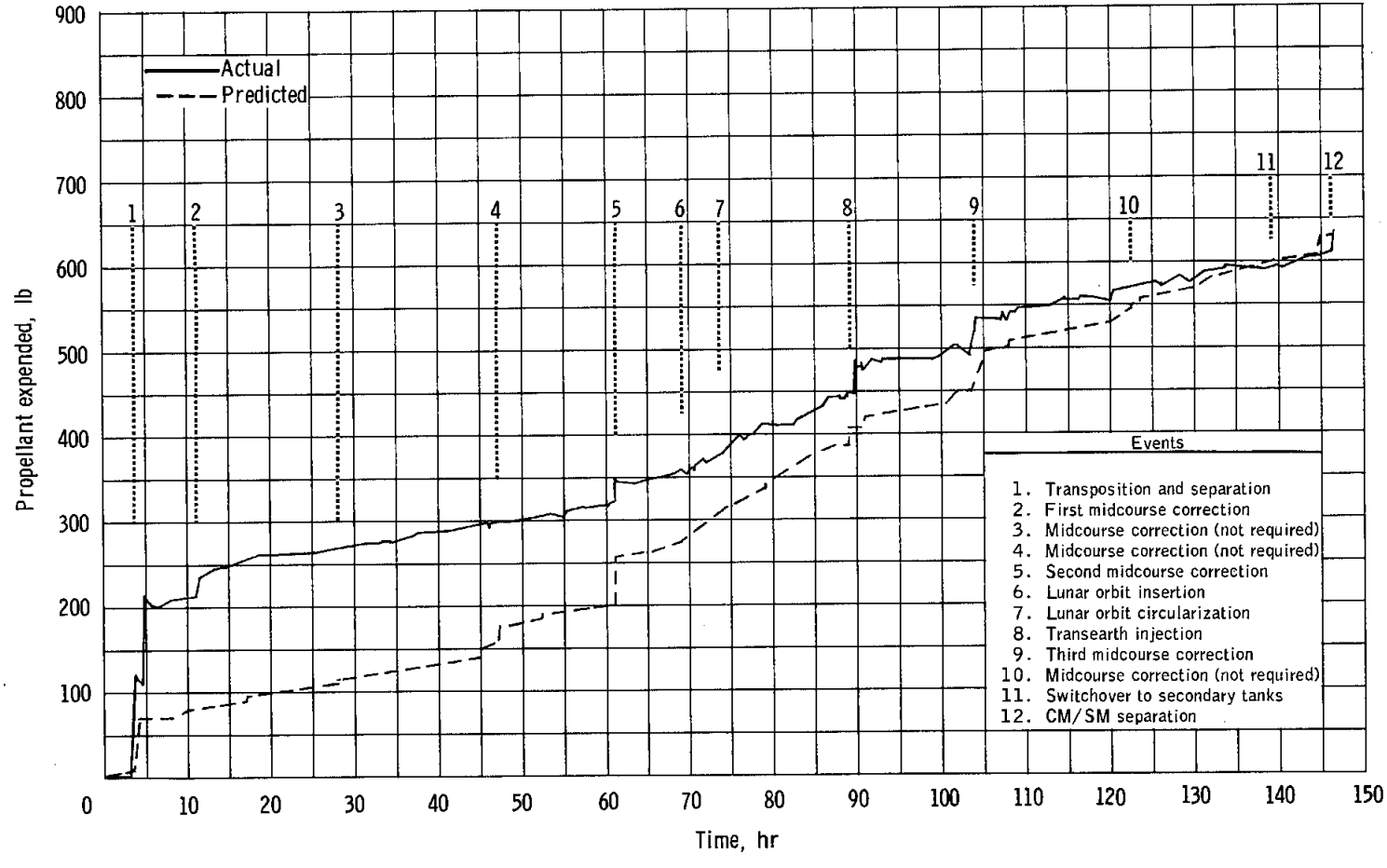

Figure 6.10-1. - Total propellant expended from service module reaction control system.

NASA-S-69-674

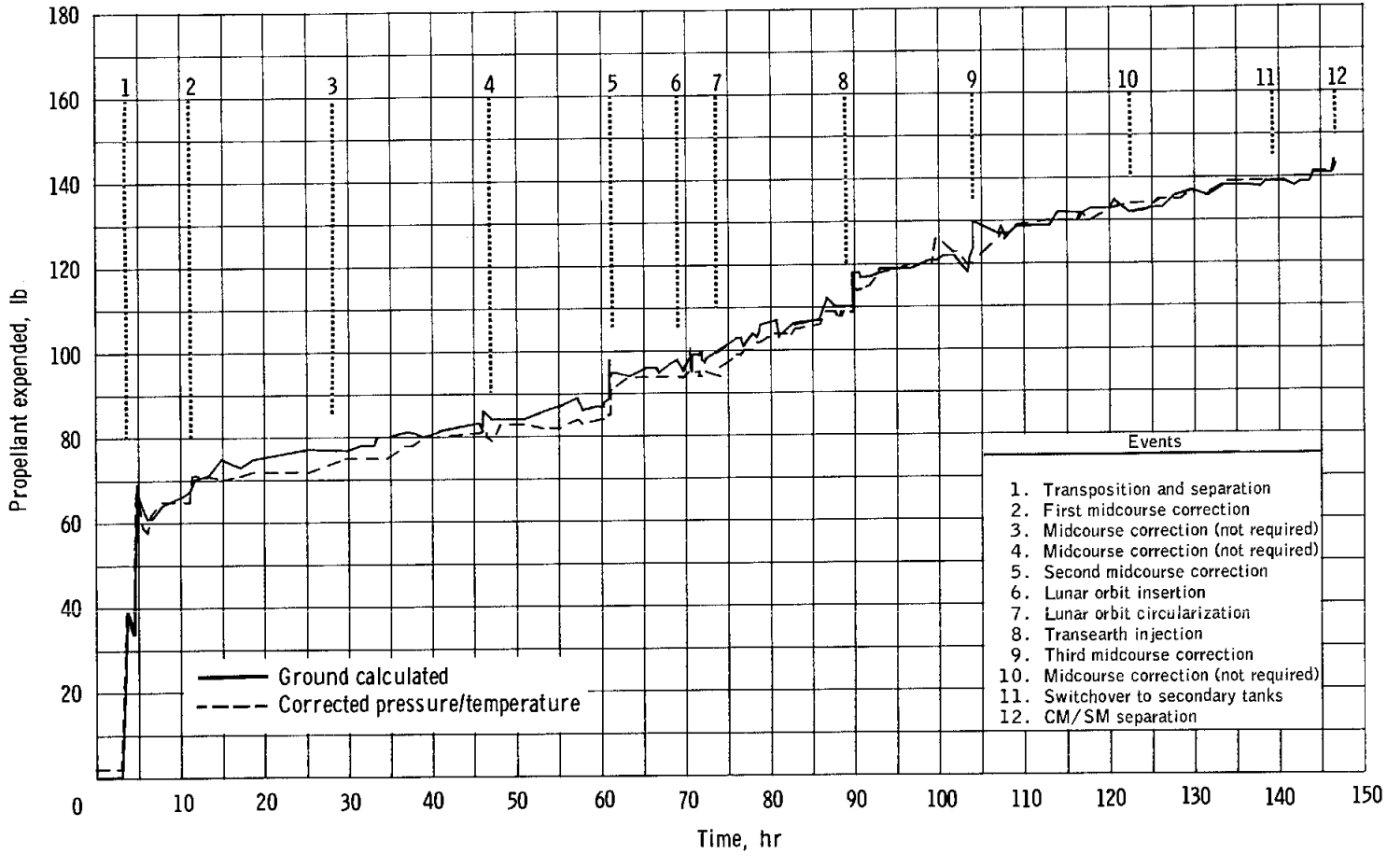

(a) Quad A.

Figure 6.10-2. - Propellants consumed from quads.

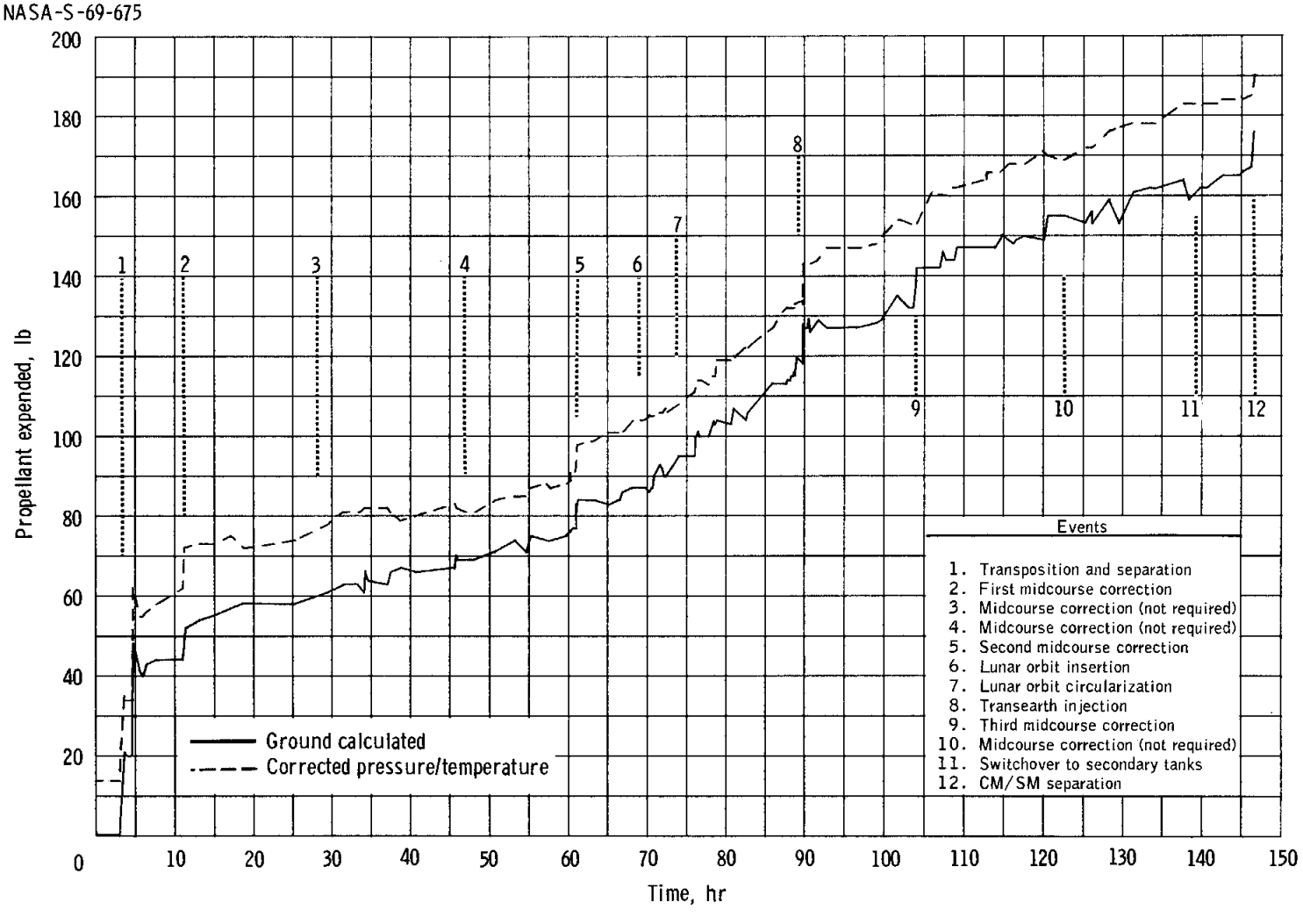

(b) Quad B.

Figure 6.10-2. - Continued.

NASA-S-69-676

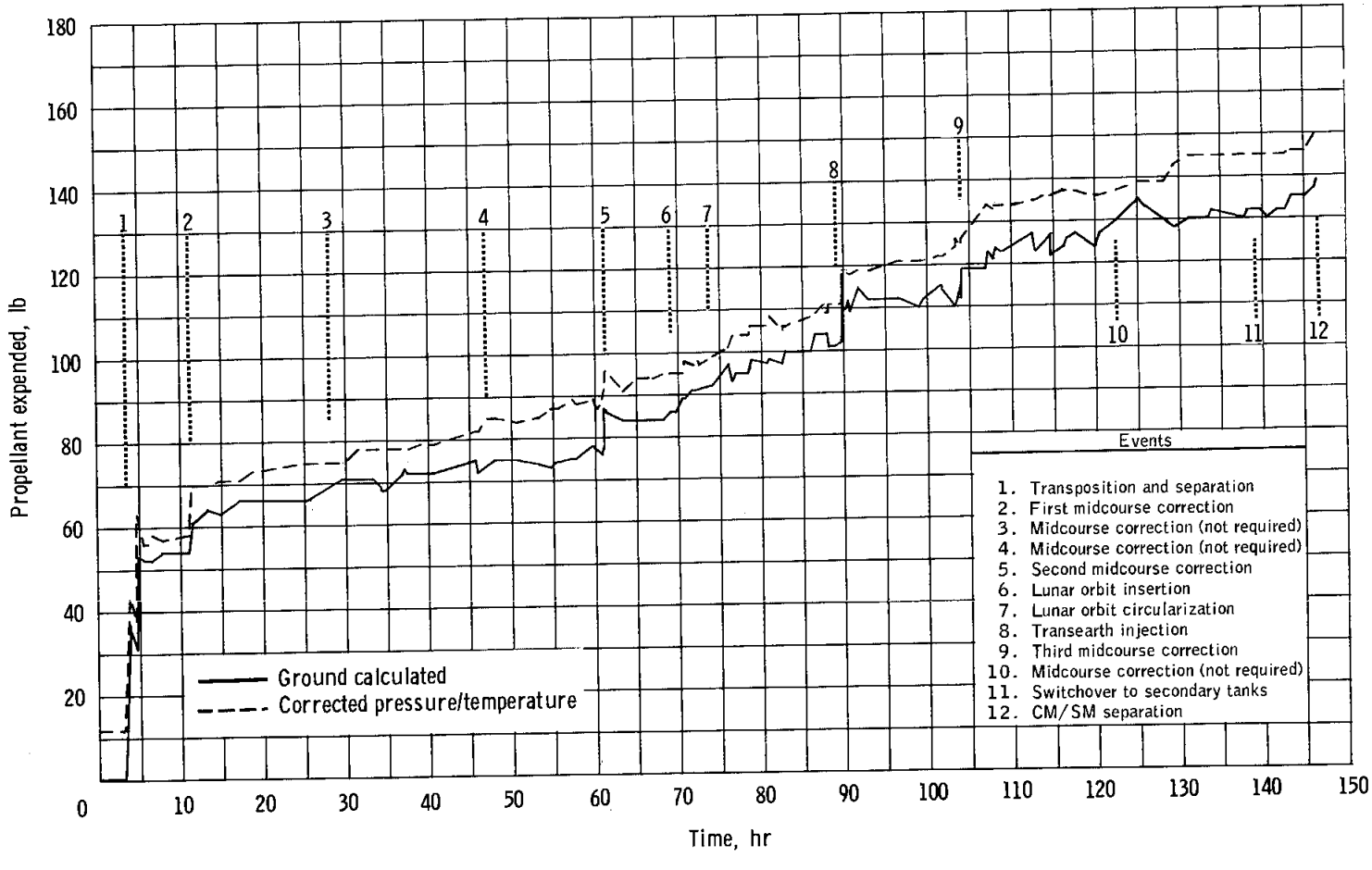

(c) Quad C.

Figure 6.10-2. - Continued.

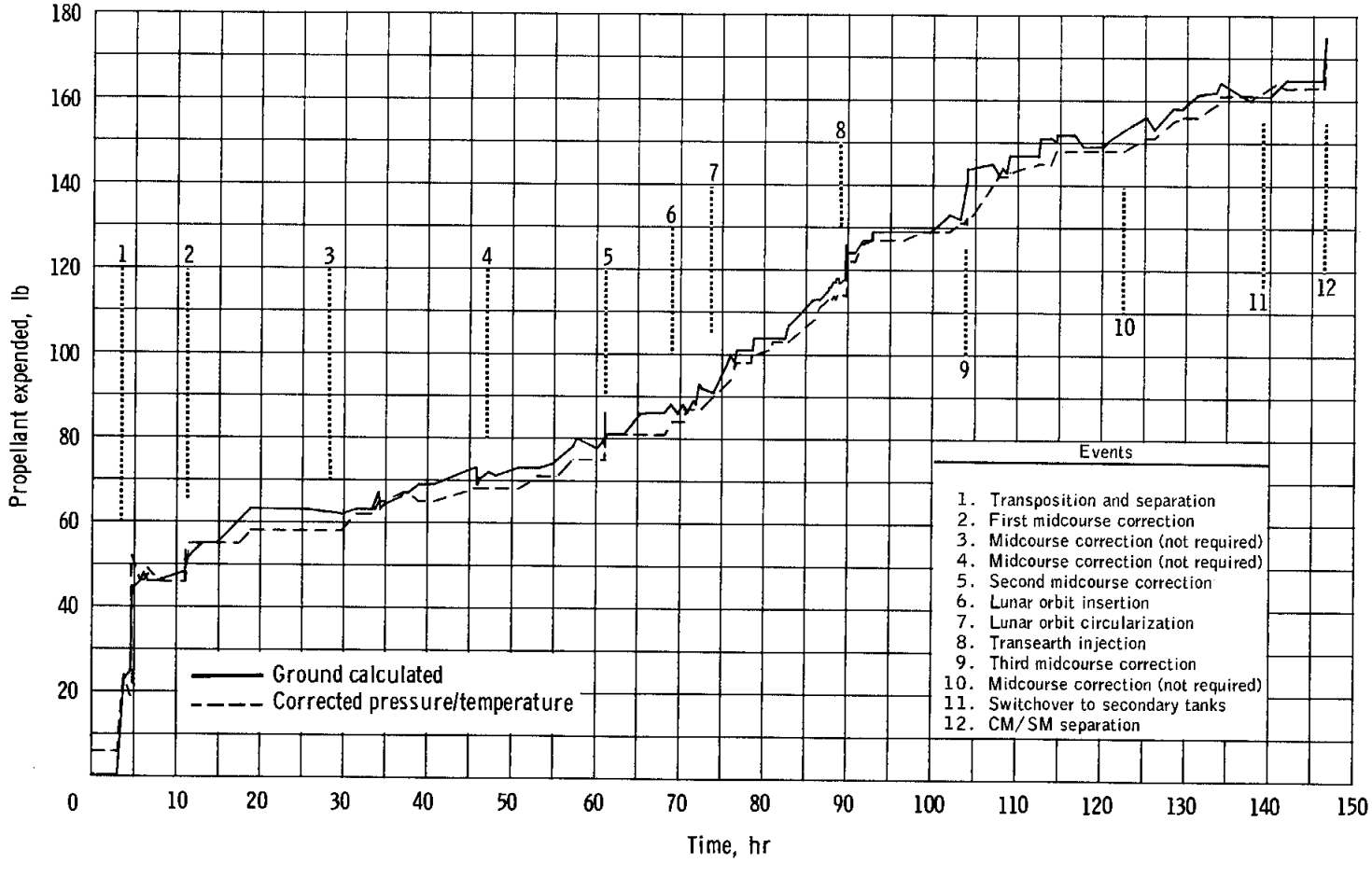

(d) Quad D.

Figure 6.10-2.- Concluded.

NASA-S-69-678

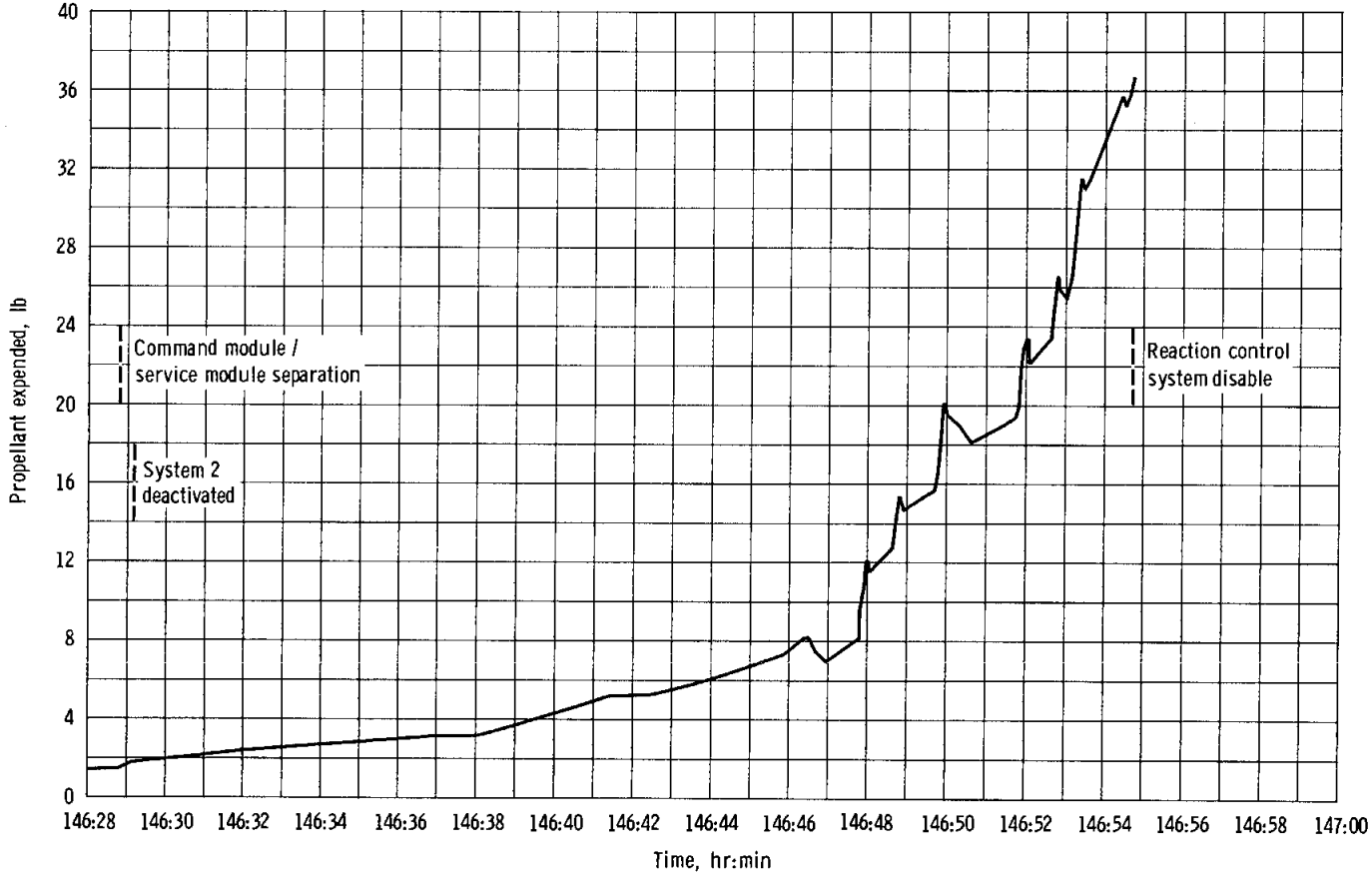

Figure 6.10-3. - Propellant expended from command module reaction control system.

6.11 SERVICE PROPULSION

Service propulsion system operation was satisfactory during the four maneuvers performed with this system. The longest engine firing was the 247-second lunar orbit insertion maneuver. Under normal conditions, none of these maneuvers would have required a plus X translation with the reaction control system to effect propellant settling. However, the fourth (transearth injection) was preceded, as planned, by a 15-second plus X translation to provide confidence in system operation had the storage tanks been emptied during the third maneuver.

A momentary drop in chamber pressure (fig. 6.11-1) was observed at the start of the first maneuver; this drop is attributed to the presence of a helium bubble in the oxidizer feed line. The trapped helium resulted from an inadequate engine-oxidizer bleed during preflight servicing. Comparable chamber pressure traces were obtained during a spacecraft ground test when the bleed procedure was also improperly conducted and during the AS-202 mission, during which the second service propulsion maneuver also exhibited helium ingestion. Chamber pressure characteristics were normal for the remaining three maneuvers. Bleed procedures have been changed in future spacecraft to preclude recurrence of trapped helium in the lines.

The propellant utilization and gaging system was utilized for loading the spacecraft; however, during the prelaunch checkout, both the fuel-sump-tank primary probe and a fuel point sensor in the storage tank did not operate properly, probably because of a short circuit. This malfunction could not be readily corrected, and since propellant reserves were relatively high in this mission, the fuel and oxidizer gaging systems were deactivated by opening the circuit breaker which was common to both.

6.11.1 Inflight Performance

The steady-state performance of the service propulsion engine was determined from a 200-second data segment of the lunar orbit insertion maneuver. Table 6.11-I contains a comparison of the calculated and predicted steady-state values. As shown in the table, the thrust and flow rates during the maneuver were approximately 2 percent less than predicted. The less-than-expected thrust and flow rates resulted from propellant-tank ullage pressures that were approximately 4 psi lower than predictions based on acceptance test data, but the pressures were within acceptable limits. The stems of the regulators which control ullage pressure were replaced prior to flight because of a quality fault in the original stems. Variations in manufacturing tolerances could account for lower regulator pressures during flight than those during acceptance testing, which was conducted using the original stems. Engine performance corrected to standard engine-acceptance inlet conditions yielded

a thrust of 20 396 pounds, a specific impulse of 313.0 seconds, and a propellant mixture ratio of 1.59. The first two values are 0.2 and 0.35 percent lower, respectively, than the values reported in the engine acceptance test log book but are within expected tolerances.

Table 6.11-II presents the measured steady-state pressures at representative time periods for the first and final service propulsion maneuvers. These pressures indicate satisfactory engine operation. The data from the lunar orbit circularization maneuver indicate normal system operation. The measured chamber pressure profiles for the first, second, and fourth service propulsion maneuvers are shown in figures 6.11-1, 6.11-2, and 6.11-3, respectively.

During the early portion of translunar coast, a drop of about 7 psi was noted in the service propulsion oxidizer tank pressure. The cause is believed to have been helium going into solution, and the decrease stopped when the oxidizer became saturated.

A summary of the start and shutdown transients for the second, third, and fourth service propulsion maneuvers is presented in table 6.11-III. All transient data for these maneuvers were within specification limits. In view of the helium ingestion problem, transients during the first maneuver are not meaningful and therefore are not shown.

The engine was started on all maneuvers using only one of two redundant sets of valves in the engine bipropellant valve assembly. This procedure was instituted to decrease the magnitude of initial chamber pressure, and therefore thrust level overshoot, characteristic of starts with both valve sets open. Noticeable decrease in the overshoot magnitude was realized. During the second and fourth maneuvers, the redundant valve set was opened approximately 3 seconds after ignition to maximize operational reliability for the remainder of the firing.

The engine firings for the lunar orbit insertion and the transearth injection maneuvers were longer than planned by approximately 4.9 and 5.7 seconds, respectively, to achieve the required velocity change. The lower thrust caused by the decreased tank pressures can account for the increased firing times.

During all four service propulsion maneuvers, the measured oxidizer interface pressure was approximately 8 psi lower than expected. The oxidizer interface pressure reading was such that malfunctioning instrumentation is very unlikely because the measured pressures were valid for no-flow conditions. Analysis of the flight data confirm that the interface pressure could not be low by 8 psi. For example, the lunar orbit insertion maneuver would have been 10 seconds longer had the indicated pressure been valid for this sensor location, immediately upstream of the flow orifice. A measurement port, located immediately downstream of the flow orifice at

the engine interface and used during acceptance testing, would normally be plugged. A transducer at this downstream location would have responded in the same manner as observed during the mission. When a new engine was installed at the launch site, the interface pressure transducer could have been installed in the wrong location in relation to the orifice and yielded the data bias seen. However, the engineering work sheets do not substantiate an improper sensor location, and another installation error may have existed.

6.11.2 Propellant Loading

The oxidizer tanks were loaded to an indicated quantity of 100.9 percent at a tank pressure of 109 psia and an oxidizer temperature of 69° F. The fuel tanks were loaded to an indicated quantity of 100.9 percent at a tank pressure of 113 psia and a fuel temperature of 70° F. A density determination was made for two oxidizer and two fuel samples. Based on these density values and indicated tank load percentages, the actual propellant loads were determined to be:

	Actual	Planned
Oxidizer, lb	25 105.1	25 090.0
Fuel, lb	15 730.9	15 695.0
Total, lb	40 836.0	40 785.0

6.11.3 Thermal Control

All service propulsion temperatures were maintained well within redline limits. No heater operation was required, since passive thermal control was effective in maintaining temperature stability. The minimum and maximum temperatures at specific locations are given in table 6.11-IV.

TABLE 6.11-I.- STEADY-STATE PERFORMANCE DURING LUNAR ORBIT INSERTION

Parameter	50 sec after ignition			200 sec after ignition		
	Predicted	Measured	Calculated	Predicted	Measured	Calculated
Instrumented						
Oxidizer tank pressure, psia	179	174	175	180	175	176
Fuel tank pressure, psia	177	174	173	178	175	174
Oxidizer interface pressure, psia	166	154	162	166	154	162
Fuel interface pressure, psia	174	169	169	174	170	170
Engine chamber pressure, psia	102	100	100	102	102	100
Derived						
Oxidizer flowrate, lb/sec	40.9		40.2	40.8		40.2
Fuel flowrate, lb/sec	25.7		25.2	25.7		25.2
Propellant mixture ratio	1.59		1.59	1.58		1.59
Vacuum specific impulse, sec	314.2		313.0	314.2		313.0
Vacuum thrust, lb	20 924		20 498	20 899		20 466

TABLE 6.11-II.- STEADY-STATE PRESSURES DURING
FIRST MIDCOURSE CORRECTION AND TRANSEARTH INJECTION

Measured pressures	First midcourse correction (2 sec after ignition)	Transearth injection	
		80 sec after ignition	180 sec after ignition
Oxidizer tank, psia	169	175	176
Fuel tank, psia	169	174	176
Oxidizer interface, psia[a]	152	158	158
Fuel interface, psia	167	173	174
Engine chamber, psia	95	103	104

[a]Data considered erroneous. Data low by approximately 8 psi.

TABLE 6.11-III.- SERVICE PROPULSION TRANSIENT DATA

Parameter	Specification limit		Service propulsion maneuver		
	Single valve set	Dual valve set	Lunar orbit insertion	Lunar orbit circularization	Transearth injection
Total vacuum impulse from ignition to 90 percent steady-state thrust, lbf-sec	[a]460 ± 250 [b]460 ± 250	--	504.7	665.5	683.7
Time from ignition to 90 percent steady-state thrust, sec	0.675 ± 0.100	--	0.660	0.620	0.650
Chamber pressure overshoot peak, percent of nominal	120	--	113	110.5	112.8
Total vacuum impulse from cutoff signal to zero thrust, lbf-sec	[a]12 500 ± 2500 [b]12 500 ± 500	[a]13 500 ± 2500 [b]13 500 ± 500	11 625	10 031	11 933
Time from cutoff to 10 percent steady-state thrust, sec	1.075 ± 0.175	1.075 ± 0.175	1.24	0.901	1.01

[a]Engine-to-engine tolerance.

[b]Run-to-run tolerance.

TABLE 6.11-IV.- MAXIMUM AND MINIMUM SERVICE PROPULSION TEMPERATURES

Measurement location	Temperature, °F			
	Minimum		Maximum	
	Redline	Actual	Redline	Actual
Engine bipropellant valve	30	62	160	[a]121
Fuel engine line	25	64	110	85
Oxidizer engine line	25	65	110	85
Oxidizer system line	30	62	110	71
Fuel system line	30	67	110	84
Oxidizer propellant utilization valve inlet	30	61	110	83
Oxidizer propellant utilization valve outlet	30	59	110	79

[a]Maximum soakback temperature after transearth injection maneuver.

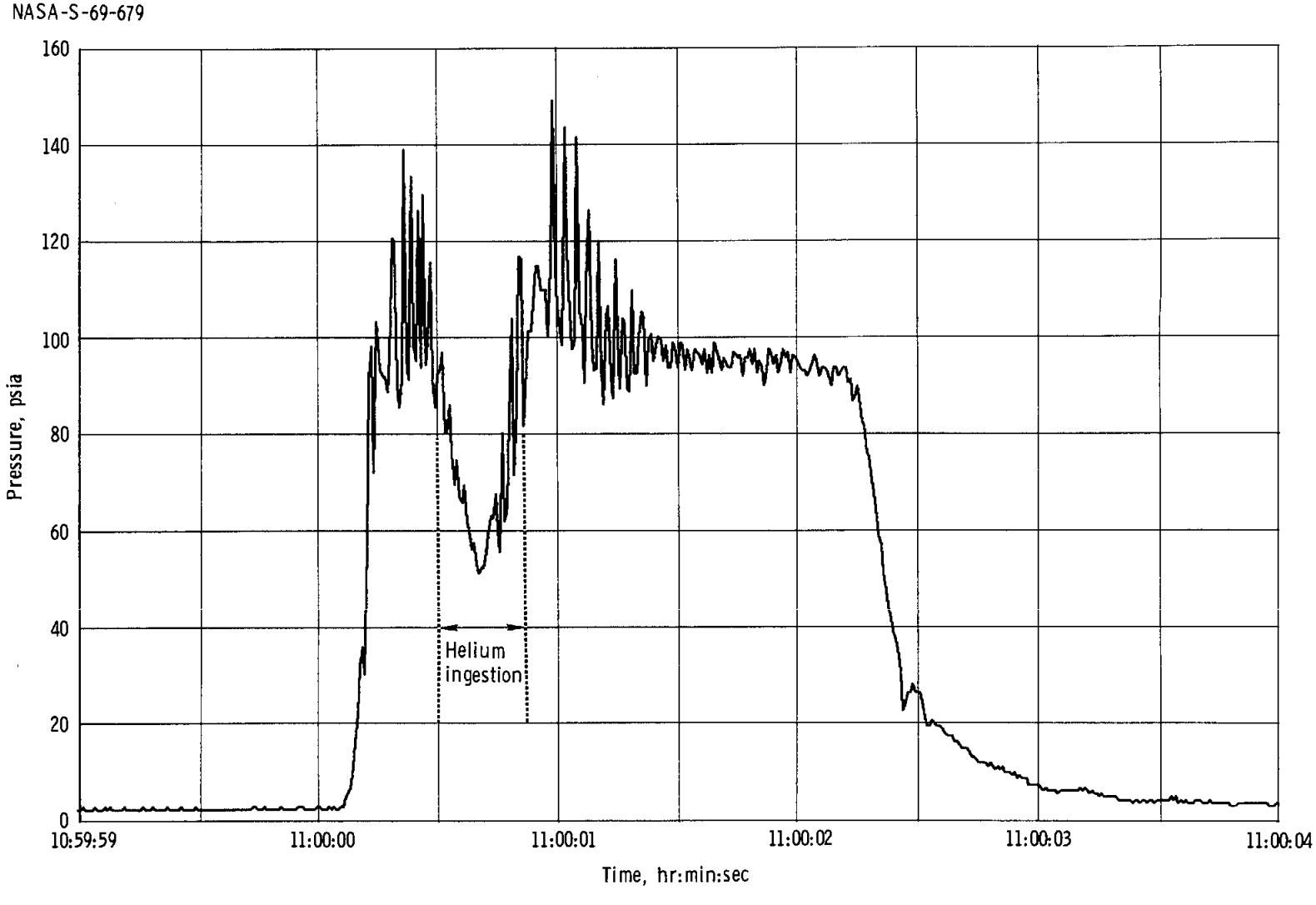

Figure 6.11-1. - Chamber pressure during first service propulsion maneuver.

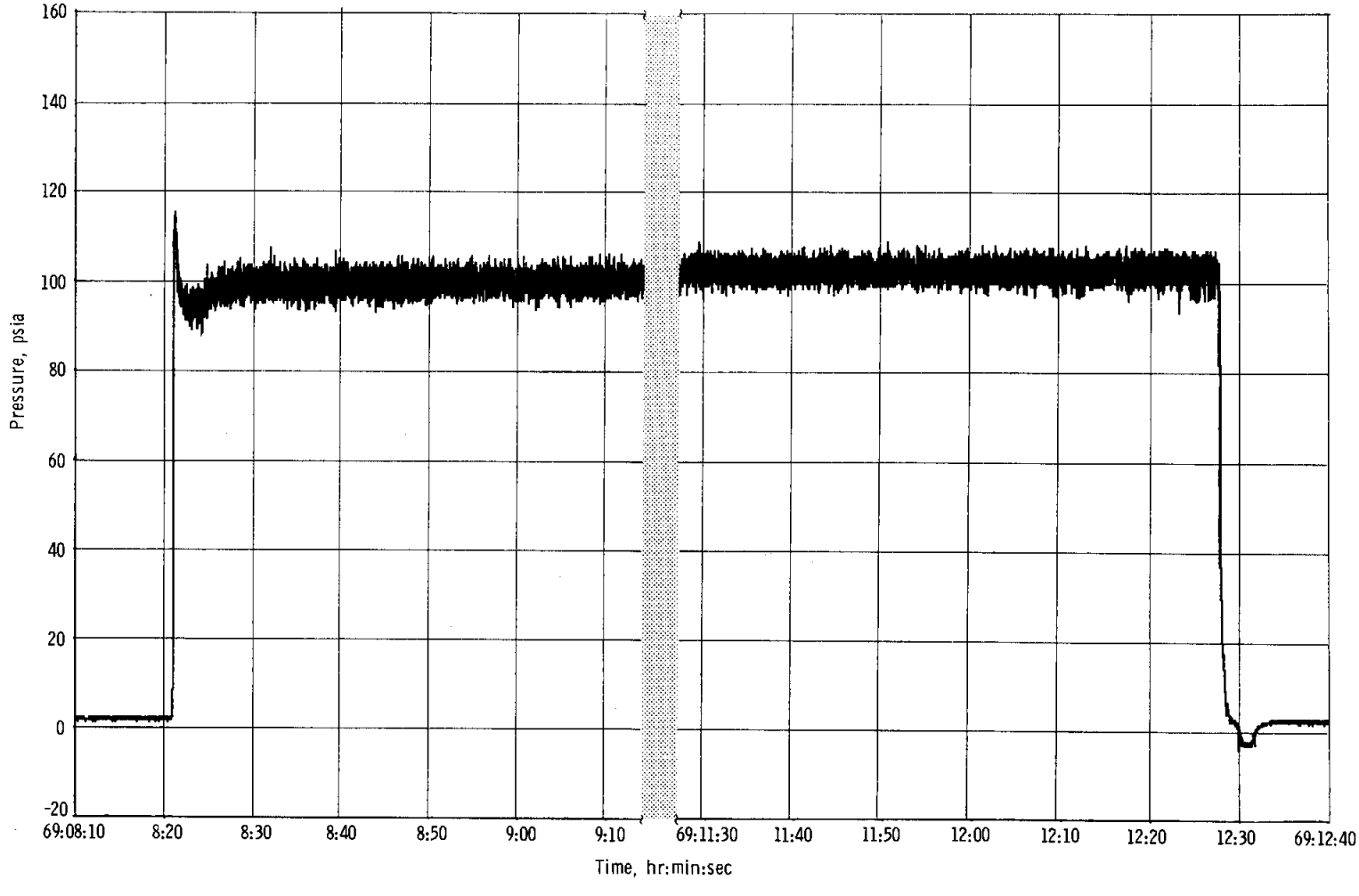

Figure 6.11-2. - Chamber pressure during second service propulsion maneuver.

NASA-S-69-681

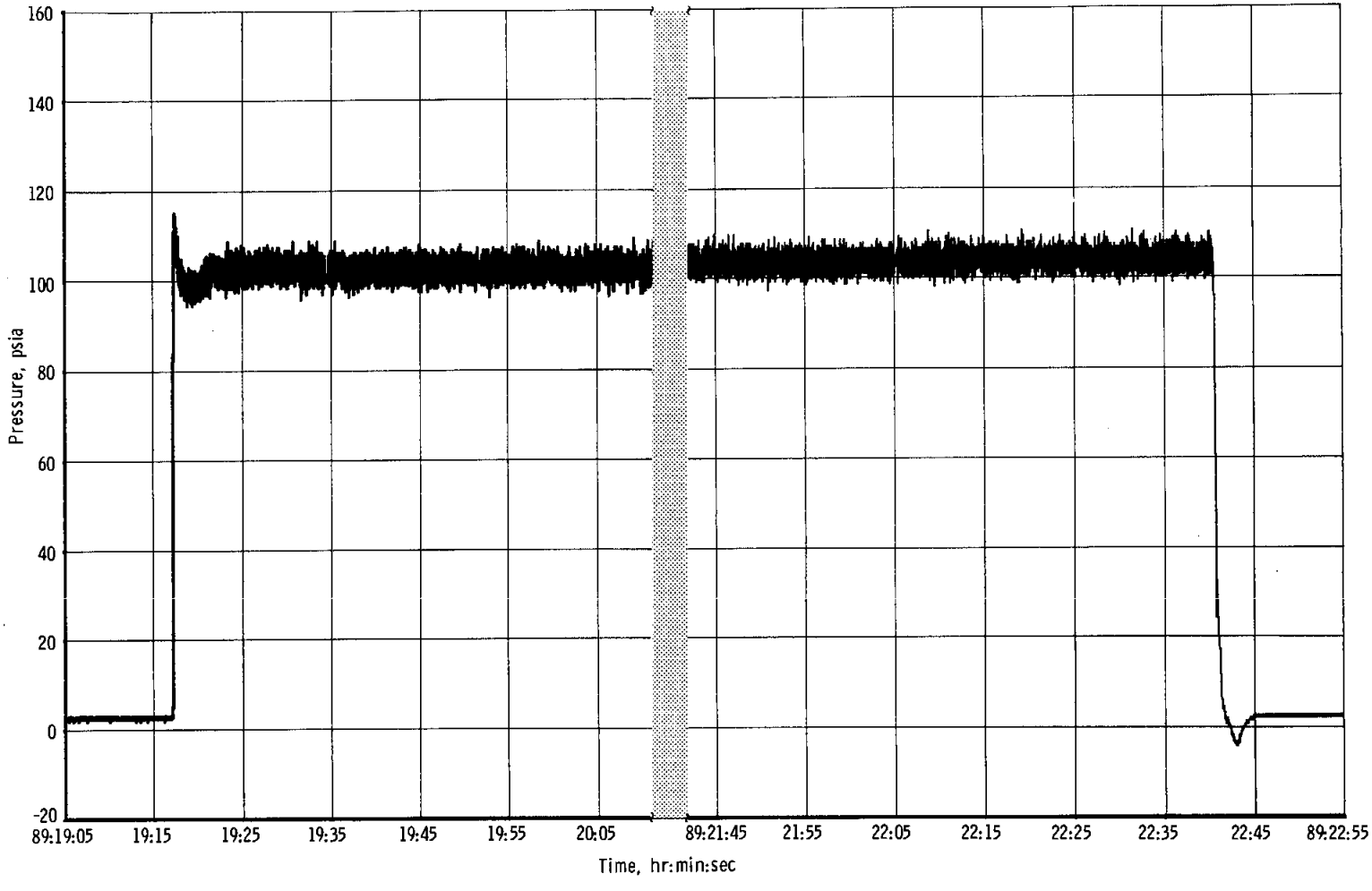

Figure 6.11-3. - Chamber pressure during fourth service propulsion maneuver.

6.12 CREW SYSTEMS

The environmental control system was required to operate under the translunar coast, lunar orbit, and transearth coast thermal environments. The performance of the system was satisfactory during all these phases. The crew remained comfortable, and the spacecraft equipment was maintained in a favorably controlled thermal condition.

6.12.1 Pressure-Suit and Cabin Circuits

The cabin pressure reached 6.2 psid at 52 seconds after launch and the relief valve began relieving. At approximately 0:05:20 the valve sealed at 5.92 psia, and at 2:25:00 the cabin pressure decreased to the cabin regulator operating pressure. The launch parameters for the suit and cabin circuits are shown in figure 6.12-1. The cabin pressure decayed rapidly during the early phase of the mission because the waste management dump valve was open to accelerate oxygen enrichment of the cabin air (60-percent oxygen and 40-percent nitrogen prior to launch). The oxygen enrichment cabin purge was terminated at 8:06:00. The cabin and suit circuits operated normally throughout the mission and during entry (fig. 6.12-2).

Lithium hydroxide element usage.- Twenty lithium hydroxide elements were stowed onboard, including two installed in the environmental control unit canister. The carbon dioxide partial pressure varied between 0.2 and 0.3 mm Hg during most of the mission and reached a maximum of 0.8 mm Hg prior to one of the element changes. A total of 13 element changes were made, and all were satisfactory.

Cabin fans.- The crew turned the cabin fans off early in the mission to reduce the noise level. During a subsequent check of cabin temperature, the fans were turned on for a short time, and the crew reported that fan 2 was quite noisy (see section 12). The fans were turned off for the remainder of the mission. Postflight tests indicate that the fans had not malfunctioned. The noise was probably caused by a resonant condition within the duct system for the existing environment.

Cabin humidity.- The cabin humidity level remained within a comfortable range, and the crew noted no moisture or free water in the cabin until about 52 hours. At this time, moisture appeared on the cabin walls. This resulted from the earlier adjustment of the glycol mixing valve to 50° to 55° F to raise the cabin temperature to a more comfortable level. The mixing valve adjustment also affected the suit heat exchanger temperature such that the moisture content in the cabin increased. When the mixing valve was returned to the automatic mode, condensation on the cool walls disappeared, and control was normal for the remainder of the mission.

6.12.2 Thermal Control System

Coolant system operation during the early phase of the mission was normal. At approximately 21 minutes, the radiators were activated, and the outlet temperature rapidly decreased to a normal value, less than the inlet temperature of 73° F.

To prevent attitude perturbation resulting from evaporator operation, the primary glycol evaporator was manually deactivated for the translunar coast phase. The radiator outlet temperatures varied normally between 30° and 45° F during translunar coast and the evaporator was not required. The primary evaporator was activated for lunar orbit, but it dried out during the first and fourth revolutions. The dryout condition was anticipated based on Apollo 7 experience. After each dryout, the evaporator was reserviced, and it operated satisfactorily for six consecutive revolutions. During the transearth coast phase, the evaporator was deactivated until just prior to entry. After activation, it again dried out twice (fig. 6.12-3), but the secondary coolant loop operated efficiently during entry and maintained the gas temperature at the suit heat exchanger outlet at a comfortable level.

Except for the anticipated primary evaporator dryout problem, coolant loop performance during lunar orbit was satisfactory. The radiators and evaporator rejected an average load of 5500 Btu/hr over a radiator outlet temperature range of 18° to 66° F.

Typical operation of the coolant system is shown in figure 6.12-4 for lunar orbits 6 and 7. When the radiator outlet temperature reaches 50° F, the water evaporator automatically starts, as shown by the evaporator outlet temperature drop to 40° F. Approaching the night cycle, the radiator outlet temperature drops, and a thermal transient, caused by the proportioning valve adjusting the flow between the two radiator panels, precedes the evaporator turning off (see fig. 6.12-4). The mixing valve is then operated in response to the radiator outlet temperature, as indicated by the evaporator outlet temperature. The mixing valve maintained the anticipated evaporator outlet temperatures (42° to 48° F) after recovering from an initial control transient, allowing the outlet temperature to decrease to an undershoot of 6° F. In each case, the mixing valve maintained proper control after the transient.

At 120:03:50, the primary radiator outlet temperature abruptly increased from 30° F to the upper limit of the transducer (108° F), and agreed with the onboard indication. This condition is believed to be associated with the measuring circuit, since other measurements in the system do not confirm the change nor can the thermal dynamics of the system support such a change.

6.12.3 Water Management

About 2 hours prior to launch, the potable water was chlorinated with one ampule of chlorine and one ampule of buffer. At lift-off, the potable and waste tank quantities were 71 and 73 percent, respectively. The potable tank, which is supplied by water from fuel-cell production, became full at about 8 hours, and except for the small amount of water consumed by the crew, this tank remained full for the entire mission. After landing, 38.4 and 36.0 pounds of water remained in the potable and waste tanks, respectively. A total of approximately 153 pounds of water was dumped during the six manual overboard dumps.

At 143:53:00, prior to entry, the potable tank quantity decreased abruptly from 104.4 percent to 57 percent. The indicated quantity became erratic after the initial decrease and reached a minimum of 21 percent at 144:39:00 after initiation of the spacecraft maneuver to entry attitude. Additional erratic readings persisted until landing. The abrupt changes were the result of a failure in the potable tank quantity measuring system and were not caused by water leakage. (See section 12.)

The crew reported that the taste of the chlorinated water was acceptable.

6.12.4 Postlanding Ventilation

The crew estimated 2 to 3 quarts of water entered the cabin through the cabin pressure relief valve at landing. Postflight tests were conducted on the valve installed in the spacecraft. Test results indicate that, with both sides of the valve in the closed position, gaseous leakage through the system is 60 scc/min at a differential pressure of 18 inches of water. The differential pressure was increased up to 13 psi, with no significant increase in leakage. Test results indicate that the valve operated as designed and would not have allowed water ingestion if properly closed.

The postlanding ventilation system was activated after the command module was returned from stable II (apex down) to the stable I position. Additional water entered the command module through the postlanding ventilation valves, which were then closed. The system was activated again and performed satisfactorily.

NASA-S-69-682

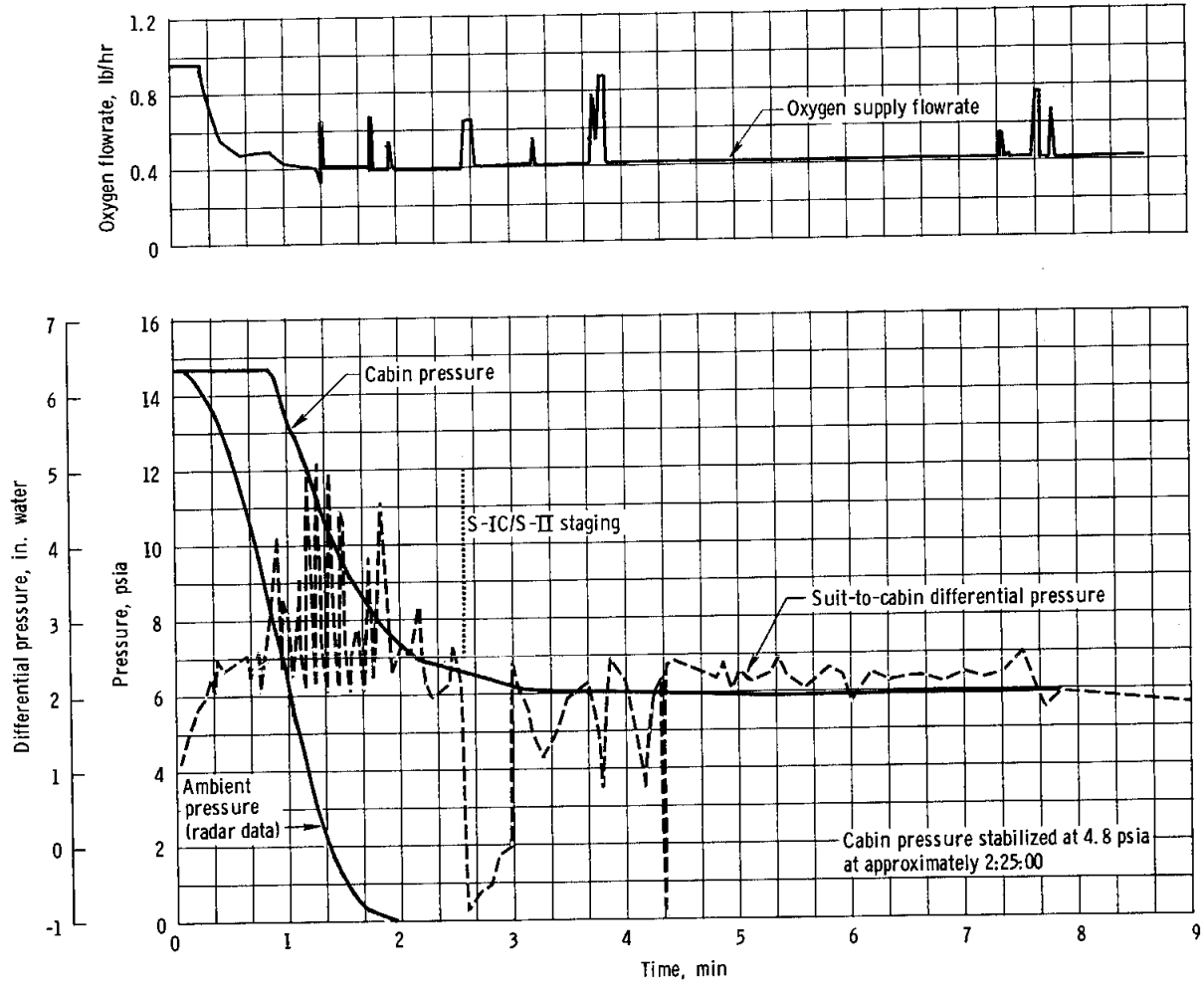

Figure 6.12-1. - Cabin and ambient pressure and suit pressure and oxygen flow during launch.

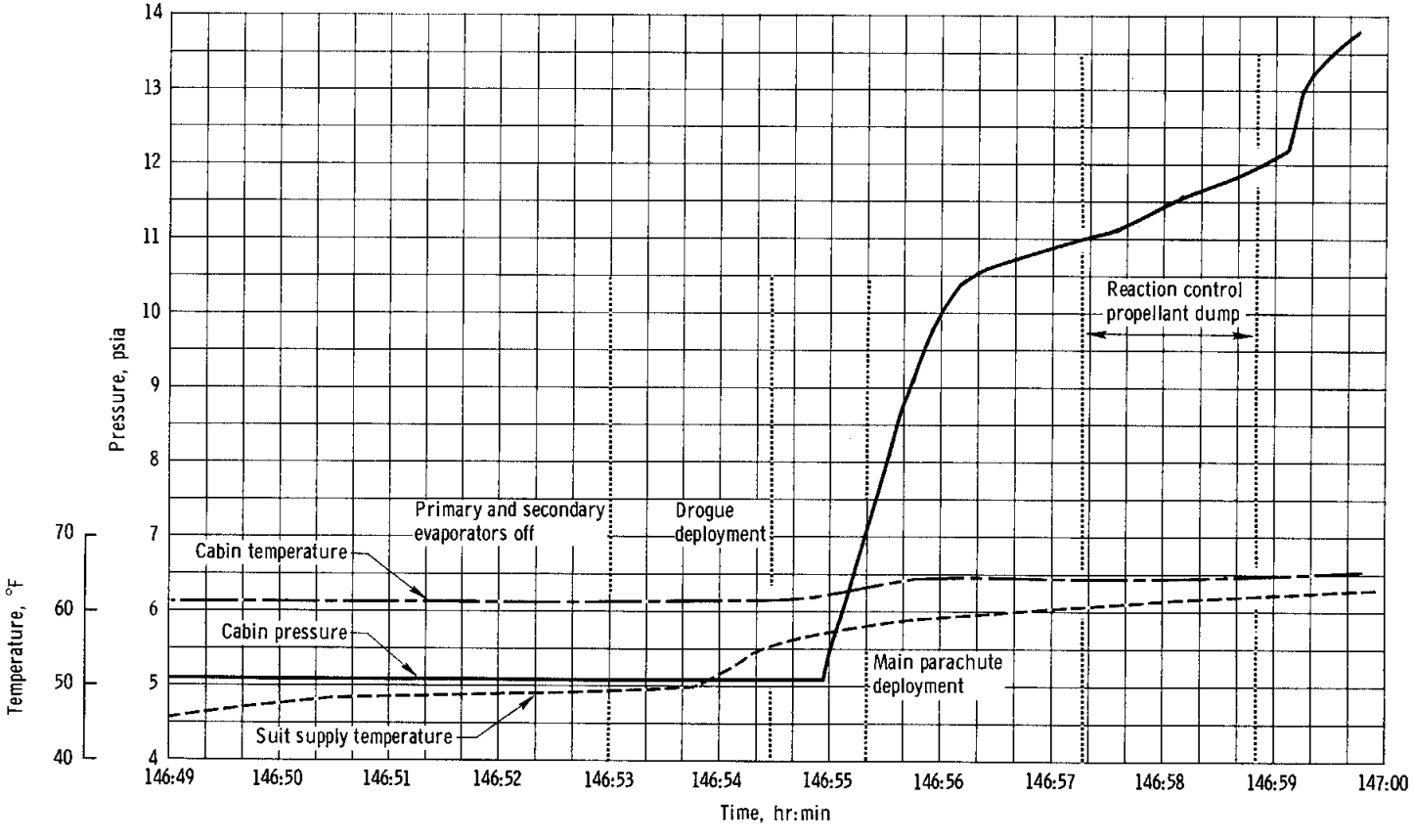

Figure 6.12-2. - Cabin pressure and temperatures during entry.

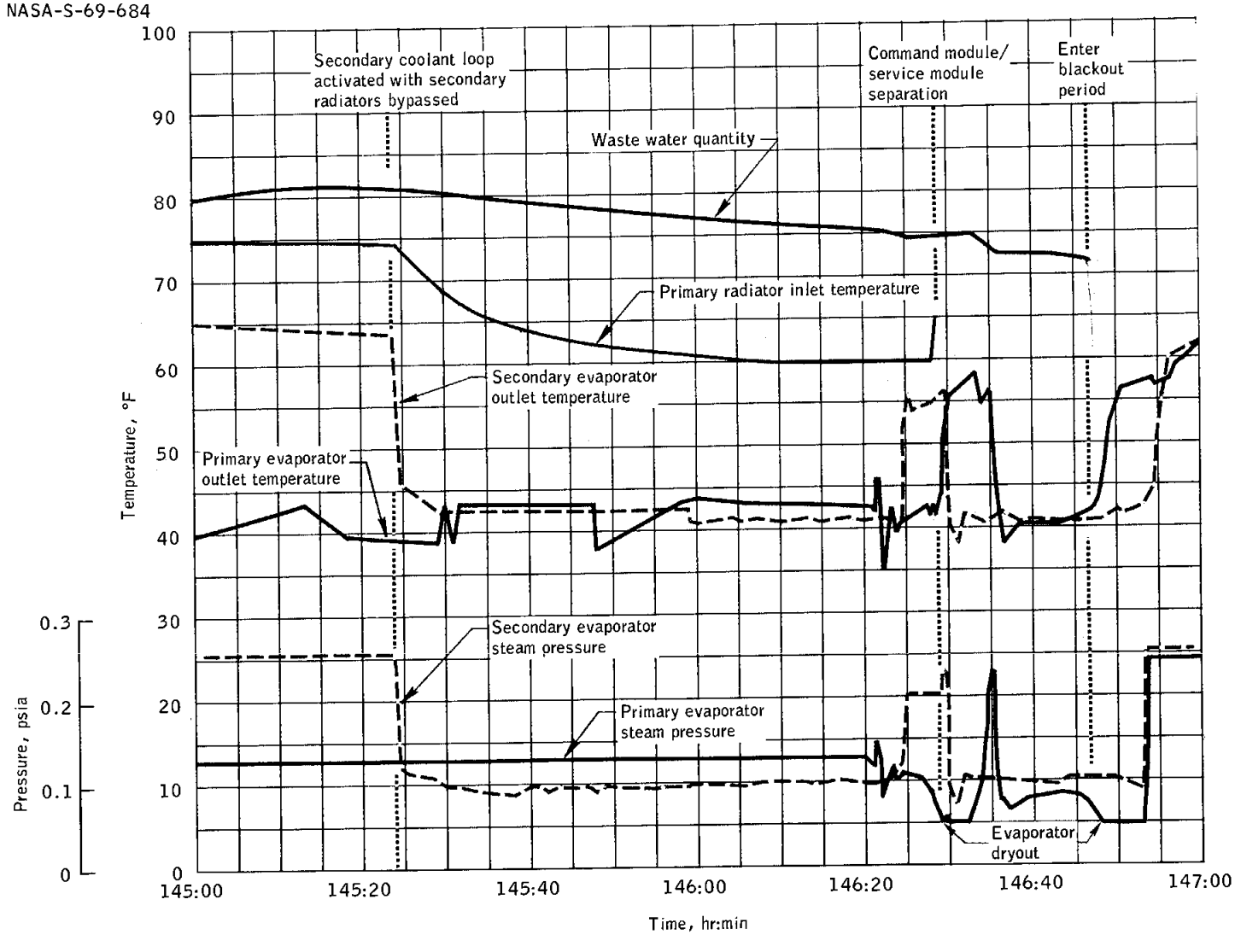

Figure 6.12-3.- Primary and secondary coolant loop operation during entry.

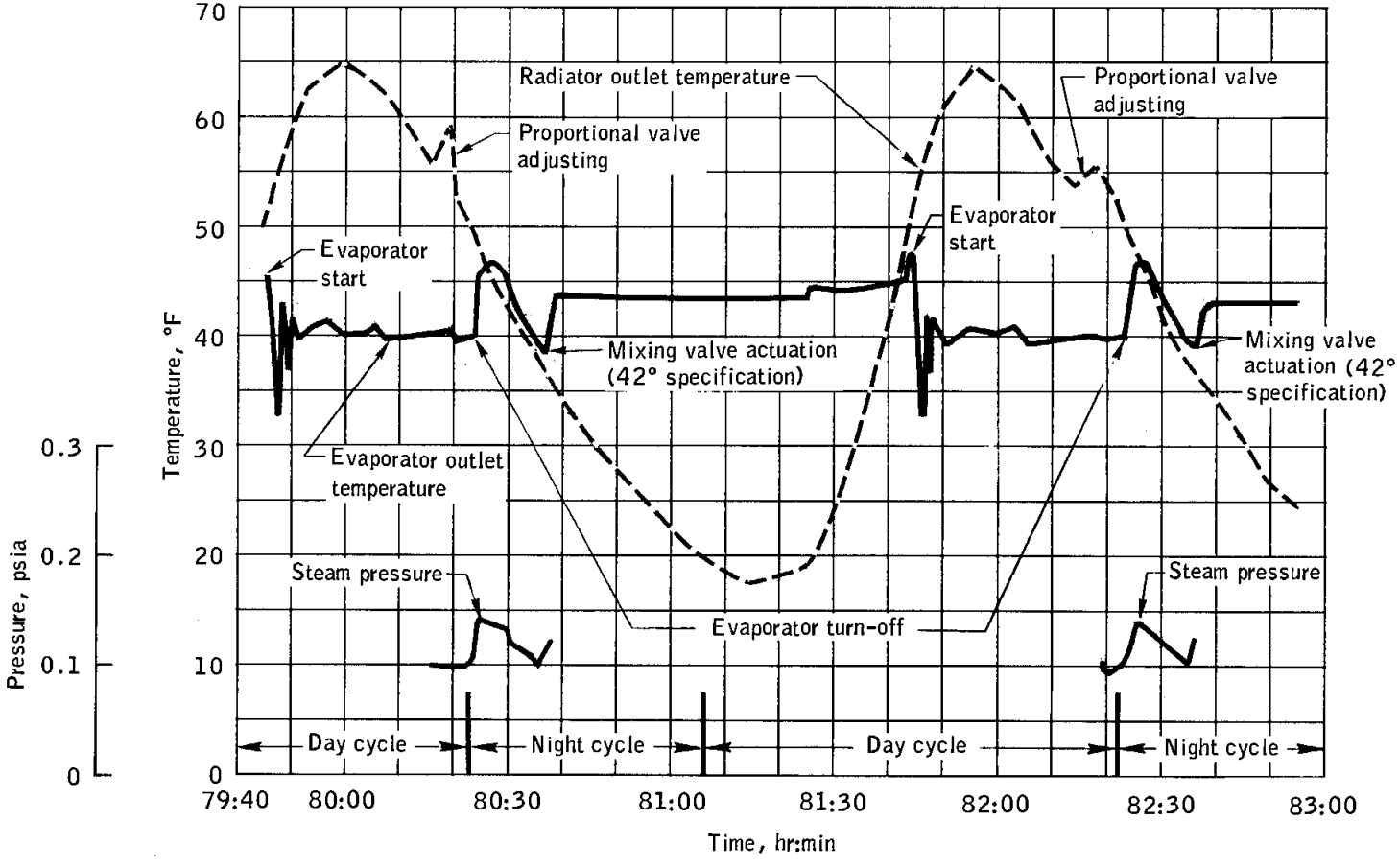

Figure 6.12-4.- Radiator operation during sixth and seventh lunar orbits.

6.13 CREW STATION

This section contains an evaluation of major crew provisions, controls and displays, spacecraft windows, interior lighting, and equipment stowage.

6.13.1 Crew Provisions

The pressure garment assemblies (including helmets and gloves) were worn during launch. The helmets and gloves were removed approximately 1 hour after launch, and the pressure garments were removed and stowed by approximately 4 hours.

The crew expressed some dissatisfaction with the waste management system, complaining of problems similar to those disclosed on Apollo 7, namely the awkwardness of the urine transfer cuffs and the fit of the fecal collection device. In addition, the crew was dissatisfied with the method of dumping the urine collection transfer assemblies. With the present procedure, the assemblies must be emptied through a fitting on the pressure suit before the suit is doffed on launch day. This procedure is time consuming and imposes an inconvenience on the crew during one of their busiest time periods. For future missions, a new device stowed in the spacecraft will enable dumping of the assemblies without going through the pressure suit fitting. Thus, the suit can be doffed early and the dumping of the urine can be delayed until a more convenient time.

The Lunar Module Pilot stated postflight that the biomedical harness leads were positioned such as to interfere with urination. Because of a similar problem on Apollo 7, a configuration change, to move the harness up by approximately 4 inches, is in effect for Apollo 9 and subsequent missions.

One of the T-adapters which connect the lightweight headsets or the communications carriers to the spacecraft was reported to have produced intermittent communications. A spare was substituted and corrected the deficiency. Postflight testing has not revealed a problem with this particular T-adapter.

The intervalometer, used to time the shutter on the camera, was effectively used. The inflight exerciser worked well; however, the lines were reported to be too long. The "kitchen timer" recommended after Apollo 7 proved to be very useful, particularly during fuel cell purges. The glareshades and meter covers were not too effective. Even with the shades in place over the mission event timer, the meter face still had to be shielded to read digits.

The crew was satisfied with the inflight coveralls. One bootie and the shoulder area of one jacket began to fray, but this did not present any problem.

The lightweight headsets were used twice during the mission and were unacceptable, primarily because of interference with the T-adapter, which tended to push the headsets off the crewman's head.

During the flight, the eyepiece of the scanning telescope became unscrewed and was found floating in the cabin.

Equipment stowage was adequate; however, after about 30 minutes in earth parking orbit, the dual life jacket worn by the Command Module Pilot was inadvertently inflated.

6.13.2 Displays and Controls

Panel nomenclature and markings were satisfactory. Prior to the flight, various caution and warning data and operating information were placed on the main display console and proved to be valuable to the crew. All spacecraft controls were operated satisfactorily.

6.13.3 Windows

As experienced on Apollo 7, windows 1, 3, and 5 became contaminated early in the flight. The center (hatch) window began to fog during earth parking orbit, and by 6 hours this window was unusable. Modifications for subsequent spacecraft should eliminate this condition; further discussion is contained in section 12.

6.14 CONSUMABLES

The usage of all liquid consumables, including cryogenics, is summarized in this section. Electrical power consumption is discussed in section 6.5.

6.14.1 Service Propulsion System Propellants

The total service propulsion system propellant loadings and consumption values are shown below. The loadings were calculated from gaging system readings and measured densities prior to lift-off.

	Fuel, lb	Oxidizer, lb
Loaded		
In tanks	15 652.3	24 981.4
In lines	78.6	123.7
	15 730.9	25 105.1
Consumed	11 651.9	18 808.6
Remaining at separation	4 079.0	6 296.5

6.14.2 Reaction Control System Propellants

Service module.- The propellant utilization and loading data for the service module reaction control system are presented below. Consumption was calculated from telemetered helium tank pressure histories using the relationships between pressures, volume, and temperature.

	Fuel, lb	Oxidizer, lb
Loaded		
Quad A	110.6	226.2
Quad B	110.2	226.9
Quad C	110.5	224.5
Quad D	109.3	224.2
	440.6	901.8
Consumed	220.5	414.5
Remaining at separation	220.1	487.3

Command module.- The propellant loading and utilization data for the command module reaction control system are tabulated below. Consumption was calculated from pressure, volume, and temperature relationships.

	Fuel, lb	Oxidizer, lb
Loaded		
System A	44.2	78.7
System B	44.2	78.2
	88.4	156.9
Consumed		
System A	12.0	22.2
System B	0.7	0.4
	12.7	22.6
Remaining at parachute deploy		
System A	32.2	56.5
System B	43.5	77.8
	75.7	134.3

6.14.3 Cryogenics

The cryogenic hydrogen and oxygen quantities loaded and consumed are given in the following table.

	Hydrogen, lb	Oxygen, lb
Loaded		
Tank 1	25.6	322.2
Tank 2	25.9	317.2
	51.5	639.4
Consumed		
Tank 1	13.4	130.4
Tank 2	13.2	124.0
	26.6	254.4
Remaining at separation		
Tank 1	12.2	191.5
Tank 2	12.7	193.5
	24.9	385.0

6.14.4 Water

The water quantities loaded, consumed, produced, and expelled during the mission are summarized in the following table.

	Water, lb
Loaded	
Potable water tank	25
Waste water tank	44
Produced inflight	
Fuel cells	220
Lithium hydroxide	20
Dumped overboard (including urine)	198
Evaporated	28
Remaining postflight	
Potable water tank	38
Waste water tank	42

7.0 FLIGHT CREW

7.1 FLIGHT CREW PERFORMANCE

The Apollo 8 crew members were Commander, F. Borman; Command Module Pilot, J. A. Lovell; and Lunar Module Pilot, W. A. Anders. This section presents summaries of training, inflight activities, operational equipment use, and photographic exercises.

7.1.1 Training

The crew completed preflight training essentially as planned and were well prepared for the mission. The effectiveness of their training is indicated by the highly satisfactory performance during the mission.

The possibility of conducting Apollo 8 as a lunar orbit flight was first discussed with the crew on August 10, 1968; for a year prior to that date, the crew had been training for an earth orbit mission. A new training program for the crew was initiated immediately. While the program contained mission options of either earth orbit or circumlunar, it was conducted with most emphasis on a lunar orbit mission so as to cause the least impact should the mission be redefined. The official decision to conduct a lunar orbit mission was not made until November 12, 1968, five weeks before the scheduled launch. The brief period available for training demanded maximum utilization of all training resources. The greatest obstacles were developing detailed mission techniques and procedures, preparing a flight plan, and implementing these on Command Module Simulator 3. Although this simulator was initially very limited in capability for Apollo 8, expedient modifications resulted in adequate training support after November 1, 1968.

The crew were well prepared for a nominal mission, but the severe training load did impose some compromises, as noted in the Pilots' Report.

7.1.2 Flight Activities

The crew performed the mission in an outstanding manner and all mission objectives were met.

A minor change to the flight plan for the seventh, eighth, and ninth lunar orbits deleted all non-essential activities in order to provide for necessary crew rest and preparation for the transearth injection maneuver. Figure 7.1-1 shows the flight plan as it was accomplished, and section 3 provides a description of the actual mission.

The pre-translunar injection period progressed very smoothly and the crew adhered to the scheduled work/rest cycle except when the flight plan was changed.

At approximately 4 hours 45 minutes, a second separation maneuver was required to achieve a satisfactory separation rate between the S-IVB and the spacecraft. A star sighting scheduled for about 4 hours 15 minutes was delayed 1-1/2 hours because of the poor sighting environment. Before adequate data could be collected, the sighted star was occulted by the earth; the sighting was again rescheduled and successfully performed at about 7 hours, using two stars. The initiation of passive thermal control was thus delayed about 2 hours.

An alignment of the inertial measurement unit at 26 hours and a navigation sighting at 26 hours 30 minutes were cancelled because the sleep period for the Command Module and Lunar Module Pilots was extended and because the next midcourse correction was not required. To allow for additional crew rest and communications tests, the platform alignment scheduled for 33 hours 45 minutes and the star sighting for 34 hours 15 minutes were delayed until 36 hours and 36 hours 30 minutes, respectively. Passive thermal control was reinitiated at 37 hours. At 45 hours, a star sighting was performed as scheduled, but the number of sightings was increased from five to eight sets to compensate for previous deletions. Only one set of four was obtained using star 33 because sighting was difficult against the bright lunar horizon. The crew performed two sets instead of one on each of stars 34 and 40. The crew had developed a high degree of proficiency in making the star sightings.

The crew initially adhered to the lunar-orbit flight plan and performed all scheduled tasks. However, because of increasing crew fatigue, the Commander made the decision at 84 hours 30 minutes to cancel all activities in lunar orbit, except for a required platform alignment and subsequent preparation for transearth injection. Television was, however, transmitted as scheduled and extended through terminator crossing. Details on lunar photography are covered later in this section. Transearth injection was accomplished normally.

During transearth coast, at about 91 hours 30 minutes, a star sighting was performed as scheduled, except that sightings on stars 10 and 11 were cancelled because of crew fatigue. Passive thermal control was initiated at 92 hours and interrupted only once for the next 14 hours.

Because of a crew procedural error, the onboard state vector and platform alignment were destroyed at 106 hours 26 minutes. Subsequent realignment was performed at 106 hours 45 minutes to reestablish onboard data. The only transearth midcourse correction was performed at 104 hours. The small velocity errors after this time did not require further corrections. Command module/service module separation and entry were performed normally by the crew.

Passive thermal control was performed according to the flight plan except when conflicts existed with other attitude constraints. Pitch and yaw attitudes during this rolling maneuver were revised to improve communications, to change sun/earth/spacecraft geometry, and to negate spacecraft propulsive-vent effects on the trajectory.

Alignments of the inertial measurement unit were deleted whenever platform drift was not enough to warrant an alignment or when midcourse corrections or navigation sightings were cancelled.

Four of the seven midcourse corrections were not performed because of the small velocity errors present (less than 1 ft/sec). See figure 7.1.1 for time of accomplishment of the flight plan activities and section 5 for details of the maneuver parameters.

Waste water dumps and fuel cell purges were scheduled at specific times as the flight progressed to preclude trajectory dispersions prior to a maneuver and to prevent ejected ice particles from obscuring the star field in the optics during alignment sightings.

After landing, the spacecraft was pulled over to a stable II (apex-down) flotation position by the parachutes, and the crew operated the uprighting system to return to stable I.

Crew performance was exceptionally good under the work load requirements throughout the mission, and crew equipment operated satisfactorily with but the few exceptions noted.

7.1.3 Photographic Activities

This section discusses photographic activities and the extent to which the photographic objectives were achieved. In pursuing these objectives, the crew completed photographic exercises in an excellent manner. Over 800 70-mm still photographs were obtained. Of these, 600 were good-quality reproductions of lunar surface features. The remainder of these photographs were of the S-IVB during separation and venting, and long-distance earth and lunar photography. Over 700 feet of 16-mm film was also exposed during S-IVB separation, lunar landmark photography through the sextant, lunar surface sequence photography, and documentation of intravehicular activity.

The still photography contributed significantly to knowledge of the lunar environment. A description of the photographic equipment is included in section 4.

Many valuable observations were made by the crew. As expected, the crew could recognize surface features in shadow zones and extremely bright

areas of the lunar surface; these features are not well delineated in photographs. This recognition, combined with the photographic information, enabled new interpretations of lunar surface features and phenomena. As a result, lunar-surface lighting constraints for the lunar landing mission were widened.

The vertical stereo strip photography of the lunar surface was performed as planned, except that time notations on exposures were not made because other, more essential operations were pressing. The photographic target-chart exposure schedule was followed, and good imagery was obtained for all of the lunar surface that was photographed. Selenodetic control of the areas photographed on the lunar far side will be improved using the Apollo 8 information.

As an alternate to the planned oblique stereo-strip photography, the crew elected to mount the camera in the window and expose the type-3400 black-and-white film at constant camera settings. Through use of the intervalometer, excellent photographic coverage was obtained without crew involvement, other than for maintaining spacecraft attitude. The exposure settings used were 1/250 second and f/5.6.

The photography to evaluate exhaust effects on spacecraft windows was performed as planned, except that the sun incidence angle was approximately 70 degrees instead of the planned 85 degrees. Spotmeter readings on the sun-illuminated window were taken.

Good quality 16- and 70-mm photographs of the S-IVB and adapter panels were obtained from long distances.

Photography of lunar landmarks using the sextant was accomplished essentially as planned, except that the time and exposure information was not recorded. Most of the imagery is excellent.

Photography of the lunar terminator was obtained, but no photographs of the north-of-track terminator were taken on the lunar far side.

Long-distance earth photography of general interest highlighted global weather and terrain features. Lunar photography was not accomplished during translunar coast because of rigid attitude constraints. However, good quality photography of most of the moon disk was accomplished during transearth coast.

Approximately 50 percent of the proposed lunar targets of opportunity were photographed but, because of attitude constraints, available photographic stations, and window degradation, almost all were located south of the orbital ground track. An abundance of good quality zero-phase (along the sun line) photography was obtained at various sun incidence angles to the lunar surface.

NASA-S-69-686

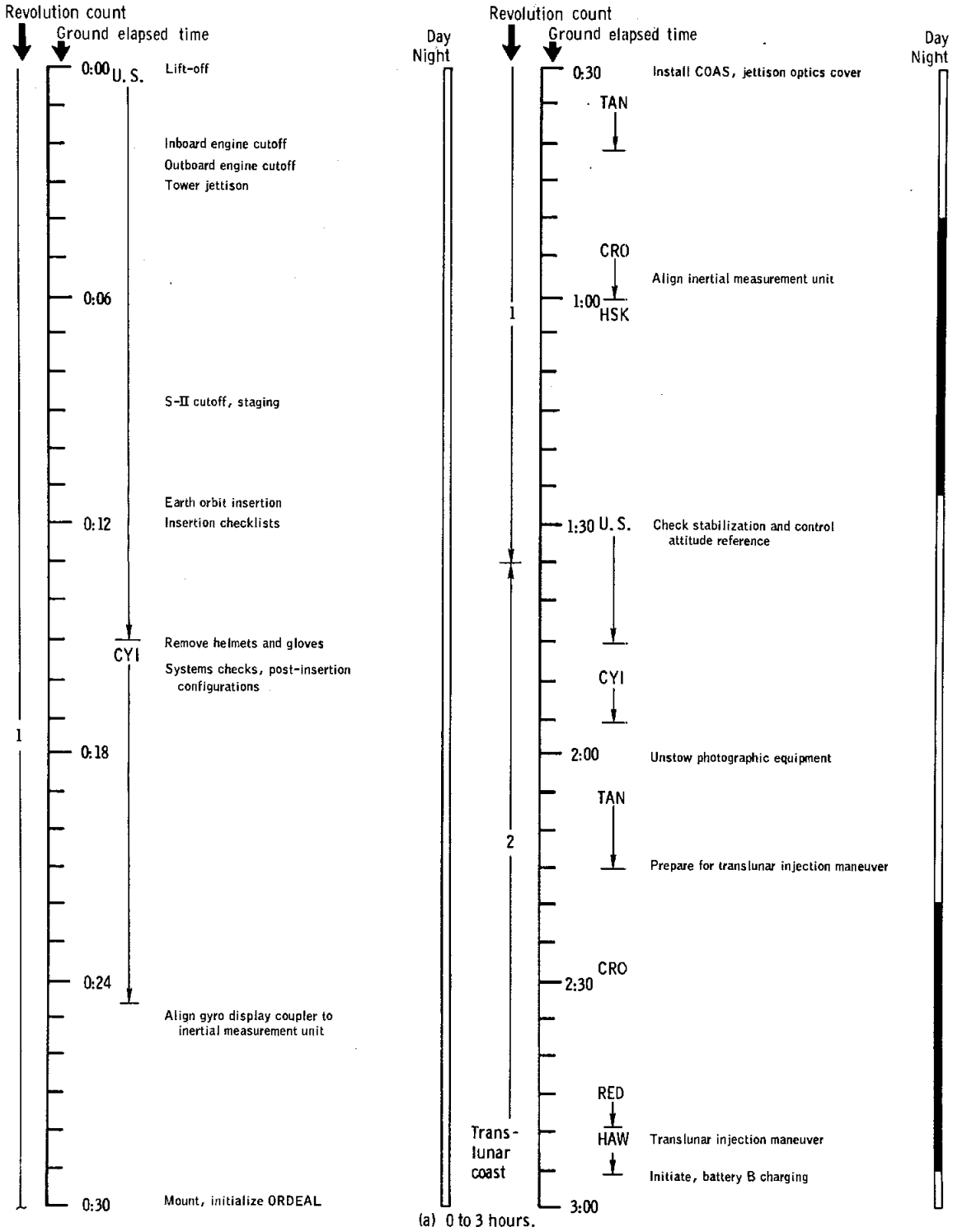

(a) 0 to 3 hours.

Figure 7.1-1. - Summary flight plan.

NASA-S-69-687

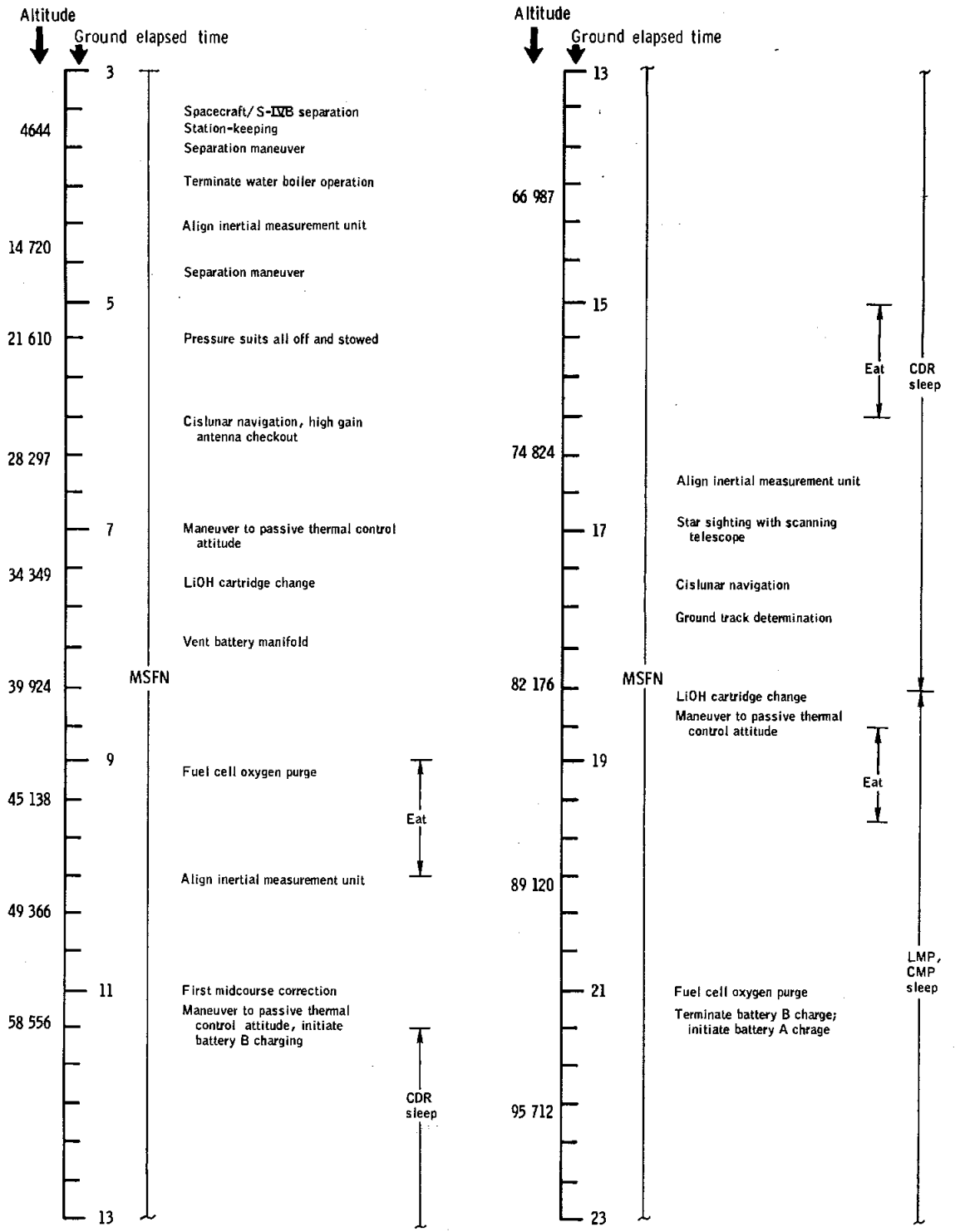

(b) 3 to 23 hours.

Figure 7.1-1. - Continued.

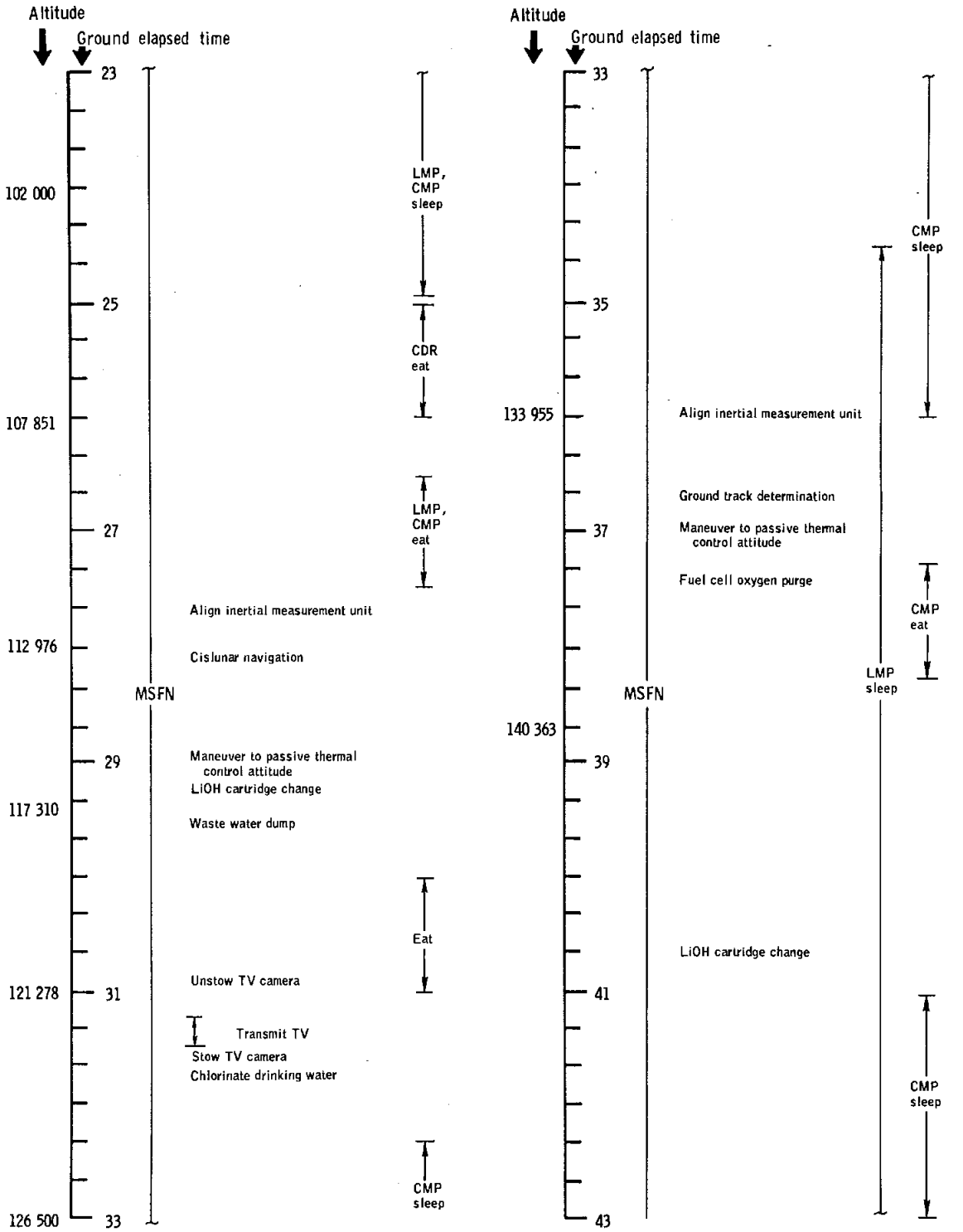

(c) 23 to 43 hours.

Figure 7.1-1. - Continued.

NASA-S-69-689

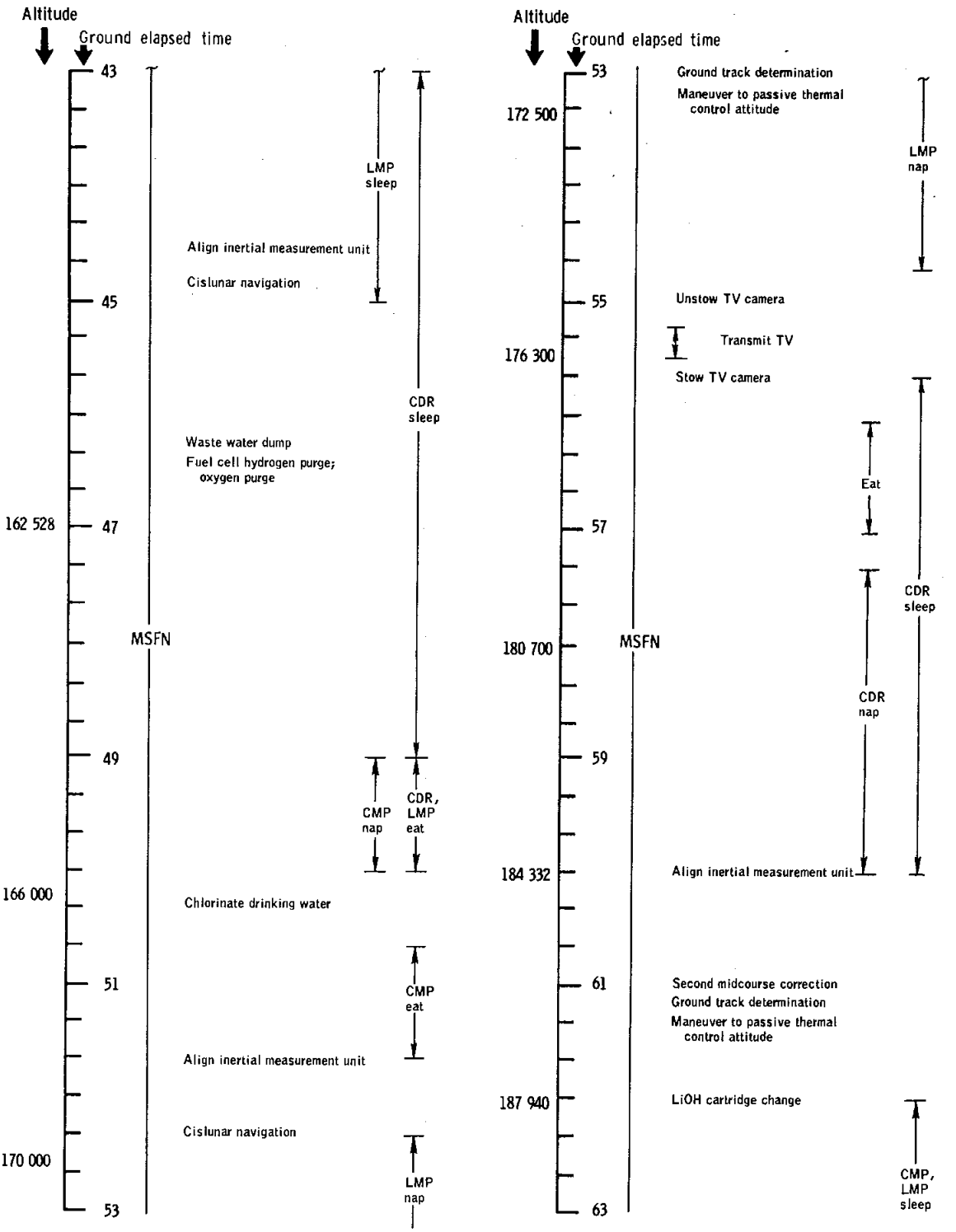

(d) 43 to 63 hours.

Figure 7.1-1. - Continued.

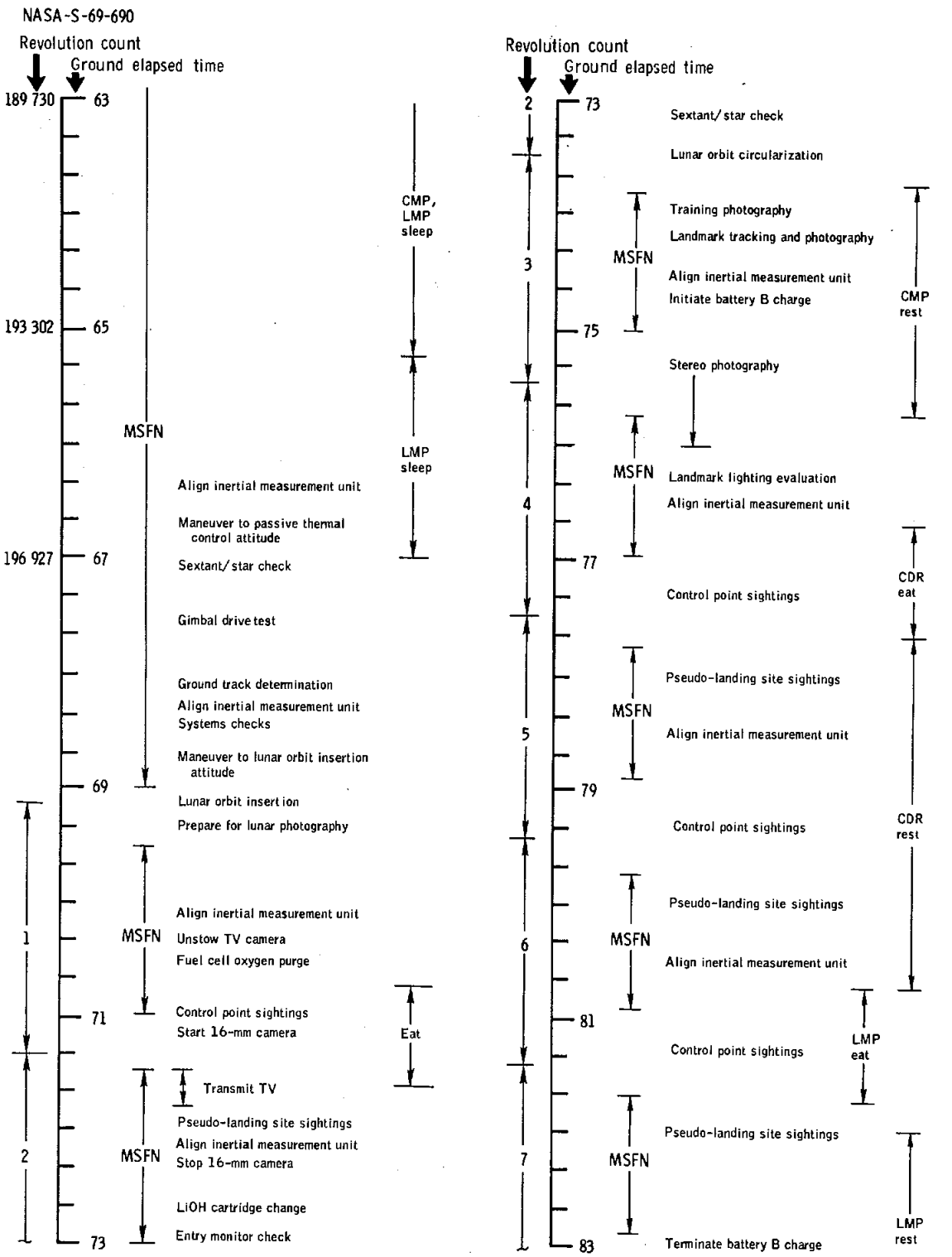

(e) 63 to 83 hours.

Figure 7.1-1. - Continued.

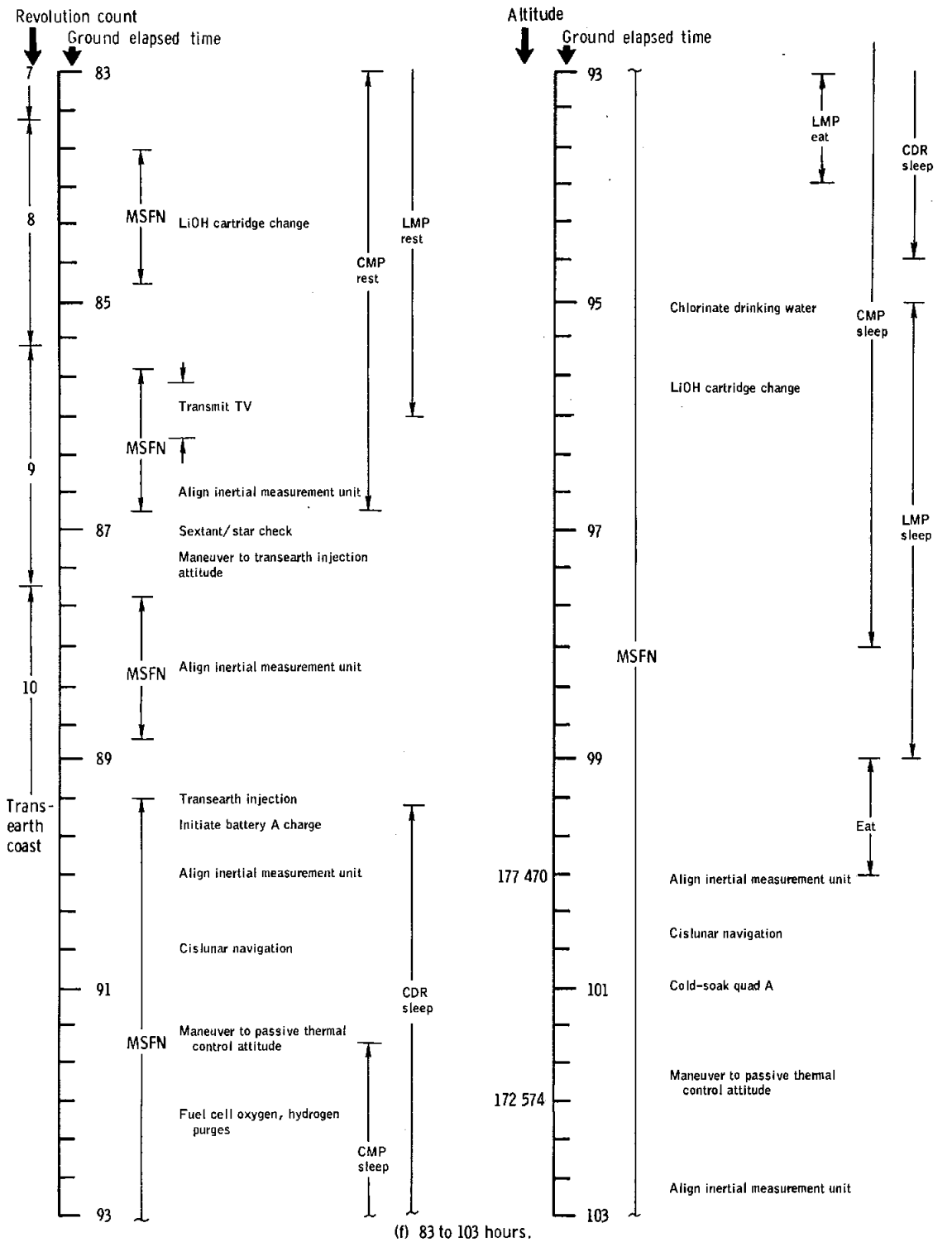

(f) 83 to 103 hours.

Figure 7.1-1. - Continued.

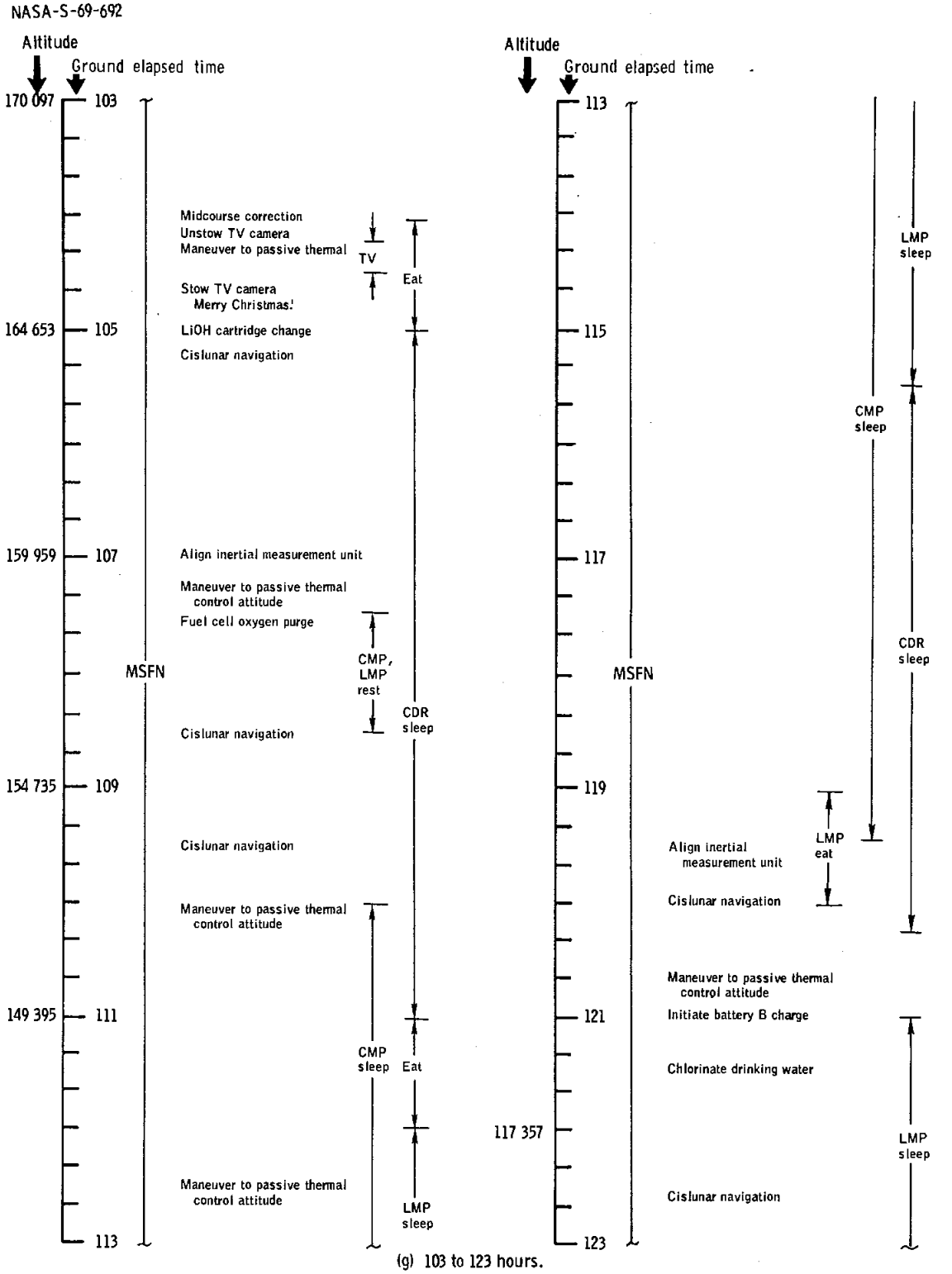

(g) 103 to 123 hours.

Figure 7.1-1.- Continued.

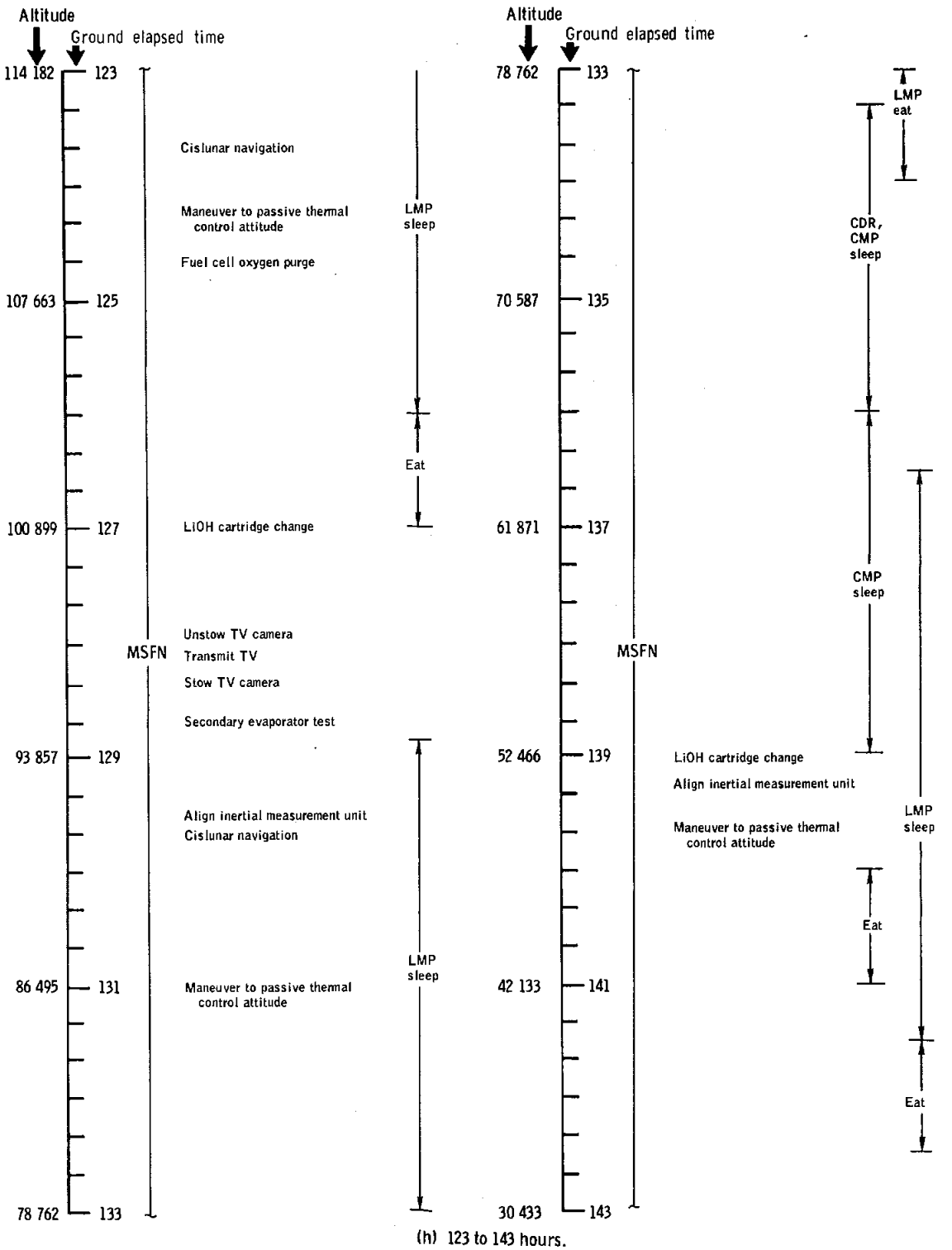

(h) 123 to 143 hours.

Figure 7.1-1. - Continued.

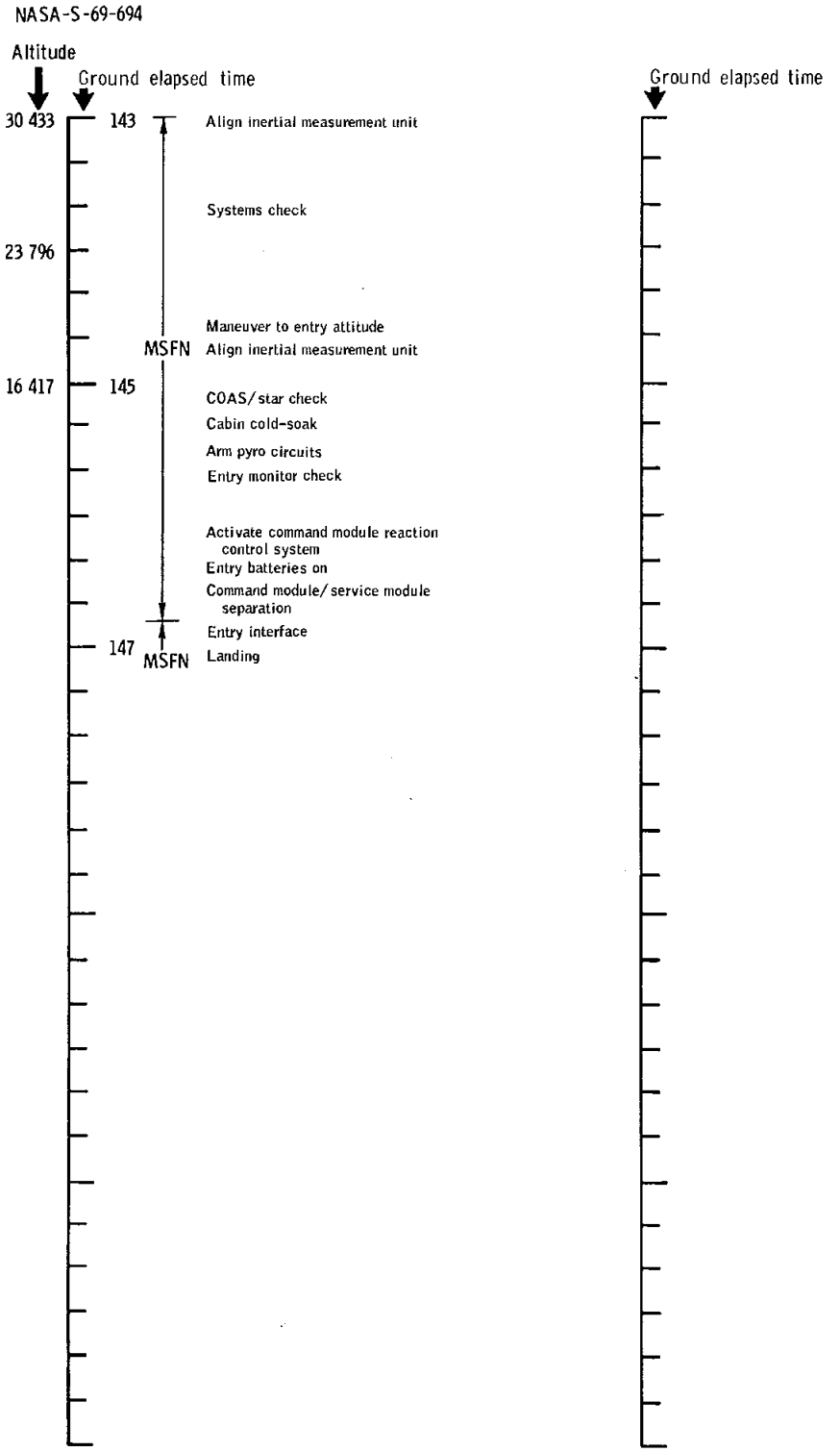

(i) 143 hours to landing.

Figure 7.1-1. - Concluded.

Apollo 8 flight crew

Command Module Pilot J. Lovell, Lunar Module Pilot W. Anders, and Commander F. Borman

7.2 PILOTS' REPORT

7.2.1 Mission Preparation

Prior to the proposal of a lunar mission profile for Apollo 8, the crew training was oriented to an earth orbital rendezvous mission using a command and service module and a lunar module. On August 10, 1968, the crew was first informed that a lunar orbit flight was under consideration. On August 19, 1968, the crew was notified of a change in mission assignments and was instructed to train for a new mission having circumlunar and lunar-orbit options, using a command and service module only. The results of the Apollo 7 mission would determine whether the Apollo 8 mission would be a lunar orbital, circumlunar, or earth-orbital mission. An immediate decision was made to concentrate all crew training on the lunar orbital mission, the most difficult of the three profiles and the one least covered by previous training. Most of the mission guidelines, including launch day, time in lunar orbit, and overall mission time, were determined in late August.

The Apollo 8 crew was assigned Command Module Simulator 3 at Cape Kennedy, and the first simulation exercise for the mission was conducted there on September 9, 1968. The normal training week through November consisted of 3 or 4 days at Cape Kennedy and the remainder of the 6-day work week at Houston attending meetings or using Houston-based simulators.

An important contribution to crew preparedness in the limited training time was the effective use of a training support team which followed the hardware, coordinated the preparation of checklists, and handled the numerous problems associated with the spacecraft stowage list.

The crew moved into special quarters on December 10, 1968, and controls were established to limit, as much as possible, contact with persons displaying symptoms associated with the flu, colds, and other illnesses.

All required equipment was available at Cape Kennedy to support crew training in a timely manner. Because of the 10-hour work days on the simulators, the physical conditioning program was not as extensive nor as regular as preferred. However, no adverse physical effects were noticed during nor after the mission because of this deficiency.

The crew schedule on launch day was excellent. Ample time was allocated for all activities, and the crew ingress time was met without undue haste. The final countdown was smooth and precise and was conducted with excellent discipline, and the crew had no difficulty in following the proceedings. The last 10 seconds of the countdown were

well handled, and the blockhouse communicator was the only person transmitting. During the countdown, no unusual or unexpected noises, vibrations, nor other disturbing occurrences were noted and no swaying or movement of the launch vehicle was noticed.

7.2.2 Powered Flight Phase

Although the engine ignition sequence began 9 seconds before lift-off, no noise or vibration was apparent until 3 seconds before lift-off. From that time until lift-off, the primary sensations were a general vibration and an increasing noise level. Lift-off was easily discernible by the slight but sudden acceleration. From lift-off until the vehicle cleared the tower, the noise level continued to increase, and definite, but light, random lateral accelerations were sensed.

The radio call of "tower clear" was received by the crew; however, the noise level continued to increase until any form of communication from the ground or between crew members was impossible for about 35 seconds. This condition could have prevented the crew from receiving an identifiable abort-request call.

The cabin pressure began to relieve as scheduled, accompanied by a rather loud surging noise. As the launch proceeded past 42 seconds, the noise level dropped off considerably and the remainder of first-stage operation was characterized by a smooth continuous increase in acceleration until inboard engine cutoff, when the acceleration leveled off at about 1g. The first-stage separation sequence was abrupt, with a sudden decrease in acceleration.

Tower jettison was accompanied by only a minimum noise level and no other physical sensations. Powered flight on the S-II stage was smooth and quiet until the last 45 seconds of S-II operation, when a slight longitudinal oscillation, estimated to be about 10 Hz and ±0.1g, was discernible.

Both S-IC/S-II and S-II/S-IVB staging was accompanied by a small flash visible through the center hatch window. None of the spacecraft windows were clouded by either staging sequence or tower jettison. Guidance initiation was accompanied by a definite pitch-down maneuver until the horizon was in the middle of the left rendezvous window. The remainder of the S-IVB flight was smooth and quiet, and cutoff was accompanied by no significant rates.

7.2.3 Earth Parking Orbit and Translunar Injection

The post-insertion checklist was completed smoothly. The time available was adequate to perform all the checks and procedures required in the first 20 minutes after insertion. In maneuvering under the couch to unstow equipment, the Command Module Pilot inadvertently actuated one side of his dual life preserver. He removed the life preserver and continued with his functions. All scheduled procedures, including optics jettison and platform fine alignment, for the earth parking orbit phase were accompanied without difficulty.

Attitude control of the S-IVB was extremely smooth, and it was impossible to feel or hear the S-IVB attitude control engines as they fired, although they could be seen on the dark side. Preparations for the translunar injection maneuver went smoothly and according to the flight plan. The timeline for the earth parking orbit prior to translunar injection was efficiently planned and effectively completed. This plan should be standardized to the maximum extent possible for future lunar missions. S-IVB re-ignition was on time, and guidance during translunar injection was very precise. S-IVB shutdown was nominal, and the separation attitude was achieved by a three-axis maneuver.

7.2.4 Translunar Coast

Spacecraft separation from the S-IVB was accomplished by rotating the translational hand controller counterclockwise, and after a programmed 3-second delay, separation occurred with a very noticeable acceleration. The entry monitor system, set up to monitor the separation velocity change, jumped to plus 100.4 ft/sec at separation (see section 12). The crew maneuvered the spacecraft so they could view the S-IVB, and no difficulty was experienced in station-keeping. Lighting conditions in the separation attitude were excellent, and the spacecraft/launch-vehicle adapter panels were observed as they separated to the rear of the S-IVB.

Approximately 20 minutes after separation, a 1.5 ft/sec separation maneuver radially outward from the earth was conducted. The maneuver did not provide a comfortable clearance, and approximately 1 hour later another radial impulse of 7.7 ft/sec was applied.

Basic translunar crew activities consisted of two midcourse corrections, navigation, earth photography, urine and waste water dumps, lithium hydroxide cartridge changes, water chlorination, and communication checks, plus the normal necessities to maintain life and housekeeping functions.

Initial translunar navigation, scheduled for about 4 hours, was delayed because of the second separation maneuver. At the beginning of the cislunar navigation, a star of opportunity could not be obtained to

perform the optics calibration. This was caused by the closeness of the earth, the daylight conditions, and the millions of particles created by S-IVB venting. Automatic optic-system routines were used to acquire the first navigation star when an optics calibration was finally performed. A total of 27 sets of navigation sightings were accomplished in the translunar phase.

During the first star/earth-horizon sighting, the horizon was very indistinct viewed through the sextant, and the crew had difficulty ascertaining the top of the atmosphere. There was, however, what appeared to be a definite horizon line where the atmosphere and earth horizon met. This line was enhanced by the colored filter. Insufficient sightings were accomplished near the earth to ascertain whether or not this line could be used as a horizon. No problems were involved in defining a good earth horizon for marking during later star/earth-horizon sightings. Star/lunar-horizon sightings in the translunar phase were complicated by the nearness of the moon to the sun. The moon appeared in the sextant as a thin crescent. The area around the moon was milky white in appearance because of solar light scattering in the optics. The dark horizon could not be seen. Between the two translunar midcourse corrections, the state vector was updated only by onboard navigation.

Early in translunar flight, a rolling mode of passive thermal control was instituted using ground-computed pitch and yaw attitudes. Maneuvers to these attitudes were accomplished through the automatic maneuver mode. The stabilization and control system was then selected, and a roll rate of 1 rev/hr was established. Pitch and yaw manual attitude switches were placed in rate command, and the maximum attitude deadband was selected.

Two translunar midcourse correction maneuvers were accomplished to refine the trajectory. The first correction required a 24.8 ft/sec change in velocity, and the residuals were trimmed out using the reaction control system. This maneuver provided a means of verifying the service propulsion operation prior to the lunar orbit insertion maneuver. All onboard indications were normal during the maneuver. The second correction consisted of a 2 ft/sec reaction control system maneuver.

Ten platform alignments were completed during the translunar phase. The only problem encountered in the alignment procedures was the failure to recycle the optics zero switch after turning on optics power. (See section 6.9.) The identification of the star selected by the computer for the alignment program was not always possible because of the variation in light-scattering associated with spacecraft orientation.

Staggered work/rest cycles were planned for the translunar phase of flight to maintain continuous systems monitoring, provide effective antenna switching during passive thermal control, and monitor spacecraft attitude to prevent drifting into gimbal lock.

7.2.5 Lunar Orbit Operations

The lunar orbit insertion maneuver was initiated on time. The bank A propellant valves were used at initiation of the maneuver, and 3 seconds later, the bank B valves were opened with a perceptible increase in chamber pressure. Cutoff occurred after 246.5 seconds, with some small residuals which were not trimmed out. Lunar-orbit camera and navigation-sighting equipment was unstowed and prepared according to the flight plan.

Because the hatch window was almost totally obscured, the side and rendezvous windows were used for ground-track and navigation-sighting fix familiarization. One 70-mm camera contained high-speed black-and-white film for possible dim-light photography. This camera was to be reloaded with standard film prior to sunrise.

Ground-track determination with the crewman optical alignment sight was begun at sunrise on the second lunar revolution. Ground-track determination on the far side was more difficult than expected because of the large uncertainity in the maps of that region. Large and/or distinct features were observed and compared favorably with the dead reckoning position along the lunar ground track. Pilotage was less difficult on the near side because of the increased accuracy of the maps. During the daylight portion of each pass, the central points and landmarks were located without too much difficulty. Most photographic targets south of track were covered up to the subsolar point, including some additional targets of opportunity. The television camera was prepared with the recommended red filters taped over the wide angle lens. After acquisition, the television camera was turned on, and a running commentary was given on those features viewed.

During the third revolution, the circularization maneuver was accomplished using the service propulsion system. Engine cutoff occurred on time with very small residuals. Post-maneuver systems checks were accomplished, and battery B recharge was initiated. A sequence of six far-side terminator exposures was taken south of the spacecraft track. Slightly after signal acquisition, the flight controllers reported that the primary evaporator had dried out and required reservicing. (See section 6.12.) The lunar-landing training photography was initiated while the spacecraft was approaching the landing site, and the recommended camera f-stops and shutter speeds were utilized. The 70-mm camera was not loaded with dim-light photography film because of the poor spacecraft orientation and poor lighting conditions for this type of photography. However, it was planned to do all dim-light photography during the eighth revolution in conjunction with the solar corona and zodiacal light tasks.

The vertical stereo strip photography was initiated, as planned, on the fourth revolution, and additional targets of opportunity north and

south of the spacecraft track were photographed. Landing site acquisition was easy, particularly on the earth side because of the breakup of rough terrain by the mare areas. Onboard maps, photographs, and ground-updated acquisition times were adequate to pinpoint the desired locations. Optical ground tracking was good with the resolve and medium speed modes for lunar orbit velocities. Tracking with the sextant down to about 7 degrees of trunnion angle was easy. This procedure should be investigated for lunar module tracking. The best spacecraft attitude for ground tracking appears to be 10 degrees pitch up from the local horizontal. The moon horizon is a good gage for acquiring landmarks; however, all selected landmarks should be near an easily recognizable feature for early recognition. Five marks on a control point were accomplished with no spacecraft pitch-down required.

From just prior to the initial point through pseudo-landing-site B-2 on the fourth revolution, lighting conditions looked satisfactory for a lunar module landing. Ground features were easily distinguishable, and reflected light from the surface was not harsh nor glaring. Shadows in this region caused terrain features to stand out, and a complete crater circumference could be seen with little difficulty. Crater patterns such as doublets and triplets were easily recognizable. No surface objects such as large boulders were seen during this pass. As expected, the area just prior to the terminator had extremely long shadows that tended to distort surface features. All prominent features such as craters, mountains, peaks, etc., could be easily tracked with the command module optics. The best objects to track were small craters in the vicinity of some unusual feature which permitted easy acquisition. However, the crater needed to be clear of any shadows from larger crater walls.

In addition, the Command Module Pilot believes that the lighting conditions present in the fourth revolution from the first initial point to pseudo-landing-site B-1 are adequate to perform lunar module landing operations and are superior to earthshine terrain and areas of higher sun angles.

Prior to sunrise on the fifth revolution, the zodiacal light was observed through the scanning telescope.

The Commander terminated his rest period during the seventh revolution and decided to terminate all further lunar-orbit tasks to permit additional rest for the other two crewmen prior to preparation for transearth injection. A television exercise was begun after earth acquisition on the ninth revolution and was concluded at the near-side terminator. Standard nightside activities were accomplished, and equipment was stowed in preparation for transearth injection.

7.2.6 Transearth

All spacecraft systems were checked and prepared for transearth injection during the tenth revolution. The inertial measurement unit was realigned and the spacecraft maneuvered to the proper maneuver attitude. Transearth injection was accomplished normally, and the bank A and B valves were operated in the same manner as for the lunar orbit insertion maneuver.

The transearth coast phase consisted of one midcourse maneuver, a lunar navigation, platform alignments, passive thermal control, earth-moon photography, and normal spacecraft housekeeping activities. At approximately 104 hours, the only transearth midcourse correction was performed, using the service module reaction control system.

A total of 46 sets of navigation sightings were completed during the transearth phase using computer program 23. The handling characteristics of the spacecraft using the minimum-impulse controller were more sensitive transearth than translunar because of the much lighter fuel load.

Initial star/lunar-horizon sightings were complicated by the moon's irregular horizon when the spacecraft was in proximity. The sextant reticle was very hard to see through with a space background near the earth's horizon. Long eye-relief optics were used on one set of star/earth-horizon sightings.

A total of six reference matrix alignments and two preferred-option alignments were completed during the transearth phase of flight. In addition, an inertial measurement unit orientation was accomplished during this period.

The passive thermal control procedure used was the same as that followed during the translunar phase. Preparation for entry began 2 hours prior to reaching 400 000-foot altitude and included normal equipment stowage and reorientation of the spacecraft to the separation attitude. The maneuver to complete a horizon check was made using the stabilization and control system in the rate command mode. When the horizon appeared in the window at the predicted time, the spacecraft was yawed left 45 degrees for command module/service module separation.

Separation was highlighted by a loud "bang" and a slight acceleration, but the service module was not seen.

The command module was returned to zero degrees yaw with single-ring minimum-impulse control. The horizon was then tracked using this control mode until the pitch error needle on the guidance and control display went to zero. At that time, control was transferred to the digital autopilot with the backup control system in rate command.

7.2.7 Entry and Landing

The 0.05g light was illuminated at the predicted instant. The 0.05g was preceded by an ionization trail that became steadily brighter during the first phase of atmospheric flight. The ionization became so bright that the spacecraft interior was bathed in a cold blue light as bright as normal daytime. The automatic entry was successfully monitored on the entry monitor system display. One ring of the reaction control system provided the required control throughout entry.

The first indication of reaching more dense atmosphere came with a full-scale-high reading on the steam duct pressure, followed by movement of the altimeter. At 30 000 feet, the earth landing system was switched to automatic, and apex cover jettison, drogue deployment, and main parachute deployment were all normal. The command module was very stable throughout atmospheric flight, including the drogue and main parachute periods.

After the main parachutes were deployed, the remaining portion of the entry checklist was accomplished. During the normal reaction control system dump procedure, the illumination provided by the burning propellants was adequate for a visual check of the three main parachutes.

The altimeter was very accurate, and about the time it read zero, the command module contacted the water with a severe shock. The force of the landing apparently caused water to enter the cabin through the cabin pressure relief valve and to douse the left side of the Commander.

The water distracted the attention of the Commander and caused a momentary delay in releasing the main parachutes. As a result, the spacecraft was pulled over to a stable II attitude. The uprighting compressors were activated to inflate the flotation bags and upright the spacecraft, which required approximately 4-1/2 minutes. After uprighting, communications were established with the recovery forces, and the postlanding checklist was completed. Some water came through the postlanding vent valves when they were first opened. This water was probably trapped above the valves after uprighting. Some slight valve leakage was noted due to the rough sea state. The dye marker was deployed and observed by helicopter pilots, but swimmer interphone communications did not work (see section 12). Because of the sea state, the swimmers had difficulty in deploying the flotation collar. An attempt was made to repressurize the hatch-opening cylinder, but an incorrect checklist procedure resulted in venting instead. The secondary bottle was difficult to puncture using the needle valve handle, even with assistance from the torque tool. When daylight became sufficient, the hatch was opened by the swimmers, and egress and pickup were accomplished nominally. Prior to egress, the spacecraft was powered down, and all circuit breakers were pulled.

7.2.8 Systems Performance

Spacecraft systems performed superbly with only minor exceptions. System checks were limited to the verification of critical component operation prior to translunar injection and lunar orbit insertion and to activation of backup components for verifying adequate redundancy. More specific observations of particular systems are contained in the following paragraphs.

Guidance and navigation system.- Except for optics power, the guidance and navigation system was powered-up for the entire flight, and no abnormalities were noted. One computer restart, which resulted from improper operator input, was encountered.

The optics performed satisfactorily; however, the light transmittance through the scanning telescope was marginal. Even with a good dark background, it was still difficult to recognize lower magnitude navigation stars.

Light interference depended on spacecraft attitude with respect to the sun. At certain quadrants of rotation during passive thermal control, the scanning telescope had a shaft of light some 20 degrees in depth across the entire field of view. Star recognition during this period was impossible.

Optic drive in all modes appeared smoother than experienced in simulators. The auto-optics system functioned correctly both in the cislunar navigation and alignment programs and the landmark tracking program in lunar orbit.

Both the scanning telescope and sextant eye pieces which screw into their mounts tended to back off in zero gravity. At one time, the telescope eye piece was found floating several inches from the mount. In addition, the telescope was difficult to keep in focus.

Sequential events.- The sequential events system accomplished all intended tasks of the nominal mission profile. Because of the concern with five "Criticality 1" switches, crew procedures were changed prior to launch to circumvent the very remote possibility of the dangerous effects associated with a malfunction of any one of these five switches. All pyrotechnic activations were positive and on time. The uprighting system worked nominally, although after the spacecraft had been returned to stable I, one flotation bag switch was inadvertently placed to VENT and the center bag partially deflated.

Electrical power.- The electrical power system worked nominally, and only a slight variation in performance among the three fuel cells was noticed. Battery charging was accomplished as planned. The low main-bus

voltage problem experienced on Apollo 7 was avoided by effective battery warm-up and spacecraft power-down sequences prior to command module/service module separation. Post-separation voltage levels were approximately 27.5 V dc. These procedures were satisfactory for future missions; however, the secondary coolant loop should be powered up.

Environmental control.- Cabin temperature and relative humidity were generally pleasant, and odors were removed within a reasonable time. To reduce the cabin noise level, the cabin fans were turned off after orbital insertion. During the initial portion of the translunar phase, evaporator operation was inhibited, and manual control of primary glycol mixing inlet temperatures was initiated to increase cabin temperatures slightly. This reduced the effectiveness of water removal in the suit heat exchanger and condensation began to form on the hatch and cold oxygen and glycol lines. Some water was removed with the vacuum system. Automatic mixing was reactivated prior to lunar orbit insertion. The spacecraft was comfortably warm and dry during the transearth phase. During the latter part of the first daylight pass in lunar orbit, the primary evaporator dried out, and evaporator outlet temperatures began to increase. An initial reservice of the evaporator was attempted and the unit was immediately put back in service to preclude overheating of the inertial measurement unit. The evaporator dried out again, was reserviced during the following nighttime pass, and operated normally until it was deactivated after transearth injection. (Editor's note: The heat load was sufficiently high at this time to preclude dryout.) The primary and secondary evaporators were activated prior to command module/service module separation, and again the primary unit dried out and was reserviced. The primary system continued to function well until the early stages of entry but then dried out again. A last reservice was attempted during g force buildup but was abandoned when 3g was reached. Other environmental control failures included an erroneous full-scale-high indication of primary radiator outlet temperature in lunar orbit and an indication of loss of potable water during the entry phase of the flight.

Periodic variations in cabin temperature were noticed during passive thermal control maneuvering. By eliminating the sunlight coming through the windows during one-half of each revolution, the temperature variations were damped out.

Cryogenics.- The cryogenic fans were operated manually on a predetermined schedule and prior to all thrusting maneuvers. No cryogenic caution and warning lights were experienced, and the usage was as expected.

Communications.- The communications system performance was excellent. S-band up-voice quality was good, and after resolution of a ground problem, both high- and low-bit-rate voice on the data storage equipment was

reported as satisfactory. Unfortunately, considerable data logging and lunar surface observations were inhibited while the low-bit-rate mode for recording on the data storage equipment was believed to be unacceptable. The problems associated with real-time analysis of recorded voice quality and the coupling of the record-rate/fidelity with the PCM bit rate pointed out the need for a simple and reliable means of onboard voice recording. The omnidirectional antenna switching task was somewhat bothersome. The high-gain antenna worked nominally in the manual and automatic modes but did not perform as the crew expected in the reacquisition mode during passive thermal control. In the reacquisition mode, the antenna would track to the scan limit and lose two-way lock. Instead of going to the predetermined position for reacquisition, it appeared that an "earth-presence" signal was still present, and the antenna would continue to attempt to track and shift beam widths up against the mechanical limits. (Editor's note: Antenna operations in this mode were normal. The earth-presence signal was present because of the strong signal strengths from the ground stations at the range the test was conducted.) Automatic gain control of approximately 2 volts was present much of the time, and the antenna would eventually work its way around to a position where it could acquire lock-on as the earth came into view.

VHF range capability tests were conducted just after lunar orbit insertion and prior to entry and indicated an effective range of 8000 to 12 000 n. mi.

Service propulsion.- The operation of the service propulsion system was excellent. To reduce starting transients, the engine was started using the service propulsion system A propellant valves. The system B valves were actuated approximately 3 and 5 seconds after ignition for the lunar orbit insertion and transearth injection maneuvers, respectively.

Reaction control.- The service module and command module reaction control systems performed nominally throughout the flight. Minimum impulse attitude control was easy and conserved fuel. The rate-command/attitude-hold mode was quite positive. Command module reaction control system preheat was not required prior to entry.

8.0 BIOMEDICAL EVALUATION

This section is an abstract of Apollo 8 medical findings and anomalies. A comprehensive biomedical evaluation will be published as a separate medical report.

During the 6.1-day lunar orbital flight, the three crewmen accumulated 441 man-hours of space flight experience. For the first time in the space program, the crew reported symptoms of motion sickness during the adaptation phase of the intravehicular activity.

As in Apollo 7, the inflight real-time operational medical support was limited to biomedical monitoring on a time-shared basis. The Apollo 8 crew participated in a series of special medical studies designed to assess the changes incident to space flight. The final results and analysis of these studies are not yet complete and will be reported later.

A preliminary analysis of the biomedical data confirms that the command module provides a habitable environment that permits the program objectives to be achieved without compromise to crew health and safety. The physiological changes observed postflight were generally consistent with those noted in earlier flights.

8.1 BIOINSTRUMENTATION PERFORMANCE

The bioinstrumentation harnesses were modified because of the difficulties experienced during the Apollo 7 flight. The modified bioharnesses used by the Commander and the Command Module Pilot were satisfactory throughout the flight.

The quality of the Lunar Module Pilot's sternal electrocardiogram signal dropped suddenly at about 115 hours. The baseline shifted frequently and the signal-conditioner output was intermittently blocked; however, the quality of the impedance pneumogram remained excellent. An inflight switch of the input leads from a sternal to an axillary electrocardiograph signal resulted in excellent, noise-free data. A loose connection of the biosensor to the skin was probably responsible for the degraded signal. Postflight examination of the bioharnesses demonstrated no failures of any kind.

The maximum temperature reached by the dc-dc converter during the mission was approximately 120° F, as measured by temperature-sensitive indicator tape, and agrees with the predicted maximum.

In summary, performance of the bioinstrumentation system was good, and the modifications made subsequent to the Apollo 7 flight proved effective.

8.2 PHYSIOLOGICAL DATA

The inflight biomedical results are based on approximately 24 hours of good quality data samples for each crewman. Descriptive statistics for heart rates are given in table 8-I. The Command Module Pilot's heart rate ranged from 51 to 88 beats/min and was lower and less variable than those of the other two crewmen (Commander's ranged from 60 to 103; Lunar Module Pilot's from 63 to 101). The data reflect normal variations, and annotated plots of cardiac activity for critical phases of the mission are shown in figure 8-1. Attempts to plot heart rate versus acceleration were only partially successful because of noise in the data. Heart rates were highest during the transearth injection maneuver at the end of the lunar-orbit phase, but the rates quickly returned to normal levels.

Results of attempts to fit the collected heart rate data to sine waves that would describe the daily physiological variations are given in table 8-II. All results are based on data that do not include sleep. These results indicate that the Commander, the Command Module Pilot, and the Lunar Module Pilot operated on a daily circadian cycle of 24.3, 25.4, and 22.3 hours, respectively. Based on this circadian model, the expected (baseline) daily heart rates for the respective crewmen were 81(±2), 73(±2), and 83(±2) beats/min. A comparison of the baseline rates for the Commander and Command Module Pilot from this mission and these same crewmen during the Gemini VII mission shows that heart rates were significantly lower for the Gemini flight and suggests that the Apollo 8 mission was more strenuous and demanding.

The changes in baseline heart rate and periodicity given in table 8-II are most readily attributed to sampling problems and to lengthened activity periods associated with the lunar orbit phase. These and the results given in table 8-I suggest that human circadian variations in heart rate are not influenced by the variations in lighting levels during earth-orbit flights. The results further indicate that about 10 percent of the variation seen in heart rates for these crewmen would be a function of the time of day they were being monitored.

The ground systems for processing biomedical data performed well, although off-line processing frequently resulted in spuriously high variability estimates thought to be caused by erroneous cardiotachometer outputs during signal lock-on and loss. Efforts are being made to correct variability using appropriate analog and digital filters.

8.3 MEDICAL OBSERVATIONS

Following normal physical cues during powered flight, each crewman experienced the characteristic feeling of fullness of the head after orbital insertion. The Lunar Module Pilot was aware of this sensation for about 24 hours, compared with 4 hours for the Commander.

This was the first manned flight in which the crewmen experienced symptoms of a mild motion sickness, identical to incipient mild seasickness. Soon after leaving their couches, all three crew members experienced nausea as a result of rapid body movements. At no time was any abnormal eye movement (nystagmus) or disorientation noted by the crew. It is expected that less motion initially after leaving the couches would have alleviated the symptoms of motion sickness experienced. Therefore, it is suggested for Apollo 9 that the crew make initial movements in the weightless state in a cautious manner to preclude the onset of motion sickness. The duration of symptoms varied between 2 and 24 hours but did not interfere with operational effectiveness.

The Command Module Pilot and the Lunar Module Pilot each took one Lomotil tablet prophylactically when the exact nature of their medical problem was still unclear to them. The Lunar Module Pilot also took one Marezine tablet, with good results. His symptoms completely subsided, and no additional medication was used or required for control of these mild symptoms of motion sickness.

Following subsidence of symptoms and adaptation to movement within the zero-g environment, each crewman was then able to perform rapid head movements and tilting without difficulty or recurrence of the problem.

Inflight illness.- After the Commander's symptoms of motion sickness dissipated, he experienced additional symptoms of an inflight illness believed to be unrelated to motion sickness.

When the Commander was unable to fall asleep 2 hours into his initial rest period at 11:00:00, he took a 100-mg sleeping tablet, which induced approximately 5 hours of sleep described as "fitful." Upon awakening, the Commander felt nauseated and had a moderate occiptal headache. He took two 5-grain aspirin tablets and then went from the sleep station to his couch to rest. The nausea, however, became progressively worse, retching occurred, and vomiting happened twice. After termination of his first sleep period, the Commander also became aware of some increased gastrointestinal distress and was concerned that diarrhea might occur.

As the mission progressed, the medical flight controller had the impression that the Commander was experiencing an acute viral gastroenteritis. This tentative diagnosis was based upon the delayed transmission

of a recorded voice report that the Commander had a headache, a sore throat, loose bowels, and had vomited twice. A conversation between the chief medical flight controller and the Commander verified that the previous report was correct, but that the Commander was feeling much better. The Commander also stated that he had not taken any medication for his illness, which he described as a "24-hour intestinal flu." Just prior to the Apollo 8 launch, an epidemic of acute viral gastroenteritis lasting 24 hours was present in the Cape Kennedy area.

The Commander's temperature was 97.5° F on two occasions subsequent to his nausea and vomiting. The Commander was advised to take one Lomotil tablet and to use the Marezine if the nausea should return; however, the Commander did not take this medication because his inflight illness soon remitted completely, and no further treatment was required.

In the postflight medical debriefing, the Commander reported that his symptoms may have been a side effect of the sleeping tablet. It was disclosed that during his preflight trial of this drug, he had experienced a mild "hangover" and an uncomfortable feeling bordering on nausea. When he used this same drug on two occasions during the flight, he experienced symptoms identical to those encountered in the drug trial. During the debriefing, his vomitus was described as liquid in character and presented no difficulty to aspiration.

Work/rest cycles.- The very busy flight schedule precluded simultaneous sleep and resulted in large departures from normal circadian periodicity, thus causing fatigue. The wide dispersions of the work/rest cycles are given in figure 8-2. A "practical shift" of 3 hours before or 8 hours after the start of the usual Cape Kennedy sleep period is shown for the Command Module Pilot and Lunar Module Pilot. The Commander experienced a "practical shift" of 11 hours before to 2.5 hours later than his assumed Cape Kennedy sleep time. The scheduled sleep and that actually obtained are compared in figure 8-3. Real-time changes to the flight plan were required because of crew fatigue, particularly during the last few orbits before the transearth injection maneuver.

Crew status reporting procedures.- Evaluation of crew status procedures was a detailed test objective, and food, water, exercise, and sleep magnitudes were logged to enhance medical knowledge. A significant amount of water and exercise information, however, was not recovered.

Inflight exercise.- A calibrated inflight exercise program was not planned for the Apollo 8 flight, and inflight exercise was solely for crew relaxation. Exercise times were estimated at 10 minutes a day for each crewman. The Apollo 8 crew generally demonstrated more cardiovascular deconditioning in their postflight lower body negative pressure and ergometry tests than the Apollo 7 crew, despite a shorter mission duration.

The fact that the Apollo 7 crew exercised 45 minutes a day for each crewman, 4-1/2 times as much as the Apollo 8 crew, appears to account for the observed difference in cardiovascular deconditioning.

8.4 FOOD

An account of food packages remaining after the flight showed that the caloric intake was 1475, 1503, and 1230 cal/day for the Commander, Command Module Pilot, and Lunar Module Pilot, respectively. During the postflight medical debriefing, the crew reported that the freeze dehydrated food was adequate but monotonous in taste. They stated, however, that the special wet-pack food, consisting of Christmas turkey chunks and gravy, was the tastiest meal of the flight. No problems were encountered in eating the wet-pack food with a spoon in weightlessness, nor was any difficulty experienced with food crumbs floating in the cabin. They also stated that too much food was contained in each meal package (the approximate caloric value of the meals for one day was 2500 calories).

8.5 WATER

The results of the daily water tabulation are shown in the following table.

Crewman	Water consumed, oz						
	Flight day						Total
	0	1	2	3	4	5	
Commander	57	56	99	100	-	-	312
Command Module Pilot	57	59	84	86	-	-	286
Lunar Module Pilot	79	84	86	96	-	-	335

The water consumption data are missing for flight days 4 and 5. Serial postflight body weights indicate, however, that the Apollo 8 crew was in a state of negative water balance at the time of landing, and postflight physical examinations also confirmed this finding. Prior to flight, the spacecraft water system was loaded with water containing 8 mg/liter free chlorine. The system was then soaked for a 6-hour period, flushed, and filled with non-chlorinated water. At 2-1/2 hours before lift-off, the

potable water system was chlorinated using the inflight equipment and procedure. During flight, the crew performed 6 chlorinations of the potable water system at approximately 24-hour intervals. Postflight analysis of the potable water samples obtained 17 hours after the final inflight chlorination showed a free chlorine residual of 0.1 mg/liter in the hot water food preparation port and 2.0 mg/liter in the water gun. No microbial organisms were cultured from potable water samples taken 14 hours after landing. Chemical analysis of the potable water indicated a nickel concentration of 2.42 mg/liter (maximum recommended level is 0.5 mg/liter). However, no adverse affect was noted on the crew. The high nickel concentration cannot be attributed to the presence of chlorine in the water system, since it has also been observed in non-chlorinated spacecraft water systems.

8.6 PHYSICAL EXAMINATIONS

Preflight medical evaluations were accomplished at 30, 14, and 5 days before flight, and a cursory physical examination was performed on the morning of the flight. A comprehensive physical examination was performed immediately after recovery.

In general, all three crewmen were moderately fatigued postflight and demonstrated moderate cardiovascular deconditioning. They tolerated the ergometry test very well, but all three crewmen showed an initial elevation of heart rate in the neighborhood of 120 beats/min. Significantly higher heart rates, lower blood pressures, and narrower pulse pressures were noted during the postflight lower body negative pressure tests, as compared with the preflight tests. Only one crewman completed the test. The other two crewmen developed presyncopal symptoms and were forced to terminate the test prematurely.

Six days after recovery, the Lunar Module Pilot developed a mild pharyngitis which evolved into a common cold syndrome with coryza and non-productive cough. He received symptomatic therapy and fully recovered 6 days later. The Commander developed a common cold 12 days after the flight, and symptomatic treatment resulted in complete recovery after 7 days.

TABLE 8-I.- APOLLO 8 CREW HEART RATE

Phase	Commander			Command Module Pilot			Lunar Module Pilot		
	Mean	Median	Standard deviation	Mean	Median	Standard deviation	Mean	Median	Standard deviation
Prelaunch	80	72	24	76	75	9	75	74	11
Launch	118	113	24	--	--	--	--	--	--
Earth orbit	93	87	20	71	71	8	98	99	12
Translunar coast	80	75	20	69	67	16	83	82	17
Lunar orbit	80	75	22	73	70	16	84	84	13
Transearth coast	81	76	20	67	63	16	78	75	22
Average baseline rate for entire mission	81.6		26.6	69.3		19.4	82.0		22.6
Day									
0	79	74	20	73	71	11	85	85	12
1	94	82	32	68	65	18	78	75	23
2	80	75	20	71	68	15	83	82	17
3	83	73	28	69	66	13	88	83	28
4	77	73	19	69	65	16	84	79	23
5	78	73	21	66	62	18	72	72	16

TABLE 8-II.- CIRCADIAN VARIATION IN HEART RATE

	Gemini VII		Apollo 8		
	Command Pilot	Pilot	Commander	Command Module Pilot	Lunar Module Pilot
Sampled data					
No. samples	600	600	239	239	239
Mean, beats/min	73.1	66.3	82.5	72.9	84.4
Standard deviation, beats/min	9.3	10.9	18.1	20.8	17.3
Calculated					
Fitted curve parameters					
Period (biological day), hr	23.5	23.5	24.3	25.4	22.3
Amplitude of variation, beats/min	7.3	8.2	9.3	8.7	7.6
Phase of variation, hr*	20.2	19.8	18.9	16.4	22.2
Baseline, beats/min	71.2	64.3	80.8	73.3	83.0
Circadian ratio**	0.10	0.13	0.11	0.12	0.09
Standard error					
Period, hr	2.98	3.18	5.5	6.9	5.0
Amplitude, beats/min	0.69	0.85	3.8	4.8	3.7
Phase, hr	0.35	0.40	1.1	1.9	1.7
Baseline, beats/min	0.35	0.44	2.0	2.3	1.9

*Referenced to local launch time (Gemini VII - 2:30 p.m. e.s.t.; Apollo 8 - 7:51 a.m. e.s.t.).

**Amplitude/baseline, or variation due to circadian effects.

NASA-S-69-695

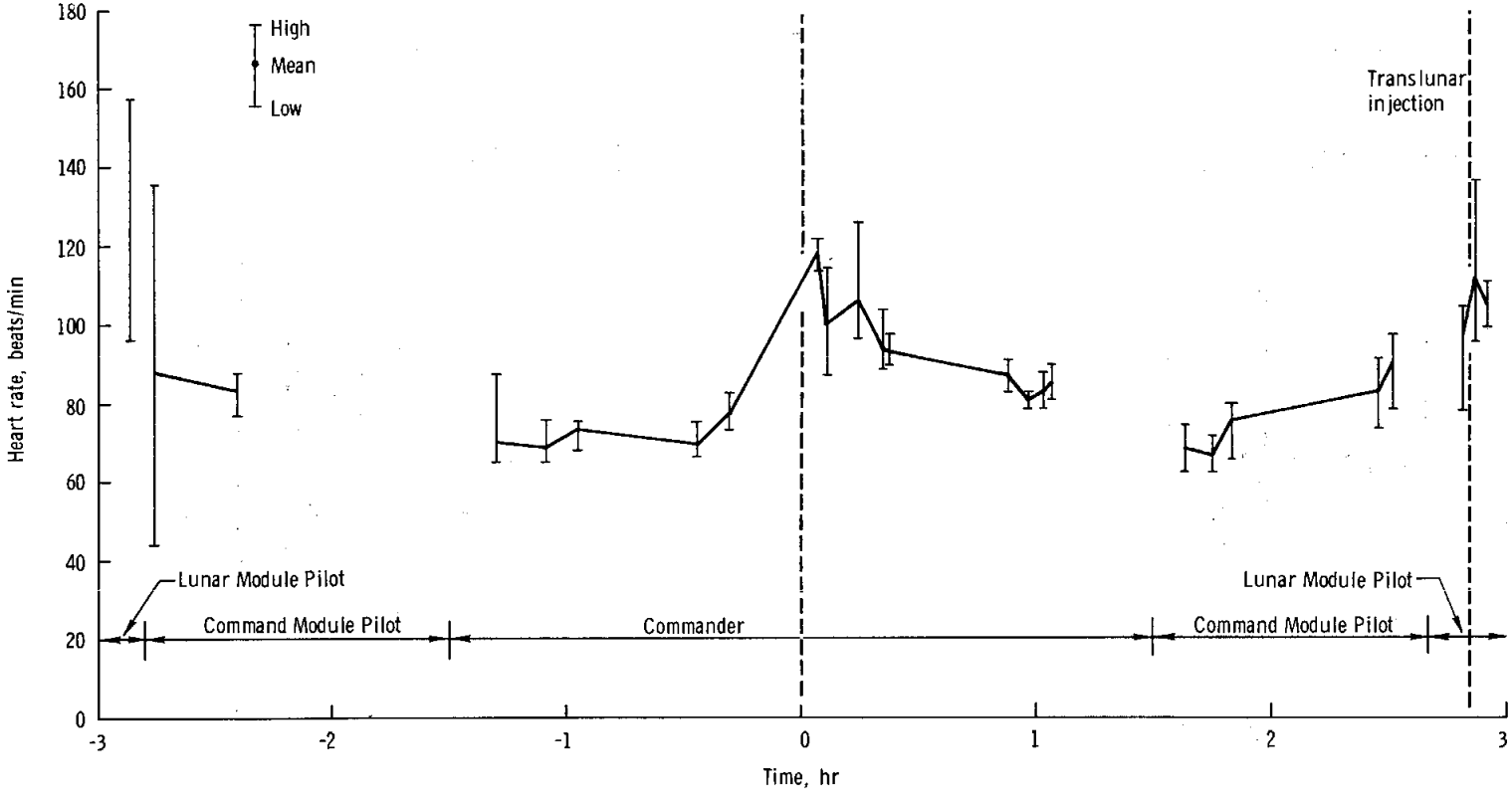

(a) Prelaunch, launch, and translunar injection.

Figure 8-1.- Crew heart rates.

NASA-S-69-696

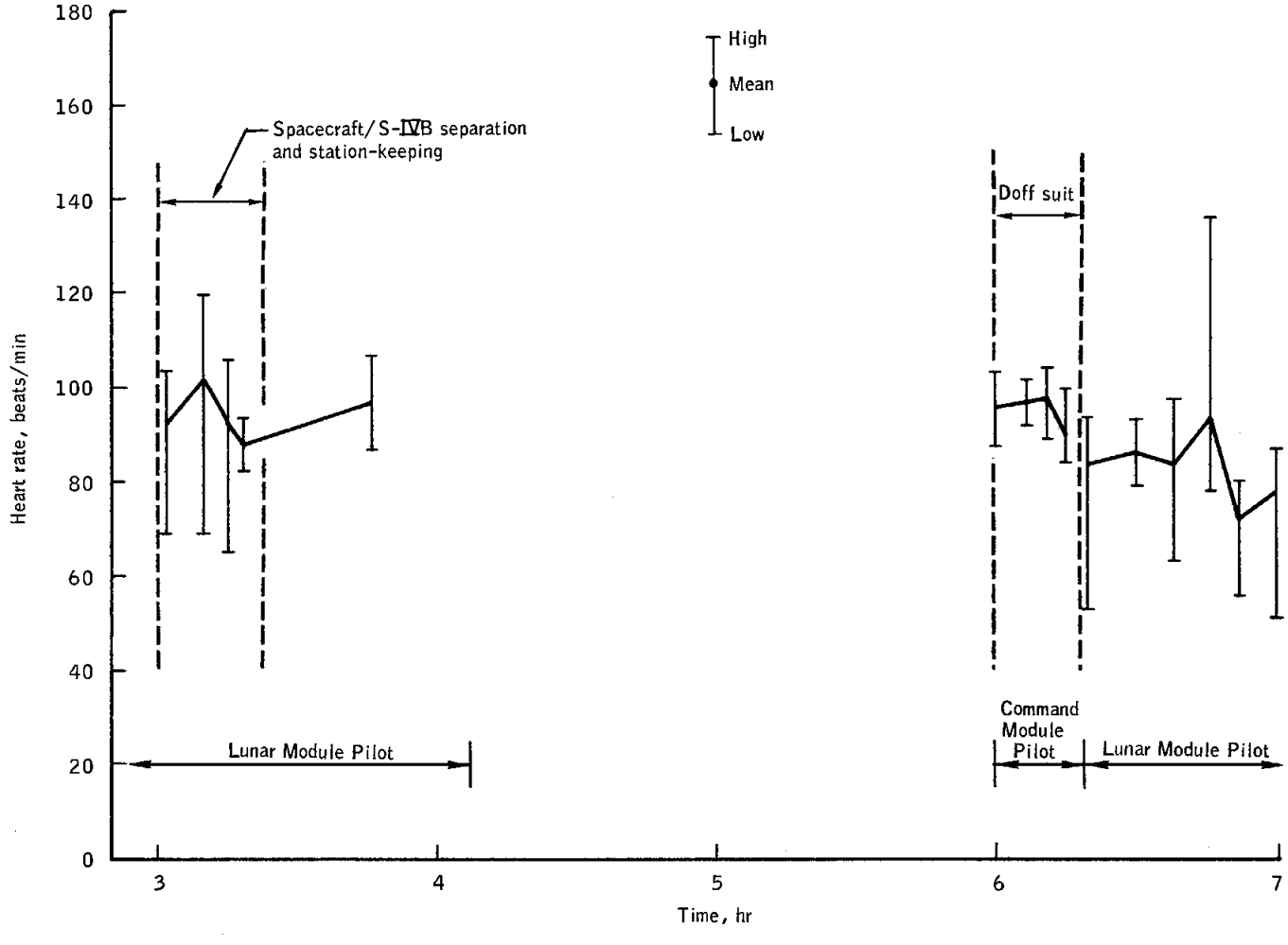

(b) Translunar coast.

Figure 8-1.- Continued.

NASA-S-69-697

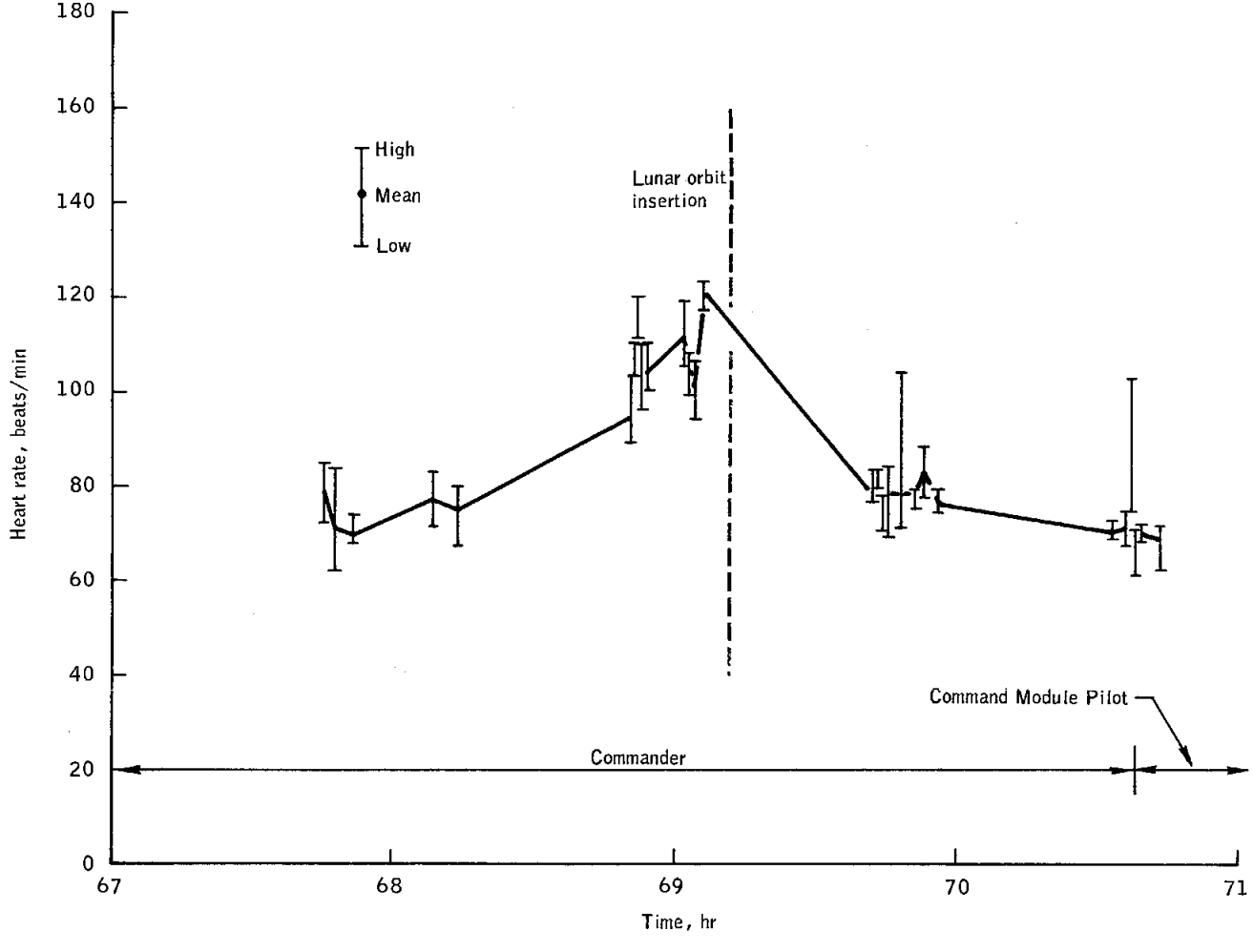

(c) Lunar orbit insertion.

Figure 8-1.- Continued.

NASA-S-69-698

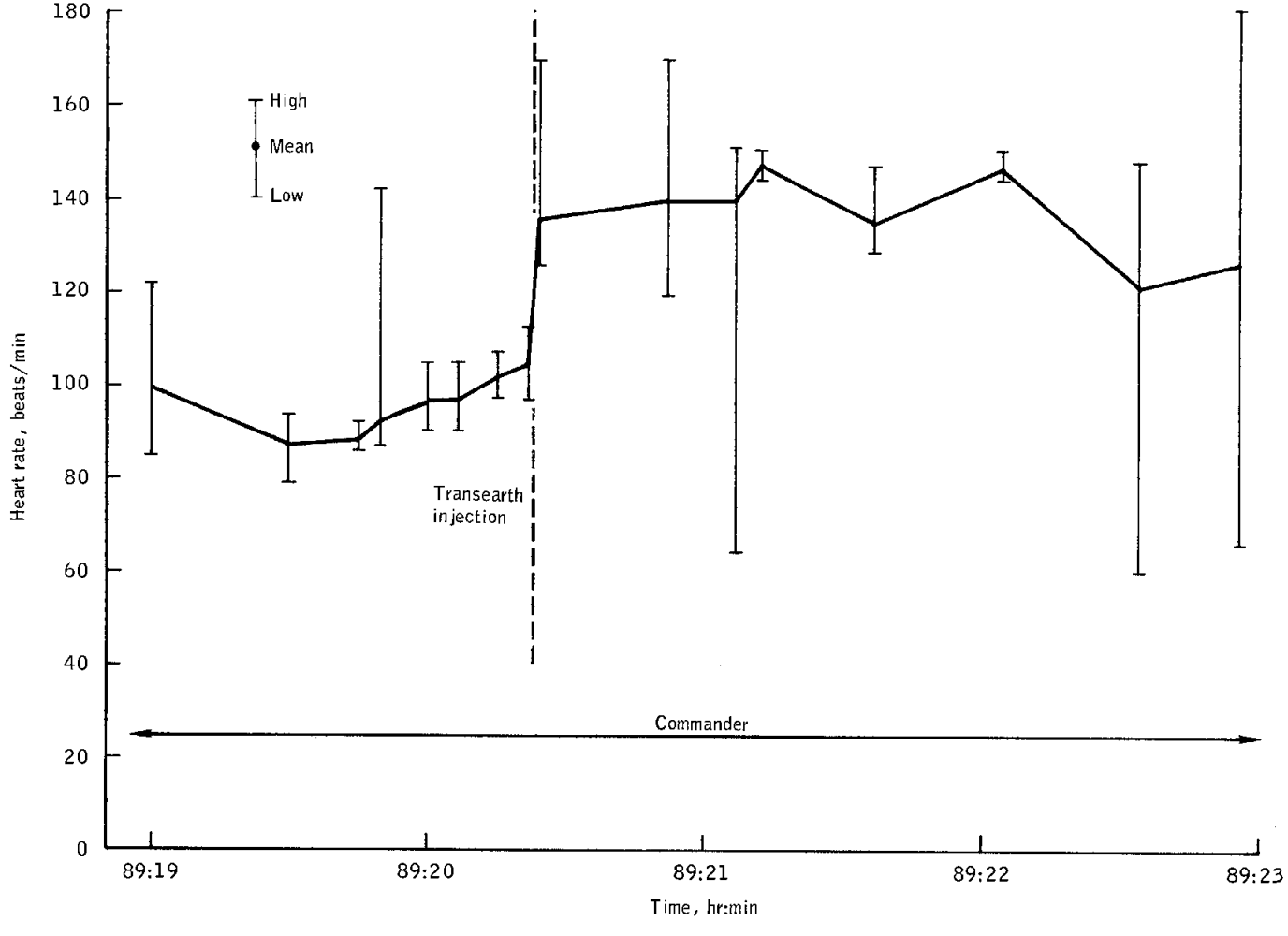

(d) Transearth injection.

Figure 8-1.- Concluded.

NASA-S-69-699

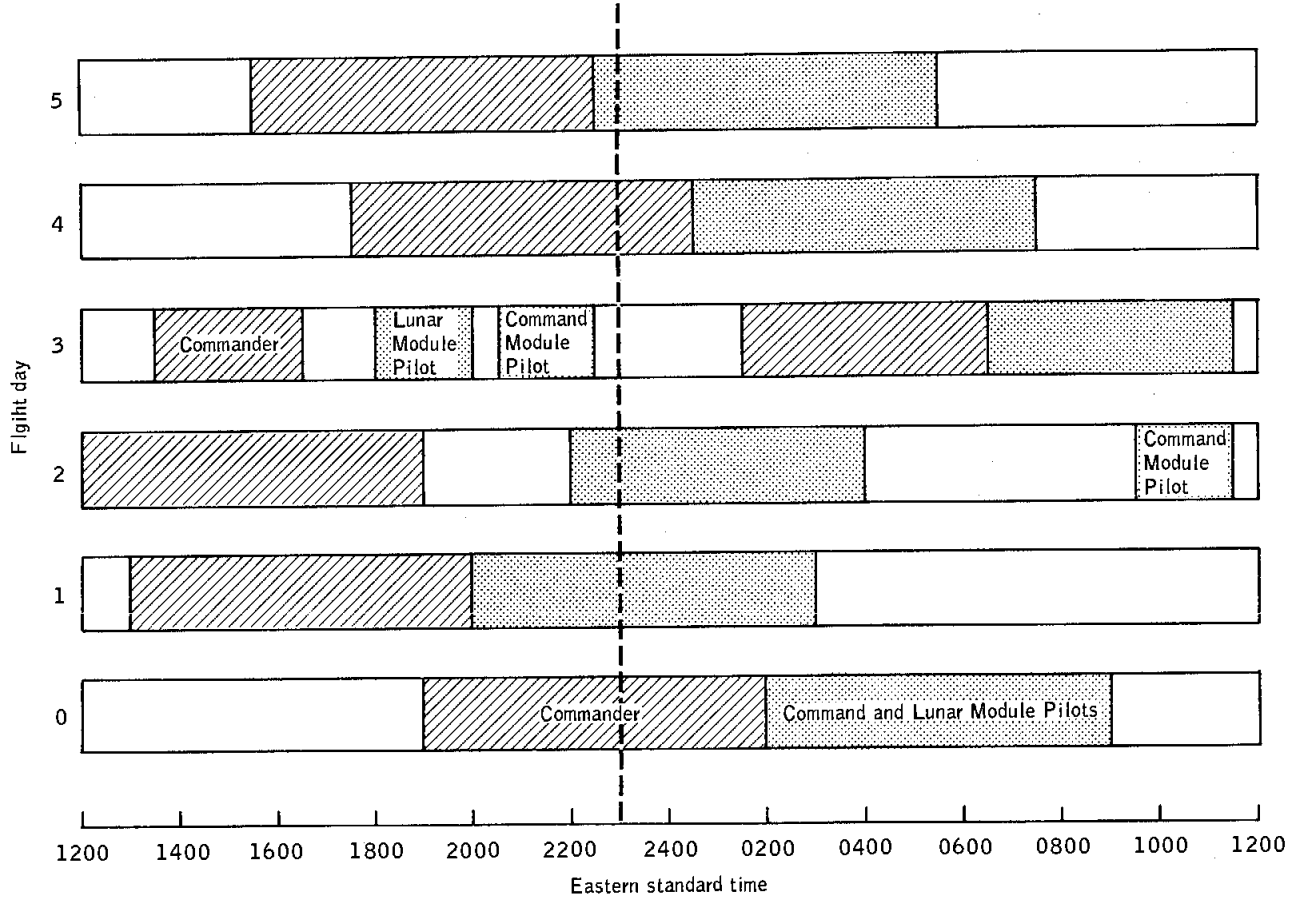

Figure 8-2.- Crew rest cycles.

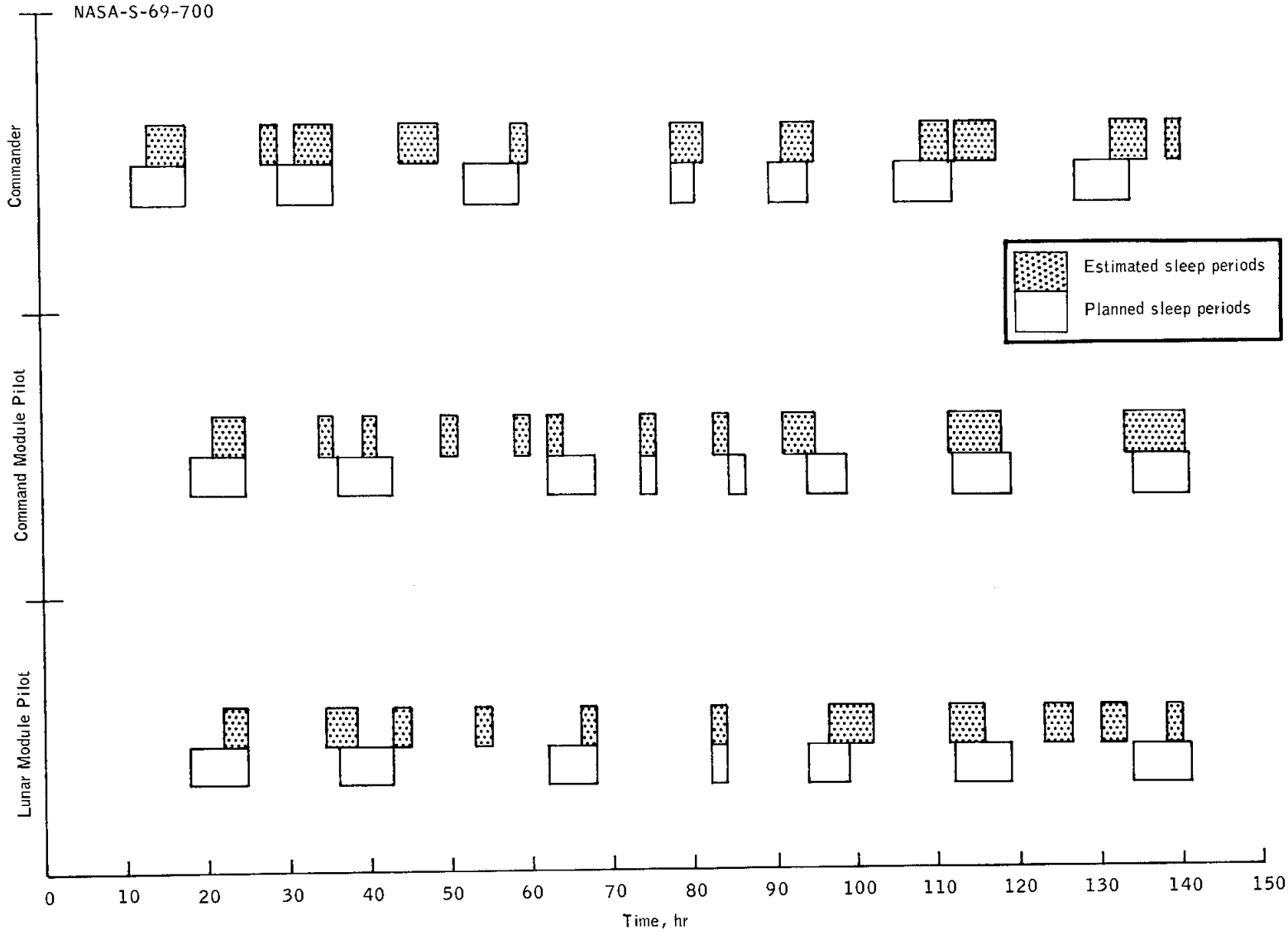

Figure 8-3.- Planned and crew-estimated sleep.

9.0 MISSION SUPPORT PERFORMANCE

This section of the report is based upon real-time observations. Therefore, statements based on actual events may not agree with the final analysis of the data in other sections of the report.

9.1 FLIGHT CONTROL

All aspects of the flight control operations were excellent, demonstrating the capability to support a lunar mission.

During the launch phase, ground systems support was nominal, except at 20 seconds a malfunction occurred in the communication processor at the Goddard Space Flight Center. The processor was disabled for 4 minutes, and all 2.4 kbps data were lost, but there was no impact on the mission because the 40.8 kbps data were prime.

A slight longitudinal oscillation was reported at 0:08:13 during second stage firing; however, cutoff was nominal, and voice communications during this phase were excellent.

After the optics cover was jettisoned at 0:42:05, the crew performed star checks over the Carnarvon station to verify their platform alignment. During the second revolution, at 1:56:00, all spacecraft systems were approved for translunar injection. The translunar injection maneuver occurred on time while the spacecraft was over the *Mercury* tracking ship. Engine cutoff for the maneuver occurred at 2:55:52, over Hawaii.

During the translunar coast phase, the S-IVB maneuver to the proper separation attitude began at 3:10:55. The S-IVB/spacecraft separation occurred at 3:20:55. All adapter panels jettisoned, and the high gain antenna was deployed.

The first maneuver to increase the distance between the spacecraft and S-IVB was executed with the reaction control system at 3:40:00. The resultant velocity change was approximately 1.15 ft/sec, as compared with the desired value of 1.50 ft/sec. Shortly after this maneuver, the crew reported that the S-IVB was still uncomfortably close and requested an additional maneuver to increase the separation distance. After appropriate ground-based analyses based on platform gimbal angles, a reaction control system maneuver of 8 ft/sec was recommended. The maneuver was executed at 4:45:00, and the actual velocity change was 7.7 ft/sec. This velocity change was larger than required to insure adequate spacecraft separation during the planned maneuver to place the S-IVB in a solar orbit. Because of this second separation maneuver, the scheduled flight

plan events were delayed approximately 2 hours to permit additional tracking and ground-computed vector resolution.

The first midcourse correction resulted in a velocity change of 24.8 ft/sec, and the precision was such that only a 2.0 ft/sec correction at 60:59:54 was required prior to lunar orbit insertion.

A 3:00:00, the service propulsion oxidizer tank pressure had dropped 7 psi in 45 minutes. The pressure continued to decrease slowly until 16:00:00, when it stabilized. The suspected cause was helium going into solution in the oxidizer; the decrease stopped when the oxidizer became saturated.

During the first midcourse maneuver, a momentary drop in the service propulsion engine chamber pressure was noted and was attributed to helium ingestion caused by insufficient feedline bleeding during propellant loading. The system was approved for the lunar orbit insertion maneuver.

At approximately 20:00:00, based on the crew's previous inability to recognize only the brightest stars through the telescope, the backup alignment stars were changed to Sirius as primary and Rigel as secondary.

At 31:10:00, the first televison transmissions were attempted. The wide-angle lens was used to obtain excellent pictures of the inside of the cabin; however, when the telephoto lens was used, the attempted pictures of the earth were not received. It appeared that the lens was passing too much light, and a procedure for taping certain filters from the still camera to the television camera was passed to the crew. Subsequent transmissions using the telephoto lens were of satisfactory quality. (See section 6.7 for further discussion.)

The lunar orbit insertion and circularization maneuvers were nominally performed at 69:08:20 and at 73:35:06, respectively, and the only observed discrepancy was a slightly low thrust. (See section 6.11.)

The crew performed all planned functions during the first six lunar orbits but elected to delete stereo photography, control point navigation, and landing site sightings during the seventh, eighth, and ninth orbits because of extreme fatigue. The transearth injection maneuver was performed at 89:19:17, as planned.

During transearth coast, the velocity counter in the entry monitor system continued to count after the first transearth midcourse maneuver and stopped at minus 6.9 ft/sec, when the system was turned off. When the counter was returned to AUTO with the function switch in delta V, it jumped to 19 or 20 ft/sec. At 114 hours, a complete set of system tests was conducted, and normal system operation was indicated. It was reported that the shock of the pyrotechnics at the time of separation from the S-IVB

caused the delta V counter to jump by 100 ft/sec. After further system analysis and consideration of preflight characteristics, the entry monitor system was approved for use during entry. (See section 12 for further discussion.)

At approximately 107 hours, during a series of star/horizon sightings, program 01, which performs prelaunch initialization, was accidentally selected by the crew, and this caused the computer to perform coarse align and overlay certain erasable memory locations. Once a coarse align is performed, all knowledge of the current inertial reference material is lost. Further, the navigation weighting matrix (W-matrix) is invalidated and would need to be reinitialized for fresh derivation by additional navigation sightings. There was some concern about what would occur during a state vector integration, since the state-vector time and W-matrix time are synchronous. Therefore, the W-matrix was invalidated by setting the proper flag in memory to zero. After completing all recommended procedures, an analysis of a memory dump revealed no problems, and total computer recovery was achieved.

During the transearth coast, a final midcourse correction was deleted, since performing it would only result in a 0.04-degree change in flight-path angle at entry.

9.2 NETWORK PERFORMANCE

The Mission Control Center and the Manned Space Flight Network were placed on mission status for Apollo 8 on December 12, 1968. The support provided by all elements of the Mission Control Center and the Manned Space Flight Network was excellent.

Operations of the Real Time Computer Complex were satisfactory, and only minor problems were experienced throughout the mission period. At approximately 11:51:00, all data processing by the mission operations computer and the dynamic standby computer were lost for 10 minutes because of an uninterruptible instruction sequence in both computers. Corrective action has been taken to eliminate the computer-program error which caused this problem.

Air-to-ground communications throughout the mission were outstanding, with the exception of several minor keying problems. Telemetry support was successful and command operations were excellent throughout the mission.

Ground communications support was adequate; however, several communications failures were experienced. Restoration of two major circuit outages was accomplished. Just after lift-off, the Goddard Space Flight

Center on-line communications processor faulted with the resulting loss of the secondary 2.4 kbs data links. The 4-minute period required to isolate and correct this loss is excessive, and procedures will be found to reduce this time. At approximately 36:00:00, a 20-minute communications failure which affected numerous Manned Space Flight Network circuits was attributed to a faulty fuse alarm.

9.3 RECOVERY OPERATIONS

9.3.1 Landing Areas and Recovery Force Deployment

The Department of Defense provided recovery forces commensurate with the probability of a spacecraft landing within a specified area and with any special problems associated with such a landing (table 9.3-I). The locations of the elements are shown in figures 9.3-1 through 9.3-4.

9.3.2 Command Module Location and Retrieval

First contact with the spacecraft by recovery forces occurred at 1540 G.m.t. during entry as a simultaneous reception of direction-finding signals from the S-Band equipment and visual sighting by the HC-130 aircraft. Soon after this contact, the primary recovery ship, *U.S.S. Yorktown*, had intermittent radar contact with the spacecraft and was able to determine position fixes at 270, 109, and 62 n. mi. uprange of the ship. Voice contact between the spacecraft and an E-1B recovery aircraft (Air Boss 1) was established on 296.8 MHz at 1 minute after main-parachute deployment. The VHF recovery beacon was also received by the aircraft and helicopters. Visual observation of the flashing light was made by the helicopter crew and by persons on the *Yorktown*.

Landing occurred at 1552 G.m.t. The landing point calculated by the recovery forces was latitude 8 degrees 7.5 minutes north and longitude 165 degrees 1.2 minutes west. After landing, visual observation of the flashing light and reception of the recovery beacon were temporarily lost when the spacecraft went to the stable II (apex down) flotation attitude. Six minutes 3 seconds elapsed between the time of loss of beacon signal and the time the crew reported that they were upright.

Before the mission, a ground rule had been established that unless the flight crew required immediate aid, the recovery operation would be delayed until daylight. Therefore, the recovery forces held their positions around the spacecraft until first light at 1635 G.m.t., when swimmers from the helicopter were deployed to install the flotation collar. The hatch was opened and at 1714 G.m.t., the crew was hoisted into the helicopter and brought aboard ship 1 hour 28 minutes after landing. The

command module was retrieved by the *Yorktown* 2 hours 28 minutes after landing. The retrieval point was latitude 8 degrees 4.9 minutes north and longitude 165 degrees 4.0 minutes west.

The following is a chronological listing of significant events that occurred during the recovery operation on December 27, 1968.

Time, G.m.t.	Event
1540	Aircraft received direction-finding signals and visually acquired spacecraft during entry
1541	*Yorktown* radar contact with command module 270 n. mi. uprange
1542	*Yorktown* radar contact with command module 109 n. mi. uprange
1543	*Yorktown* radar contact with command module 60 n. mi. uprange
1547	Voice contact with flight crew by helicopter on 296.8 MHz
	Recovery beacon contact by aircraft on 243.0 MHz
	Flashing light visible on recovery helicopter 3
1548	Flashing light visible on *Yorktown*
1552	Command module landed and went to stable II position
1558	Spacecraft uprighted
1635	Swimmers deployed
1658	Flotation collar inflated
1703	Hatch open
1706	Crew in life raft
1714	Crew in helicopter
1720	Crew aboard *Yorktown*
1813	*Yorktown* arrived at spacecraft
1820	Spacecraft hoisted aboard *Yorktown*

Weather conditions reported by the *USS Yorktown* at 1635 G.m.t. were:

Wind direction, deg true	70
Wind speed, knots	19
Water temperature, °F	82
Cloud cover	2000 scattered 9000 overcast
Visibility, n. mi.	10
Wave height, ft	6
Wave direction, deg true	110

9.3.3 Direction Finding Equipment

The following table summarizes the recovery force's reception of the S-band and the VHF recovery beacon.

S-band

Aircraft	Time of first contact, G.m.t.	Type receiver	Aircraft position
Hawaii Rescue 1 (HC-130)	1540	AN/ARD-17	11°35'N 166°45'W

VHF Recovery Beacon

Aircraft	Time of first contact, G.m.t.	Range of reception, n. mi.	Type receiver	Aircraft position
Hawaii Rescue 1 (HC-130)	1547	215	AN/ARD-17	11°10'N 167°05'W
Hawaii Rescue 2 (HC-130)	1550	212	AN/ARD-17	50°30'N 162°44'W
Recovery 1 (SH-3A)	1549	47	SARAH	8°45'N 156°30'W
Recovery 2 (SH-3A)	1547	47	SARAH	7°55'N 164°20'W
Recovery 3 (SH-3A)	1547	1	SARAH	8°08'N 165°02'W
Air Boss 1 (E-1B)	1547	50	ARA-25	8°40'N 165°40'W

9.3.4 Command Module Deactivation

The command module was offloaded from the *Yorktown* on December 29, 1968, at Ford Island, Hawaii. The Landing Safing Team started the evaluation and deactivation procedures at 2100 G.m.t. An inspection verified that all normally activated command module pyrotechnics had fired. The remainder of the pyrotechnics were safed by removal of the initiators. The reaction control system propellants were expelled into ground support equipment and disposed of in a safe area, but the expelled quantities were immeasurable. Deactivation was completed on January 1, 1969. At 2100 G.m.t. January 2, 1969, the command module was received at the contractor's facility in Downey, California.

9.3.5 Command Module Postrecovery Inspection

The following is a summary of observations made during the recovery operation.

a. The swimmers were not able to communicate with the flight crew on the swimmer interphone (see section 12).

b. Two of the six strands on the recovery loop were parted during the spacecraft retrieval (see section 12).

c. Approximately 3-3/4 gallons of water was found inside the command module.

d. Recovery antenna 1 was bent during retrieval operations.

e. Two areas of the aft heat shield were separated from the spacecraft, but the vertical cleavage around the edges of the areas from where sections were missing indicated that they had been jarred loose during or after landing (fig. 9.3-5) (see section 6.4).

TABLE 9.3-I.- RECOVERY SUPPORT

Landing area	Maximum retrieval time, hr	Maximum access time, hr	Support		Remarks
			No.	Unit	
Launch site	--	2	1	LCU	Landing craft utility (landing craft with command module retrieval capability)
			2	LVTR	Landing vehicle tracked retriever (tracked amphibious vehicle with command module retrieval capability)
			1	HH-3E	Helicopter with pararescue team
			2	HH-53C	Helicopter capable of lifting the command module; each with pararescue team
			2	ARS/ATF	Salvage ship
Launch abort	24 to 48	4	1	LPH	Landing platform helicopter, USS Guadalcanal
			5	SH-3D	Helicopter with swimmers for camera capsule retrieval
			1	LKA	Attack cargo ship, USS Rankin
			1	AIS	Apollo instrumentation ship, USNS Vanguard
			1	LPA	Attack transport, USS Sandoval
			1	AO	Fleet oiler, USS Chukawan
			3	HC-130	Fixed-wing search and rescue aircraft with pararescue team
Earth orbital secondary					
West Atlantic	26	6	1	LPH	USS Guadalcanal
Mid-Pacific	26	6	2	DD	Destroyers, USS Nicholas and Cochrane
East Atlantic	26	6	1	AO	USS Chuckawan
West Pacific	26	6	1	DD	USS Rupertus (on standby; never activated)
			8	HC-130	Two each staged at Japan, Hawaii, Bermuda, and the Azores
Deep space secondary	32	3	1	LPA	Attack transport, USS Francis Marion
			2	HC-130	Staged at Ascension Island
Primary	14	3	1	CVS	Primary recovery ship, USS Yorktown
			1	DD	USS Cochrane
			3	HC-130	Staged at Hawaii
			4	SH-3A	Three helicopters with swimmers plus one photographic platform
			2	E-1B	Fixed-wing air control and communications relay aircraft
Contingency		18	16	HC-130	Aircraft staged from Hawaii, Azores, Japan, Canal Zone, Ascension, Mauritius, and Samoa

NASA-S-69-701

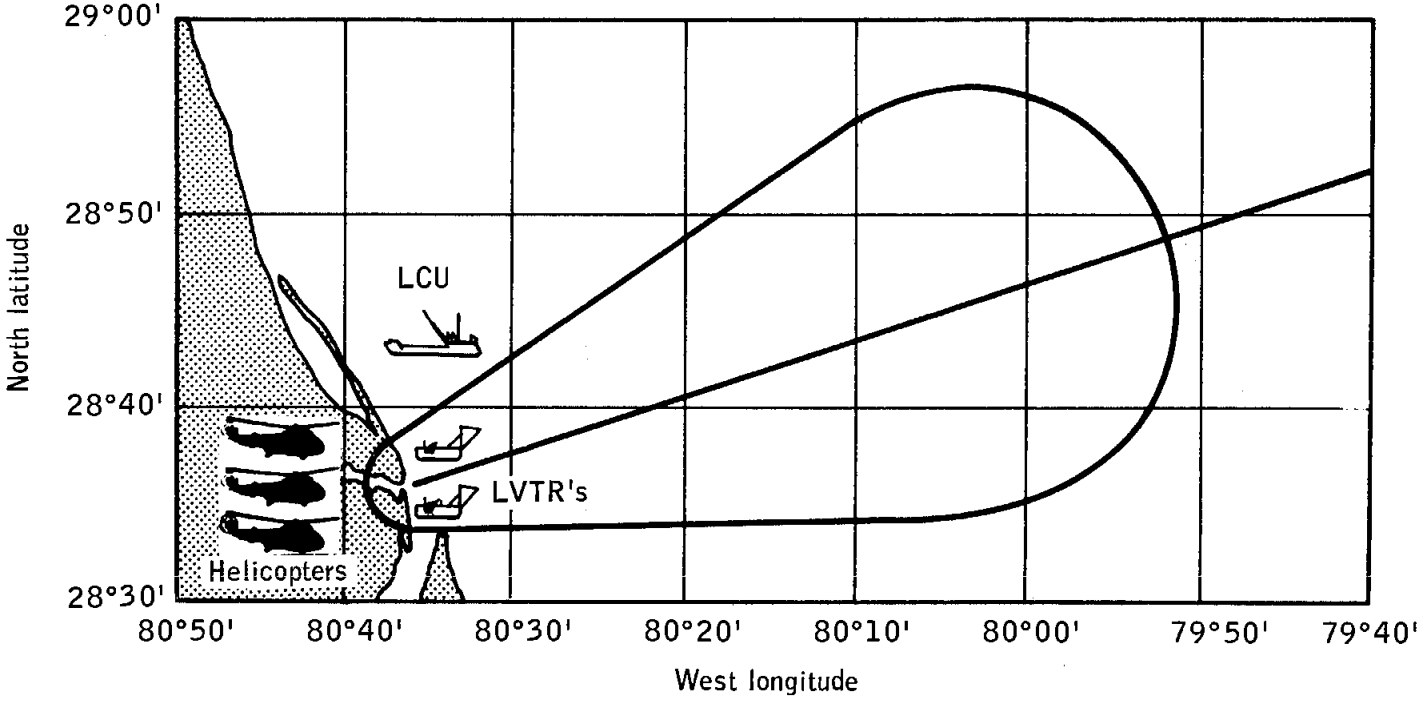

Figure 9.3-1.- Launch site area and force deployment.

NASA-S-69-702

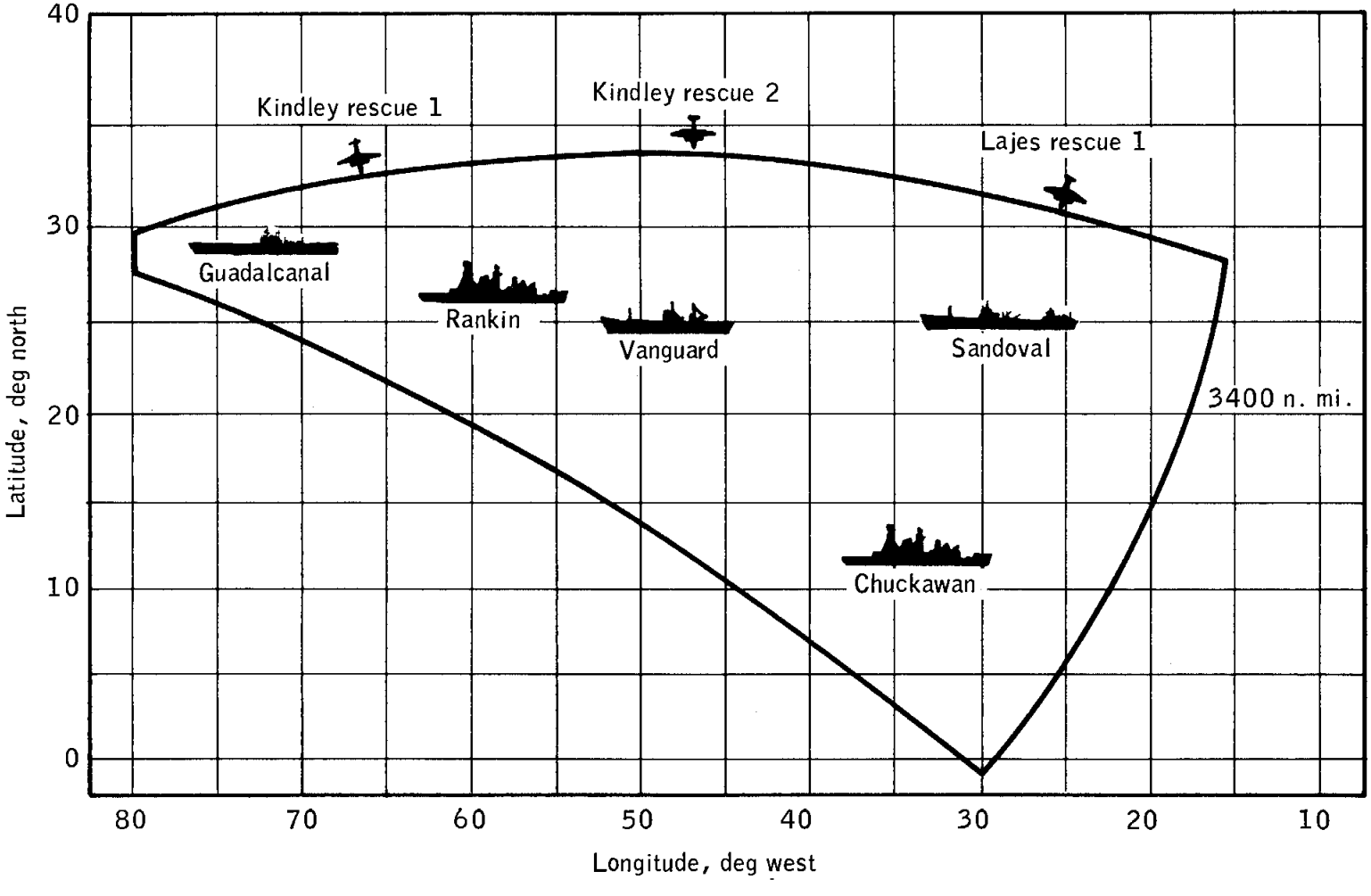

Figure 9.3-2.- Launch abort area and force deployment.

NASA-S-69-703

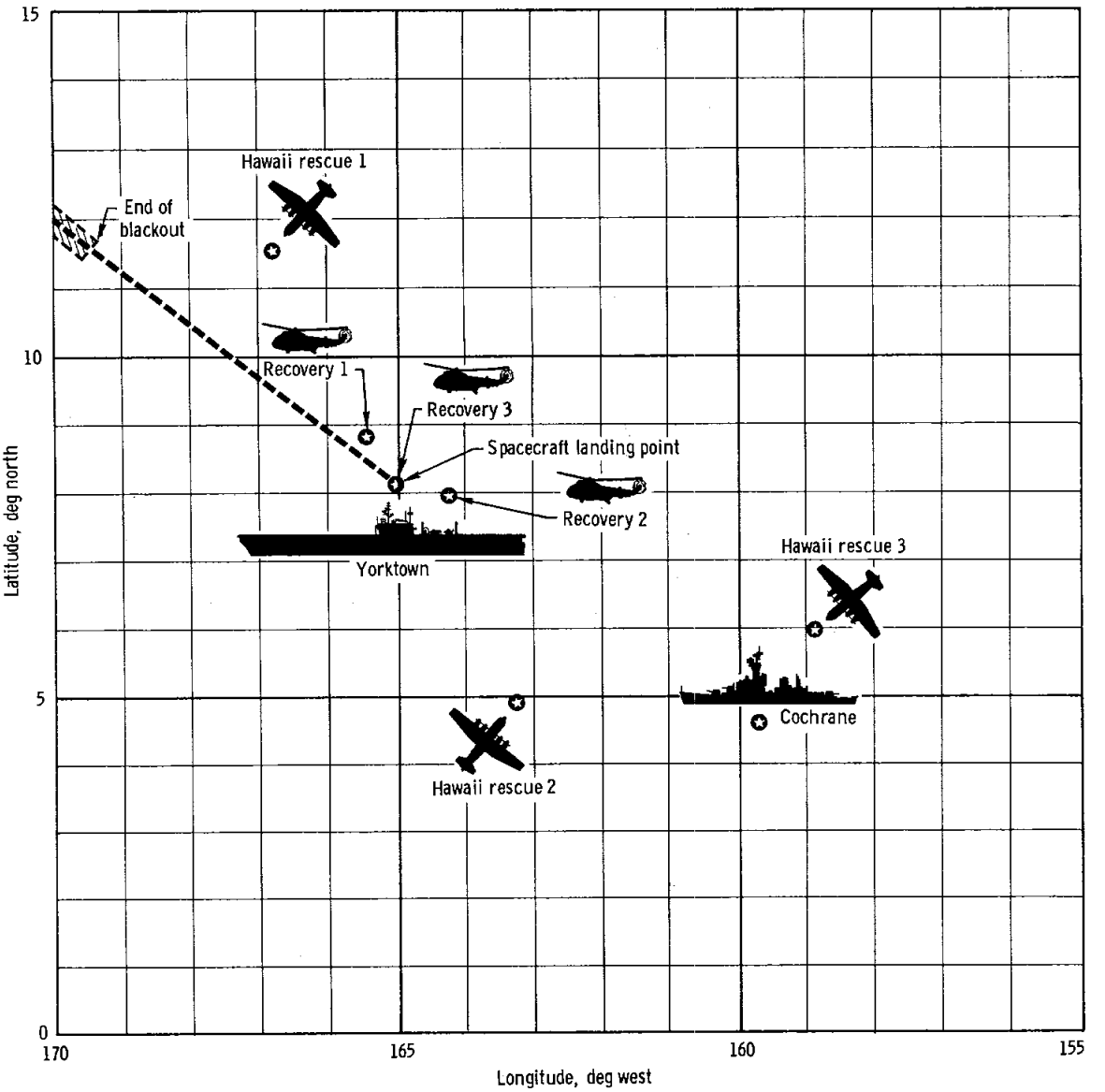

Figure 9.3-3.- Landing area and recovery force deployment.

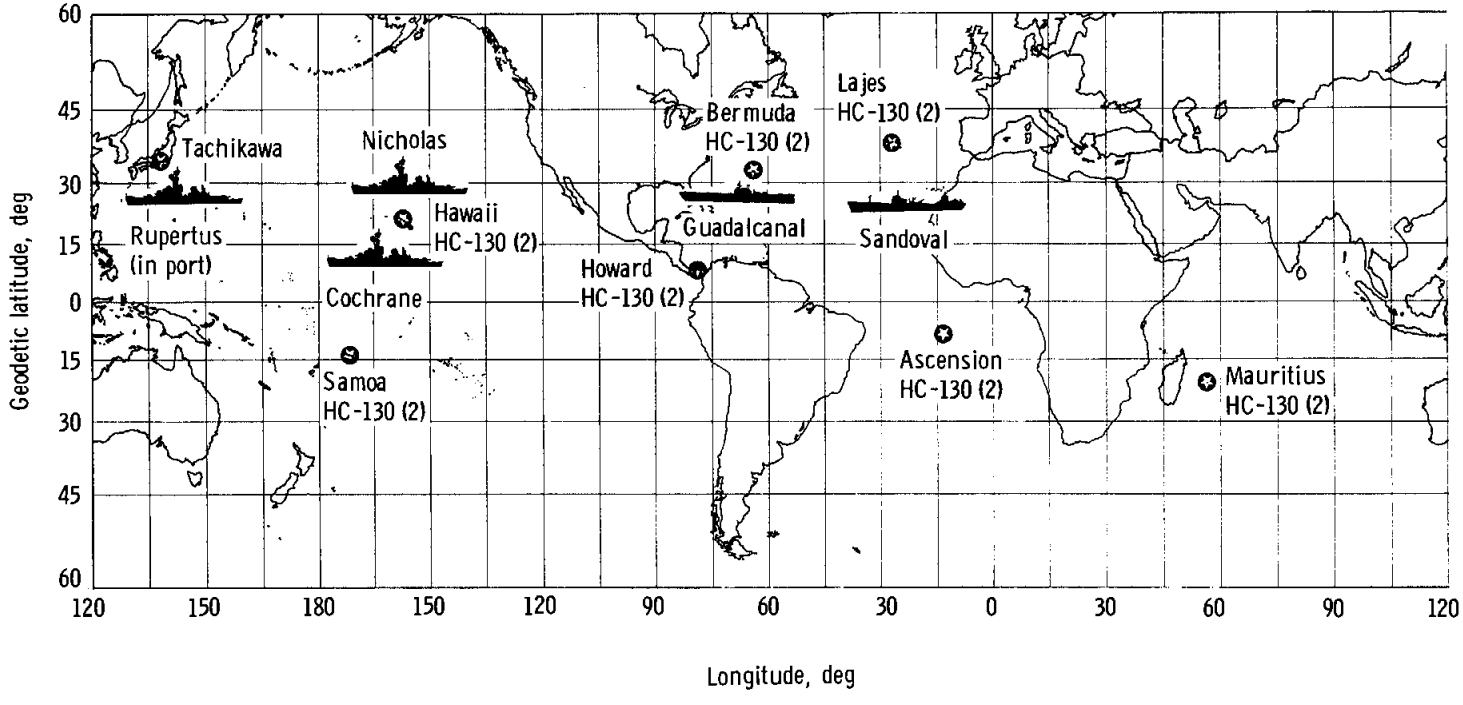

(a) Prior to translunar injection.

Figure 9.3-4. - Recovery force deployment during mission.

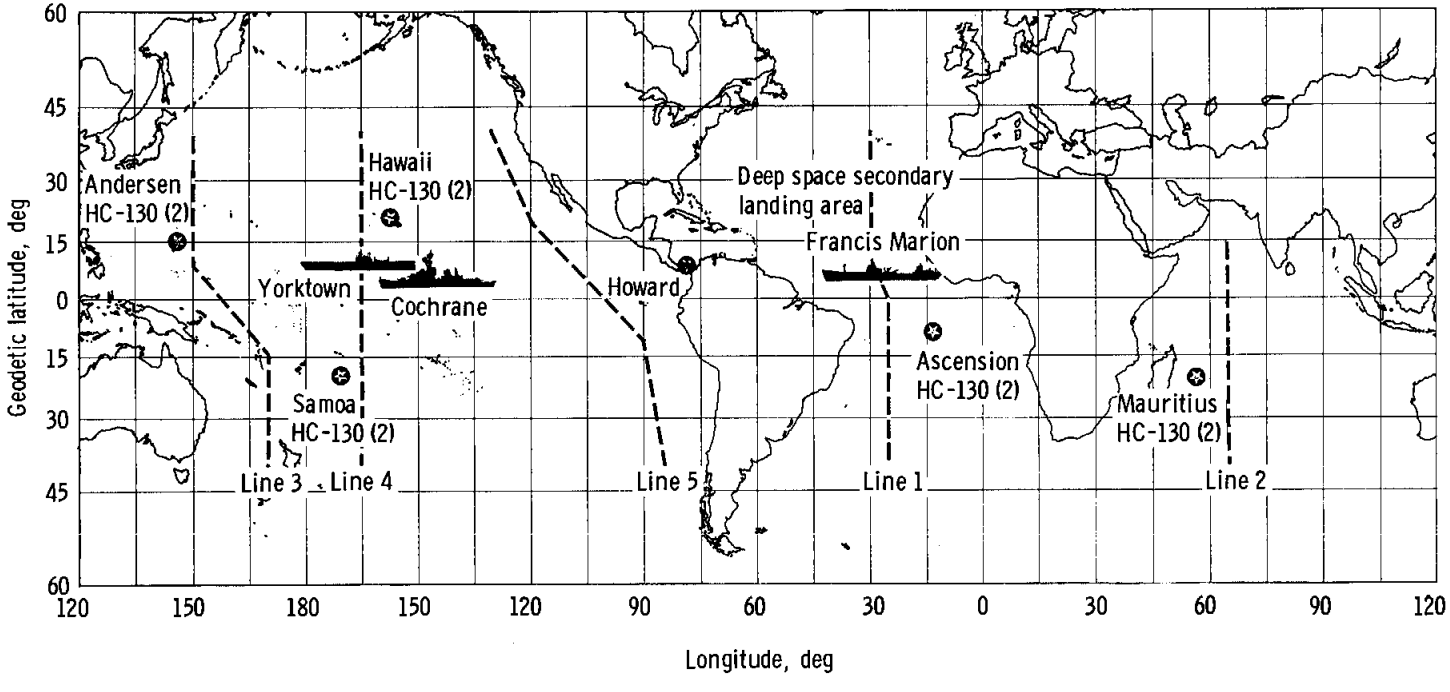

(b) After translunar injection.

Figure 9.3-4. - Concluded.

NASA-S-69-706

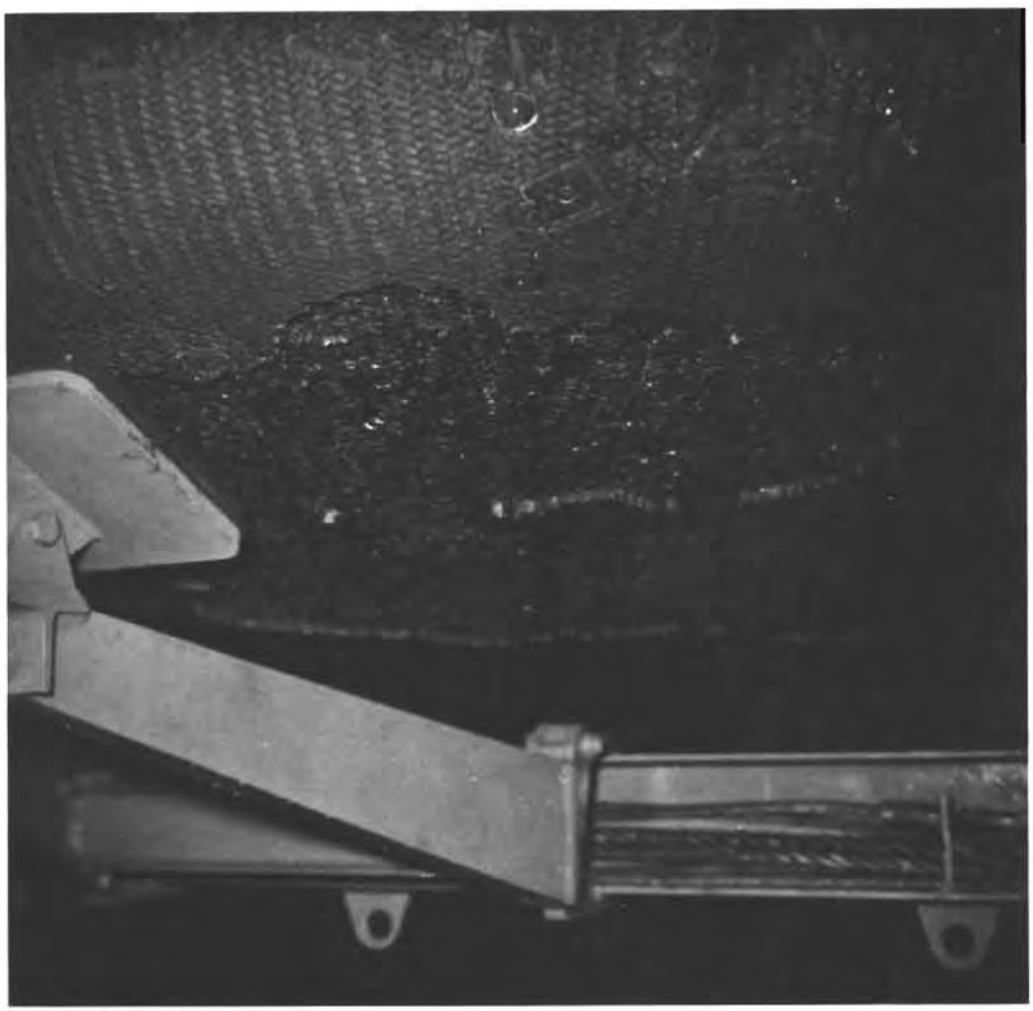

Figure 9.3-5.- Broken ablator on aft heat shield.

10.0 LAUNCH VEHICLE PERFORMANCE

Launch vehicle performance was completely nominal, and no failures or discrepancies have been identified.

Minor low-amplitude 10- and 18-Hz oscillations occurred at the S-II center engine during the low-mixture-ratio period and damped out shortly before cutoff. Also, minor low-amplitude 18-Hz oscillations in S-II outboard engine pressures were noted during the same period.

After spacecraft separation, the remaining liquid oxygen and the auxiliary propulsion system propellant in the S-IVB were used to change the trajectory of the S-IVB stage. The liquid oxygen was expelled through the J-2 engine in approximately 300 seconds, and the auxiliary propulsion motors were fired for approximately 700 seconds. The resulting velocity increment of 137.5 ft/sec caused the S-IVB to go past the trailing edge of the moon. Closest approach of the S-IVB to the moon was 681 n. mi., and the trajectory after passing from the lunar sphere of influence resulted in a heliocentric orbit with an aphelion of 23 165.2, a perihelion of 21 630.2, and a period of 340.8 days.

11.0 ASSESSMENT OF MISSION OBJECTIVES

The primary objectives for the Apollo 8 mission are defined in reference 2. The primary objectives were the following:

a. Demonstrate crew/space vehicle/mission support performance during a manned SaturnV mission with the command and service module

b. Demonstrate performance of nominal and selected backup lunar orbit rendezvous mission activities, including the following:

   (1) Launch vehicle targeting for translunar injection

   (2) Long-duration service propulsion maneuvers and midcourse corrections

   (3) Pre-translunar injection procedures

   (4) Translunar injection

   (5) Command and service module orbital navigation

Detailed test objectives defining the tests required to fulfill the primary mission objectives are defined in reference 3. These detailed test objectives are listed in table 11-I.

The data obtained and presented in other sections of this report are sufficient to verify that the primary mission objectives were met. However, in two cases, portions of detailed test objectives were not met. These objectives and their significance are discussed in the following paragraphs.

11.1 MIDCOURSE NAVIGATION/STAR-EARTH LANDMARK (S1.32)

The intent of objective S1.32 was to demonstrate onboard star-earth landmark optical navigation. This is a secondary objective which does not require demonstration. The accuracy of other navigation modes is sufficient to preclude the necessity of using star-earth landmarks for midcourse navigation.

11.2 LUNAR LANDMARK TRACKING (P20.111)

The intent of objective P20.111 was to establish that an onboard capability existed to compute relative position data for the lunar landing mission. This mode will be used in conjunction with the Manned Space Flight Network vehicle state-vector update. All portions of the objective were completed except for the functional test, which required the use of onboard data to determine the error uncertainties in landing-site location. Although this test was not completed, sufficient data were obtained to determine that no constraint exists for subsequent missions. A procedural error caused the time intervals between the mark designations to be too short; thus, the data may be correct but may not be representative. The accuracy of the onboard capability has not yet been determined because the data analyses are not complete. A demonstration of this technique is planned for the next lunar mission.

TABLE 11-I.- DETAILED TEST OBJECTIVES

Number	Description	Primary objectives supported	Completed
S1.27	Guidance and navigation boost monitor, Saturn V	1	Yes
S1.30	Inertial measurement unit performance	1	Yes
P1.31	Guidance and navigation entry, lunar return	1	Yes
S1.32	Midcourse navigation/star-earth landmark	1	Partial
P1.33	Midcourse navigation/star-lunar horizon	1	Yes
P1.34	Midcourse navigation/star-earth horizon	1	Yes
S1.35	Inertial measurement unit orientation determination/ visibility	1	Yes
S3.21	Service propulsion system evaluation	2	Yes
S4.5	Environmental control system, lunar return entry	1	Yes
S6.10	Omnidirectional antennas, lunar distance	1	Yes
P6.11	Spacecraft-to-ground communications, lunar distance	1	Yes
S7.30	Heat shield, lunar return	1	Yes
P7.31	Thermal control in space environment	1	Yes
P7.32	Spacecraft dynamic environment	1	Yes
P7.33	Adapter panel jettison	1	Yes
S20.104	Transposition	1	Yes
P20.105	Lunar orbit insertion maneuver	2	Yes
P20.106	Transearth injection maneuver	2	Yes
P20.107	Crew activities, lunar distance	1	Yes
S20.108	Spacecraft consumables, lunar mission	1	Yes
P20.109	Passive thermal control modes	1	Yes
P20.110	Ground support, lunar distance	1	Yes
P20.111	Lunar landmark tracking	2	Partial
P20.112	Translunar injection maneuver	2	Yes
P20.114	Midcourse correction capability	1	Yes
S20.115	Lunar mission photography	1	Yes
S20.116	Exhaust effects/spacecraft windows	1	Yes
Functional tests added during the mission			
P1.34	Star/earth horizon photography through sextant	1	Yes
P1.34	Midcourse navigation, helmets on	1	Yes
P1.34	Navigation, long eyepiece	1	Yes
P6.11	High-gain antenna, automatic reacquisition	1	Yes
P20.109	Passive thermal control, roll rate of 0.3 deg/sec	1	Yes

12.0 ANOMALY SUMMARY

This section contains a discussion of the significant anomalies from the Apollo 8 mission. A discussion of all other discrepancies is included in the appropriate sections of this report.

12.1 ENTRY MONITOR SYSTEM ERRORS

Four abnormal indications from the entry monitor system occurred at different times during the mission.

1. During the spacecraft/S-IVB separation sequence, the delta V counter jumped 100 ft/sec.

2. For the third midcourse correction, a delta V of 5 ft/sec was entered into the entry monitor system. The system counted to zero at delta V cutoff; however, it continued to count after the maneuver and was finally turned off by the crew.

3. At times when the mode switch was rapidly switched from "standby" to "automatic," the delta V counter jumped 19 to 20 ft/sec.

4. For the initial entry phase, the g/velocity trace on the entry scroll showed two short, incorrect g transients (fig. 12-1). Operation of the scroll assembly was normal in all other respects.

The entry monitor system was removed from the spacecraft, and no abnormal indications were observed in functional tests. However, during tilt-table tests, abnormal accelerometer outputs were observed when random 0.25g pulses were produced at approximately 0.8g. Detailed testing and inspection of the accelerometer disclosed a bubble in the damping fluid. The bubble may explain the behavior of the g trace during entry and the random pulses during the tilt-table test. The bubble may also be associated with the problem after the midcourse correction, in that it has been demonstrated that the time for the accelerometer to drive to null greatly increases when a bubble is present.

The accelerometer case contained 1 cubic centimeter less fluid than when it was originally filled. Indications near the fill port are that damping fluid had leaked around the O-ring seal. The seal has been changed from a screw to a plug type for units to be flown on spacecraft 106 and subsequent.

Velocity counter jumps on the order of that seen at spacecraft/S-IVB separation have been produced when an ordered series of positive and negative pulses enter the counter logic from the accelerometer output with the counter reading essentially zero. The jumps are the result of a logic race involving the sign change circuit in the counter and, therefore, cannot occur unless the counter reading is near zero. In the normal modes of operation (delta V and entry ranging) large values of velocity or range are set in and driven toward zero; therefore, no logic race occurs. If the system is used for monitoring accrued velocity, such as at separation, the counter can be manually biased away from zero to avoid the problem.

The entry monitor system is a backup mode for both delta V and entry ranging on Apollo 9. Further, entry bank angles will be furnished to the crew if both the guidance and navigation system and the entry monitor system fail.

This anomaly is still open, and an Anomaly Report will be prepared.

12.2 WINDOW FOGGING

Visibility through the hatch window was degraded to the point that the window was useless for visual observation and photography after approximately 6 hours. The two side windows (1 and 5) were fogged but to a lesser degree. The two rendezvous windows (2 and 4) remained usable throughout the flight. These conditions were consistent with what was expected as a result of the Apollo 7 window fogging analysis, which showed the primary cause to be outgassing of silicone oils from the RTV sealing material.

Figure 12-2 shows a cross section of the side windows, including the typical installation of the three windows and the location of the modification. The modification consists of a new RTV curing process to greatly reduce the residual oils.

During ground tests with the unbaked hatch window installation in a simulated flight environment, excessive deposits were produced on the inner surface of the heat shield pane within half a day. Under identical test conditions, a hatch window, cured under the new process, was subjected to a 10-day test. This test demonstrated the success of the new curing process in eliminating deposits of the silicone oils. About 2 square inches of condensation, from the moisture between the pressure panes, appeared temporarily. On flight windows, the space between panes is filled with dry nitrogen. A test under more extreme conditions has been completed to verify the adequacy of the modification for lunar missions, and preliminary results also indicate successful performance.

Windows 1, 3, and 5 on command module 104 have been refitted with insulation cured by the new process. This anomaly is closed.

12.3 NOISY CABIN FANS

During the sixth day of the mission, the cabin fans (fig. 12-3) were momentarily turned on, and the crew reported that both were noisy.

Postflight, the acoustic level of the fans, both individually and together, was measured at the three head positions on the couches, at the work stations, and in the sleep positions, with the hatches closed. The noise level is considered normal when compared to cabin fan noise previously experienced during checkout.

No blade or bearing damage was detected, and the blades moved smoothly and stopped slowly. No loose objects were found in the plenum chamber and none of the blades were nicked; loose objects and nicked blades on spacecraft 101 (Apollo 7) produced objectionable noise on that flight.

The noise level may have been caused by a resonant condition within the duct system under the existing environment. However, no further investigation is necessary; results of Apollo 7 and 8 demonstrate that the cabin fans are not required for maintenance of a comfortable environment This anomaly is closed.

12.4 POSSIBILITY OF WATER INFLOW THROUGH CABIN PRESSURE RELIEF VALVE

The Commander reported that his left shoulder was showered with water at landing, implying that sea water entered through the cabin pressure relief valve (fig. 12-4); the crew reported that both sides of the valve had been positioned to the closed position, as specified by the crew checklist.

A manual lever is connected to each side of the redundant cabin pressure relief valve. With the two levers in the closed position (dashed lines in fig. 12-4), a cam prevents the valve from opening. Any other position of the lever and cam allows the valve to open at ambient-to-cabin differential pressure of 0.3 psi. Postflight, the valves were tested to 13 psi in the closed position, and the leakage was within specification. Increasing the pressure to 25 psig caused a fine spray around the valves. However, the valves did not yield permanently. Only a negligible amount of sea water could enter by ram effect against the relief

valve. In addition, no salt deposits were evident in either valve. Further, the cam and lever rigging and lever detent positions were verified.

On the unmanned Apollo 4 and 6 flights, the cabin pressure relief valves were required to be in the boost/entry position at landing, which would allow inflow of sea water. Such inflow was apparent by H-film ingestion into one valve on Apollo 4 and by a valve frozen closed by salt deposits on Apollo 6 when the spacecraft were returned to Downey.

On Apollo 7, about 2 quarts of condensation accumulated on the aft bulkhead during the mission. Although condensation was not reported during Apollo 8, it was expected to accumulate on coolant lines which were not thermally insulated. The water which drenched the Commander's shoulder at landing could have been accumulated condensation.

No corrective action is required; the procedure for closing the valves is included in the crew checklist, and if the valves are not closed at landing, the crew will see water inflow and take appropriate action. This anomaly is closed.

12.5 BROKEN RECOVERY LOOP CABLES

Two of the six steel cables in the command module recovery loop failed while the spacecraft was being hoisted from the sea (fig. 12-5).

The recovery loop had exhibited numerous failures during tests at snatch loadings equivalent to a 32 000-pound load, and as a result, an auxiliary nylon loop was provided for installation by the swimmers. The nylon loop alone has sufficient safety margin to take the snatch loadings expected.

For spacecraft 108 and subsequent, the steel cable will be replaced with a nylon recovery loop similar to the auxiliary nylon loop. Until then, the auxiliary nylon loop, installed by the swimmers, will be used. This anomaly is closed.

12.6 LACK OF SWIMMER INTERCOMMUNICATIONS

During recovery operations, the swimmers were unable to communicate with the crew via the intercommunications system. The crew reported that the spacecraft intercom switches were in the proper position. As shown in figure 12-6, the swimmer interphone, which plugs into the spacecraft, has a push-to-talk switch and an ON-OFF switch.

Postflight, the system (using the actual swimmer interphone) was tested in the recovery configuration and operated satisfactorily, with two-way communications being established to all three crew stations.

The most probable cause of the problem is outside the spacecraft and associated with the operation of the interphone. The training procedures for operation of the interphone will be emphasized for future flights. This anomaly is closed.

12.7 POTABLE WATER TANK QUANTITY MEASUREMENT

The potable water tank quantity measurement became erratic at 143:53:00. The water system did not leak inflight, as confirmed by the facts that the correct amount of water was drained from the potable water tank and the system leakage checks were within specification after the flight.

Examination of the disassembled unit (fig. 12-7) revealed corrosion in the indicator housing, on the variable resistor, and on the actuator pulley, indicating moisture had been present in the oxygen side of the tank pressurization system. The actuator line was broken, probably as a result of postflight calibration with the pulley shaft frozen from corrosion. Analysis of the residue in the area indicated that the contaminant was urine and possibly water from the waste water tank. The contamination could have come through the oxygen bleed filter and orifice (fig. 12-8) into the indicator housing and bladder.

Moisture in the variable resistor has been demonstrated to cause erratic readings of the type observed inflight. It has also been demonstrated that when the potable water tank is full (beginning at about 90 percent), the bladder wall comes in full contact with the bladder support frame. This isolates the 20 psig oxygen supply from the bleed orifice and allows a reduction in gas bladder pressure below the contact area. With the gas bladder at reduced pressure, water and urine can enter through the filter and orifice, when urine or the waste water tank is dumped.

The quantity measuring system in the waste water tank (same type as in potable tank) was also disassembled, but no corrosion was found. The waste water tank is never allowed to be 100-percent full. However, evidence of urine was found in the bleed filter.

For Apollo 9, it is planned to terminate potable water fill at approximately 80-percent of the maximum quantity. This anomaly is closed.

12.8 FUEL CELL DEGRADATION DURING COUNTDOWN

A degradation in fuel cell performance was experienced after switching to onboard cryogenics. Gas samples from the fuel cell purge lines showed approximately 8000 ppm of nitrogen (specification limit is 30 ppm).

Figure 12-9 shows only the basic system elements associated with the problem.

During normal servicing operation, liquid oxygen flows through a subcooler, which is chilled by liquid nitrogen. Valves 1 and 2 are closed during this operation.

While servicing liquid oxygen, a leak developed in a facility liquid oxygen line, causing a safety shutdown. To preclude overpressurization because of stagnant liquid oxygen, the system was vented using the normal shutdown procedure. This procedure was incorrect in one area, which called for opening valve 1 instead of valve 2. This error allowed liquid nitrogen to flow through valve 1 into the liquid oxygen supply line. Procedures have been corrected and verified by test. This anomaly is closed.

NASA-S-69-707

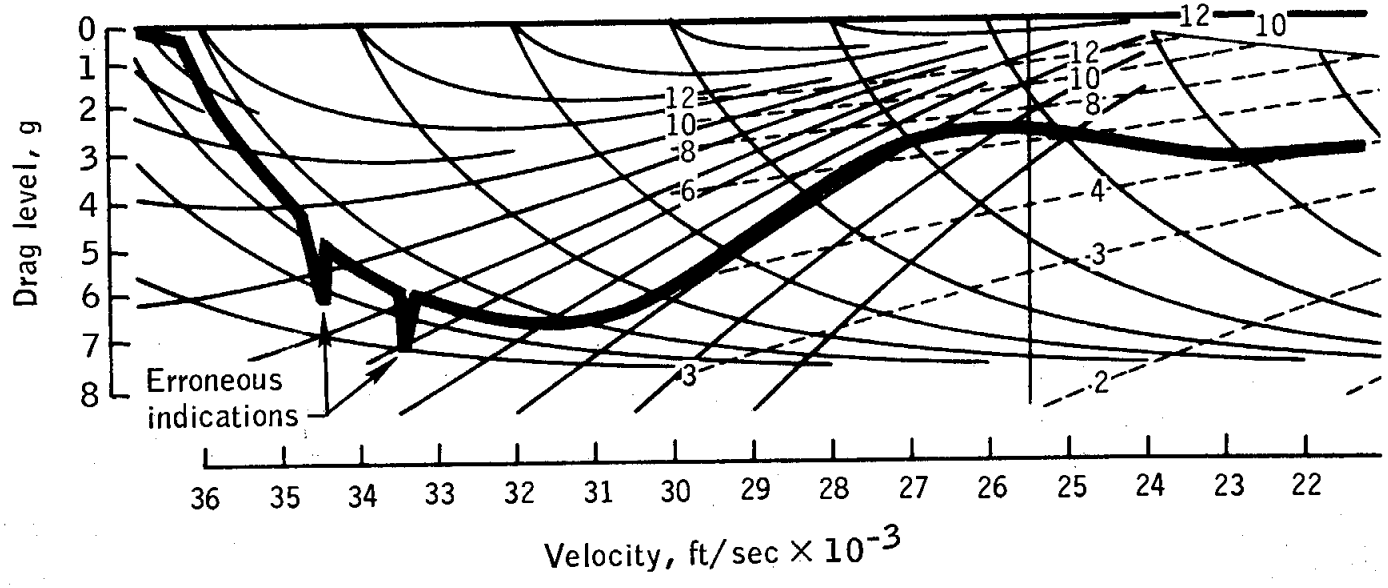

Figure 12-1.- Entry monitor system scroll.

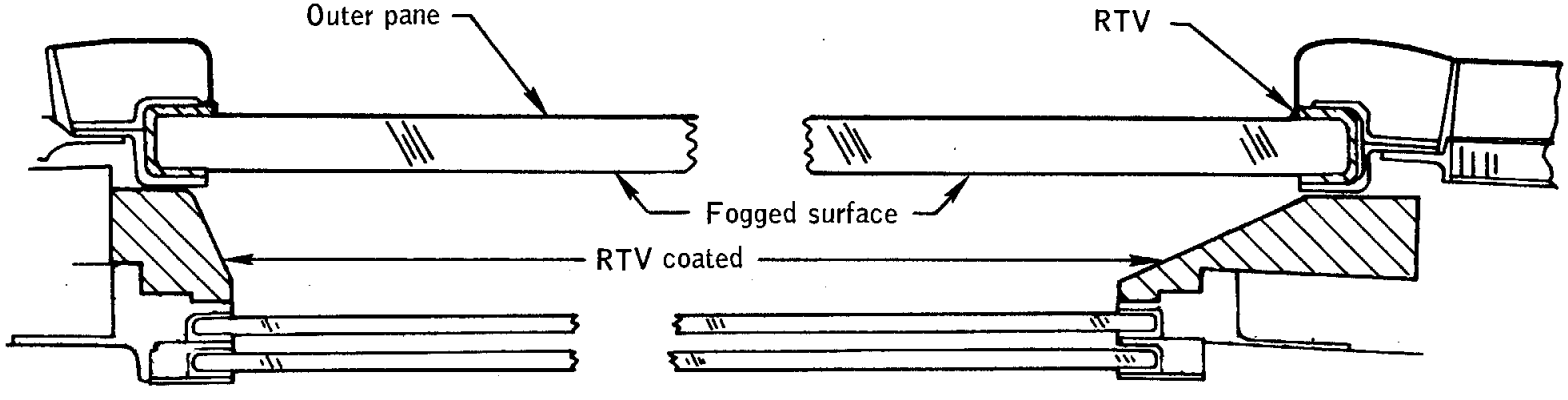

Figure 12-2.-Side window cross section (also typical for hatch window).

NASA-S-69-709

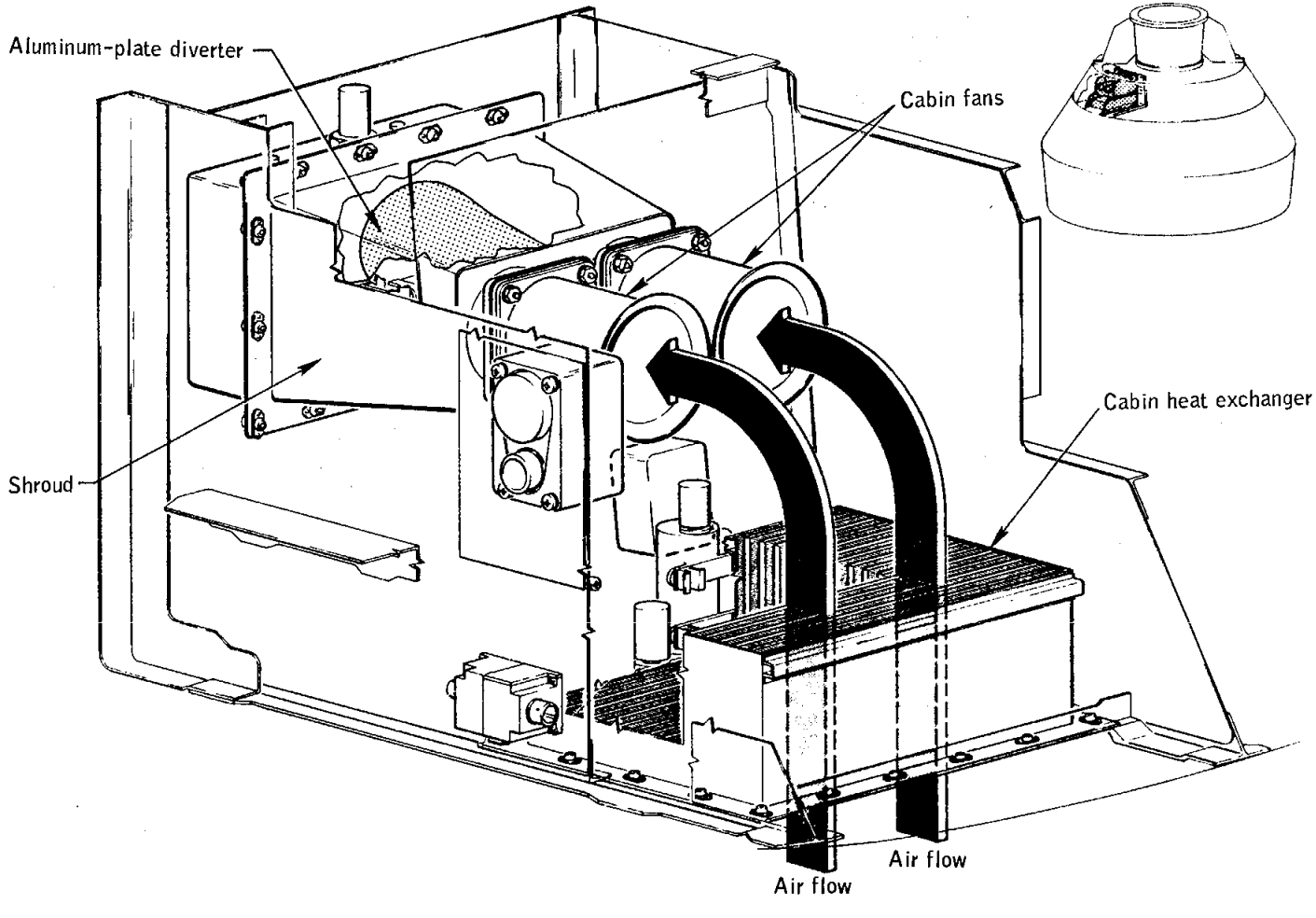

Figure 12-3.- Cabin fan installation.

NASA-S-69-710

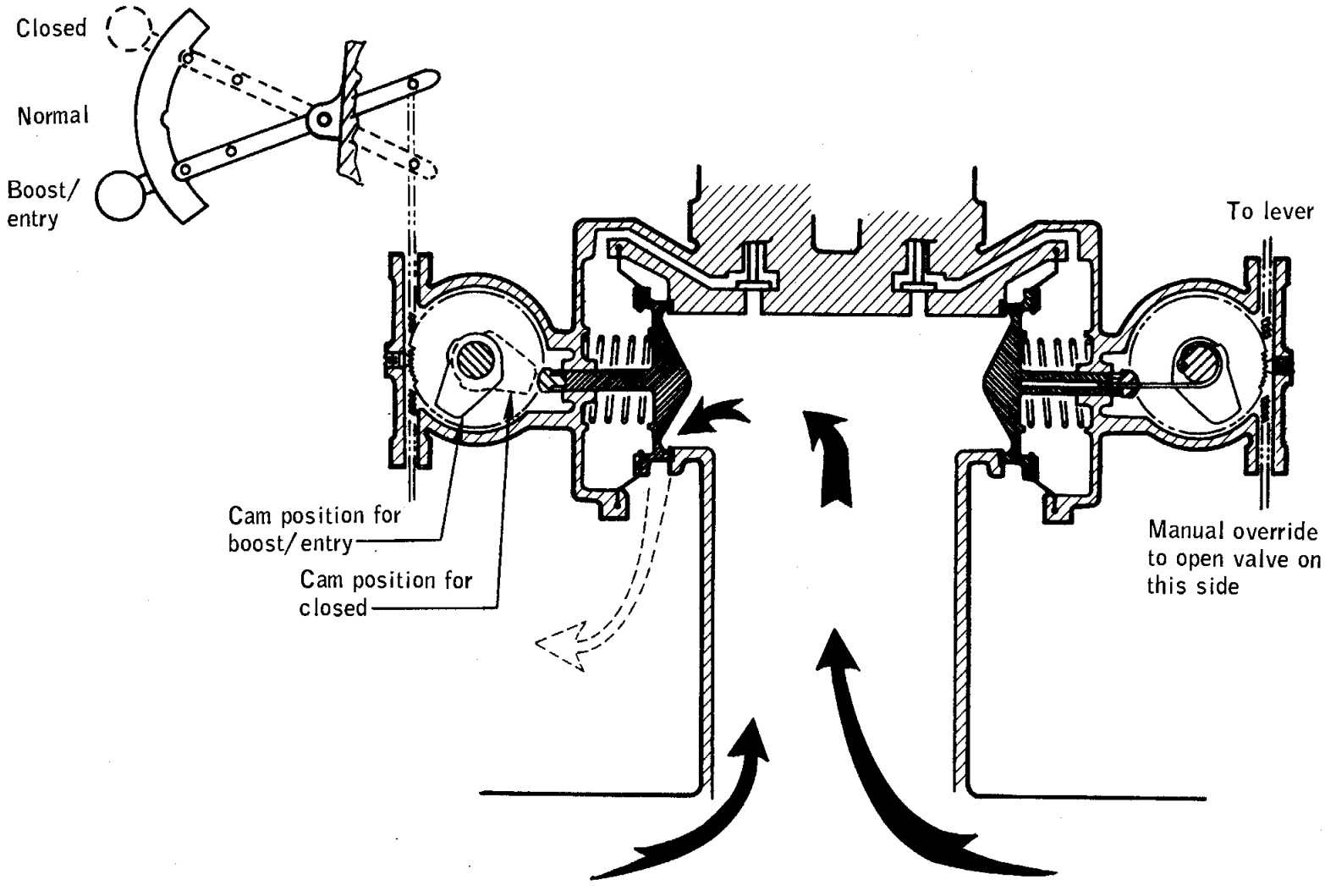

Figure 12-4.- Cabin pressure relief valve.

NASA-S-69-711

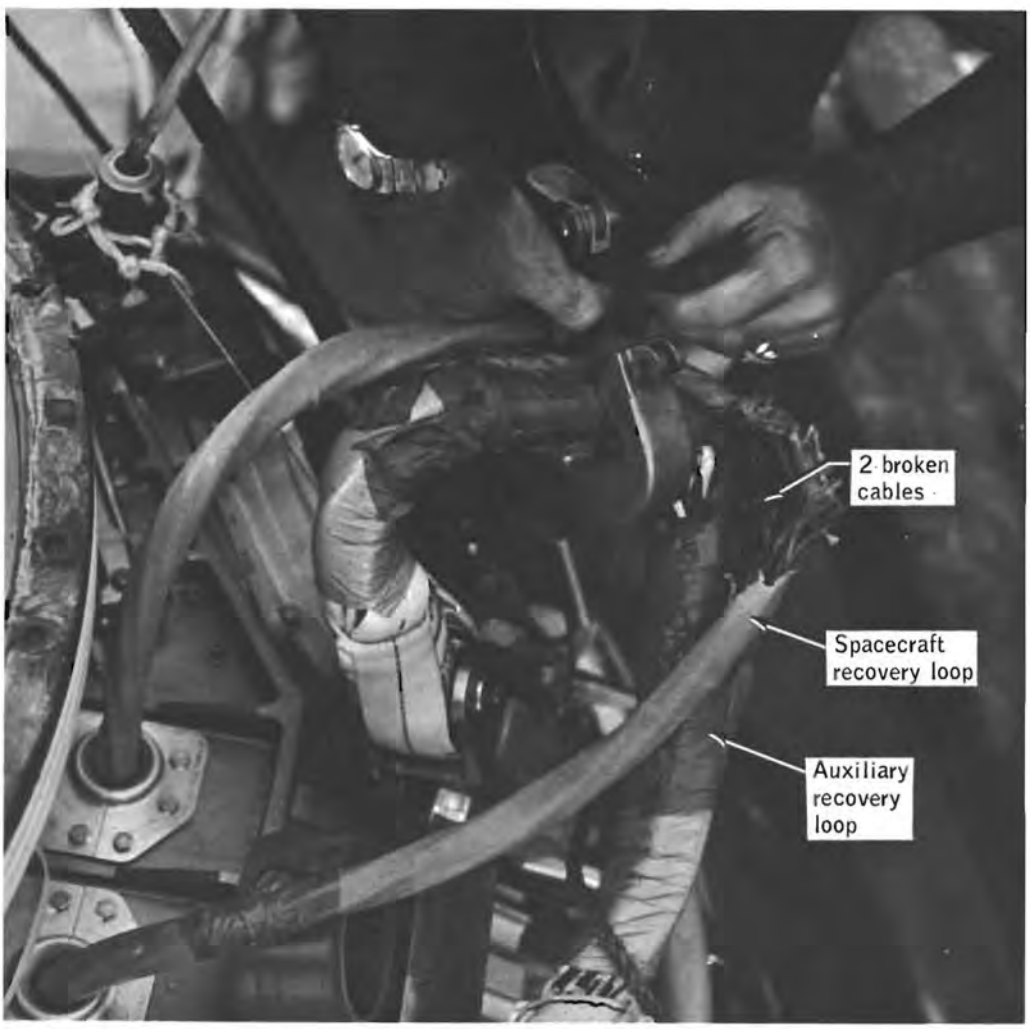

Figure 12-5.- Broken cables in spacecraft recovery loop.

NASA-S-69-712

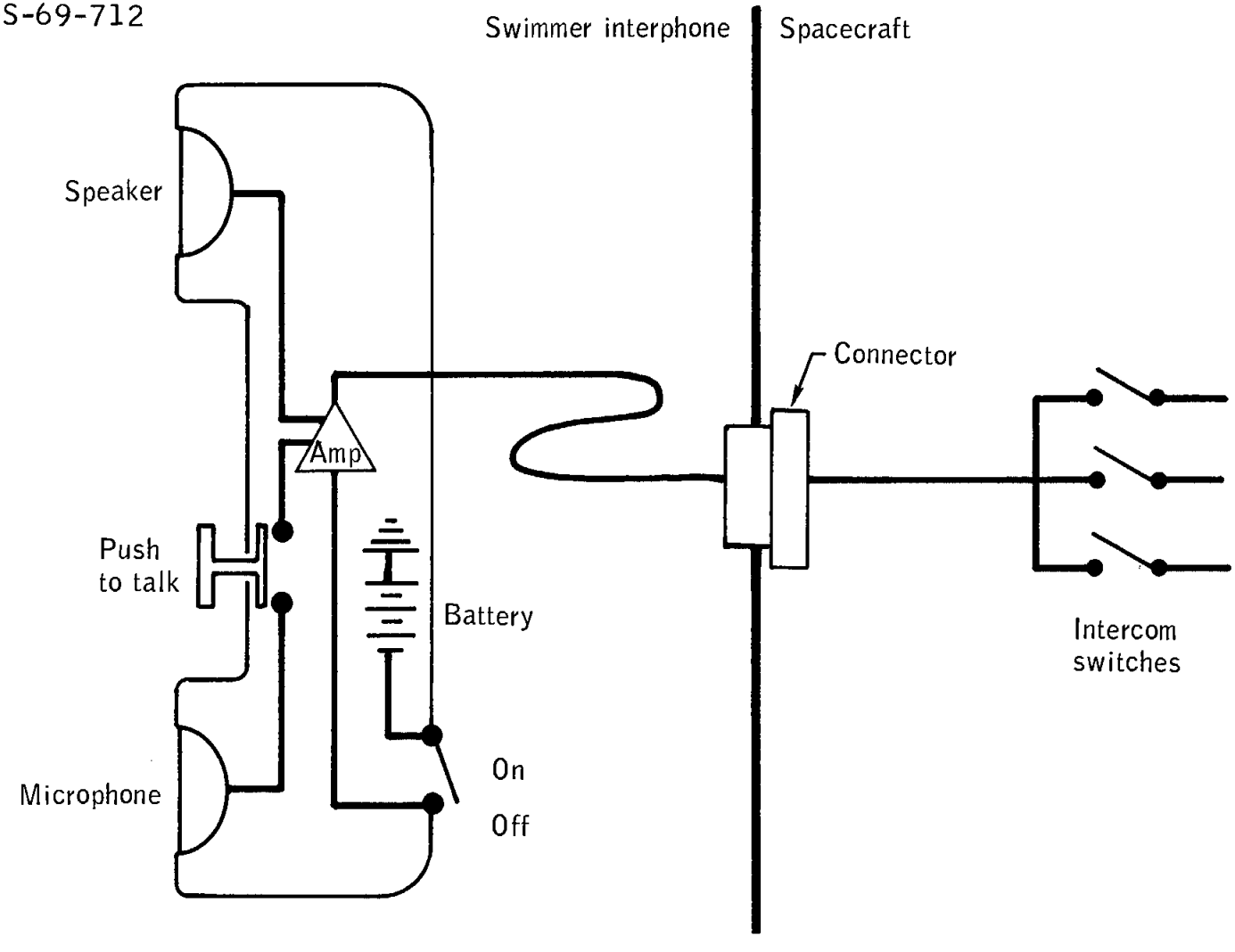

Figure 12-6.- Swimmer interphone.

NASA-S-69-713

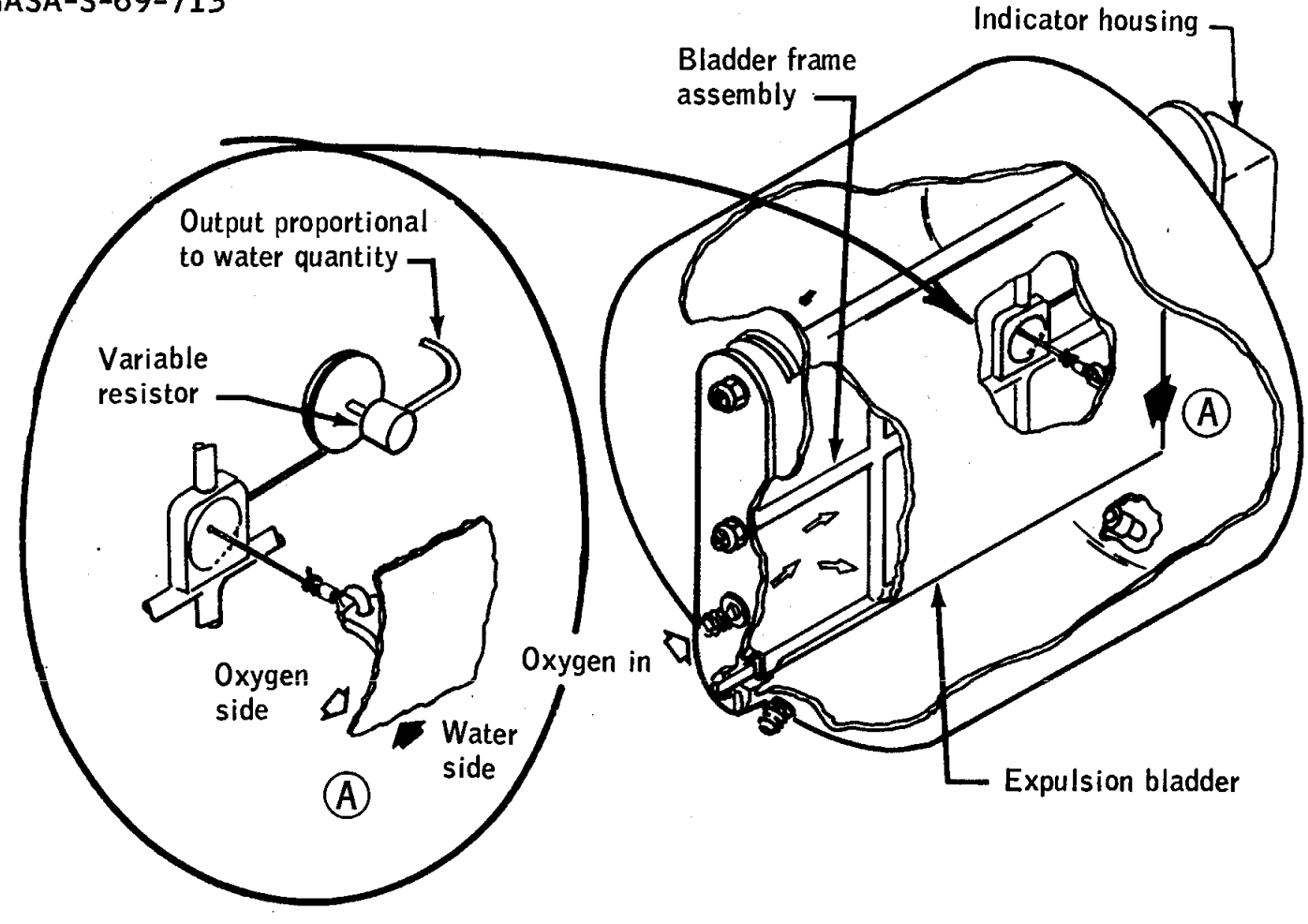

Figure 12-7.- Potable water tank.

NASA-S-69-714

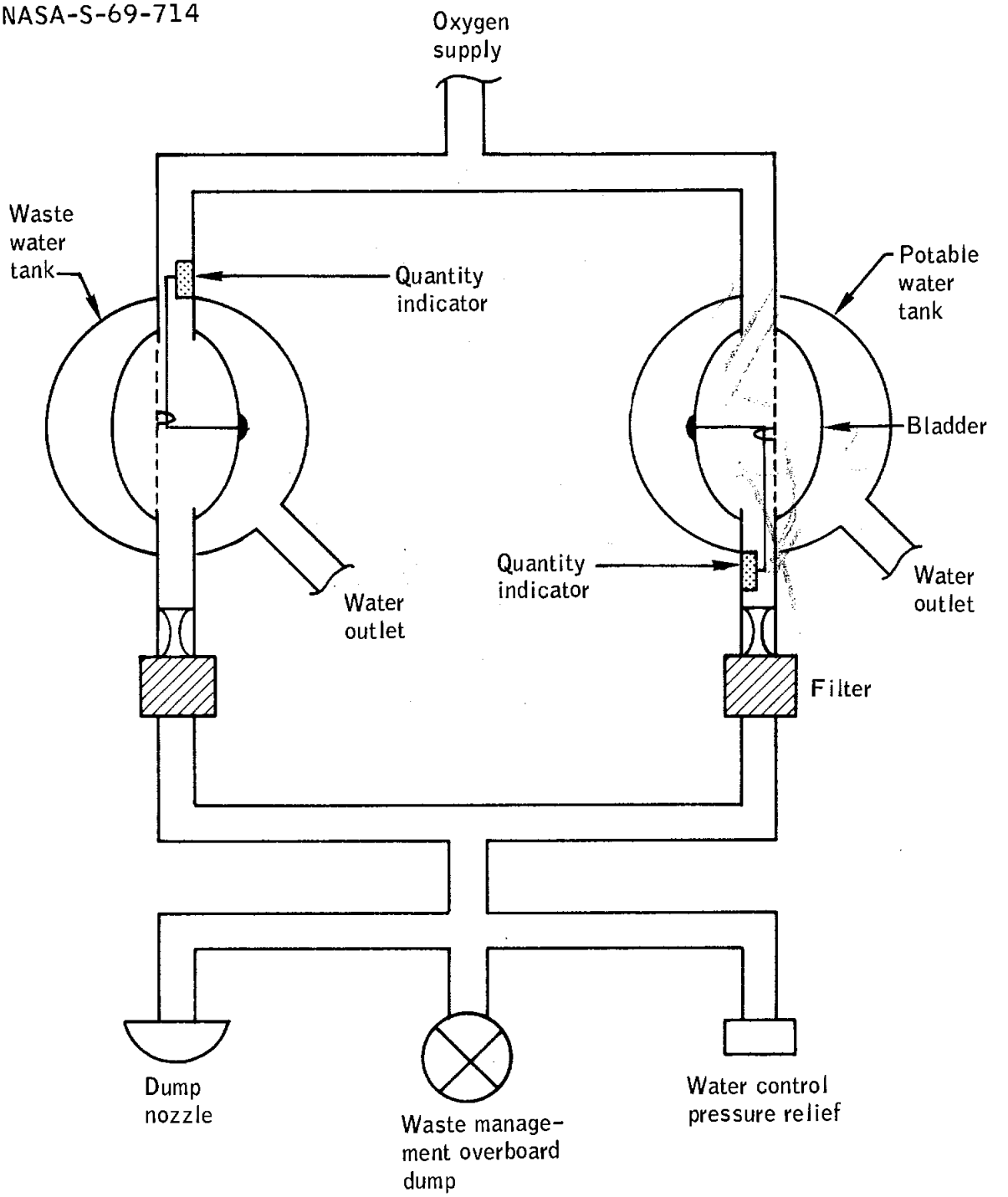

Figure 12-8.- Water tank pressurization system.

NASA-S-69-715

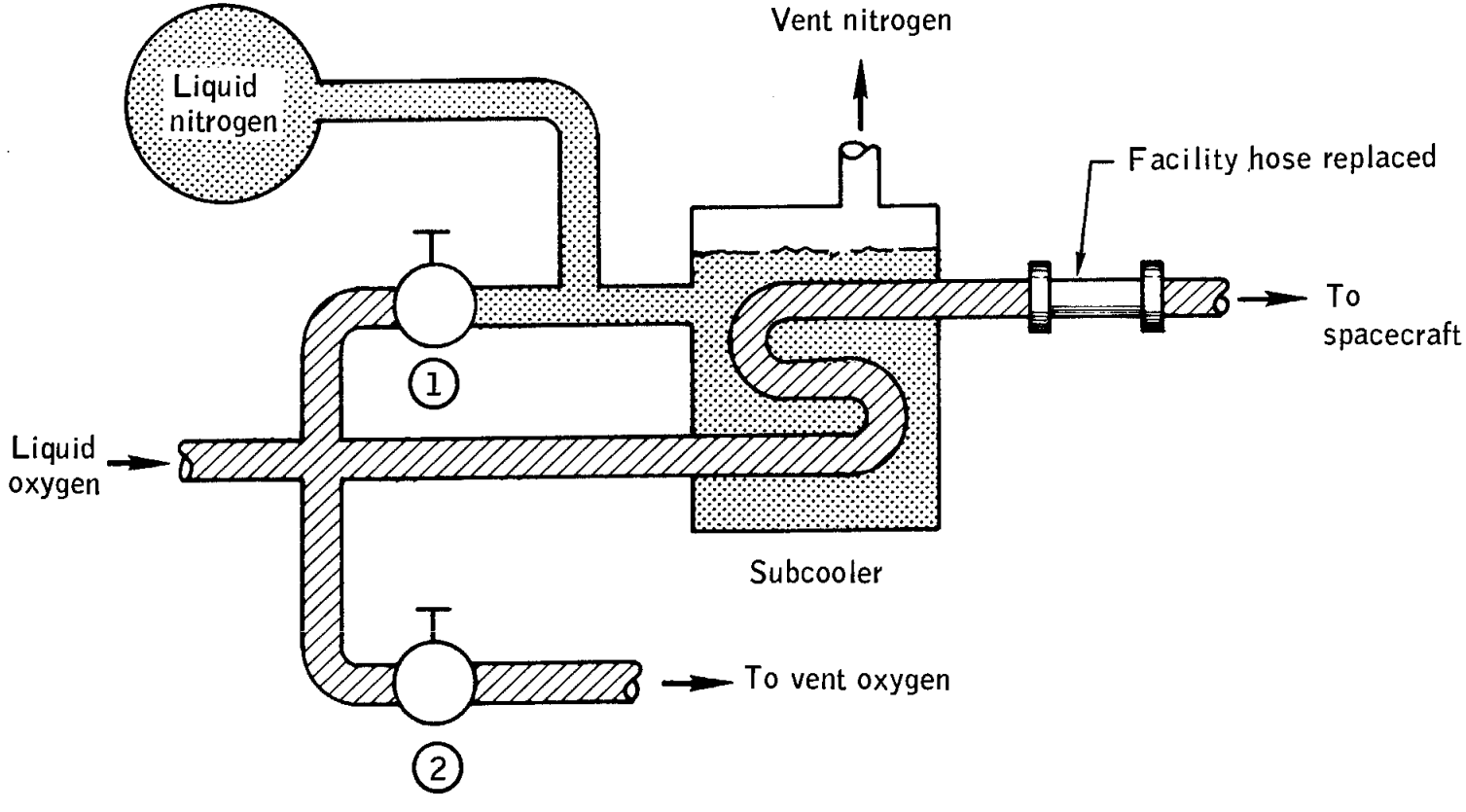

Note: Only valves pertinent to problem shown.

Figure 12-9.- Simplified schematic of cryogenic oxygen servicing unit.

13.0 CONCLUSIONS

The Apollo 8 mission, the most successful of the Apollo Program, was a bold step forward in the development of lunar landing capability. Based on the results and observations of this mission, the following conclusions are drawn from the information contained in this report.

1. The command and service module systems are operational for manned lunar flight.

2. All system parameters and consumable quantities were maintained well within their design operating limits during both cislunar and lunar-orbit flight.

3. Passive thermal control, which uses a slow rolling maneuver perpendicular to the sun line, was a satisfactory means of maintaining critical temperatures near the middle of the acceptable response ranges.

4. The navigation techniques developed for translunar and lunar-orbit flight were proved to be more than adequate to maintain required lunar-orbit-insertion and transearth-injection guidance accuracies.

5. Non-simultaneous sleep periods adversely affected the normal circadian cycle of each crew member and provided a poor environment for undisturbed rest. Flight activity scheduling for the lunar orbit coast phase also did not provide adequate time for required crew rest periods.

6. Communications and tracking at lunar distances were excellent in all modes. The high-gain antenna, flown for the first time, performed exceptionally well and withstood dynamic structural loads and vibrations which exceeded anticipated operating levels.

7. Crew observations of the lunar surface showed the "washout" effect (surface detail being obscured by backscatter) to be much less severe than anticipated. In addition, smaller surface details were visible in shadow areas at low sun angles, indicating that lighting for lunar landing should be photometrically acceptable.

8. To accommodate the change in Apollo 8 from an earth orbital to a lunar mission, preflight mission planning, crew training, and ground support reconfigurations were completed in a time period significantly shorter than usual. The required response was particularly demanding on the crew and, although not desireable on a long-term basis, exhibits a capability which had never been demonstrated.

A.0 SPACE VEHICLE DESCRIPTION

The Apollo 8 space vehicle comprised a block II configuration Apollo spacecraft (no. 103) and a Saturn V launch vehicle (SA-503). The spacecraft consisted of a launch escape system, command module, service module, spacecraft/launch-vehicle adapter, and lunar module test article. The launch vehicle consisted of S-IC, S-II, and S-IVB stages and an instrument unit. The Apollo 8 spacecraft was similar in configuration to the Apollo 7 spacecraft and the launch vehicle was similar to the Apollo 6 configuration; therefore, only the major changes are discussed in the following sections.

A.1 COMMAND AND SERVICE MODULES

A.1.1 Structures

The major changes to the command and service module structures are discussed in the following paragraphs.

Command module.- The most significant change to the command module structure was the replacement of the forward pressure and ablative hatches with the combined forward hatch (fig. A.1-1), which will be required on later missions for intravehicular transfer to the lunar module. This change resulted in the inclusion of the command module tunnel area as part of the pressure vessel. To provide more free space for intravehicular activity, all three couches in the Apollo 8 command module could be folded, whereas no couches were foldable for Apollo 7.

Lockouts were added in the impact-attentuation system for the couch struts (fig. A.1-2) and the associated strut-load/stroke criteria were modified (fig. A.1-3) to permit a lower landing deceleration threshold.

Service module.- The service-module aft bulkhead was strengthened to assure a 1.4 safety factor for Saturn V powered flight loads. The tension ties between the service module and the command module were increased in thickness from 0.135 to 0.153 inch (fig. A.1-4).

A.1.2 Emergency Detection System

The emergency detection system for Apollo 8 was nearly identical to that flown on Apollo 6. The major differences included the capability for a redundant display of launch vehicle attitude-reference failure during S-IC (first-stage) powered flight. Also, a means was provided in the

instrument unit and S-IVB stage to bypass the emergency cutoff command resulting from spacecraft/launch-vehicle separation to permit a second S-IVB ignition in the event of an early separation.

A.1.3 Communications System

The major change from the Apollo 7 communications system configuration was the addition of a high-gain S-band antenna (fig. A.1-5) to accommodate transmission and reception at lunar distances. The antenna is spring-loaded against one of the adapter panels and is deployed at panel jettison. The system is made up of a four-parabolic-dish and feed-horn array and is capable of transmission in three beam width modes and reception in two. In wide beam mode, the feed horns, located in the center of the array, are used for reception and transmission. In the medium beam mode, one of the four parabolic reflectors is used for transmission and all four are used for reception. In the narrow beam mode, all four dish reflectors are used for transmission and reception. The gains and beam widths associated with each mode are listed.

Mode	Gain, dB	Beam width, deg
Wide - Transmit	9.2	40
Receive	3.8	40
Medium - Transmit	20.7	11.3
Narrow - Transmit	26.7	3.9
Receive	23.3	4.5

The high-gain antenna can be operated both manually and automatically in acquiring and maintaining signal lock with earth-based stations. Figure A.1-3 shows the antenna in both the stowed and deployed position, as well as a schematic indicating internal electronic functions. An electronics unit, located in the service module, provides servo-drive signals to orient the antenna based on either manual or S-band signal-strength commands. The service module electronics unit uses position feedback from the antenna boom to generate the proper servo commands, and the S-band auto-acquisition commands are derived from standard onboard communications equipment. In the manual mode, the controls, position readouts, and signal-strength meter are located on main display console 2 to provide a means of positioning the antenna for maximum signal strength before switching to an automatic tracking configuration.

A.1.4 Environmental Control System

The environmental control system for Apollo 8 was modified only slightly from the Apollo 7 configuration. The primary and secondary evaporators now have wicks of increased thickness to improve the contact between the wicks and fins in the core stacks.

The pressure regulator for waste and potable water tanks and the glycol reservoir was modified to incorporate a reduced elastomer thickness and a rounded valve-seat edge to prevent sticking of the relief valve poppets.

The carbon dioxide absorber-elements housings were changed from stainless steel to polyester-coated aluminum for weight saving, and the quantity of activated charcoal was increased by 50 percent to provide improved odor-removal capability.

The suit hose connectors had an increased mechanism friction and loaded check valves in the OFF position to provide improved position retention and a more positive seal.

The revised flow-proportioning valve incorporated machined instead of cast motor-pole pieces and redesigned flexure tubes to provide improved component integrity and reliability.

A.1.5 Guidance, Navigation, and Control System

The guidance, navigation, and control system hardware was modified in two respects. In the optical system, a sun filter was added to the scanning telescope to permit solar sightings in the event of poor star visibility, and a camera adapter was installed on the sextant to permit photography of celestial bodies and landmarks. A second hardware change was incorporated into the stabilization and control system to permit switch isolation of a single reaction control system thruster.

Two changes in stored information were required as a result of the lunar mission. The computer program used for the Apollo 7 earth-orbital flight was replaced with a lunar flight version, and the entry-monitor-system scroll was modified for the higher lunar-return entry velocities.

A.1.6 Service Propulsion System

The major modifications to the service propulsion system were the substitution of a ball valve which would accommodate a lower predicted

temperature environment, the use of flow dividers in the retention reservoir to eliminate a dynamic bias in the gaging system, and the deactivation of the flight combustion stability monitor.

A.1.7 Reaction Control System

The major change to the service module reaction control system was the addition of look-angle blankets to provide thermal protection from service module structural members. In the command module reaction control system, an onboard capability for crew monitoring of helium tank temperature was provided. In addition, holes were added to the Teflon pads on propellant tanks to permit rapid helium depressurization.

A.1.8 Instrumentation System

The instrumentation system in the Apollo spacecraft is divided into two types, operational and flight qualification. The operational instrumentation for Apollo 8 was essentially the same as for Apollo 7, except in the bioinstrumentation. The input connectors and instrumentation leads in the bioharness were redesigned to provide improved reliability. The pin connectors at the bioharness disconnect were eliminated, a more flexible harness material was used, and a silicone-rubber strain-relief cuff was added at the signal conditioner input.

In addition, a nuclear particle detection system and a Van-Allen-belt dosimeter were added to the telemetry system to accomodate the cislunar radiation environment.

The flight qualification instrumentation was modified to reflect the different flight objectives for Apollo 8. Two proportional-bandwidth voltage controlled oscillators were installed in addition to the flight qualification recorder and were used to monitor acceleration, vibration, and flight loads associated with the spacecraft and the spacecraft/launch-vehicle adapter. The number of measured parameters and their recorder assignments are noted in figure A.1-6.

A.1.9 Crew Provisions

The only changes to the crew provisions were the items discussed in the following paragraphs.

Two medical accessories kits were flown in Apollo 8, whereas only one was flown on Apollo 7. One kit was basically the same as that flown on Apollo 7 with the exception of a new type of pain pill; also, a complete spare biomedical harness was provided instead of spare sensors.

The second medical accessories kit was new and included additional medications.

The metering water dispenser incorporated an ethylene-propylene O-ring in place of the neoprene unit used on Apollo 7, and the change eliminated the chlorine contamination problem.

The constant wear garments were modified to include a keeper strap for the lightweight headset.

The oxygen mask and hose assemblies incorporated an improved swivel fitting and fluorel hoses in place of the silicone-rubber hoses.

Heel restraint and head support pads were added.

The configurations of the space suits were identical to those worn by the Apollo 7 crew with the exception of the following items:

a. A foldable neck dam, stowed in a suit pocket, was provided in place of the hard-ring neck dams.

b. The suits worn by the Commander and by the Lunar Module Pilot incorporated intravehicular cover layers over extravehicular pressure-garment assemblies.

The electrical umbilicals were fabricated utilizing a fluorel outer cover construction rather than the silicone used for Apollo 7.

The oxygen umbilicals contained tie wires to decrease the possibility of an oxygen leak.

Sleep restraints were modified to provide a more stable lower leg area by relocating the existing lower foot retention straps and installing an inner support within the lower portion of the enclosure.

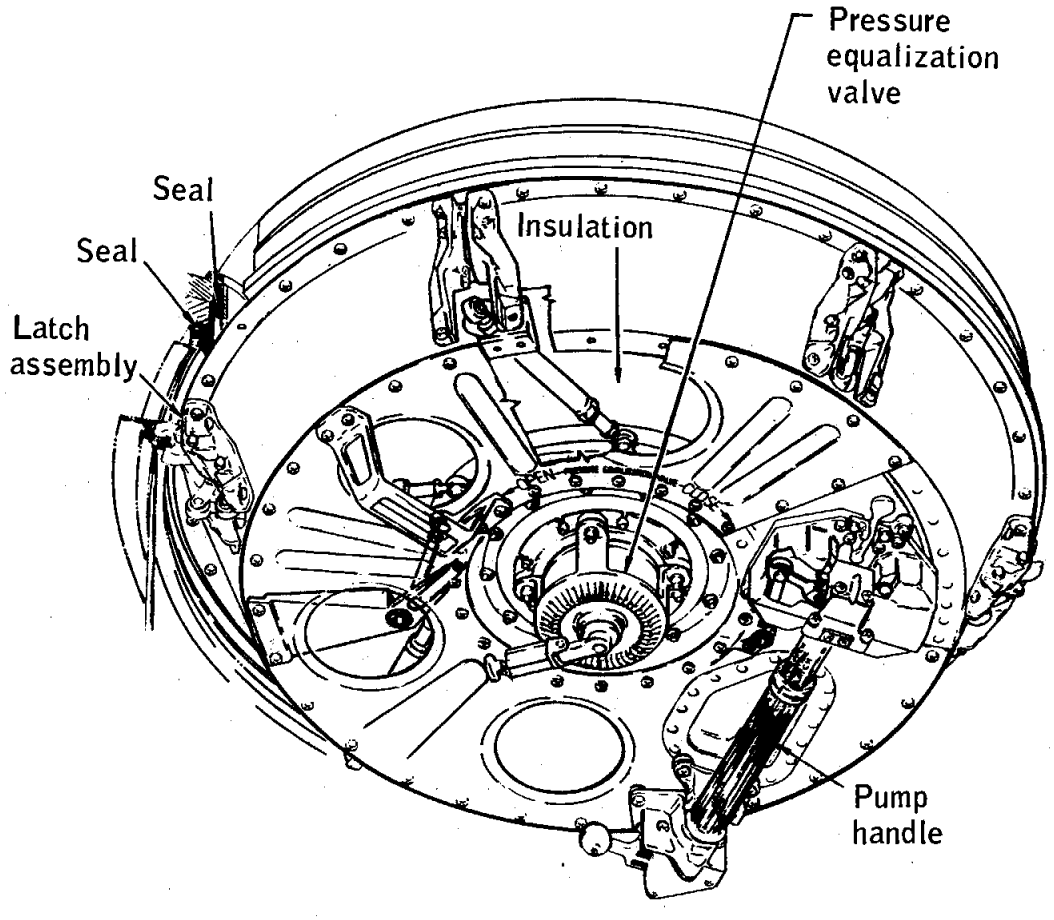

Figure A.1-1.- Combined tunnel hatch.

NASA-S-69-717

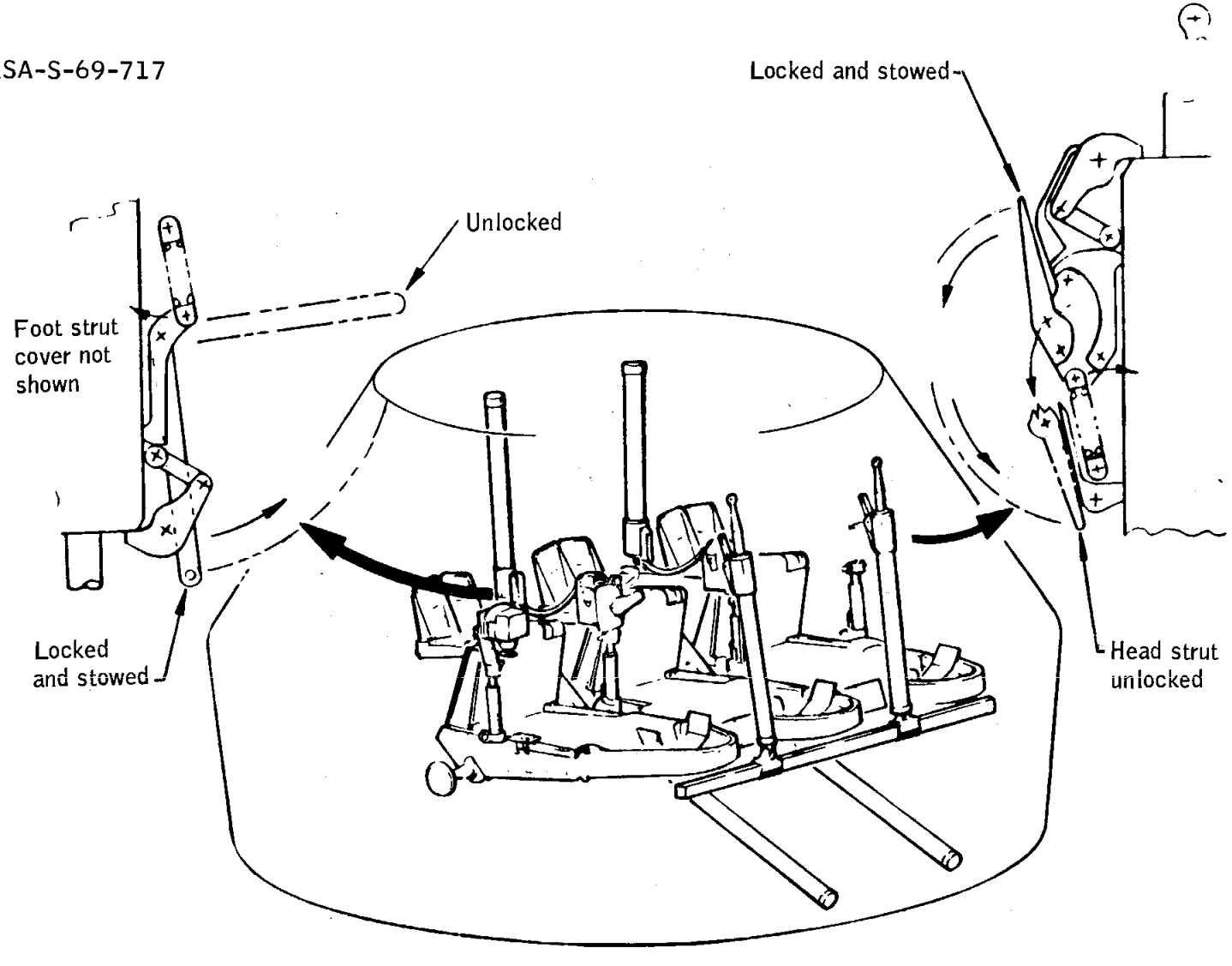

Figure A.1-2.- Crew couch struts and lockouts.

NASA-S-69-718

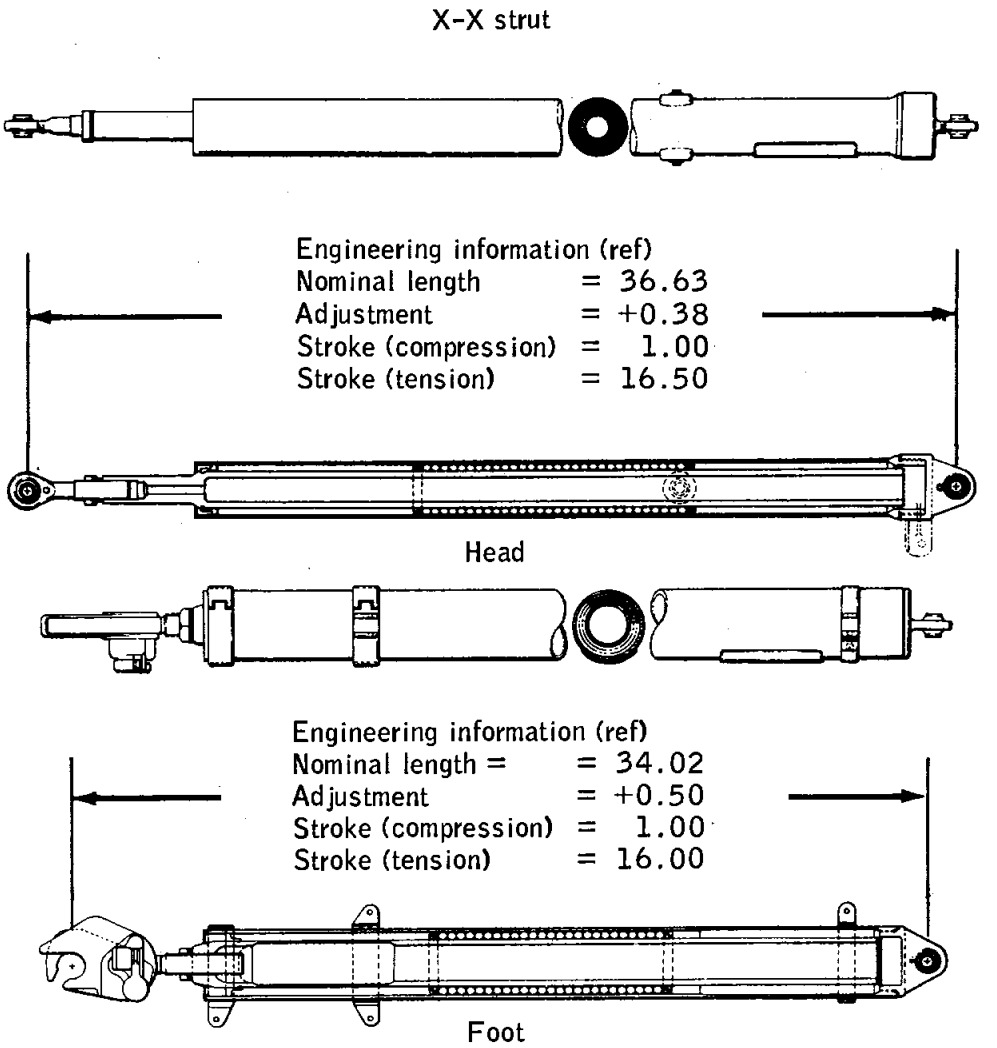

Figure A.1-3.- Landing-shock attenuation struts. (X-X typical)

NASA-S-69-719

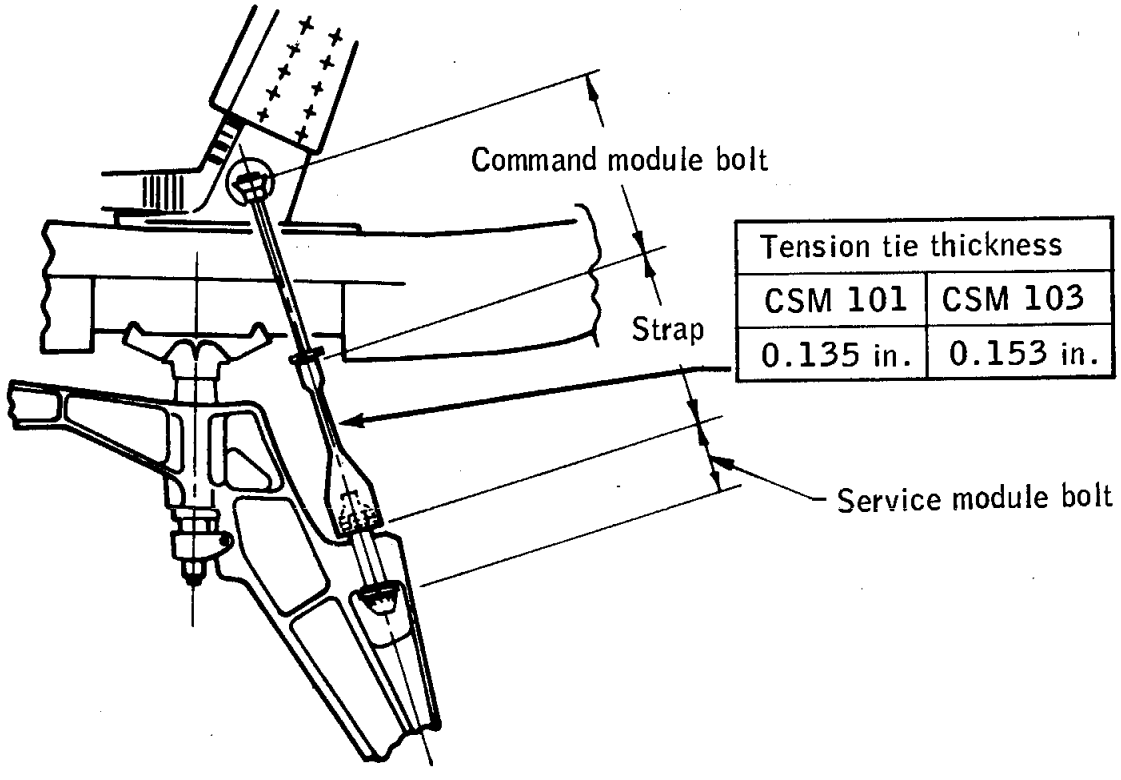

Figure A.1-4.- Block II tension tie.

NASA-S-69-720

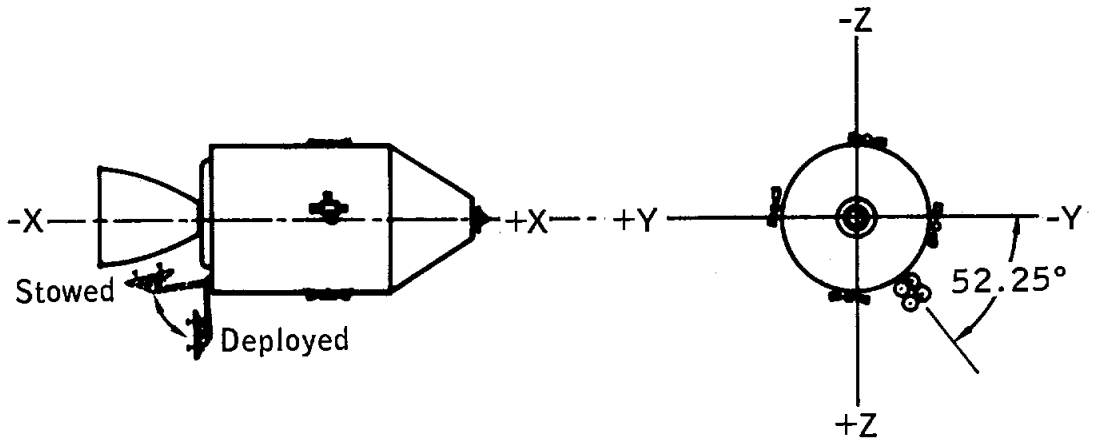

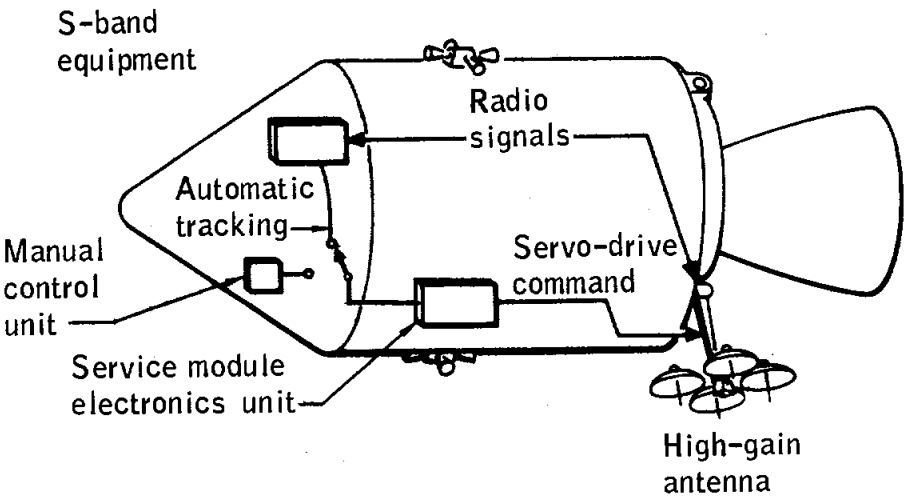

Figure A.1-5.- High-gain antenna

NASA-S-69-721

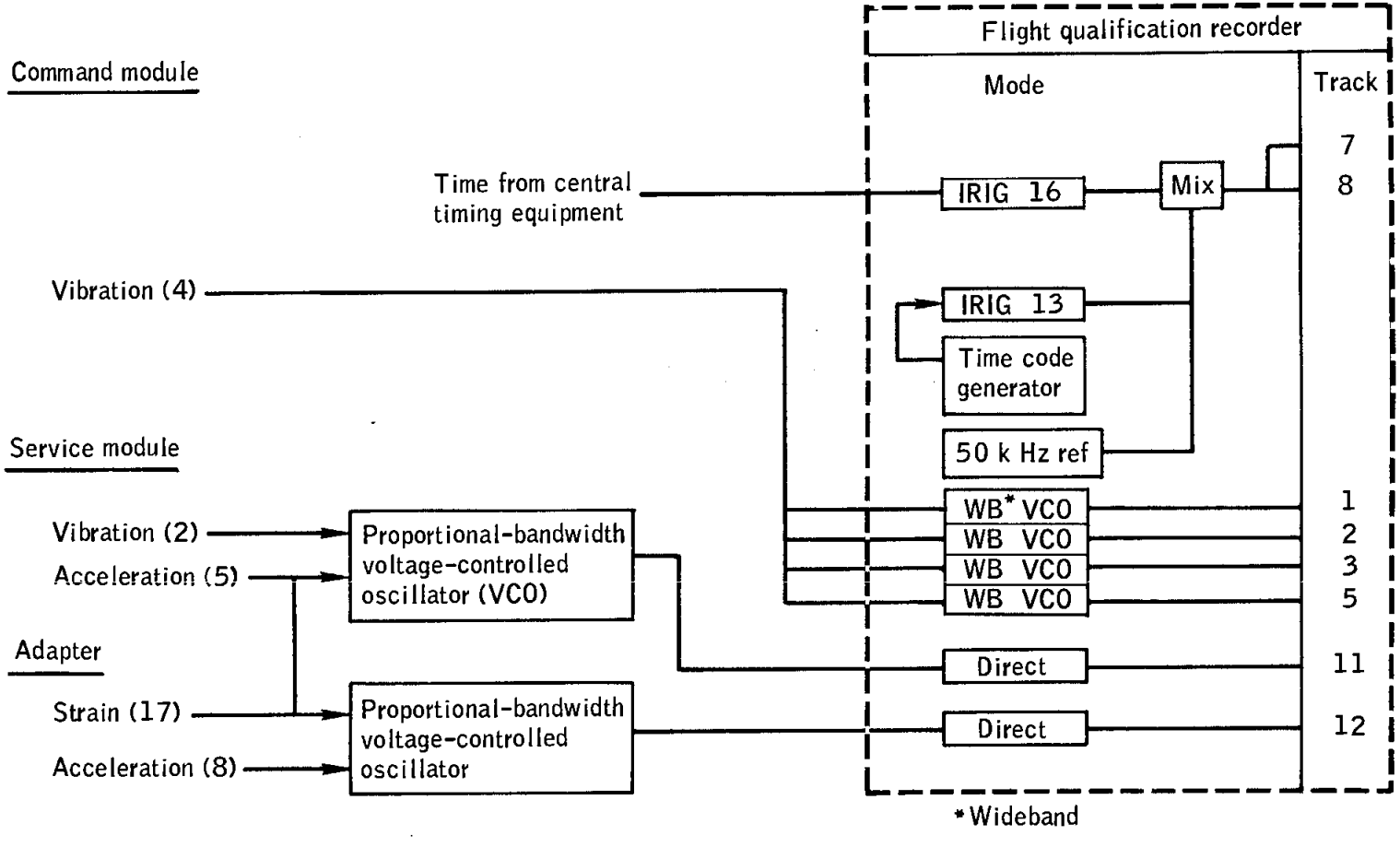

Figure A.1-6.- Flight-qualification instrumentation schematic.

A.2 LAUNCH ESCAPE SYSTEM

No major changes were made to the launch escape system.

A.3 SPACECRAFT/LAUNCH VEHICLE ADAPTER

Three significant changes were made to the spacecraft/launch vehicle adapter.

The panel-deployment mechanism was redesigned so that the panels would be jettisoned. This change involved the removal of the panel attenuation and retention systems, redesign of the hinges, and addition of spring thrusters for the panels (fig. A.3-1).

The lunar module support structure within the adapter was redesigned, and spring thrusters were added at the four support points to provide the necessary spacecraft separation force following transposition and docking with the lunar module. Because a functional lunar module was not flown in Apollo 8, these thrusters were not used, and the test article stowed at this location remained with the S-IVB stage.

The external skin of the adapter was covered with 0.03-inch cork to reduce the degradation effects of aerodynamic heating.

NASA-S-69-722

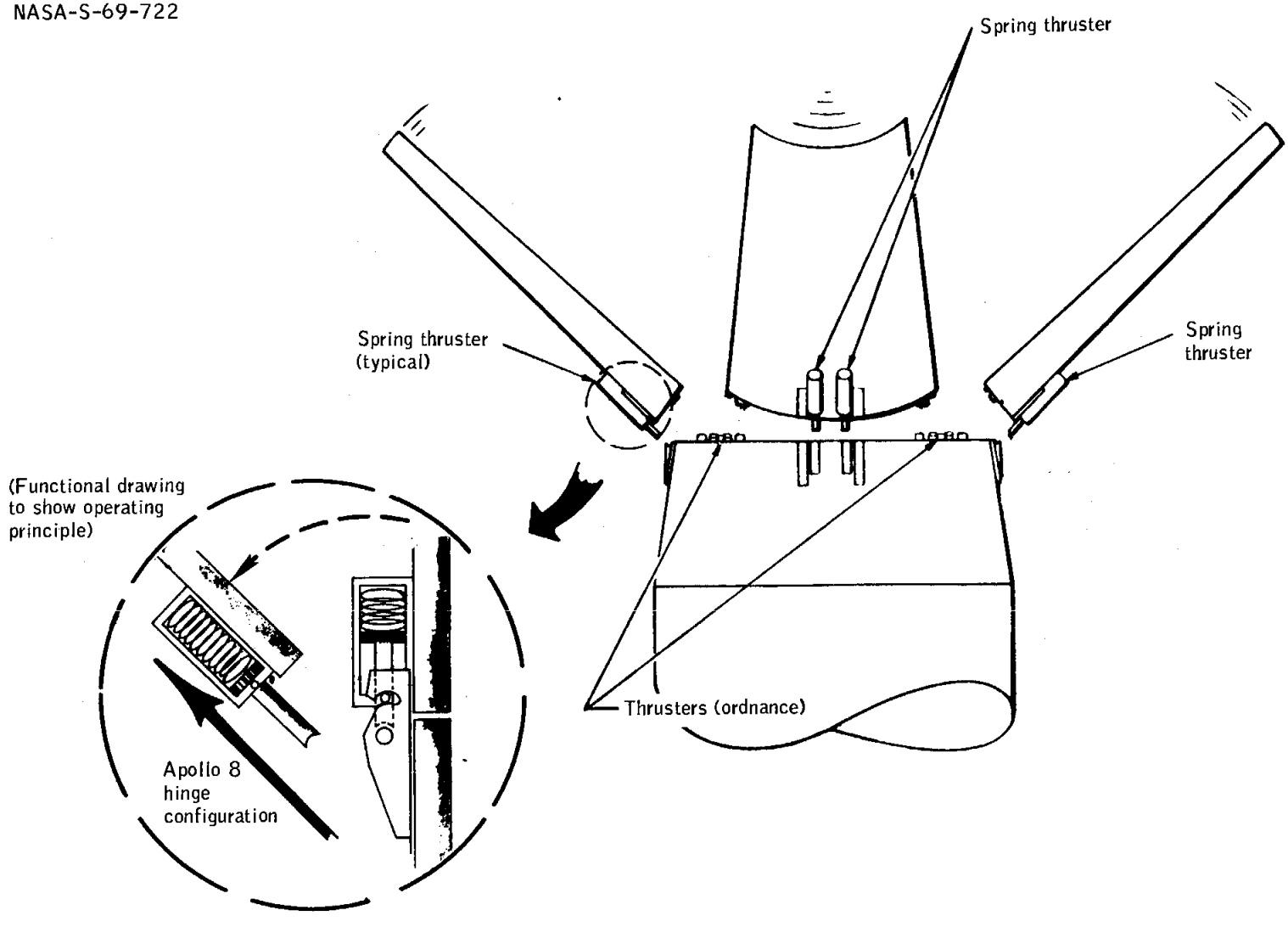

Figure A.3-1.- Adapter panel jettison system.

A.4 LAUNCH VEHICLE

The flight of Saturn V vehicle SA-503 was the third in a series of such vehicles, each of which carried a command and service module, and was the first to have a manned spacecraft. The configuration for the Apollo 8 mission was nearly identical to the SA-501 and SA-502 launch vehicles flown on Apollo 4 and Apollo 6, respectively. Some of the more significant changes from these first two missions are discussed in the following paragraphs.

In the S-IC (first) stage, the timed inboard-engine cutoff technique was the same as for Apollo 4, but the time was changed from 135 to 125.2 seconds after start of time-base 1. The outboard engines had an oxidizer-depletion cutoff, instead of the fuel-depletion cutoff on Apollo 6.

A modification was made in the S-IC stage to suppress the longitudinal thrust oscillation observed in Apollo 6. A system was installed to provide gaseous helium to a cavity in each of the liquid oxygen prevalves of the four outboard-engine suction lines. These gas-filled cavities act as a spring and serve to lower the natural frequency of the feed system and thereby prevent coupling between engine thrust oscillations and the first longitudinal mode of the vehicle structure.

Both the S-II and S-IVB stages employed an open-loop propellant utilization system for the first time on a Saturn V. In the S-II, the mixture shift was commanded by a switch selector by logic in the iterative guidance mode. The mixture ratio for the S-IVB engine was reduced from 5.5 to 5.0. The fuel and liquid-oxygen lines on the S-II and S-IVB stages were modified to reduce the possibility of propellant leak under dynamic load conditions and a vacuum environment.

In addition, the forward bulkhead on the S-II stage was changed to a lightweight configuration, and a non-propulsive liquid-oxygen vent system was added to the S-IVB to improve attitude control during orbital coast.

A.5 LUNAR MODULE TEST ARTICLE

For the Apollo 8 mission, a structural test article was installed in the spacecraft/launch vehicle adapter area for Saturn V flight-load evaluation. This module, termed lunar module test article B (LTA-B), weighed 19 900 pounds and is shown schematically in figure A.5-1. The LTA-B was instrumented to measure accelerations about all three axes.

NASA-S-69-723

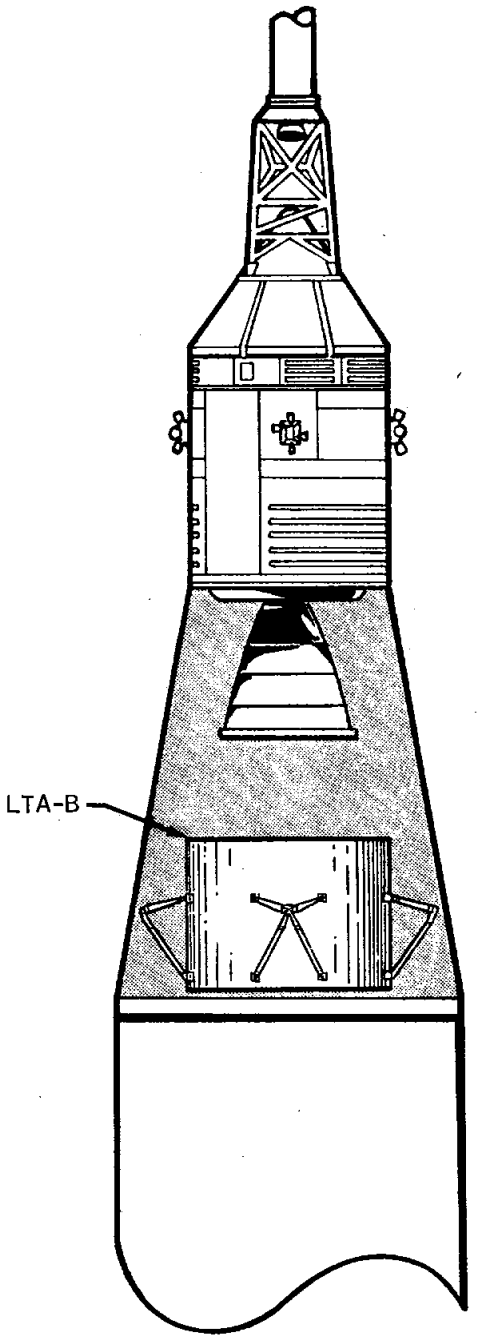

Figure A.5-1.- Lunar-module test article (LTA-B).

A.6 MASS PROPERTIES

Spacecraft mass properties for the Apollo 8 mission are summarized in table A.6-I. These data represent the conditions as determined from postflight analyses of expendable loadings and usage during the flight. Variations in spacecraft mass properties are determined for each significant mission phase from lift-off through landing. Expendables usage is based on reported real-time and postflight data presented in other sections of this report. The weights and centers of gravity of the individual command and service modules were measured prior to flight, and the inertia values were calculated. All changes incorporated after the actual weighing were monitored, and the spacecraft mass properties were updated. Spacecraft mass properties at lift-off did not vary significantly from the preflight predicted values.

TABLE A.6-I.- SPACECRAFT MASS PROPERTIES

Event	Weight, lb	Center of gravity, in.			Moment of inertia, slug-ft^2			Product of inertia, slug-ft^2		
		X_A	Y_A	Z_A	I_{XX}	I_{YY}	I_{ZZ}	I_{XY}	I_{XZ}	I_{YZ}
Lift-off	96 272	882.1	2.7	4.4	67 891	942 574	944 801	1195	5305	3282
Earth orbit insertion	87 382	839.9	2.9	4.8	67 032	550 852	553 126	3312	8022	3261
Translunar injection	87 377	839.9	2.9	4.8	67 030	550 835	553 116	3307	8004	3265
Spacecraft/S-IVB separation	63 524	933.6	4.0	6.5	34 119	78 007	80 652	-1176	-110	3170
First midcourse correction	63 307	933.6	4.0	6.5	34 119	78 017	80 666	-1785	-102	3172
Translunar coast	63 141	933.6	4.0	6.5	34 033	75 625	78 344	-1744	-93	3147
Second midcourse correction	62 845	933.6	4.1	6.4	33 955	75 530	78 269	-1750	-96	3182
Lunar orbit insertion	62 827	933.6	4.1	6.4	33 952	75 543	78 278	-1756	-83	3184
Lunar orbit coast	46 743	942.3	4.3	4.8	25 631	61 276	70 892	-1798	580	878
Lunar orbit circularization	46 716	942.3	4.3	4.8	25 629	61 281	70 897	-1800	583	878
Lunar orbit coast	46 068	943.6	4.3	4.7	25 292	59 653	69 549	-1809	679	785
Transearth injection	45 931	943.6	4.4	4.6	25 251	59 584	69 497	-1807	664	802
Transearth coast	32 100	949.1	1.1	5.9	18 290	56 168	60 083	-1424	523	-48
Third midcourse correction	32 008	949.2	1.1	5.9	18 273	56 145	60 066	-1431	531	-40
Transearth coast	31 968	949.2	1.1	5.9	18 272	56 145	60 065	-1431	530	-40
Command module/service module separation	31 768	949.4	1.2	5.8	18 237	56 119	60 042	-1460	574	-20
Command module after separation	12 179	1041.0	-0.1	5.7	5 750	5 074	4 597	54	-398	-8
Entry interface (400 000 feet)	12 171	1041.0	-0.1	5.7	5 743	5 069	4 595	53	-396	-7
Mach 10	12 035	1041.3	-0.1	5.6	5 653	4 973	4 511	52	-391	-3
Drogue deployment	11 712	1040.0	-0.1	5.7	5 579	4 745	4 293	53	-371	-1
Main parachute deployment	11 631	1039.6	-0.1	5.9	5 563	4 686	4 251	53	-346	-1
Landing	10 977	1037.9	0.0	4.9	5 372	4 287	3 945	47	-317	11

B.0 SPACECRAFT HISTORY

The history of spacecraft 103 operations at the manufacturer's plant, Downey, California, is shown in figure B-1. The spacecraft history after arrival at the Kennedy Space Center, Florida, is shown in figure B-2.

NASA-S-69-724

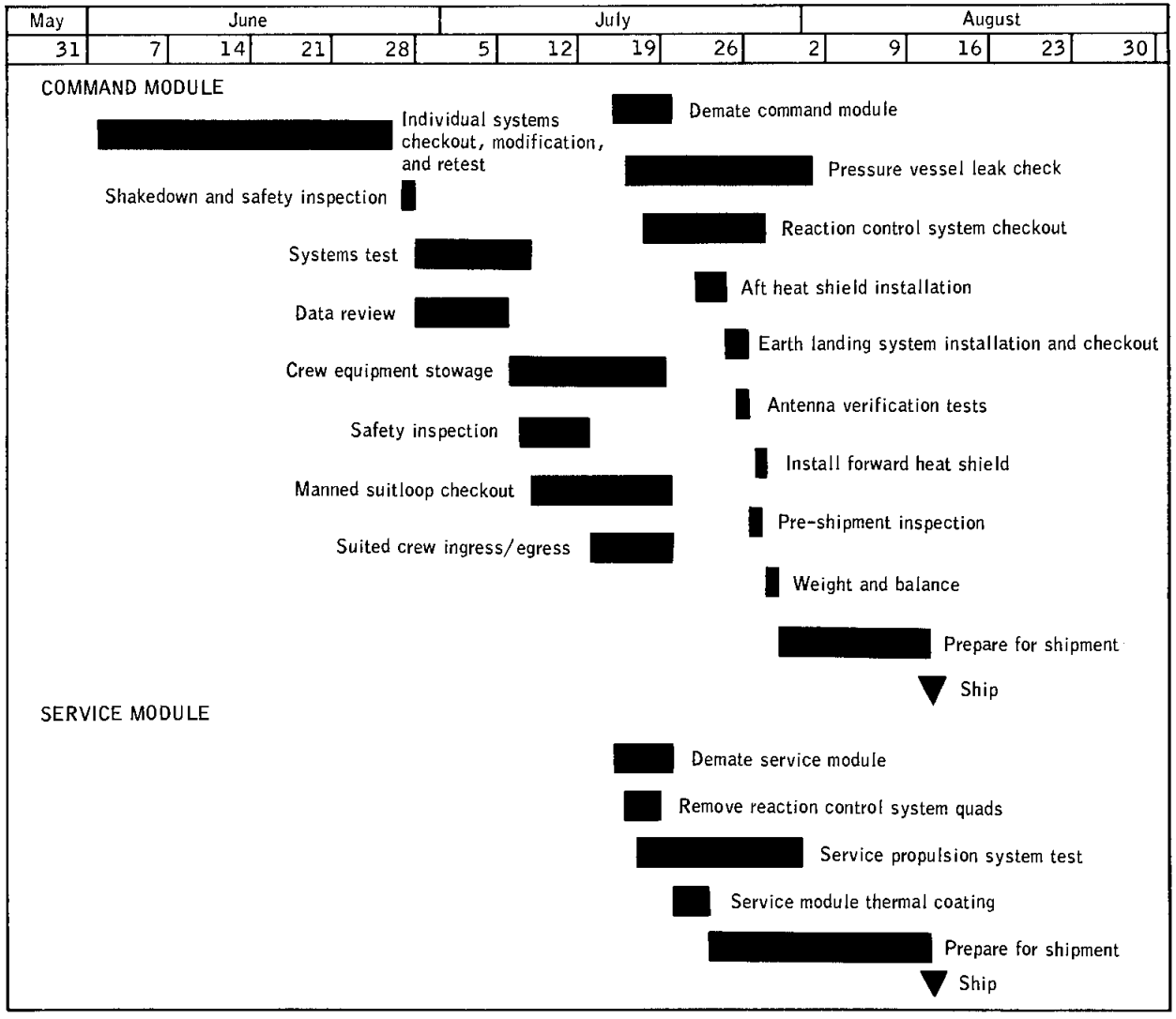

Figure B-1.- Factory checkout flow for command and service modules at contractor facility.

NASA-S-69-725

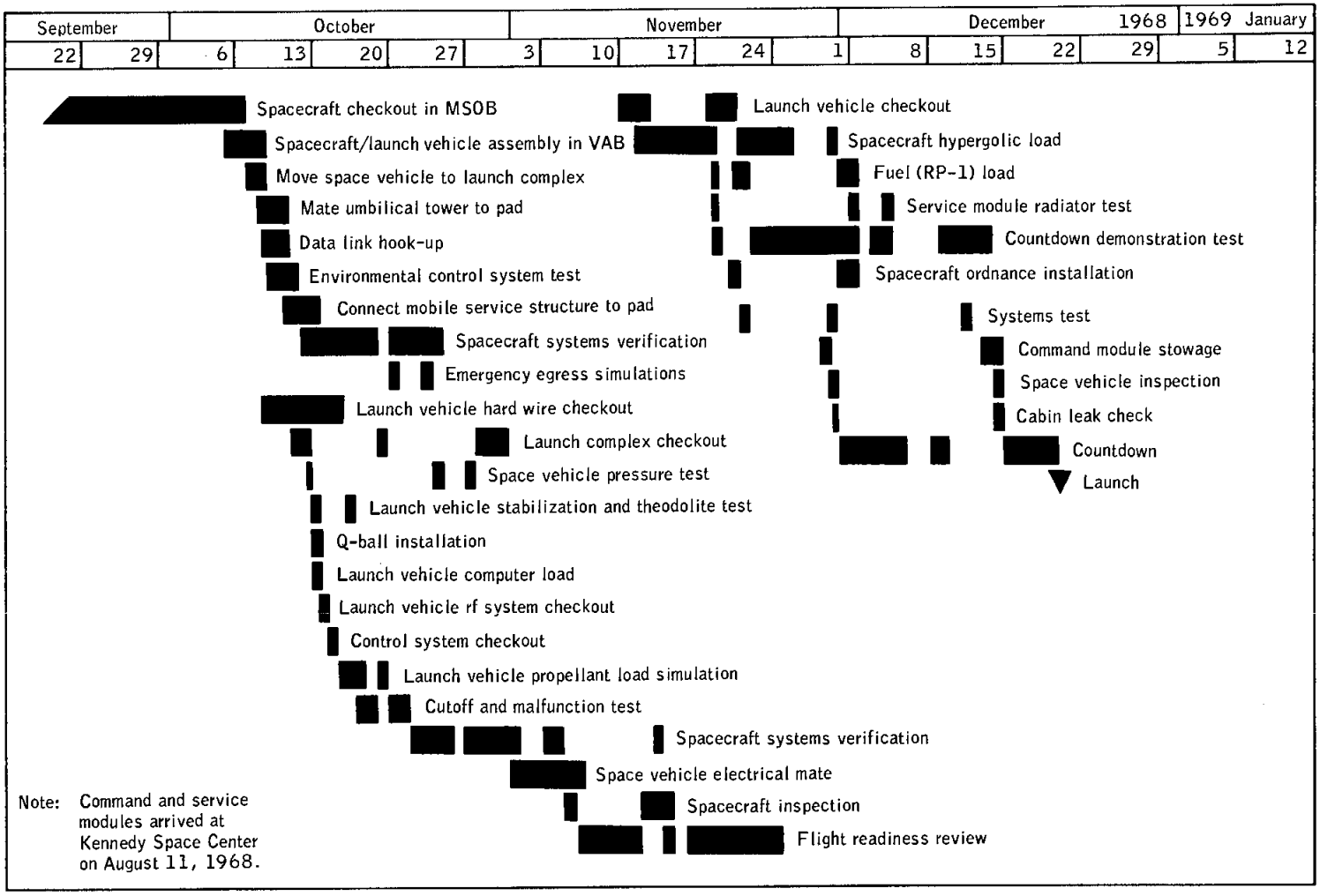

Figure B-2.- Spacecraft checkout history at Kennedy Space Center.

C.0 POSTFLIGHT TESTING

The command module arrived at the contractor's facility in Downey, California, on January 2, 1969, after reaction control system deactivation and pyrotechnic safing in Hawaii. Postflight testing and inspection of the command module for evaluation of the inflight performance and investigation of the flight irregularities were conducted at the contractor's and vendor's facilities and at the MSC in accordance with approved Apollo Spacecraft Hardware Utilization Requests (ASHUR's). The tests performed as a result of inflight problems are described in table C-I and discussed in the appropriate systems performance sections of this report. Tests being conducted for other purposes in accordance with other ASHUR's and the basic contract are not included.

TABLE C-I.- POSTFLIGHT TESTING SUMMARY

ASHUR no.	Purpose	Tests performed	Results
		Environmental Control	
103012	To determine cause for preflight calibration shift of water/glycol secondary pump outlet pressure measurement	Transducer calibration checked in command module and removed for vendor failure analysis	In-place calibration verified shift
103013	To investigate cabin fan noise reported by crew	Fan noise level measured in command module; fans removed, inspected, and power consumption tests performed	Fan connectors reversed; no other abnormal conditions
103015	To perform failure analysis of primary radiator outlet temperature measurement	Transducer calibration checked in command module and removed for vendor analysis	Nominal operation during in-place calibration
103016	To determine cause of malfunction of potable water quantity indicator	Indicator system calibration checked in command module; tank removed for vendor failure analysis	Indicator showed 50 percent regardless of actual quantity; corrosion found on oxygen side of bladder and inside indicator housing; pulley and potentiometer frozen and cable broken; water found on potentiometer, affects resistance measurement and indicator
103025	To troubleshoot environmental control water/glycol mixing valve for cause of temperature undershoot	Valve removed with environmental control unit; vendor test to determine whether control valve was sticking or thermal dynamic response was normal	
103029	To investigate possibility of water ingestion through cabin pressure relief valve at landing	Valves were leak-checked and removed for teardown and inspection, linkage adjustment and detention inspection	Leakage within specification; linkage and detention from lock cam and control lever within specification
103030	To verify calibration of waste water tank quantity indicator	Calibration test performed in command module; returned to vendor for inspection for water	Normal operation; water found in gas system, same as in the potable water tank
		Communications	
103010	To investigate reported difficulties with lightweight headsets	Headsets subjected to electrical and mechanical performance checks	No abnormal conditions; mechanical configuration unacceptable to crew

TABLE C-I.- POSTFLIGHT TESTING SUMMARY - Continued

ASHUR no.	Purpose	Tests performed	Results
		Communications - Concluded	
103011	To investigate why crew and swimmers could not communicate on interphone	Command module circuit and interphone functionally tested separately and together; interphone and connector also submerged in salt water and tested again	Normal operation
103503	To verify wiring interfaces of high gain antenna pitch and yaw position indicators (yaw indication reversed from direction of motion)	Continuity and yaw and pitch meter deflection checks for miswiring (condition existed before flight)	Normal operation; all connector wiring in cabin correct
		Reaction Control	
103502	To verify condition of the command module reaction control system	Valve leak checks performed in both systems	System 1 primary oxidizer check valve leaked slightly more than allowable; system 2 oxidizer check valve leakage within specification
		Guidance and Control	
103108	To investigate the entry monitor system abnormal indications during flight	Entry monitor control assembly removed from command module for acceptance and off-limits testing; accelerometer replaced during testing	Abnormal accelerometer outputs observed during tilt-table test (see ASHUR 103036 also); null conditions found which could cause the noted 100-ft/sec jump
103019	To investigate the jumps observed in the optic coupling display unit readout	Power-on systems testing performed	Inflight problem duplicated by procedure; system operation as designed
103036	To investigate abnormal entry monitor control assembly outputs observed during tests for ASHUR 103036	Accelerometer removed from entry monitor control assembly for failure analysis at vendor	Bubble found in the damping fluid caused erratic output
		Crew Station	
103007	To investigate possible malfunction of personnel radiation dosimeters	Dosimeters subjected to acceptance testing, high and low dose rate calibration, vibration, thermal, and electromagnetic interference testing; one unit torn down and analyzed	All three units performed within specification; low dose (below specification) response characteristics varied; high flight reading on one unit not explained

TABLE C-I.- POSTFLIGHT TESTING SUMMARY - Concluded

ASHUR no.	Purpose	Tests performed	Results
		Crew Station - Concluded	
103020	To analyze contamination on command module windows	Heat shield windows removed for infrared emission and chemical analysis of surface contamination	Products of outgassing from RTV found on inside of heat shield windows; same as on spacecraft 101 windows
103022	To investigate an excessive wear condition of the inflight coverall garment boots	Visual inspection	Wear on top surface of boots; caused by rough bottom of one boot rubbing on top of the other
103023	To determine whether the nitrogen pressure bottles for side hatch counterbalance were properly punctured	Pressure bottles and puncturing pins inspected; puncturing torques measured	Both bottles were properly punctured and pins were not damaged; puncturing torques were within specification
103024	To investigate cause for intermittent operation of a T-adapter	Functional tests, X-ray, and DITMCO performed	Normal operation
103026	To investigate a reported wiring problem in the EKG harness	Continuity checks of bioinstrumentation performed	Normal operation; problem simulated with loose connection at signal conditioner
103032	To investigate tear in one of the headrest pads	Visual inspection performed	1/2-inch tear on back side of pad; caused by incorrect installation by crewman

D.0 DATA AVAILABILITY

Table D-I is a summary of the data made available for anomaly investigation and system performance analysis. Although the table reflects only data processed from Network magnetic tapes, Network data tabulations were available during the mission with approximately a 4-hour delay, and computer words were processed after the mission for the 20-hour period after translunar injection from communications log tapes. For additional information regarding data availability, the status listing in the Central Metric Data File, building 12, MSC, should be consulted.

TABLE D-I.- DATA AVAILABILITY

Time, hr:min		Range station	Tabs or plots*	Bilevels	Computer words	Special programs	O'graphs or Brush recorder
From	To						
-00:01	+00:10	MILA	X	X	X	X	X
+00:02	00:12	BDA	X	X	X	X	X
00:09	00:17	VAN	X				
00:22	00:48	MILA(D)					X
00:51	01:00	CRO		X	X		X
00:58	01:08	HSK		X	X		X
01:05	01:30	MILA(D)					X
01:33	01:44	MILA					X
01:37	01:46	BDA		X	X		X
01:40	01:51	VAN		X	X		X
01:48	02:00	CYI		X	X		X
02:42	02:53	MER	X	X	X		X
02:48	03:00	HAW	X	X	X	X	X
02:56	04:55	GDS	X	X	X	X	X
02:59	03:23	MILA	X	X		X	X
04:54	05:36	GDS			X		
06:09	08:33	GDS		X	X	X	X
08:32	09:20	GDS		X		X	X
09:19	10:51	GDS		X	X	X	X
10:50	11:37	GDS	X	X	X	X	X
11:35	12:23	GDS		X	X	X	X
13:24	14:11	GDS		X	X	X	X
14:10	14:58	GDS		X	X	X	X
14:57	15:42	GDS			X		
15:41	16:22	GDS		X	X	X	X
16:16	17:07	GDS		X	X		X
17:10	18:36	HSK		X		X	X
21:03	21:16	HSK			X	X	
22:01	22:49	HSK			X	X	
27:30	28:00	MAD		X		X	X
29:47	30:35	ACN			X	X	
36:02	36:48	GDS		X		X	X
36:47	37:15	GDS		X	X	X	X
37:32	38:00	GDS		X		X	X
39:02	39:49	GDS		X		X	X
39:48	40:00	GDS		X		X	X
59:36	61:05	GDS	X				

*Bandpass/time history.

TABLE D-I.- DATA AVAILABILITY - Continued

Time, hr:min		Range station	Tabs or plots*	Bilevels	Computer words	Special programs	O'graphs or Brush recorder
From	To						
60:42	61:11	HSK		X	X	X	X
60:55	61:43	GDS					X
61:04	61:25	GDS		X	X	X	X
66:39	66:55	HSK			X		
66:55	67:01	HSK		X	X		X
67:01	67:49	HSK			X	X	
67:47	68:16	HSK		X	X	X	X
68:16	68:34	HSK			X		
68:34	69:00	HSK			X	X	
68:57	69:32	HSK(D)	X	X	X	X	X
70:13	70:59	HSK			X	X	
71:40	72:09	HSK			X	X	
72:08	72:21	MAD			X		
72:32	73:02	MAD			X	X	
73:02	73:47	MAD(D)	X		X	X	
75:50	76:05	MAD			X	X	
76:02	76:17	MAD	X		X		
77:13	77:46	MAD(D)	X		X		
77:46	78:01	MAD		X	X		X
78:04	78:19	MAD			X		
78:19	78:32	MAD		X	X		X
80:19	80:31	MILA		X			X
80:56	81:43	GDS	X		X		
82:55	83:41	GDS	X		X		X
84:54	85:40	GDS	X				
86:53	87:38	GDS	X				
87:45	87:56	HSK		X	X		X
88:51	89:24	HSK(D)	X	X	X		X
89:27	90:28	HSK	X				
89:47	89:59	HSK		X	X		X
104:04	105:05	GDS		X	X		X
106:30	106:48	GDS		X	X		X
111:30	111:39	GDS		X	X	X	X
111:37	112:23	GDS		X		X	X
111:45	112:19	GDS			X	X	
112:22	113:00	HSK		X	X	X	X
127:40	127:46	GDS	X		X	X	

*Bandpass/time history.

TABLE D-I.- DATA AVAILABILITY - Concluded

Time, hr:min		Range station	Tabs or plots*	Bilevels	Computer words	Special programs	O'graphs or Brush recorder
From	To						
127:45	127:49	GDS			X	X	
139:13	139:22	HSK	X	X	X		X
144:47	145:48	GWM	X	X	X	X	X
145:47	146:36	GWM	X	X	X	X	X
146:36	147:00	DSE	X	X	X	X	X
00:00	00:11	FQTR	X			X	X
02:49	02:57	FQTR				X	X
03:20	03:22	FQTR				X	X
11:00	11:01	FQTR				X	X
69:08	69:12	FQTR				X	X
89:19	89:20	FQTR				X	X

REFERENCES

1. Marshall Space Flight Center: Apollo 8 Mission Report, Launch Vehicle. (This report has not yet been released; therefore, no report number can be cited.)

2. Office of Manned Space Flight: Apollo Flight Mission Assignments. M-D MA 500-11 (SE 010-000-1), December 4, 1968.

3. Manned Spacecraft Center: Mission Requirements, SA-503/CSM 103, C' Type Mission, (Lunar Orbit). SPD 8-R-027, November 16, 1968.

APOLLO SPACECRAFT FLIGHT HISTORY

(Continued from inside front cover)

Mission	Spacecraft	Description	Launch date	Launch site
Apollo 4	SC-017 LTA-10R	Supercircular entry at lunar return velocity	Nov. 9, 1967	Kennedy Space Center, Fla.
Apollo 5	LM-1	First lunar module flight	Jan. 22, 1968	Cape Kennedy, Fla.
Apollo 6	SC-020 LTA-2R	Verification of closed-loop emergency detection system	April 4, 1968	Kennedy Space Center, Fla.
Apollo 7	SC-101	First manned flight; earth-orbital	Oct. 11, 1968	Cape Kennedy, Fla.
Apollo 8	SC-103	First manned lunar orbital flight; first manned Saturn V launch	Dec. 21, 1968	Kennedy Space Center, Fla.